Comprehensive Second-Order Adjoint Sensitivity Analysis Methodology (2nd-ASAM) Applied to a Subcritical Experimental Reactor Physics Benchmark: III. Effects of Imprecisely Known Microscopic Fission Cross Sections and Average Number of Neutrons per Fission

D. G. Cacuci [1],*, R. Fang [1], J. A. Favorite [2], M. C. Badea [1] and F. Di Rocco [1]

[1] Center for Nuclear Science and Energy, Department of Mechanical Engineering, University of South Carolina, Columbia, SC 29208, USA; fangr@cec.sc.edu (R.F.); badea@cec.sc.edu (M.C.B.); federicodirocco90@gmail.com (F.D.R.)

[2] Los Alamos National Laboratory, Applied Physics (X) Division, MS F663, Los Alamos, NM 87545, USA; fave@lanl.gov

* Correspondence: cacuci@cec.sc.edu

Abstract: The Second-Order Adjoint Sensitivity Analysis Methodology (2nd-ASAM) is applied to compute the first-order and second-order sensitivities of the leakage response of a polyethylene-reflected plutonium (PERP) experimental system with respect to the following nuclear data: Group-averaged isotopic microscopic fission cross sections, mixed fission/total, fission/scattering cross sections, average number of neutrons per fission (ν), mixed ν/total cross sections, ν/scattering cross sections, and ν/fission cross sections. The numerical results obtained indicate that the 1st-order relative sensitivities for these nuclear data are smaller than the 1st-order sensitivities of the PERP leakage response with respect to the total cross sections but are larger than those with respect to the scattering cross sections. The vast majority of the 2nd-order unmixed sensitivities are smaller than the corresponding 1st-order ones, but several 2nd-order mixed relative sensitivities are larger than the 1st-order ones. In particular, several 2nd-order sensitivities for ^{239}Pu are significantly larger than the corresponding 1st-order ones. It is also shown that the effects of the 2nd-order sensitivities of the PERP benchmark's leakage response with respect to the benchmark's parameters underlying the average number of neutrons per fission, ν, on the moments (expected value, variance, and skewness) of the PERP benchmark's leakage response distribution are negligible by comparison to the corresponding effects (on the response distribution) stemming from uncertainties in the total cross sections, but are larger than the corresponding effects (on the response distribution) stemming from uncertainties in the fission and scattering cross sections.

1. Introduction

This work, designated as "Part III," continues the presentations of results, commenced in Part I [1] and set forth in Part II [2], produced within the ongoing second-order comprehensive sensitivity analysis to nuclear data of the polyethylene-reflected plutonium (PERP) metal sphere benchmark described

in [3]. The computational model of the PERP benchmark is solved using the multigroup discrete ordinates neutron transport code PARTISN [4], comprising the following imprecisely known nuclear data parameters: 180 group-averaged total microscopic cross sections, 21,600 group-averaged scattering microscopic cross sections, 120 parameters describing the fission process, 60 parameters describing the fission spectrum, 10 parameters describing the system's sources, and 6 isotopic number densities.

This work presents the numerical results for the 60 first-order sensitivities of the PERP's leakage response with respect to the benchmark's group-averaged fission cross sections, along with the results for the 60×60 second-order sensitivities of the PERP Benchmark's leakage response to the group-averaged microscopic fission cross sections, 60×180 mixed 2nd-order sensitivities to the fission and total microscopic cross sections, and $60 \times 21,600$ mixed 2nd-order sensitivities to the fission and scattering microscopic cross sections. These sensitivities have been computed by specializing the general expressions derived by Cacuci [5] to the PERP benchmark. Section 2 of this work presents computational results for the 1st-order and 2nd-order sensitivities of the PERP benchmark's leakage response with respect to the group-averaged microscopic fission cross sections. Section 3 reports numerical results for the matrix of mixed 2nd-order leakage sensitivities to the group-averaged fission and total microscopic cross sections. Section 4 reports numerical results for the matrix of mixed 2nd-order leakage sensitivities to the group-averaged fission and scattering microscopic cross sections.

Section 5 presents computational results for the 60 first-order and 60×60 second-order unmixed sensitivities of the PERP benchmark's leakage response with respect to the parameters underlying the average number, ν, of neutrons per fission. Section 6 reports numerical results for the 60×180 matrix of mixed 2nd-order leakage sensitivities to ν and total microscopic cross sections. Section 7 reports numerical results for the $60 \times 21,600$ matrix of mixed 2nd-order leakage sensitivities to ν and scattering microscopic cross sections. Section 8 reports numerical results for the 60×60 matrix of mixed 2nd-order leakage sensitivities to ν and fission microscopic cross sections.

Section 9 presents the impact of the 1st- and 2nd-order sensitivities on the *uncertainties* induced in the leakage response by the imprecisely known group-averaged fission microscopic cross section. Section 10 presents the impact of the 1st- and 2nd-order sensitivities on the *uncertainties* induced in the leakage response by the imprecisely known parameters underlying the average number of neutrons per fission (ν).

Section 11 concludes this work. The computational results for the sensitivities of the PERP leakage response to the remaining imprecisely known fission spectrum, isotopic atomic number densities, and including the source parameters will be reported in subsequent publications.

2. Computation of 1st- and 2nd-Order Sensitivities of the PERP Leakage Response to Fission Cross Sections

The physical system considered in this work is the same poly<u>e</u>thylene-<u>r</u>eflected <u>p</u>lutonium (acronym: PERP) metal sphere benchmark [3] as was considered in the 2nd-order sensitivity and uncertainty analyses performed for the group-averaged total microscopic cross sections [1] and the group-averaged scattering cross sections [2], respectively. As in [1,2], the neutron flux is computed by solving numerically the neutron transport equation using the PARTISN [4] multigroup discrete ordinates transport code. For the PERP benchmark under consideration, PARTISN [4] solves the following multi-group approximation of the neutron transport equation with a spontaneous fission source provided by the code SOURCES4C [6]:

$$B^g(\boldsymbol{\alpha})\varphi^g(r, \boldsymbol{\Omega}) = Q^g(r), \quad g = 1, \ldots, G, \tag{1}$$

$$\varphi^g(r_d, \boldsymbol{\Omega}) = 0, \boldsymbol{\Omega} \cdot \mathbf{n} < 0, \quad g = 1, \ldots, G \tag{2}$$

where r_d denotes the external radius of the PERP benchmark, and where

$$
\begin{aligned}
B^g(\boldsymbol{\alpha})\varphi^g(r,\boldsymbol{\Omega}) &\triangleq \boldsymbol{\Omega}\cdot\nabla\varphi^g(r,\boldsymbol{\Omega}) + \Sigma_t^g(r)\,\varphi^g(r,\boldsymbol{\Omega}) \\
&- \sum_{g'=1}^{G}\int_{4\pi}\Sigma_s^{g'\to g}(r,\boldsymbol{\Omega'}\to\boldsymbol{\Omega})\,\varphi^{g'}(r,\boldsymbol{\Omega'})d\boldsymbol{\Omega'} - \chi^g(r)\sum_{g'=1}^{G}\int_{4\pi}(\nu\Sigma)_f^{g'}(r)\,\varphi^{g'}(r,\boldsymbol{\Omega'})d\boldsymbol{\Omega'},
\end{aligned}
\tag{3}
$$

$$
Q^g(r) \triangleq \sum_{k=1}^{N_f}\lambda_k N_{k,1} F_k^{SF} \nu_k^{SF} e^{-E^g/a_k}\sinh\sqrt{b_k E^g}, \quad g=1,\dots,G.
\tag{4}
$$

In Equation (1), the vector $\boldsymbol{\alpha}$ denotes the "vector of imprecisely known model parameters", which has been defined in [1] as $\boldsymbol{\alpha} \triangleq \left[\boldsymbol{\sigma}_t; \boldsymbol{\sigma}_s; \boldsymbol{\sigma}_f; \boldsymbol{\nu}; \mathbf{p}; \mathbf{q}; \mathbf{N}\right]^{\dagger}$, having the vector-components $\boldsymbol{\sigma}_t$, $\boldsymbol{\sigma}_s$, $\boldsymbol{\sigma}_f$, $\boldsymbol{\nu}$, $\mathbf{p}$, $\mathbf{q}$ and $\mathbf{N}$ which comprise the various model parameters for the microscopic total cross sections, scattering cross sections, fission cross sections, average number of neutrons per fission, fission spectra, sources, and isotopic number densities, respectively.

The PARTISN [4] calculations used MENDF71X 618-group cross sections [7] collapsed to $G=30$ energy groups, with group boundaries, E^g, as presented in [1]. The MENDF71X library uses ENDF/B-VII.1 Nuclear Data [8].

The total neutron leakage from the PERP sphere, denoted as $L(\boldsymbol{\alpha})$, will depend (indirectly, through the neutron flux) on all of the imprecisely known model parameters and is defined as follows:

$$
L(\boldsymbol{\alpha}) \triangleq \int_{S_b} dS \sum_{g=1}^{G}\int_{\boldsymbol{\Omega}\cdot\mathbf{n}>0} d\boldsymbol{\Omega}\,\boldsymbol{\Omega}\cdot\mathbf{n}\,\varphi^g(r,\boldsymbol{\Omega})
\tag{5}
$$

Part I [1] has reported the results for the 1st- and 2nd-order sensitivities of the leakage response with respect to the total and capture microscopic cross sections for $\partial L(\boldsymbol{\alpha})/\partial\boldsymbol{\sigma}_t$ and $\partial^2 L(\boldsymbol{\alpha})/\partial\boldsymbol{\sigma}_t\partial\boldsymbol{\sigma}_t$, respectively. Part II [2] has presented the results for the 1st-order sensitivities of the leakage response with respect to the scattering microscopic cross sections $\partial L(\boldsymbol{\alpha})/\partial\boldsymbol{\sigma}_s$ and for the 2nd-order sensitivities $\partial^2 L(\boldsymbol{\alpha})/\partial\boldsymbol{\sigma}_s\partial\boldsymbol{\sigma}_s$, and $\partial^2 L(\boldsymbol{\alpha})/\partial\boldsymbol{\sigma}_s\partial\boldsymbol{\sigma}_t$. This work reports the computational results for the 1st-order sensitivities $\partial L(\boldsymbol{\alpha})/\partial\boldsymbol{\sigma}_f$ and $\partial L(\boldsymbol{\alpha})/\partial\boldsymbol{\nu}$, and for the 2nd-order sensitivities $\partial^2 L(\boldsymbol{\alpha})/\partial\boldsymbol{\sigma}_f\partial\boldsymbol{\sigma}_f$, $\partial^2 L(\boldsymbol{\alpha})/\partial\boldsymbol{\sigma}_f\partial\boldsymbol{\sigma}_t$, $\partial^2 L(\boldsymbol{\alpha})/\partial\boldsymbol{\sigma}_f\partial\boldsymbol{\sigma}_s$, $\partial^2 L(\boldsymbol{\alpha})/\partial\boldsymbol{\nu}\partial\boldsymbol{\nu}$, $\partial^2 L(\boldsymbol{\alpha})/\partial\boldsymbol{\nu}\partial\boldsymbol{\sigma}_t$, $\partial^2 L(\boldsymbol{\alpha})/\partial\boldsymbol{\nu}\partial\boldsymbol{\sigma}_s$ and $\partial^2 L(\boldsymbol{\alpha})/\partial\boldsymbol{\nu}\partial\boldsymbol{\sigma}_f$, and compares these results to those reported in Parts I and II. The components of the vector of model parameters $\boldsymbol{\alpha} \triangleq \left[\boldsymbol{\sigma}_t; \boldsymbol{\sigma}_s; \boldsymbol{\sigma}_f; \boldsymbol{\nu}; \mathbf{p}; \mathbf{q}; \mathbf{N}\right]^{\dagger}$ have been defined in [1] and are described in the Appendix A, for convenient reference.

2.1. First-Order Sensitivities $\partial L(\boldsymbol{\alpha})/\partial\boldsymbol{\sigma}_f$

The first-order sensitivity of the PERP leakage response to the group-averaged microscopic fission cross sections, which will be denoted as $\left[\partial L(\boldsymbol{\alpha})/\partial f_j\right]_{f=\sigma_f}$, comprises two types of contributions. The first type of contributions, which will be denoted as $\left[\partial L(\boldsymbol{\alpha})/\partial f_j\right]_{f=\sigma_f}^{(1)}$, arises from quantities that involve the macroscopic fission cross sections directly, while the second type of contributions stems indirectly, through the macroscopic total cross sections, which comprise the fission cross sections in their definitions. The contributions $\left[\partial L(\boldsymbol{\alpha})/\partial f_j\right]_{f=\sigma_f}^{(1)}$ are computed using the following particular forms of Equations (152), (156) and (157) in [5]. For convenient referencing, the corresponding equations from [5] used in this work were reproduced in Appendix B.

$$
\left[\frac{\partial L(\boldsymbol{\alpha})}{\partial f_j}\right]_{f=\sigma_f}^{(1)} = \sum_{g=1}^{G}\int_V dV\int_{4\pi}d\boldsymbol{\Omega}\,\psi^{(1),g}(r,\boldsymbol{\Omega})\sum_{g'=1}^{G}\int_{4\pi}d\boldsymbol{\Omega'}\frac{\partial\left[\left(\nu\Sigma_f\right)^{g'}\right]}{\partial f_j}\chi^g\varphi^{g'}(r,\boldsymbol{\Omega'}), \quad j=1,\dots,J_{\sigma f}.
\tag{6}
$$

The multigroup adjoint fluxes $\psi^{(1),g}(r,\boldsymbol{\Omega})$ appearing in Equation (6) are the solutions of the following 1st-Level Adjoint Sensitivity System (1st-LASS):

$$A^{(1),g}(\boldsymbol{\alpha})\psi^{(1),g}(r,\boldsymbol{\Omega}) = \boldsymbol{\Omega}\cdot\mathbf{n}\delta(r-r_d), \quad g=1,\ldots,G, \tag{7}$$

$$\psi^{(1),g}(r_d,\boldsymbol{\Omega}) = 0, \boldsymbol{\Omega}\cdot\mathbf{n} > 0, \quad g=1,\ldots,G, \tag{8}$$

where the adjoint operator $A^{(1),g}(\boldsymbol{\alpha})$ takes on the following particular form of Equation (149) in [5]:

$$
\begin{aligned}
&A^{(1),g}(\boldsymbol{\alpha})\psi^{(1),g}(r,\boldsymbol{\Omega}) \\
&\triangleq -\boldsymbol{\Omega}\cdot\nabla\psi^{(1),g}(r,\boldsymbol{\Omega}) + \Sigma_t^g\psi^{(1),g}(r,\boldsymbol{\Omega}) - \sum_{g'=1}^{G}\int_{4\pi}d\boldsymbol{\Omega}'\Sigma_s^{g\to g'}(\boldsymbol{\Omega}\to\boldsymbol{\Omega}')\,\psi^{(1),g'}(r,\boldsymbol{\Omega}') \\
&-\nu\Sigma_f^g\sum_{g'=1}^{G}\int_{4\pi}d\boldsymbol{\Omega}'\chi^{g'}\,\psi^{(1),g'}(r,\boldsymbol{\Omega}'), \quad g=1,\ldots,G.
\end{aligned}
\tag{9}
$$

The second type of contributions, which will be denoted as $\left[\partial L(\boldsymbol{\alpha})/\partial f_j\right]_{f=\sigma_f}^{(2)}$, includes the contributions stemming from the total cross sections, since the total cross sections comprises the fission cross sections. The contributions are computed using Equation (150) in [5] in conjunction with the relations $\frac{\partial L}{\partial t_j}\frac{\partial t_j}{\partial f_j} = \frac{\partial L}{\partial f_j}$ and $\frac{\partial \Sigma_t^g}{\partial t_j}\frac{\partial t_j}{\partial f_j} = \frac{\partial \Sigma_t^g}{\partial f_j}$, to obtain:

$$\left[\frac{\partial L(\boldsymbol{\alpha})}{\partial f_j}\right]_{f=\sigma_f}^{(2)} = -\sum_{g=1}^{G}\int_V dV\int_{4\pi}d\boldsymbol{\Omega}\,\psi^{(1),g}(r,\boldsymbol{\Omega})\varphi^g(r,\boldsymbol{\Omega})\frac{\partial \Sigma_t^g}{\partial f_j}, \quad j=1,\ldots,J_{\sigma f}. \tag{10}$$

Adding Equations (6) and (10) yields the following expression:

$$
\begin{aligned}
\left[\frac{\partial L(\boldsymbol{\alpha})}{\partial f_j}\right]_{f=\sigma_f} &= \left[\frac{\partial L(\boldsymbol{\alpha})}{\partial f_j}\right]_{f=\sigma_f}^{(1)} + \left[\frac{\partial L(\boldsymbol{\alpha})}{\partial f_j}\right]_{f=\sigma_f}^{(2)} \\
&= \sum_{g=1}^{G}\int_V dV\int_{4\pi}d\boldsymbol{\Omega}\,\psi^{(1),g}(r,\boldsymbol{\Omega})\sum_{g'=1}^{G}\int_{4\pi}d\boldsymbol{\Omega}'\frac{\partial\left[(\nu\Sigma_f)^{g'}\right]}{\partial f_j}\chi^g\varphi^{g'}(r,\boldsymbol{\Omega}') \\
&- \sum_{g=1}^{G}\int_V dV\int_{4\pi}d\boldsymbol{\Omega}\,\psi^{(1),g}(r,\boldsymbol{\Omega})\varphi^g(r,\boldsymbol{\Omega})\frac{\partial \Sigma_t^g}{\partial f_j}, \quad \text{for } j=1,\ldots,J_{\sigma f}.
\end{aligned}
\tag{11}
$$

For the PERP benchmark, the cross-sections in every material are treated in the PARTISN [4] calculations as being space-independent within the respective material. When the parameters f_j correspond to the fission cross sections, i.e., $f_j \equiv \sigma_{f,i_j}^{g_j}$, thus the following relations hold:

$$\frac{\partial\left[(\nu\Sigma_f)^{g'}\right]}{\partial f_j} = \frac{\partial \sum_{m=1}^{M}\sum_{i=1}^{I}N_{i,m}\left(\nu\sigma_f\right)_i^{g'}}{\partial\sigma_{f,i_j}^{g_j}} = \frac{\partial \sum_{m=1}^{M}\sum_{i=1}^{I}N_{i,m}\nu_i^{g'}\sigma_{f,i}^{g'}}{\partial\sigma_{f,i_j}^{g_j}} = \delta_{g_jg'}N_{i_j,m_j}\nu_{i_j}^{g'}, \tag{12}$$

$$
\begin{aligned}
\frac{\partial \Sigma_t^g}{\partial f_j} &= \frac{\partial\left[\sum_{m=1}^{M}\sum_{i=1}^{I}N_{i,m}\sigma_{t,i}^g\right]}{\partial\sigma_{f,i_j}^{g_j}} = \frac{\partial\left\{\sum_{m=1}^{M}\sum_{i=1}^{I}N_{i,m}\left[\sigma_{f,i}^g+\sigma_{c,i}^g+\sum_{g'=1}^{G}\sigma_{s,l=0,i}^{g\to g'}\right]\right\}}{\partial\sigma_{f,i_j}^{g_j}} \\
&= \frac{\partial\left[\sum_{m=1}^{M}\sum_{i=1}^{I}N_{i,m}\sigma_{f,i}^g\right]}{\partial\sigma_{f,i_j}^{g_j}} = \delta_{g_jg}N_{i_j,m_j},
\end{aligned}
\tag{13}
$$

where the subscripts i_j, g_j and m_j denote the isotope, energy group and material associated with the parameter f_j, respectively; and where $\delta_{g_jg'}$ and δ_{g_jg} denote the Kronecker-delta functionals (e.g.,

$\delta_{g_jg} = 1$ if $g_j = g$; $\delta_{g_jg} = 0$ if $g_j \neq g$). Inserting Equations (12) and (13) into Equation (11) yields the following expression for computational purposes:

$$\frac{\partial L(\boldsymbol{\alpha})}{\partial \sigma_{f,i}^g} = N_{i,m} \int_V dV v_i^g \varphi_0^g(r) \sum_{g'=1}^{G} \chi^{g'} \xi_0^{(1),g'}(r) - N_{i,m} \int_V dV \int_{4\pi} d\boldsymbol{\Omega}\, \psi^{(1),g}(r,\boldsymbol{\Omega})\varphi^g(r,\boldsymbol{\Omega}),$$
$$for\ i = 1,\ldots,I;\ g = 1,\ldots,G;\ m = 1,\ldots,M, \tag{14}$$

where the flux moments $\varphi_0^g(r)$ and $\xi_0^{(1),g'}(r)$ are defined as follows:

$$\varphi_0^g(r) \triangleq \int_{4\pi} d\boldsymbol{\Omega}\, \varphi^g(r,\boldsymbol{\Omega}), \tag{15}$$

$$\xi_0^{(1),g}(r) \triangleq \int_{4\pi} d\boldsymbol{\Omega}\, \psi^{(1),g}(r,\boldsymbol{\Omega}). \tag{16}$$

The numerical values of the 1st-order relative sensitivities, $S^{(1)}\left(\sigma_{f,i}^g\right) \triangleq \left(\partial L / \partial \sigma_{f,i}^g\right)\left(\sigma_{f,i}^g / L\right)$, $i = 1,2; g = 1,\ldots,30$, of the leakage response with respect to the fission microscopic cross sections for the six isotopes contained in the PERP benchmark will be presented in Section 2.3, below, in tables that will also include comparisons with the numerical values of the corresponding 2nd-order unmixed relative sensitivities $S^{(2)}\left(\sigma_{f,i}^g, \sigma_{f,i}^g\right) \triangleq \left(\partial^2 L / \partial \sigma_{f,i}^g \partial \sigma_{f,i}^g\right)\left(\sigma_{f,i}^g \sigma_{f,i}^g / L\right)$, $i = 1,2;\ g = 1,\ldots,30$.

2.2. Second-Order Sensitivities $\partial^2 L(\boldsymbol{\alpha}) / \partial \boldsymbol{\sigma}_f \partial \boldsymbol{\sigma}_f$

The equations needed for deriving the expression of the 2nd-order sensitivities $\partial^2 L(\boldsymbol{\alpha}) / \partial \boldsymbol{\sigma}_f \partial \boldsymbol{\sigma}_f$ are obtained by particularizing Equations (158), (160), (177) and (179) in [5] to the PERP benchmark. The contribution stemming directly from the fission cross section is obtained by particularizing Equation (179) in [5] to the PERP benchmark, which yields:

$$\left(\frac{\partial^2 L}{\partial f_j \partial f_{m_2}}\right)^{(1)} = \sum_{g=1}^{G} \int_V dV \int_{4\pi} d\boldsymbol{\Omega}\, \psi^{(1),g}(r,\boldsymbol{\Omega}) \sum_{g'=1}^{G} \int_{4\pi} d\boldsymbol{\Omega}' \varphi^{g'}(r,\boldsymbol{\Omega}')\chi^g \frac{\partial^2\left[(\nu\Sigma_f)^{g'}\right]}{\partial f_j \partial f_{m_2}}$$
$$+ \sum_{g=1}^{G} \int_V dV \int_{4\pi} d\boldsymbol{\Omega}\, u_{1,j}^{(2),g}(r,\boldsymbol{\Omega}) \frac{\partial\left[(\nu\Sigma_f)^g\right]}{\partial f_{m_2}} \sum_{g'=1}^{G} \int_{4\pi} d\boldsymbol{\Omega}' \chi^{g'} \psi^{(1),g'}(r,\boldsymbol{\Omega}')$$
$$+ \sum_{g=1}^{G} \int_V dV \int_{4\pi} d\boldsymbol{\Omega}\, u_{2,j}^{(2),g}(r,\boldsymbol{\Omega}) \sum_{g'=1}^{G} \int_{4\pi} d\boldsymbol{\Omega}' \varphi^{g'}(r,\boldsymbol{\Omega}')\chi^g \frac{\partial\left[(\nu\Sigma_f)^{g'}\right]}{\partial f_{m_2}}, \tag{17}$$
$$for\ j = 1,\ldots,J_{\sigma f}; m_2 = 1,\ldots,J_{\sigma f},$$

where the 2nd-level adjoint functions, $u_{1,j}^{(2),g}(r,\boldsymbol{\Omega})$ and $u_{2,j}^{(2),g}(r,\boldsymbol{\Omega}), j = 1,\ldots,J_{\sigma f}, g = 1,\ldots,G$, are the solutions of the following 2nd-Level Adjoint Sensitivity System (2nd-LASS) presented in Equations (183)–(185) of [5]:

$$B^g\left(\boldsymbol{\alpha}^0\right) u_{1,j}^{(2),g}(r,\boldsymbol{\Omega}) = \sum_{g'=1}^{G} \int_{4\pi} d\boldsymbol{\Omega}' \varphi^{g'}(r,\boldsymbol{\Omega}')\chi^g \frac{\partial\left[(\nu\Sigma_f)^{g'}\right]}{\partial f_j}, j = 1,\ldots,J_{\sigma f};\ g = 1,\ldots,G, \tag{18}$$

$$u_{1,j}^{(2),g}(r_d,\boldsymbol{\Omega}) = 0, \boldsymbol{\Omega} \cdot \mathbf{n} < 0;\ j = 1,\ldots,J_{\sigma f};\ g = 1,\ldots,G, \tag{19}$$

$$A^{(1),g}\left(\boldsymbol{\alpha}^0\right) u_{2,j}^{(2),g}(r,\boldsymbol{\Omega}) = \frac{\partial\left[(\nu\Sigma_f)^g\right]}{\partial f_j} \sum_{g'=1}^{G} \int_{4\pi} d\boldsymbol{\Omega}' \chi^{g'} \psi^{(1),g'}(r,\boldsymbol{\Omega}'),\ j = 1,\ldots,J_{\sigma f};\ g = 1,\ldots,G, \tag{20}$$

$$u_{2,j}^{(2),g}(r_d,\boldsymbol{\Omega}) = 0, \boldsymbol{\Omega} \cdot \mathbf{n} > 0;\ j = 1,\ldots,J_{\sigma f};\ g = 1,\ldots,G. \tag{21}$$

The parameters f_j and f_{m_2} in Equations (17), (18) and (20) correspond to the fission cross sections, and are therefore denoted as $f_j \equiv \sigma_{f,i_j}^{g_j}$ and $f_{m_2} \equiv \sigma_{f,i_{m_2}}^{g_{m_2}}$, respectively, where the subscripts i_{m_2} and g_{m_2} refer to the isotope and energy groups associated with the parameter f_{m_2}, respectively, and where the index m_2 is defined in Equation (17). Noting that

$$\frac{\partial^2 \Sigma_t^g}{\partial f_j \partial f_{m_2}} = \frac{\partial^2 \Sigma_t^g}{\partial \sigma_{f,i_j}^{g_j} \partial \sigma_{f,i_{m_2}}^{g_{m_2}}} = 0, \tag{22}$$

$$\frac{\partial\left[\left(\nu\Sigma_f\right)^g\right]}{\partial f_{m_2}} = \frac{\partial \sum_{m=1}^{M} \sum_{i=1}^{I} N_{i,m}\left(\nu\sigma_f\right)_i^g}{\partial \sigma_{f,i_{m_2}}^{g_{m_2}}} = \frac{\partial \sum_{m=1}^{M} \sum_{i=1}^{I} N_{i,m}\nu_i^g \sigma_{f,i}^g}{\partial \sigma_{f,i_{m_2}}^{g_{m_2}}} = \delta_{g_{m_2} g} N_{i_{m_2},m_{m_2}}\nu_{i_{m_2}}^g, \tag{23}$$

$$\frac{\partial\left[\left(\nu\Sigma_f\right)^{g'}\right]}{\partial f_{m_2}} = \frac{\partial \sum_{m=1}^{M} \sum_{i=1}^{I} N_{i,m}\left(\nu\sigma_f\right)_i^{g'}}{\partial \sigma_{f,i_{m_2}}^{g_{m_2}}} = \frac{\partial \sum_{m=1}^{M} \sum_{i=1}^{I} N_{i,m}\nu_i^{g'} \sigma_{f,i}^{g'}}{\partial \sigma_{f,i_{m_2}}^{g_{m_2}}} = \delta_{g_{m_2} g'} N_{i_{m_2},m_{m_2}}\nu_{i_{m_2}}^{g'}, \tag{24}$$

$$\frac{\partial\left[\left(\nu\Sigma_f\right)^g\right]}{\partial f_j} = \frac{\partial \sum_{m=1}^{M} \sum_{i=1}^{I} N_{i,m}\left(\nu\sigma_f\right)_i^g}{\partial \sigma_{f,i_j}^{g_j}} = \frac{\partial \sum_{m=1}^{M} \sum_{i=1}^{I} N_{i,m}\nu_i^g \sigma_{f,i}^g}{\partial \sigma_{f,i_j}^{g_j}} = \delta_{g_j g} N_{i_j,m_j}\nu_{i_j}^g, \tag{25}$$

and inserting the results obtained in Equation (12) and in Equations (22)–(25) into Equations (18), (20) and (17) reduces the latter equation to the following expression:

$$\left(\frac{\partial^2 L}{\partial f_j \partial f_{m_2}}\right)^{(1)} = N_{i_{m_2},m_{m_2}}\nu_{i_{m_2}}^{g_{m_2}} \int_V dV \left[U_{1,j;0}^{(2),g_{m_2}}(r) \sum_{g'=1}^{G} \chi^{g'} \xi_0^{(1),g'}(r) + \varphi_0^{g_{m_2}}(r) \sum_{g=1}^{G} \chi^g U_{2,j;0}^{(2),g}(r)\right], \tag{26}$$

where

$$U_{1,j;0}^{(2),g}(r) \triangleq \int_{4\pi} d\Omega\, u_{1,j}^{(2),g}(r,\Omega), \tag{27}$$

$$U_{2,j;0}^{(2),g}(r) \triangleq \int_{4\pi} d\Omega\, u_{2,j}^{(2),g}(r,\Omega), \tag{28}$$

and where the 2nd-level adjoint functions, $u_{1,j}^{(2),g}(r,\Omega)$ and $u_{2,j}^{(2),g}(r,\Omega)$, $j = 1,\ldots,J_{\sigma f}$; $g = 1,\ldots,G$ are the solutions of the following simplified form of the 2nd-Level Adjoint Sensitivity System (2nd-LASS) shown in Equations (18) and (20):

$$B^g\left(\alpha^0\right) u_{1,j}^{(2),g}(r,\Omega) = N_{i_j,m_j}\nu_{i_j}^{g_j} \chi^g \varphi_0^{g_j}(r), \quad j = 1,\ldots,J_{\sigma f}; \ g = 1,\ldots,G, \tag{29}$$

$$A^{(1),g}\left(\alpha^0\right) u_{2,j}^{(2),g}(r,\Omega) = \delta_{g_j g} N_{i_j,m_j}\nu_{i_j}^g \sum_{g'=1}^{G} \chi^{g'} \xi_0^{(1),g'}(r), \quad j = 1,\ldots,J_{\sigma f}; \ g = 1,\ldots,G, \tag{30}$$

subject to the boundary conditions shown in Equations (19) and (21), respectively.

The remaining contributions to $\left(\frac{\partial^2 L}{\partial f_j \partial f_{m_2}}\right)_{(f=\sigma_f, f=\sigma_f)}$ stem from Equation (158) in [5], which are obtained by using this equation in conjunction with the relations $\frac{\partial^2 L}{\partial t_j \partial t_{m_2}} \frac{\partial t_j}{\partial f_j} \frac{\partial t_{m_2}}{\partial f_{m_2}} = \frac{\partial^2 L}{\partial f_j \partial f_{m_2}}$, $\frac{\partial \Sigma_t^g}{\partial t_{m_2}} \frac{\partial t_{m_2}}{\partial f_{m_2}} = \frac{\partial \Sigma_t^g}{\partial f_{m_2}}$, and $\frac{\partial^2 \Sigma_t^g}{\partial t_j \partial t_{m_2}} \frac{\partial t_j}{\partial f_j} \frac{\partial t_{m_2}}{\partial f_{m_2}} = \frac{\partial^2 \Sigma_t^g}{\partial f_j \partial f_{m_2}}$, which gives:

$$
\begin{aligned}
\left(\frac{\partial^2 L}{\partial f_j \partial f_{m_2}}\right)^{(2)} = & -\sum_{g=1}^{G} \int_V dV \int_{4\pi} d\Omega \, \psi^{(1),g}(r,\Omega) \varphi^g(r,\Omega) \frac{\partial^2 \Sigma_t^g}{\partial f_j \partial f_{m_2}} \\
& -\sum_{g=1}^{G} \int_V dV \int_{4\pi} d\Omega \left[\psi_{1,j}^{(2),g}(r,\Omega) \psi^{(1),g}(r,\Omega) + \psi_{2,j}^{(2),g}(r,\Omega) \varphi^g(r,\Omega)\right]\frac{\partial \Sigma_t^g}{\partial f_{m_2}}, \\
& for \; j = 1, \ldots, J_{\sigma f}, \; m_2 = 1, \ldots, J_{\sigma f},
\end{aligned}
\tag{31}
$$

where the 2nd-level adjoint functions $\psi_{1,j}^{(2),g}(r,\Omega)$ and $\psi_{2,j}^{(2),g}(r,\Omega)$, $j = 1, \ldots, J_{\sigma f}$; $g = 1, \ldots, G$, are the solutions of the following particular form of the 2nd-Level Adjoint Sensitivity System (2nd-LASS) presented in Equations (164)–(166) of [5]:

$$
B^g(\boldsymbol{\alpha}^0)\psi_{1,j}^{(2),g}(r,\Omega) = -\varphi^g(r,\Omega)\frac{\partial \Sigma_t^g}{\partial f_j}, \; j = 1, \ldots, J_{\sigma f}; \; g = 1, \ldots, G,
\tag{32}
$$

$$
\psi_{1,j}^{(2),g}(r_d,\Omega) = 0, \; \Omega \cdot \mathbf{n} < 0; \; j = 1, \ldots, J_{\sigma f}; \; g = 1, \ldots, G,
\tag{33}
$$

$$
A^{(1),g}(\boldsymbol{\alpha}^0)\psi_{2,j}^{(2),g}(r,\Omega) = -\psi^{(1),g}(r,\Omega)\frac{\partial \Sigma_t^g}{\partial f_j}, \; j = 1, \ldots, J_{\sigma f}; \; g = 1, \ldots, G,
\tag{34}
$$

$$
\psi_{2,j}^{(2),g}(r_d,\Omega) = 0, \; \Omega \cdot \mathbf{n} > 0; \; j = 1, \ldots, J_{\sigma f}; \; g = 1, \ldots, G.
\tag{35}
$$

The expressions of the various derivatives appearing in Equations (31), (32), and (34) are obtained as follows:

$$
\frac{\partial^2 \Sigma_t^g}{\partial f_j \partial f_{m_2}} = \frac{\partial^2 \Sigma_t^g}{\partial \sigma_{f,i_j}^{g_j} \partial \sigma_{f,i_{m_2}}^{g_{m_2}}} = 0,
\tag{36}
$$

$$
\frac{\partial \Sigma_t^g}{\partial f_{m_2}} = \frac{\partial\left[\sum_{m=1}^{M}\sum_{i=1}^{I} N_{i,m}\sigma_{t,i}^g\right]}{\partial \sigma_{f,i_{m_2}}^{g_{m_2}}} = \frac{\partial\left[\sum_{m=1}^{M}\sum_{i=1}^{I} N_{i,m}\sigma_{f,i}^g\right]}{\partial \sigma_{f,i_{m_2}}^{g_{m_2}}} = \delta_{g_{m_2}g} N_{i_{m_2},m_{m_2}},
\tag{37}
$$

where the subscript m_{m_2} refers to the material associated with the parameter f_{m_2}. Inserting Equations (36), (37) and (13) into Equations (31)–(34) yields the following simplified expression:

$$
\left(\frac{\partial^2 L}{\partial f_j \partial f_{m_2}}\right)^{(2)} = -N_{i_{m_2},m_{m_2}}\int_V dV \int_{4\pi} d\Omega \left[\psi_{1,j}^{(2),g_{m_2}}(r,\Omega)\psi^{(1),g_{m_2}}(r,\Omega) + \psi_{2,j}^{(2),g_{m_2}}(r,\Omega)\varphi^{g_{m_2}}(r,\Omega)\right],
\tag{38}
$$

where the 2nd-level adjoint functions $\psi_{1,j}^{(2),g}(r,\Omega)$ and $\psi_{2,j}^{(2),g}(r,\Omega)$, $j = 1, \ldots, J_{\sigma f}$; $g = 1, \ldots, G$, are the solutions of the following simplified 2nd-Level Adjoint Sensitivity System (2nd-LASS):

$$
B^g(\boldsymbol{\alpha}^0)\psi_{1,j}^{(2),g}(r,\Omega) = -\delta_{g_j g} N_{i_j,m_j}\varphi^g(r,\Omega), \; j = 1, \ldots, J_{\sigma f}; \; g = 1, \ldots, G,
\tag{39}
$$

$$
A^{(1),g}(\boldsymbol{\alpha}^0)\psi_{2,j}^{(2),g}(r,\Omega) = -\delta_{g_j g} N_{i_j,m_j}\psi^{(1),g}(r,\Omega), \; j = 1, \ldots, J_{\sigma f}; \; g = 1, \ldots, G,
\tag{40}
$$

subject to the boundary conditions shown in Equations (33) and (35), respectively.

Additional contributions stem from Equation (160) in [5], in conjunction with the relation $\frac{\partial^2 L}{\partial t_j \partial f_{m_2}} \frac{\partial t_j}{\partial f_j} = \frac{\partial^2 L}{\partial f_j \partial f_{m_2}}$, which takes on the following particular form:

$$
\begin{aligned}
\left(\frac{\partial^2 L}{\partial f_j \partial f_{m_2}} \right)^{(3)} &= \sum_{g=1}^{G} \int_V dV \int_{4\pi} d\mathbf{\Omega}\, \psi_{2,j}^{(2),g}(r,\mathbf{\Omega}) \sum_{g'=1}^{G} \int_{4\pi} d\mathbf{\Omega}'\, \varphi^{g'}(r,\mathbf{\Omega}') \chi^g \frac{\partial \left[(\nu \Sigma_f)^{g'} \right]}{\partial f_{m_2}} \\
&+ \sum_{g=1}^{G} \int_V dV \int_{4\pi} d\mathbf{\Omega}\, \psi_{1,j}^{(2),g}(r,\mathbf{\Omega}) \frac{\partial \left[(\nu \Sigma_f)^g \right]}{\partial f_{m_2}} \sum_{g'=1}^{G} \int_{4\pi} d\mathbf{\Omega}'\, \chi^{g'} \psi^{(1),g'}(r,\mathbf{\Omega}'), \\
& \quad for\ \ j = 1,\dots, J_{\sigma f};\ \ m_2 = 1,\dots, J_{\sigma f}.
\end{aligned}
\tag{41}
$$

Inserting the results obtained in Equations (23) and (24) into Equation (41), and performing the respective angular integrations, yields the following simplified expression for Equation (41):

$$
\left(\frac{\partial^2 L}{\partial f_j \partial f_{m_2}} \right)^{(3)} = N_{i_{m_2}, m_{m_2}} \nu_{i_{m_2}}^{g m_2} \int_V dV \left[\xi_{1,j;0}^{(2),g m_2}(r) \sum_{g'=1}^{G} \chi^{g'} \xi_0^{(1),g'}(r) + \varphi_0^{g m_2}(r) \sum_{g=1}^{G} \chi^g \xi_{2,j;0}^{(2),g}(r) \right],
\tag{42}
$$

where the flux moments $\xi_{1,j;0}^{(2),g m_2}(r)$ and $\xi_{2,j;0}^{(2),g}(r)$ are defined as follows:

$$
\xi_{1,j;0}^{(2),g}(r) \triangleq \int_{4\pi} d\mathbf{\Omega}\, \psi_{1,j}^{(2),g}(r,\mathbf{\Omega}),
\tag{43}
$$

$$
\xi_{2,j;0}^{(2),g}(r) \triangleq \int_{4\pi} d\mathbf{\Omega}\, \psi_{2,j}^{(2),g}(r,\mathbf{\Omega}).
\tag{44}
$$

Further contributions stem from Equation (177) in [5] in conjunction with the relations $\frac{\partial^2 L}{\partial f_j \partial t_{m_2}} \frac{\partial t_{m_2}}{\partial f_{m_2}} = \frac{\partial^2 L}{\partial f_j \partial f_{m_2}}$ and $\frac{\partial \Sigma_t^g}{\partial t_{m_2}} \frac{\partial t_{m_2}}{\partial f_{m_2}} = \frac{\partial \Sigma_t^g}{\partial f_{m_2}}$, as follows:

$$
\begin{aligned}
\left(\frac{\partial^2 L}{\partial f_j \partial f_{m_2}} \right)^{(4)} &= - \sum_{g=1}^{G} \int_V dV \int_{4\pi} d\mathbf{\Omega} \left[u_{1,j}^{(2),g}(r,\mathbf{\Omega}) \psi^{(1),g}(r,\mathbf{\Omega}) + u_{2,j}^{(2),g}(r,\mathbf{\Omega}) \varphi^g(r,\mathbf{\Omega}) \right] \frac{\partial \Sigma_t^g}{\partial f_{m_2}}, \\
& \quad for\ \ j = 1,\dots, J_{\sigma f};\ \ m_2 = 1,\dots, J_{\sigma f}.
\end{aligned}
\tag{45}
$$

Inserting the results obtained in Equation (37) into Equation (45) reduces the latter to the following expression:

$$
\left(\frac{\partial^2 L}{\partial f_j \partial f_{m_2}} \right)^{(4)} = -N_{i_{m_2}, m_{m_2}} \int_V dV \int_{4\pi} d\mathbf{\Omega} \left[u_{1,j}^{(2),g m_2}(r,\mathbf{\Omega}) \psi^{(1),g m_2}(r,\mathbf{\Omega}) + u_{2,j}^{(2),g m_2}(r,\mathbf{\Omega}) \varphi^{g m_2}(r,\mathbf{\Omega}) \right],
\tag{46}
$$

Collecting the partial contributions obtained in Equations (26), (38), (42) and (46), yields the following result:

$$
\begin{aligned}
\left(\frac{\partial^2 L}{\partial f_j \partial f_{m_2}} \right)_{(f=\sigma_f, f=\sigma_f)} &= \sum_{i=1}^{4} \left(\frac{\partial^2 L}{\partial f_j \partial f_{m_2}} \right)^{(i)} \\
&= N_{i_{m_2}, m_{m_2}} \nu_{i_{m_2}}^{g m_2} \int_V dV \left[u_{1,j;0}^{(2),g m_2}(r) \sum_{g'=1}^{G} \chi^{g'} \xi_0^{(1),g'}(r) + \varphi_0^{g m_2}(r) \sum_{g=1}^{G} \chi^g U_{2,j;0}^{(2),g}(r) \right] \\
&- N_{i_{m_2}, m_{m_2}} \int_V dV \int_{4\pi} d\mathbf{\Omega} \left[\psi_{1,j}^{(2),g m_2}(r,\mathbf{\Omega}) \psi^{(1),g m_2}(r,\mathbf{\Omega}) + \psi_{2,j}^{(2),g m_2}(r,\mathbf{\Omega}) \varphi^{g m_2}(r,\mathbf{\Omega}) \right] \\
&+ N_{i_{m_2}, m_{m_2}} \nu_{i_{m_2}}^{g m_2} \int_V dV \left[\xi_{1,j;0}^{(2),g m_2}(r) \sum_{g'=1}^{G} \chi^{g'} \xi_0^{(1),g'}(r) + \varphi_0^{g m_2}(r) \sum_{g=1}^{G} \chi^g \xi_{2,j;0}^{(2),g}(r) \right] \\
&- N_{i_{m_2}, m_{m_2}} \int_V dV \int_{4\pi} d\mathbf{\Omega} \left[u_{1,j}^{(2),g m_2}(r,\mathbf{\Omega}) \psi^{(1),g m_2}(r,\mathbf{\Omega}) + u_{2,j}^{(2),g m_2}(r,\mathbf{\Omega}) \varphi^{g m_2}(r,\mathbf{\Omega}) \right], \\
& \quad for\ \ j = 1,\dots, J_{\sigma f};\ m_2 = 1,\dots, J_{\sigma f}.
\end{aligned}
\tag{47}
$$

2.3. Numerical Results for $\partial^2 L(\boldsymbol{\alpha})/\partial\boldsymbol{\sigma}_f\partial\boldsymbol{\sigma}_f$

The 2nd-order absolute sensitivities of the leakage response with respect to the fission cross sections, i.e., $\partial^2 L/\partial\sigma_{f,i}^g\partial\sigma_{f,k}^{g'}$, $i,k = 1,\ldots,N_f$; $g,g' = 1,\ldots,G$, for the $N_f = 2$ fissionable isotopes and $G = 30$ energy groups of the PERP benchmark are computed using Equation (47). The (Hessian) matrix $\partial^2 L/\partial f_j\partial f_{m_2}$, $j = 1,\ldots,J_{\sigma f}$; $m_2 = 1,\ldots,J_{\sigma f}$ of 2nd-order absolute sensitivities has dimensions $J_{\sigma f} \times J_{\sigma f} (= 60 \times 60)$, since $J_{\sigma f} = G \times N_f = 30 \times 2$. For convenient comparisons, the numerical results presented in this section are presented in unit-less values of the relative sensitivities that correspond to $\partial^2 L/\partial f_j\partial f_{m_2}$, $j = 1,\ldots,J_{\sigma f}$; $m_2 = 1,\ldots,J_{\sigma f}$, which are denoted as $\mathbf{S}^{(2)}\left(\sigma_{f,i}^g,\sigma_{f,k}^{g'}\right)$ and are defined as follows:

$$\mathbf{S}^{(2)}\left(\sigma_{f,i}^g,\sigma_{f,k}^{g'}\right) \triangleq \frac{\partial^2 L}{\partial\sigma_{f,i}^g\partial\sigma_{f,k}^{g'}}\left(\frac{\sigma_{f,i}^g\sigma_{f,k}^{g'}}{L}\right), \quad i,k = 1,2; \ g,g' = 1,\ldots,30. \tag{48}$$

The numerical results obtained for the matrix $\mathbf{S}^{(2)}\left(\sigma_{f,i}^g,\sigma_{f,k}^{g'}\right)$, $i,k = 1,2$; $g,g' = 1,\ldots,30$, have been partitioned into $N_f \times N_f = 4$ submatrices, each of dimensions $G \times G(= 30 \times 30)$; the summary of the main features of each submatrix is presented in Table 1. The results for the submatrices are presented in the following form: when a submatrix comprises elements with relative sensitivities with absolute values greater than 1.0, the total number of such elements are counted and shown in the table. Otherwise, if the relative sensitivities of all elements of a submatrix have values lying in the interval $(-1.0, 1.0)$, only the element having the largest absolute value in the submatrix is listed in Table 1, together with the phase-space coordinates of that element. The submatrix $\mathbf{S}^{(2)}\left(\sigma_{f,1}^g,\sigma_{f,1}^{g'}\right)$ in Table 1 comprises components with absolute values greater than 1.0; it will therefore be discussed in detail in subsequent sub-sections of this section.

Table 1. Summary presentation of the matrix $\mathbf{S}^{(2)}\left(\sigma_{f,i}^g,\sigma_{f,k}^{g'}\right)$, $i,k = 1,2$; $g,g' = 1,\ldots,30$.

Isotopes	$k = 1$ (^{239}Pu)	$k = 2$ (^{240}Pu)
$i = 1$ (^{239}Pu)	$\mathbf{S}^{(2)}\left(\sigma_{f,1}^g,\sigma_{f,1}^{g'}\right)$ 11 elements with absolute values > 1.0	$\mathbf{S}^{(2)}\left(\sigma_{f,1}^g,\sigma_{f,2}^{g'}\right)$ Max. value = 6.97×10^{-2} at $g = 12$, $g' = 12$
$i = 2$ (^{240}Pu)	$\mathbf{S}^{(2)}\left(\sigma_{f,2}^g,\sigma_{f,1}^{g'}\right)$ Max. value = 6.97×10^{-2} at $g = 12$, $g' = 12$	$\mathbf{S}^{(2)}\left(\sigma_{f,2}^g,\sigma_{f,2}^{g'}\right)$ Max. value = 3.60×10^{-3} at $g = 12$, $g' = 12$

The 2nd-order mixed sensitivities $\partial^2 L(\boldsymbol{\alpha})/\partial\boldsymbol{\sigma}_f\partial\boldsymbol{\sigma}_f$ are mostly positive. Among all the $J_{\sigma f} \times J_{\sigma f} (= 60 \times 60)$ elements in the matrix $\mathbf{S}^{(2)}\left(\sigma_{f,i}^g,\sigma_{f,k}^{g'}\right)$, $i,k = 1,2$; $g,g' = 1,\ldots,30$, a total of 3508 out of 3600 elements have positive values, and most of them are very small, as indicated in Table 1. However, among all the $J_{\sigma f} \times J_{\sigma f} (= 60 \times 60)$ elements, 11 of them have very large relative sensitivities, with values greater than 1.0, as noted in the table. All of these larger sensitivities reside in the sub-matrix $\mathbf{S}^{(2)}\left(\sigma_{f,1}^g,\sigma_{f,1}^{g'}\right)$, and relate to the fission cross sections in isotope ^{239}Pu. The overall maximum relative sensitivity is $S^{(2)}\left(\sigma_{f,1}^{12},\sigma_{f,1}^{12}\right) = 1.348$. Additional details about the sub-matrix $\mathbf{S}^{(2)}\left(\sigma_{f,1}^g,\sigma_{f,1}^{g'}\right)$ are provided in the following section. Also noted in Table 1 are the results that all of the mixed 2nd-order relative sensitivities involving the fission cross sections of isotope ^{240}Pu (i.e., $\sigma_{f,2}^g$) have absolute values smaller than 1.0. The elements with the maximum absolute value in each of the respective submatrices relate to the fission cross sections for the 12th energy group of isotopes ^{239}Pu and ^{240}Pu.

2.3.1. Second-Order Unmixed Relative Sensitivities $S^{(2)}\left(\sigma_{f,i}^g, \sigma_{f,i}^g\right), i = 1, 2; g = 1, \ldots, 30$

The 2nd-order unmixed sensitivities $S^{(2)}\left(\sigma_{f,i}^g, \sigma_{f,i}^g\right) \triangleq \left(\partial^2 L/\partial \sigma_{f,i}^g \partial \sigma_{f,i}^g\right)\left(\sigma_{f,i}^g \sigma_{f,i}^g / L\right)$, $i = 1, 2$, $g = 1, \ldots, 30$, which are the elements on the diagonal of the matrix $\mathbf{S}^{(2)}\left(\sigma_{f,i}^g, \sigma_{f,k}^{g'}\right)$, $i, k = 1, 2$; $g, g' = 1, \ldots, 30$, can be directly compared to the values of the 1st-order relative sensitivities $S^{(1)}\left(\sigma_{f,i}^g\right) \triangleq \left(\partial L/\partial \sigma_{f,i}^g\right)\left(\sigma_{f,i}^g / L\right)$, $i = 1, 2$; $g = 1, \ldots, 30$, for the leakage response with respect to the fission cross section parameters. These comparisons are presented in Tables 2 and 3 for the two fissionable isotopes contained in the PERP benchmark. Table 2 compares the 1st-order to the 2nd-order relative sensitivities for isotope 1 (^{239}Pu). This comparison indicates that the values of the 2nd-order sensitivities are comparable to, and generally smaller than, the corresponding values of the 1st-order sensitivities for the same energy group, except for the 12th energy group, where the 2nd-order relative sensitivity is larger. The largest values (shown in bold in the table) for the 1st-order and 2nd-order relative sensitivities both related to the 12th energy group of isotope ^{239}Pu. It is noteworthy that all of the 1st-order relative sensitivities are positive, signifying that an increase in $\sigma_{f,1}^g$ will cause an increase in L.

Comparing the corresponding results in Table 2 in this work with Table 5 of Part I [1] and Table 6 of Part II [2] reveals that the absolute values of the 1st-order relative sensitivities with respect to the fission cross sections are significantly smaller than the corresponding 1st-order relative sensitivities with respect to the total cross sections, but they are approximately one order of magnitude larger than the corresponding 1st-order relative sensitivities with respect to the 0th-order self-scattering cross sections for isotope ^{239}Pu. Likewise, the absolute values of the 2nd-order unmixed relative sensitivities with respect to the fission cross sections are approximately 50–90% smaller than the corresponding 2nd-order unmixed relative sensitivities to the total cross sections, but they are approximately one to two orders of magnitudes larger than the corresponding 2nd-order unmixed relative sensitivities for the 0th-order self-scattering cross sections for isotope ^{239}Pu.

Table 2. Comparison of 1st-order relative sensitivities $\left(\partial L/\partial \sigma_{f,i=1}^g\right)\left(\sigma_{f,i=1}^g / L\right), g = 1, \ldots, 30$ and 2nd-order relative sensitivities $\left(\partial^2 L/\partial \sigma_{f,i=1}^g \partial \sigma_{f,k=1}^g\right)\left(\sigma_{f,1}^g \sigma_{f,1}^g / L\right)$, $g = 1, \ldots, 30$, for isotope 1 (^{239}Pu).

g	1st-Order	2nd-Order	g	1st-Order	2nd-Order
1	0.00039	−0.00016	16	0.197	−0.001
2	0.00080	−0.00033	17	0.075	−0.023
3	0.00231	−0.00091	18	0.042	−0.018
4	0.011	−0.0038	19	0.036	−0.019
5	0.050	−0.014	20	0.036	−0.025
6	0.129	−0.008	21	0.033	−0.031
7	0.585	0.559	22	0.029	−0.029
8	0.489	0.353	23	0.025	−0.029
9	0.589	0.536	24	0.024	−0.019
10	0.612	0.580	25	0.020	−0.025
11	0.569	0.487	26	0.019	−0.024
12	**0.882**	**1.348**	27	0.017	−0.011
13	0.611	0.584	28	0.010	−0.003
14	0.393	0.188	29	0.014	−0.016
15	0.222	0.023	30	0.131	−0.153

Table 3. Comparison of 1st-order relative sensitivities $\left(\partial L/\partial\sigma^g_{f,i=2}\right)\left(\sigma^g_{f,i=2}/L\right), g = 1,\ldots,30$ and 2nd-order relative sensitivities $\left(\partial^2 L/\partial\sigma^g_{f,i=2}\partial\sigma^g_{f,k=2}\right)\left(\sigma^g_{f,i=2}\sigma^g_{f,k=2}/L\right), g = 1,\ldots,30,$ for isotope 2 (^{240}Pu).

g	1st-Order	2nd-Order	g	1st-Order	2nd-Order
1	2.642×10^{-5}	-6.237×10^{-7}	16	6.361×10^{-4}	-5.532×10^{-9}
2	4.790×10^{-5}	-1.173×10^{-6}	17	2.769×10^{-4}	-3.154×10^{-7}
3	1.350×10^{-4}	-3.098×10^{-6}	18	1.399×10^{-4}	-1.919×10^{-7}
4	6.524×10^{-4}	-1.461×10^{-5}	19	7.740×10^{-5}	-8.545×10^{-8}
5	3.138×10^{-3}	-5.479×10^{-5}	20	1.254×10^{-4}	-3.111×10^{-7}
6	7.612×10^{-3}	-3.207×10^{-5}	21	6.055×10^{-5}	-1.048×10^{-7}
7	3.300×10^{-2}	1.771×10^{-3}	22	5.724×10^{-6}	-1.080×10^{-9}
8	2.796×10^{-2}	1.150×10^{-3}	23	3.435×10^{-6}	-5.246×10^{-10}
9	3.210×10^{-2}	1.584×10^{-3}	24	9.157×10^{-7}	-2.867×10^{-11}
10	3.229×10^{-2}	1.600×10^{-3}	25	2.862×10^{-6}	-4.747×10^{-10}
11	2.868×10^{-2}	1.226×10^{-3}	26	4.661×10^{-8}	-1.384×10^{-13}
12	4.568×10^{-2}	3.602×10^{-3}	27	5.471×10^{-6}	-1.214×10^{-9}
13	1.904×10^{-2}	5.649×10^{-4}	28	7.800×10^{-6}	-2.129×10^{-9}
14	3.365×10^{-3}	1.359×10^{-5}	29	1.965×10^{-8}	-3.219×10^{-14}
15	8.900×10^{-4}	3.629×10^{-7}	30	7.126×10^{-7}	-4.394×10^{-12}

Table 3 presents the results for the 1st-order and 2nd-order unmixed relative sensitivities for isotope 2 (^{240}Pu). These results show that the values for both the 1st- and 2nd-order relative sensitivities are all very small, and the absolute values of the 2nd-order unmixed relative sensitivities are at least one order of magnitude smaller than the corresponding values of the 1st-order ones for all energy groups. The largest 1st-order relative sensitivity is $S^{(1)}\left(\sigma^{12}_{f,i=2}\right) = 4.568 \times 10^{-2}$, and the largest 2nd-order unmixed relative sensitivity is $S^{(2)}\left(\sigma^{12}_{f,i=2}, \sigma^{12}_{f,k=2}\right) = 3.602 \times 10^{-3}$; both occur for the 12th energy group of the fission cross section of ^{240}Pu.

2.3.2. Second-Order Relative Sensitivities $\mathbf{S}^{(2)}\left(\sigma^g_{f,i=1}, \sigma^{g'}_{f,k=1}\right), g, g' = 1,\ldots,30$

Figure 1 depicts the 2nd-order mixed relative sensitivity results obtained for $\mathbf{S}^{(2)}\left(\sigma^g_{f,i=1}, \sigma^{g'}_{f,k=1}\right) \triangleq \left(\partial^2 L/\partial\sigma^g_{f,i=1}\partial\sigma^{g'}_{f,k=1}\right)\left(\sigma^g_{f,i=1}\sigma^{g'}_{f,k=1}/L\right), g, g' = 1,\ldots,30,$ for the leakage response with respect to the fission cross sections of ^{239}Pu. This matrix is symmetrical with respect to its principal diagonal. As shown in Figure 1, the largest 2nd-order relative sensitivities are concentrated in the energy region confined by the energy groups $g = 7,\ldots,14$ and $g' = 7,\ldots,14$. The numerical values of these elements are presented in Table 4. Shown in bold in this Table are 11 sensitivities, all involving the 12th energy group of the fission cross sections $\sigma^{g=12}_{f,i=1}$ or $\sigma^{g'=12}_{f,k=1}$ of ^{239}Pu, which have values greater than 1.0. The largest value among these sensitivities is attained by the relative 2nd-order unmixed sensitivity $S^{(2)}\left(\sigma^{g=12}_{f,i=1}, \sigma^{g'=12}_{f,k=1}\right) = 1.348$. Figure 1 also shows that the majority (877 out of 900) of the elements of $\mathbf{S}^{(2)}\left(\sigma^g_{f,i=1}, \sigma^{g'}_{f,k=1}\right)$ have positive 2nd-order relative sensitivities. The remaining 23 elements are located mostly on the diagonal of $\mathbf{S}^{(2)}\left(\sigma^g_{f,i=1}, \sigma^{g'}_{f,k=1}\right)$ and have negative values, as presented in Table 2, above.
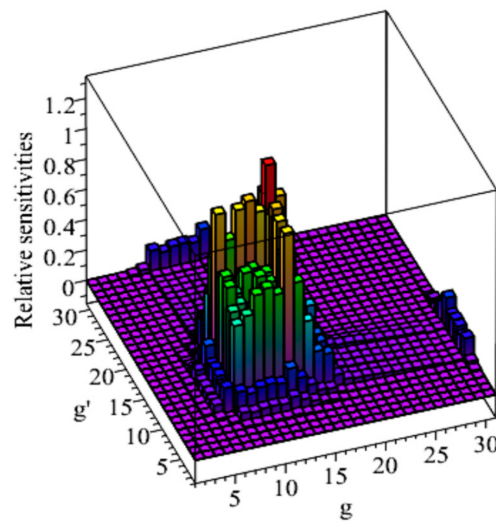
Figure 1. The matrix of sensitivities $\mathbf{S}^{(2)}\left(\sigma_{f,i=1}^{g}, \sigma_{f,k=1}^{g'}\right)$, $g, g' = 1, \ldots, 30$, for ^{239}Pu.

Table 4. Components of $\mathbf{S}^{(2)}\left(\sigma_{f,i=1}^{g}, \sigma_{f,k=1}^{g'}\right)$, $g, g' = 1, \ldots, 30$ having values greater than 1.0.

Groups	$g' = 6$	7	8	9	10	11	12	13	14
$g = 6$	−0.008	0.163	0.136	0.163	0.170	0.158	0.244	0.169	0.109
7	0.163	0.558	0.609	0.732	0.762	0.707	**1.095**	0.758	0.488
8	0.136	0.609	0.353	0.607	0.633	0.589	0.911	0.631	0.406
9	0.163	0.732	0.607	0.536	0.758	0.707	**1.095**	0.757	0.487
10	0.170	0.762	0.633	0.758	0.580	0.732	**1.137**	0.787	0.506
11	0.158	0.707	0.589	0.707	0.732	0.487	**1.054**	0.731	0.470
12	0.244	**1.095**	0.911	**1.095**	**1.137**	**1.054**	**1.348**	**1.130**	0.728
13	0.169	0.758	0.631	0.757	0.787	0.731	**1.130**	0.584	0.502
14	0.109	0.488	0.406	0.487	0.506	0.470	0.728	0.502	0.188

3. Mixed Second-Order Sensitivities of the PERP Total Leakage Response with Respect to the Parameters Underlying the Benchmark's Fission and Total Cross Sections

This Section presents the computation and analysis of the numerical results for the 2nd-order mixed sensitivities $\partial^2 L(\boldsymbol{\alpha}) / \partial \boldsymbol{\sigma}_f \partial \boldsymbol{\sigma}_t$, of the leakage response with respect to the group-averaged fission and total microscopic cross sections of all isotopes of the PERP benchmark. As has been shown by Cacuci [5], these mixed sensitivities can be computed using two distinct expressions, involving distinct 2nd-level adjoint systems and corresponding adjoint functions, by considering either the computation of $\partial^2 L(\boldsymbol{\alpha}) / \partial \boldsymbol{\sigma}_f \partial \boldsymbol{\sigma}_t$ or the computation of $\partial^2 L(\boldsymbol{\alpha}) / \partial \boldsymbol{\sigma}_t \partial \boldsymbol{\sigma}_f$. These two distinct paths for computing the 2nd-order sensitivities with respect to group-averaged fission and total microscopic cross sections will be presented in Section 3.1 and, respectively, Section 3.2. The end results produced by these two distinct paths must be identical to one another, thus providing a mutual "solution verification" that the respective computations were performed correctly. Moreover, the computational time for these two distinct paths can be much different, and one of them provides the best computational speed, as will be further illustrated by the numerical results presented in Section 3.3.

3.1. Computing the Second-Order Sensitivities $\partial^2 L(\boldsymbol{\alpha}) / \partial \boldsymbol{\sigma}_f \partial \boldsymbol{\sigma}_t$

The equations needed for deriving the expression of the 2nd-order sensitivities $\partial^2 L(\boldsymbol{\alpha}) / \partial \boldsymbol{\sigma}_f \partial \boldsymbol{\sigma}_t$ are obtained by particularizing Equations (158) and (177) in [5] to the PERP benchmark and adding

their respective contributions. The expression obtained by particularizing Equation (177) in [5] takes on the following form:

$$
\left(\frac{\partial^2 L}{\partial f_j \partial t_{m_2}}\right)^{(1)} = -\sum_{g=1}^{G} \int_V dV \int_{4\pi} d\Omega \left[u_{1,j}^{(2),g}(r,\Omega)\psi^{(1),g}(r,\Omega) + u_{2,j}^{(2),g}(r,\Omega)\varphi^g(r,\Omega)\right]\frac{\partial \Sigma_t^g}{\partial t_{m_2}},
$$
$$
for \ \ j = 1,\ldots,J_{\sigma f}; \ \ m_2 = 1,\ldots,J_{\sigma t}. \tag{49}
$$

The parameters f_j and t_{m_2} in Equation (49) correspond to the fission cross sections and total cross sections, and are therefore denoted as $f_j \equiv \sigma_{f,i_j}^{g_j}$ and $t_{m_2} \equiv \sigma_{t,i_{m_2}}^{g_{m_2}}$, respectively. Noting that

$$
\frac{\partial \Sigma_t^g}{\partial t_{m_2}} = \frac{\partial \Sigma_t^g}{\partial \sigma_{t,i_{m_2}}^{g_{m_2}}} = \frac{\partial \left(\sum_{m=1}^{M}\sum_{i=1}^{I} N_{i,m}\sigma_{t,i}^g\right)}{\partial \sigma_{t,i_{m_2}}^{g_{m_2}}} = \delta_{g_{m_2}g}N_{i_{m_2},m_{m_2}}, \tag{50}
$$

and inserting the result obtained in Equation (50) into Equation (49), yields:

$$
\left(\frac{\partial^2 L}{\partial f_j \partial t_{m_2}}\right)^{(1)} = -N_{i_{m_2},m_{m_2}}\int_V dV \int_{4\pi} d\Omega \left[u_{1,j}^{(2),g_{m_2}}(r,\Omega)\psi^{(1),g_{m_2}}(r,\Omega) + u_{2,j}^{(2),g_{m_2}}(r,\Omega)\varphi^{g_{m_2}}(r,\Omega)\right],
$$
$$
for \ \ j = 1,\ldots,J_{\sigma f}; \ \ m_2 = 1,\ldots,J_{\sigma t}. \tag{51}
$$

The contributions stemming from Equation (158) in [5], in conjunction with the relations $\frac{\partial^2 L}{\partial t_j \partial t_{m_2}}\frac{\partial t_j}{\partial f_j} = \frac{\partial^2 L}{\partial f_j \partial t_{m_2}}$ and $\frac{\partial^2 \Sigma_t^g}{\partial t_j \partial t_{m_2}}\frac{\partial t_j}{\partial f_j} = \frac{\partial^2 \Sigma_t^g}{\partial f_j \partial t_{m_2}}$, yields the following expression:

$$
\left(\frac{\partial^2 L}{\partial f_j \partial t_{m_2}}\right)^{(2)} = -\sum_{g=1}^{G} \int_V dV \int_{4\pi} d\Omega \, \psi^{(1),g}(r,\Omega)\varphi^g(r,\Omega)\frac{\partial^2 \Sigma_t^g}{\partial f_j \partial t_{m_2}}
$$
$$
-\sum_{g=1}^{G} \int_V dV \int_{4\pi} d\Omega \left[\psi_{1,j}^{(2),g}(r,\Omega)\psi^{(1),g}(r,\Omega) + \psi_{2,j}^{(2),g}(r,\Omega)\varphi^g(r,\Omega)\right]\frac{\partial \Sigma_t^g}{\partial t_{m_2}}, \tag{52}
$$
$$
for \ j = 1,\ldots,J_{\sigma f}, \ \ m_2 = 1,\ldots,J_{\sigma t},
$$

where the adjoint functions $\psi_{1,j}^{(2),g}(r,\Omega)$ and $\psi_{2,j}^{(2),g}(r,\Omega), j = 1,\ldots,J_{\sigma f}; g = 1,\ldots,G$ are the solutions of the 2nd-Level Adjoint Sensitivity System (2nd-LASS) as presented in Equations (33), (35), (39)and (40). Noting that

$$
\frac{\partial^2 \Sigma_t^g}{\partial f_j \partial t_{m_2}} = \frac{\partial^2 \Sigma_t^g}{\partial \sigma_{f,i_j}^{g_j} \partial \sigma_{t,i_{m_2}}^{g_{m_2}}} = 0, \tag{53}
$$

and inserting the results obtained in Equations (53) and (50) into Equation (52), yields:

$$
\left(\frac{\partial^2 L}{\partial f_j \partial t_{m_2}}\right)^{(2)} = -N_{i_{m_2},m_{m_2}}\int_V dV \int_{4\pi} d\Omega \left[\psi_{1,j}^{(2),g_{m_2}}(r,\Omega)\psi^{(1),g_{m_2}}(r,\Omega) + \psi_{2,j}^{(2),g_{m_2}}(r,\Omega)\varphi^{g_{m_2}}(r,\Omega)\right],
$$
$$
for \ j = 1,\ldots,J_{\sigma f}, \ \ m_2 = 1,\ldots,J_{\sigma t}. \tag{54}
$$

Combining the partial contributions obtained in Equations (51) and (54), yields the following result:

$$
\left(\frac{\partial^2 L}{\partial f_j \partial t_{m_2}}\right)_{(f=\sigma_f, t=\sigma_t)} = \left(\frac{\partial^2 L}{\partial f_j \partial t_{m_2}}\right)^{(1)} + \left(\frac{\partial^2 L}{\partial f_j \partial t_{m_2}}\right)^{(2)}
$$
$$
= -N_{i_{m_2},m_{m_2}}\int_V dV \int_{4\pi} d\Omega \left[\psi_{1,j}^{(2),g_{m_2}}(r,\Omega)\psi^{(1),g_{m_2}}(r,\Omega) + \psi_{2,j}^{(2),g_{m_2}}(r,\Omega)\varphi^{g_{m_2}}(r,\Omega)\right]
$$
$$
-N_{i_{m_2},m_{m_2}}\int_V dV \int_{4\pi} d\Omega \left[u_{1,j}^{(2),g_{m_2}}(r,\Omega)\psi^{(1),g_{m_2}}(r,\Omega) + u_{2,j}^{(2),g_{m_2}}(r,\Omega)\varphi^{g_{m_2}}(r,\Omega)\right], \tag{55}
$$
$$
for \ j = 1,\ldots,J_{\sigma f}; m_2 = 1,\ldots,J_{\sigma t}.
$$

3.2. Alternative Path: Computing the Second-Order Sensitivities $\partial^2 L(\boldsymbol{\alpha})/\partial\boldsymbol{\sigma}_t\partial\boldsymbol{\sigma}_f$

As mentioned earlier, the mixed 2nd-order sensitivities $\partial^2 L(\boldsymbol{\alpha})/\partial\boldsymbol{\sigma}_f\partial\boldsymbol{\sigma}_t$ can also be computed using the alternative expression for $\partial^2 L(\boldsymbol{\alpha})/\partial\boldsymbol{\sigma}_t\partial\boldsymbol{\sigma}_f$. The equations needed for deriving the expression for $\partial^2 L(\boldsymbol{\alpha})/\partial\boldsymbol{\sigma}_t\partial\boldsymbol{\sigma}_f$ are obtained by particularizing Equations (158) and (160) in [5] to the PERP benchmark, where Equation (160) provides the direct contributions to the mixed sensitivities $\partial^2 L(\boldsymbol{\alpha})/\partial\boldsymbol{\sigma}_t\partial\boldsymbol{\sigma}_f$, while Equation (158) provides contributions to these sensitivities arising indirectly from the total cross sections. The expression obtained by particularizing Equation (160) in [5] takes the following form:

$$
\left(\frac{\partial^2 L}{\partial t_j \partial f_{m_2}}\right)^{(1)} = \sum_{g=1}^{G} \int_V dV \int_{4\pi} d\boldsymbol{\Omega}\, \psi_{1,j}^{(2),g}(r,\boldsymbol{\Omega}) \frac{\partial\left[(\nu\Sigma_f)^g\right]}{\partial f_{m_2}} \sum_{g'=1}^{G} \int_{4\pi} d\boldsymbol{\Omega'} \chi^{g'} \psi^{(1),g'}(r,\boldsymbol{\Omega'})
$$
$$
+ \sum_{g=1}^{G} \int_V dV \int_{4\pi} d\boldsymbol{\Omega}\, \psi_{2,j}^{(2),g}(r,\boldsymbol{\Omega}) \sum_{g'=1}^{G} \int_{4\pi} d\boldsymbol{\Omega'} \varphi^{g'}(r,\boldsymbol{\Omega'}) \chi^g \frac{\partial\left[(\nu\Sigma_f)^{g'}\right]}{\partial f_{m_2}}, \tag{56}
$$
$$
\text{for } j = 1,\dots,J_{\sigma t}; \quad m_2 = 1,\dots,J_{\sigma f},
$$

where the adjoint functions $\psi_{1,j}^{(2),g}(r,\boldsymbol{\Omega})$ and $\psi_{2,j}^{(2),g}(r,\boldsymbol{\Omega})$, $j=1,\dots,J_{\sigma t}$; $g=1,\dots,G$ are the solutions of the 2nd-Level Adjoint Sensitivity System (2nd-LASS) presented in Equations (32), (34), (39) and (40) of Part I [1], which are reproduced below for convenient reference:

$$
B^g\!\left(\boldsymbol{\alpha}^0\right)\psi_{1,j}^{(2),g}(r,\boldsymbol{\Omega}) = -\delta_{g_j g} N_{i_j,m_j}\varphi^g(r,\boldsymbol{\Omega}), \ \ j=1,\dots,J_{\sigma t}; \ \ g=1,\dots,G, \tag{57}
$$

$$
\psi_{1,j}^{(2),g}(r_d,\boldsymbol{\Omega}) = 0, \ \boldsymbol{\Omega}\cdot\mathbf{n} < 0; \ j=1,\dots,J_{\sigma t}; \ g=1,\dots,G, \tag{58}
$$

$$
A^{(1),g}\!\left(\boldsymbol{\alpha}^0\right)\psi_{2,j}^{(2),g}(r,\boldsymbol{\Omega}) = -\delta_{g_j g} N_{i_j,m_j}\psi^{(1),g}(r,\boldsymbol{\Omega}), \ \ j=1,\dots,J_{\sigma t}; \ \ g=1,\dots,G, \tag{59}
$$

$$
\psi_{2,j}^{(2),g}(r_d,\boldsymbol{\Omega}) = 0, \ \boldsymbol{\Omega}\cdot\mathbf{n} > 0; \ j=1,\dots,J_{\sigma t}; \ g=1,\dots,G. \tag{60}
$$

The parameters t_j and f_{m_2} in Equation (56) correspond to the total cross sections and fission cross sections, and are therefore denoted as $t_j \equiv \sigma_{t,i_j}^{g_j}$ and $f_{m_2} \equiv \sigma_{f,i_{m_2}}^{g_{m_2}}$, respectively. Inserting the results obtained in Equations (23) and (24) into Equation (56), yields:

$$
\left(\frac{\partial^2 L}{\partial t_j \partial f_{m_2}}\right)^{(1)} = N_{i_{m_2},m_{m_2}} \nu_{i_{m_2}}^{g_{m_2}} \int_V dV \left[\xi_{1,j;0}^{(2),g_{m_2}}(r) \sum_{g'=1}^{G} \chi^{g'} \xi_0^{(1),g'}(r) + \varphi_0^{g_{m_2}}(r) \sum_{g=1}^{G} \chi^g \xi_{2,j;0}^{(2),g}(r) \right], \tag{61}
$$
$$
\text{for } j = 1,\dots,J_{\sigma t}; \quad m_2 = 1,\dots,J_{\sigma f}.
$$

The contributions stemming from Equation (158) in [5], in conjunction with the relations $\frac{\partial^2 L}{\partial t_j \partial t_{m_2}}\frac{\partial t_{m_2}}{\partial f_{m_2}} = \frac{\partial^2 L}{\partial t_j \partial f_{m_2}}$, $\frac{\partial^2 \Sigma_t^g}{\partial t_j \partial t_{m_2}}\frac{\partial t_{m_2}}{\partial f_{m_2}} = \frac{\partial^2 \Sigma_t^g}{\partial t_j \partial f_{m_2}}$ and $\frac{\partial \Sigma_t^g}{\partial t_{m_2}}\frac{\partial t_{m_2}}{\partial f_{m_2}} = \frac{\partial \Sigma_t^g}{\partial f_{m_2}}$, yields:

$$
\left(\frac{\partial^2 L}{\partial t_j \partial f_{m_2}}\right)^{(2)} = -\sum_{g=1}^{G} \int_V dV \int_{4\pi} d\boldsymbol{\Omega}\, \psi^{(1),g}(r,\boldsymbol{\Omega}) \varphi^g(r,\boldsymbol{\Omega}) \frac{\partial^2 \Sigma_t^g}{\partial t_j \partial f_{m_2}}
$$
$$
- \sum_{g=1}^{G} \int_V dV \int_{4\pi} d\boldsymbol{\Omega} \left[\psi_{1,j}^{(2),g}(r,\boldsymbol{\Omega}) \psi^{(1),g}(r,\boldsymbol{\Omega}) + \psi_{2,j}^{(2),g}(r,\boldsymbol{\Omega}) \varphi^g(r,\boldsymbol{\Omega}) \right] \frac{\partial \Sigma_t^g}{\partial f_{m_2}}, \tag{62}
$$
$$
\text{for } j = 1,\dots,J_{\sigma t}, \quad m_2 = 1,\dots,J_{\sigma f}.
$$

Noting that

$$
\frac{\partial^2 \Sigma_t^g}{\partial t_j \partial f_{m_2}} = \frac{\partial^2 \Sigma_t^g}{\partial \sigma_{t,i_j}^{g_j} \partial \sigma_{f,i_{m_2}}^{g_{m_2}}} = 0, \tag{63}
$$

and inserting the results obtained in Equations (37) and (63) into Equation (62), yields:

$$
\left(\frac{\partial^2 L}{\partial t_j \partial f_{m_2}}\right)^{(2)} = -N_{i_{m_2}, m_{m_2}} \int_V dV \int_{4\pi} d\Omega \left[\psi_{1,j}^{(2),g_{m_2}}(r,\Omega)\psi^{(1),g_{m_2}}(r,\Omega) + \psi_{2,j}^{(2),g_{m_2}}(r,\Omega)\varphi^{g_{m_2}}(r,\Omega)\right], \quad (64)
$$
$$
for \ j = 1,\ldots,J_{\sigma t}, \ m_2 = 1,\ldots,J_{\sigma f}.
$$

Adding Equations (61) and (64), yields the following result:

$$
\left(\frac{\partial^2 L}{\partial t_j \partial f_{m_2}}\right)_{(t=\sigma_t, f=\sigma_f)} = \left(\frac{\partial^2 L}{\partial t_j \partial f_{m_2}}\right)^{(1)} + \left(\frac{\partial^2 L}{\partial t_j \partial f_{m_2}}\right)^{(2)}
$$
$$
= -N_{i_{m_2}, m_{m_2}} \int_V dV \int_{4\pi} d\Omega \left[\psi_{1,j}^{(2),g_{m_2}}(r,\Omega)\psi^{(1),g_{m_2}}(r,\Omega) + \psi_{2,j}^{(2),g_{m_2}}(r,\Omega)\varphi^{g_{m_2}}(r,\Omega)\right]
$$
$$
+N_{i_{m_2}, m_{m_2}} v_{i_{m_2}}^{g_{m_2}} \int_V dV \left[\xi_{1,j;0}^{(2),g_{m_2}}(r)\sum_{g'=1}^{G}\chi^{g'}\xi_0^{(1),g'}(r) + \varphi_0^{g_{m_2}}(r)\sum_{g=1}^{G}\chi^g\xi_{2,j;0}^{(2),g}(r)\right], \quad (65)
$$
$$
for \ j = 1,\ldots,J_{\sigma t}; m_2 = 1,\ldots,J_{\sigma f}
$$

3.3. Numerical Results for $\partial^2 L(\boldsymbol{\alpha})/\partial\boldsymbol{\sigma}_f\partial\boldsymbol{\sigma}_t$

The second-order absolute sensitivities, $\partial^2 L(\boldsymbol{\alpha})/\partial\boldsymbol{\sigma}_f\partial\boldsymbol{\sigma}_t$, of the leakage response with respect to the fission cross sections and the total cross sections for all isotopes of the PERP benchmark have been computed using Equation (55), and have been independently verified by computing $\partial^2 L(\boldsymbol{\alpha})/\partial\boldsymbol{\sigma}_t\partial\boldsymbol{\sigma}_f$ using Equation (65). Regarding the computational requirements: Computing $\partial^2 L(\boldsymbol{\alpha})/\partial\boldsymbol{\sigma}_f\partial\boldsymbol{\sigma}_t$ needs $J_{\sigma f} = G \times N_f = 30 \times 2 = 60$ forward and adjoint PARTISN transport computations for obtaining the adjoint functions $u_{1,j}^{(2),g}(r,\Omega)$ and $u_{2,j}^{(2),g}(r,\Omega), j = 1,\ldots,J_{\sigma f}; g = 1,\ldots,G$, together with additional $J_{\sigma f} = 60$ forward and adjoint PARTISN computations for obtaining the adjoint functions $\psi_{1,j}^{(2),g}(r,\Omega)$ and $\psi_{2,j}^{(2),g}(r,\Omega), j = 1,\ldots,J_{\sigma f}; g = 1,\ldots,G$. Thus, a total of 120 forward and adjoint PARTISN computations are required to obtain all the adjoint functions needed in Equation (55). In contradistinction, computing $\partial^2 L(\boldsymbol{\alpha})/\partial\boldsymbol{\sigma}_t\partial\boldsymbol{\sigma}_f$ would require $J_{\sigma t} = G \times I = 30 \times 6 = 360$ forward and adjoint PARTISN computations for obtaining the adjoint functions $\psi_{1,j}^{(2),g}(r,\Omega)$ and $\psi_{2,j}^{(2),g}(r,\Omega), j = 1,\ldots,J_{\sigma t}; g = 1,\ldots,G$ that are needed in Equation (65). It is thus evident that computing $\partial^2 L(\boldsymbol{\alpha})/\partial\boldsymbol{\sigma}_f\partial\boldsymbol{\sigma}_t$ using Equation (55) is 3 times more efficient than computing $\partial^2 L(\boldsymbol{\alpha})/\partial\boldsymbol{\sigma}_t\partial\boldsymbol{\sigma}_f$ using Equation (65).

The matrix $\partial^2 L/\partial f_j \partial t_{m_2}, j = 1,\ldots,J_{\sigma f}; m_2 = 1,\ldots,J_{\sigma f}$ has dimensions $J_{\sigma f} \times J_{\sigma t} (= 60 \times 180)$; corresponding to this matrix is the matrix denoted as $\mathbf{S}^{(2)}\left(\sigma_{f,i}^g, \sigma_{t,k}^{g'}\right)$ of 2nd-order relative sensitivities, which is defined as follows:

$$
\mathbf{S}^{(2)}\left(\sigma_{f,i}^g, \sigma_{t,k}^{g'}\right) \triangleq \frac{\partial^2 L}{\partial\sigma_{f,i}^g\partial\sigma_{t,k}^{g'}}\left(\frac{\partial\sigma_{f,i}^g\partial\sigma_{t,k}^{g'}}{L}\right), \ i = 1,2; k = 1,\ldots,6; \ g, g' = 1,\ldots,30. \quad (66)
$$

To facilitate the presentation and interpretation of the numerical results, the $J_{\sigma f} \times J_{\sigma t} (= 60 \times 180)$ matrix $\mathbf{S}^{(2)}\left(\sigma_{f,i}^g, \sigma_{t,k}^{g'}\right)$ has been partitioned into $N_f \times I = 2 \times 6$ submatrices, each of dimensions $G \times G = 30 \times 30$. The summary of the main features of each of these submatrices is presented in Table 5.

Table 5. Summary presentation of the matrix $\mathbf{S}^{(2)}\left(\sigma_{f,i}^{g}, \sigma_{t,k}^{g'}\right)$.

Isotopes	k=1 (^{239}Pu)	k=2 (^{240}Pu)	k=3 (^{69}Ga)	k=4 (^{71}Ga)	k=5 (C)	k=6 (^{1}H)
$i = 1$ (^{239}Pu)	$\mathbf{S}^{(2)}\left(\sigma_{f,1}^{g}, \sigma_{t,1}^{g'}\right)$ 35 elements with absolute values > 1.0	$\mathbf{S}^{(2)}\left(\sigma_{f,1}^{g}, \sigma_{t,2}^{g'}\right)$ Min. value = -1.67×10^{-1} at $g = 12$, $g' = 12$	$\mathbf{S}^{(2)}\left(\sigma_{f,1}^{g}, \sigma_{t,3}^{g'}\right)$ Min. value = -7.48×10^{-3} at $g = 12$, $g' = 12$	$\mathbf{S}^{(2)}\left(\sigma_{f,1}^{g}, \sigma_{t,4}^{g'}\right)$ Min. value = -5.08×10^{-3} at $g = 12$, $g' = 12$	$\mathbf{S}^{(2)}\left(\sigma_{f,1}^{g}, \sigma_{t,5}^{g'}\right)$ 1 element with absolute value > 1.0	$\mathbf{S}^{(2)}\left(\sigma_{f,1}^{g}, \sigma_{t,6}^{g'}\right)$ 48 elements with absolute values > 1.0
$i = 2$ (^{240}Pu)	$\mathbf{S}^{(2)}\left(\sigma_{f,2}^{g}, \sigma_{t,1}^{g'}\right)$ Min. value = -1.36×10^{-1} at $g = 12$, $g' = 12$	$\mathbf{S}^{(2)}\left(\sigma_{f,2}^{g}, \sigma_{t,2}^{g'}\right)$ Min. value = -8.62×10^{-3} at $g = 12$, $g' = 12$	$\mathbf{S}^{(2)}\left(\sigma_{f,2}^{g}, \sigma_{t,3}^{g'}\right)$ Min. value = -3.87×10^{-4} at $g = 12$, $g' = 12$	$\mathbf{S}^{(2)}\left(\sigma_{f,2}^{g}, \sigma_{t,4}^{g'}\right)$ Min. value = -2.63×10^{-4} at $g = 12$, $g' = 12$	$\mathbf{S}^{(2)}\left(\sigma_{f,2}^{g}, \sigma_{t,5}^{g'}\right)$ Min. value = -6.04×10^{-2} at $g = 12$, $g' = 30$	$\mathbf{S}^{(2)}\left(\sigma_{f,2}^{g}, \sigma_{t,6}^{g'}\right)$ Min. value = -7.21×10^{-1} at $g = 12$, $g' = 30$

Most of the values of the $J_{\sigma f} \times J_{\sigma t}$ ($= 10,800$) elements in the matrix $\mathbf{S}^{(2)}\left(\sigma_{f,i}^{g}, \sigma_{t,k}^{g'}\right)$, $i = 1, 2$; $k = 1, \ldots, 6$; $g, g' = 1, \ldots, 30$ are very small, and 10,704 elements out of 10,800 elements have negative values. The results in Table 5 indicate that, when the 2nd-order mixed relative sensitivities involve the fission cross sections of the isotope ^{240}Pu or the total cross sections of isotopes ^{240}Pu, ^{69}Ga and ^{71}Ga, their absolute values are all smaller than 1.0, and the element with the most negative value in each of the submatrices always relates to the fission cross sections for the 12th energy group and the total cross sections for either the 12th energy group or the 30th energy group of the isotopes. There are 84 elements with large relative sensitivities, having values greater than 1.0, as indicated in Table 5. Those large sensitivities reside in the submatrices $\mathbf{S}^{(2)}\left(\sigma_{f,1}^{g}, \sigma_{t,1}^{g'}\right)$, $\mathbf{S}^{(2)}\left(\sigma_{f,1}^{g}, \sigma_{t,5}^{g'}\right)$ and $\mathbf{S}^{(2)}\left(\sigma_{f,1}^{g}, \sigma_{t,6}^{g'}\right)$, respectively. All of these 84 large sensitivities involve the fission cross sections of isotope ^{239}Pu, and the total cross sections of isotopes ^{239}Pu, C and ^{1}H. Of the sensitivities summarized in Table 5, the single largest relative value is $S^{(2)}\left(\sigma_{f,1}^{12}, \sigma_{t,6}^{30}\right) = -13.92$.

3.3.1. Second-Order Relative Sensitivities $\mathbf{S}^{(2)}\left(\sigma_{f,1}^{g}, \sigma_{t,1}^{g'}\right)$, $g, g' = 1, \ldots, 30$

The results obtained for the 2nd-order mixed relative sensitivity of the leakage response with respect to the fission microscopic cross sections of ^{239}Pu and to the total microscopic cross sections of ^{239}Pu, denoted as $\mathbf{S}^{(2)}\left(\sigma_{f,i=1}^{g}, \sigma_{t,k=1}^{g'}\right) \triangleq \left(\partial^2 L / \partial\sigma_{f,i=1}^{g} \partial\sigma_{t,k=1}^{g'}\right)\left(\sigma_{f,i=1}^{g} \sigma_{t,k=1}^{g'} / L\right)$, $g, g' = 1, \ldots, 30$, are summarized in Table 6 and depicted in Figure 2. Almost all, namely 894 out of 900, elements in this submatrix have negative 2nd-order relative sensitivities; only 6 elements have small positive values. As shown in Figure 2, there are some large 2nd-order mixed relative sensitivities concentrated in the energy region confined by the energy groups $g = 7, \ldots, 14$ and $g' = 7, \ldots, 16$. The actual numerical values of these large elements are presented in Table 6, which comprises 35 elements having values greater than 1.0, as shown in bold in this table. The largest absolute value in this submatrix is attained by the relative 2nd-order mixed sensitivity $S^{(2)}\left(\sigma_{f,i=1}^{g=12}, \sigma_{t,k=1}^{g'=12}\right) = -2.630$, which involves the 12th energy group for both the fission and total cross sections of isotope ^{239}Pu.

Table 6. Components of $\mathbf{S}^{(2)}\left(\sigma_{f,1}^{g}, \sigma_{t,1}^{g'}\right)$, $g, g' = 1, \ldots, 30$ having values greater than 1.0.

Groups	$g' = 6$	7	8	9	10	11	12	13	14	15	16
$g = 6$	−0.091	−0.199	−0.183	−0.213	−0.213	−0.195	−0.332	−0.291	−0.241	−0.176	−0.200
7	−0.159	**−1.189**	−0.821	−0.955	−0.958	−0.876	**−1.488**	**−1.302**	**−1.080**	−0.787	−0.895
8	−0.131	−0.758	−0.921	−0.790	−0.796	−0.729	**−1.238**	**−1.083**	−0.898	−0.654	−0.743
9	−0.157	−0.908	−0.844	**−1.229**	−0.953	−0.876	**−1.487**	**−1.302**	**−1.079**	−0.786	−0.893
10	−0.164	−0.941	−0.868	**−1.015**	**−1.263**	−0.906	**−1.546**	**−1.352**	**−1.121**	−0.816	−0.927
11	−0.152	−0.875	−0.804	−0.935	−0.946	**−1.086**	**−1.431**	**−1.257**	**−1.041**	−0.758	−0.861
12	−0.236	**−1.361**	**−1.250**	**−1.452**	**−1.455**	**−1.342**	**−2.630**	**−1.941**	**−1.611**	**−1.174**	**−1.331**
13	−0.164	−0.946	−0.870	**−1.010**	**−1.013**	−0.926	**−1.588**	**−1.685**	**−1.110**	−0.811	−0.919
14	−0.105	−0.610	−0.562	−0.653	−0.654	−0.599	**−1.021**	−0.905	−0.981	−0.516	−0.592
15	−0.059	−0.345	−0.318	−0.369	−0.370	−0.339	−0.577	−0.510	−0.434	−0.464	−0.325
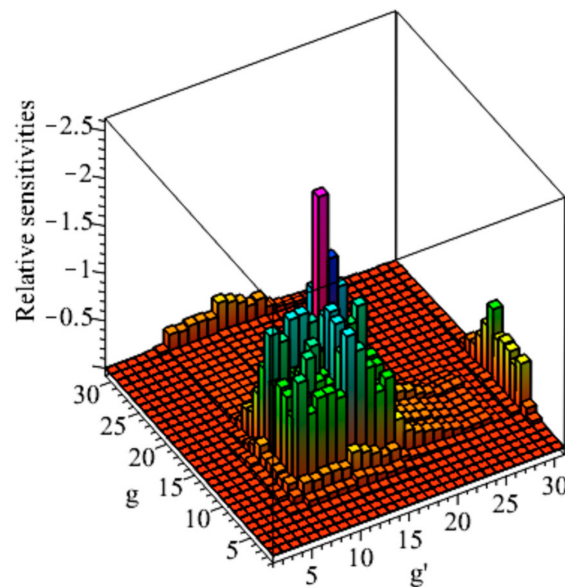
Figure 2. The matrix of sensitivities $\mathbf{S}^{(2)}\left(\sigma_{f,i=1}^{g}, \sigma_{t,k=1}^{g'}\right)$, $g, g' = 1, \ldots, 30$ for ^{239}Pu.

The absolute values of the mixed sensitivities in row $g = 12$ are the largest among all $g = 1, \ldots, 30$ rows, including rows not presented in Table 6. In other words, the absolute value of mixed relative sensitivities involving the fission cross section parameter $\sigma_{f,i=1}^{g=12}$ are always the largest among all groups $g = 1, \ldots, 30$. Similarly, the values of the mixed sensitivities in group $g' = 12$ are the most negative among all groups $g' = 1, \ldots, 30$, with one exception for the sensitivity value located in groups $g = 13$ and $g' = 12$ which is less negative than the value located in groups $g = 13$ and $g' = 13$.

3.3.2. Second-Order Relative Sensitivities $\mathbf{S}^{(2)}\left(\sigma_{f,1}^{g}, \sigma_{t,5}^{g'}\right)$, $g, g' = 1, \ldots, 30$

The matrix $\mathbf{S}^{(2)}\left(\sigma_{f,i=1}^{g}, \sigma_{t,k=5}^{g'}\right) \triangleq \left(\partial^2 L / \partial \sigma_{f,i=1}^{g} \partial \sigma_{t,k=5}^{g'}\right)\left(\sigma_{f,i=1}^{g} \sigma_{t,k=5}^{g'} / L\right)$, comprising the 2nd-order sensitivities of the leakage response with respect to the fission cross sections of isotope 1 (^{239}Pu) and the total cross sections of isotope 5 (C), contains a single large element that has an absolute value greater than 1.0, namely $S^{(2)}\left(\sigma_{f,1}^{12}, \sigma_{t,5}^{30}\right) = -1.167$.

3.3.3. Second-Order Relative Sensitivities $\mathbf{S}^{(2)}\left(\sigma_{f,1}^{g}, \sigma_{t,6}^{g'}\right)$, $g, g' = 1, \ldots, 30$

The submatrix $\mathbf{S}^{(2)}\left(\sigma_{f,i=1}^{g}, \sigma_{t,k=6}^{g'}\right) \triangleq \left(\partial^2 L / \partial \sigma_{f,i=1}^{g} \partial \sigma_{t,k=6}^{g'}\right)\left(\sigma_{f,i=1}^{g} \sigma_{t,k=6}^{g'} / L\right)$, comprising the 2nd-order relative sensitivities of the leakage response with respect to the fission microscopic cross sections of isotope 1 (^{239}Pu) and the total microscopic cross sections of isotope 6 (^{1}H), is illustrated in Figure 3. The submatrix $\mathbf{S}^{(2)}\left(\sigma_{f,1}^{g}, \sigma_{t,6}^{g'}\right)$, $g, g' = 1, \ldots, 30$ includes 48 elements that have absolute values greater than 1.0, as specified, in bold, in Table 7; 35 out of these 48 elements are located in the energy phase-space confined by the energy groups $g = 7, \ldots, 13$ and $g' = 16, \ldots, 25$. The other 13 elements are located in energy groups $g = 6, \ldots, 30$ and $g' = 30$. The largest negative value is displayed by the 2nd-order relative sensitivity of the leakage response with respect to the 12th energy group of the fission cross section for ^{239}Pu and the 30th energy group of the total cross section for ^{1}H, namely $S^{(2)}\left(\sigma_{f,1}^{12}, \sigma_{t,6}^{30}\right) = -13.92$.
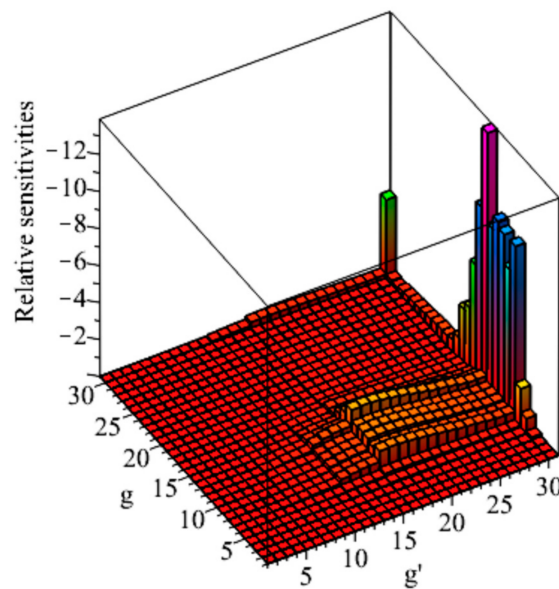
Figure 3. The matrix of sensitivities $\mathbf{S}^{(2)}\left(\sigma_{f,i=1}^{g}, \sigma_{t,k=6}^{g'}\right)$, $g, g' = 1, \ldots, 30$.

Table 7. Elements of $\mathbf{S}^{(2)}\left(\sigma_{f,i=1}^{g}, \sigma_{t,k=6}^{g'}\right)$, $g, g' = 1, \ldots, 30$, having absolute values greater than 1.0.

Groups	$g' = 15$	16	17	18	19	20	21	22	29	30
$g = 5$	−0.048	−0.099	−0.102	−0.100	−0.096	−0.091	−0.085	−0.078	−0.048	−0.833
6	−0.123	−0.252	−0.258	−0.253	−0.244	−0.231	−0.217	−0.199	−0.122	**−2.114**
7	−0.550	**−1.128**	**−1.157**	**−1.135**	**−1.093**	**−1.034**	**−0.972**	−0.892	−0.548	**−9.472**
8	−0.457	−0.936	−0.960	−0.942	−0.907	−0.858	−0.806	−0.740	−0.455	**−7.859**
9	−0.548	**−1.124**	**−1.152**	**−1.130**	**−1.088**	**−1.030**	−0.967	−0.888	−0.546	**−9.431**
10	−0.568	**−1.164**	**−1.193**	**−1.170**	**−1.127**	**−1.067**	**−1.002**	−0.920	−0.565	**−9.768**
11	−0.525	**−1.077**	**−1.104**	**−1.083**	**−1.042**	−0.987	−0.927	−0.851	−0.523	**−9.038**
12	−0.809	**−1.658**	**−1.699**	**−1.667**	**−1.605**	**−1.519**	**−1.427**	**−1.311**	−0.805	**−13.92**
13	−0.555	**−1.137**	**−1.165**	**−1.143**	**−1.100**	**−1.042**	−0.979	−0.899	−0.552	**−9.549**
14	−0.351	−0.725	−0.742	−0.728	−0.701	−0.664	−0.623	−0.573	−0.352	**−6.087**
15	−0.197	−0.404	−0.415	−0.407	−0.392	−0.371	−0.348	−0.320	−0.197	**−3.405**
16	−0.200	−0.382	−0.365	−0.359	−0.345	−0.327	−0.307	−0.282	−0.174	**−3.010**
17	−0.081	−0.169	−0.170	−0.136	−0.131	−0.124	−0.117	−0.107	−0.067	**−1.151**
18	−0.049	−0.103	−0.109	−0.112	−0.075	−0.071	−0.067	−0.062	−0.038	−0.665

As shown in Table 7, the values of the 2nd-order mixed sensitivities involving the fission cross section parameter $\sigma_{f,i=1}^{g=12}$, in energy group $g = 12$, are the most negative among all energy groups $g = 1, \ldots, 30$. In addition to the sensitivities presented in Table 7, the following 2nd-order mixed relative sensitivities of the leakage response with respect to the fission microscopic cross sections of ^{239}Pu and the total microscopic cross sections of ^{1}H have absolute values greater than 1.0: $S^{(2)}\left(\sigma_{f,1}^{12}, \sigma_{t,6}^{23}\right) = -1.213$, $S^{(2)}\left(\sigma_{f,1}^{12}, \sigma_{t,6}^{24}\right) = -1.098$, $S^{(2)}\left(\sigma_{f,1}^{12}, \sigma_{t,6}^{25}\right) = -1.042$ and $S^{(2)}\left(\sigma_{f,1}^{30}, \sigma_{t,6}^{30}\right) = -4.258$.

4. Mixed Second-Order Sensitivities of the PERP Total Leakage Response with Respect to the Parameters Underlying the Benchmark's Fission and Scattering Cross Sections

This Section presents the computation and analysis of the numerical results for the 2nd-order mixed sensitivities $\partial^2 L(\boldsymbol{\alpha}) / \partial \boldsymbol{\sigma}_f \partial \boldsymbol{\sigma}_s$, of the leakage response with respect to the group-averaged fission and scattering microscopic cross sections of all isotopes of the PERP benchmark. Similarly, the 2nd-order mixed sensitivities $\partial^2 L(\boldsymbol{\alpha}) / \partial \boldsymbol{\sigma}_f \partial \boldsymbol{\sigma}_s$ can also be computed using the alternative expressions for $\partial^2 L(\boldsymbol{\alpha}) / \partial \boldsymbol{\sigma}_s \partial \boldsymbol{\sigma}_f$. These two distinct paths for computing the 2nd-order sensitivities with respect to group-averaged fission and scattering microscopic cross sections will be presented in Section 4.1 and, respectively, Section 4.2 as follows. As will be discussed in detail in Section 4.3, below, the pathway for computing $\partial^2 L(\boldsymbol{\alpha}) / \partial \boldsymbol{\sigma}_f \partial \boldsymbol{\sigma}_s$ turns out to be 60 times more efficient than the pathway for computing $\partial^2 L(\boldsymbol{\alpha}) / \partial \boldsymbol{\sigma}_s \partial \boldsymbol{\sigma}_f$.

4.1. Computing the Second-Order Sensitivities $\partial^2 L(\boldsymbol{\alpha}) / \partial \boldsymbol{\sigma}_f \partial \boldsymbol{\sigma}_s$

The equations needed for deriving the expressions of the 2nd-order sensitivities $\partial^2 L / \partial f_j \partial s_{m_2}$, $j = 1, \ldots, J_{\sigma f}; m_2 = 1, \ldots, J_{\sigma s}$ will differ from each other depending on whether the parameter s_{m_2} corresponds to the 0th-order ($l = 0$) scattering cross sections or to the higher-order ($l \geq 1$) scattering cross sections, since, as shown in Equation (A3) of Appendix A, the 0th-order scattering cross sections contribute to the total cross sections, while the higher-order ones do not. Therefore, the zeroth order scattering cross sections must be considered separately from the higher order scattering cross sections. As described in [1] and Appendix A, the total number of zeroth-order ($l = 0$) scattering cross section comprise in $\boldsymbol{\sigma}_s$ is denoted as $J_{\sigma s, l=0}$, where $J_{\sigma s, l=0} = G \times G \times I$; and the total number of higher order (i.e., $l \geq 1$) scattering cross sections comprised in $\boldsymbol{\sigma}_s$ is denoted as $J_{\sigma s, l \geq 1}$, where $J_{\sigma s, l \geq 1} = G \times G \times I \times ISCT$, with $J_{\sigma s, l=0} + J_{\sigma s, l \geq 1} = J_{\sigma s}$. There are two distinct cases, as follows:

(1) $\left(\frac{\partial^2 L}{\partial f_j \partial s_{m_2}}\right)_{(f = \sigma_f, s = \sigma_{s, l=0})}$, $j = 1, \ldots, J_{\sigma f}$; $m_2 = 1, \ldots, J_{\sigma s, l=0}$, where the quantities f_j refer to the parameters underlying the fission microscopic cross sections, while the quantities s_{m_2} refer to the parameters underlying the 0th-order scattering microscopic cross sections; and

(2) $\left(\frac{\partial^2 L}{\partial f_j \partial s_{m_2}}\right)_{(f = \sigma_f, s = \sigma_{s, l \geq 1})}$, $j = 1, \ldots, J_{\sigma f}$; $m_2 = 1, \ldots, \sigma_{s, l \geq 1}$, where the quantities f_j refer to the parameters underlying the fission microscopic cross sections, and the quantities s_{m_2} refer to the parameters underlying the lth-order ($l \geq 1$) scattering microscopic cross sections.

4.1.1. Second-Order Sensitivities $\left(\frac{\partial^2 L}{\partial f_j \partial s_{m_2}}\right)_{(f = \sigma_f, s = \sigma_{s, l=0})}$

The equations needed for deriving the expression of the 2nd-order mixed sensitivities $\left(\frac{\partial^2 L}{\partial f_j \partial s_{m_2}}\right)_{(f = \sigma_f, s = \sigma_{s, l=0})}$ are obtained by particularizing Equations (158), (159), (177) and (178) in [5] to the PERP benchmark, where Equation (178) provides the contributions arising directly form the respective fission and scattering cross sections, while Equations (158), (159) and (177) provide contributions arising indirectly through the total cross sections, since both the fission cross sections

and the 0th-order scattering cross sections are part of the total cross sections. The expression obtained by particularizing Equation (178) in [5] to the PERP benchmark yields:

$$
\begin{aligned}
\left(\frac{\partial^2 L}{\partial f_j \partial s_{m_2}}\right)^{(1)}_{(f=\sigma_f, s=\sigma_{s,l=0})} &= \sum_{g=1}^{G} \int_V dV \int_{4\pi} d\mathbf{\Omega}\, u_{1,j}^{(2),g}(r,\mathbf{\Omega}) \sum_{g'=1}^{G} \int_{4\pi} d\mathbf{\Omega}'\, \psi^{(1),g'}(r,\mathbf{\Omega}') \frac{\partial \Sigma_s^{g\to g'}(s;\mathbf{\Omega}\to\mathbf{\Omega}')}{\partial s_{m_2}} \\
&+ \sum_{g=1}^{G} \int_V dV \int_{4\pi} d\mathbf{\Omega}\, u_{2,j}^{(2),g}(r,\mathbf{\Omega}) \sum_{g'=1}^{G} \int_{4\pi} d\mathbf{\Omega}'\, \varphi^{g'}(r,\mathbf{\Omega}') \frac{\partial \Sigma_s^{g'\to g}(s;\mathbf{\Omega}'\to\mathbf{\Omega})}{\partial s_{m_2}},
\end{aligned}
\tag{67}
$$

$$
\text{for } j=1,\dots,J_{\sigma f}; m_2=1,\dots,J_{\sigma s,l=0}.
$$

In Equation (67), the parameters indexed by f_j correspond to the fission cross sections, which means that $f_j \equiv \sigma_{f,i_j}^{g_j}$, while the parameters indexed by s_{m_2} correspond to the 0th-order scattering cross sections, so that $s_{m_2} \equiv \sigma_{s,l_{m_2}=0,i_{m_2}}^{g'_{m_2}\to g_{m_2}}$, where the subscripts i_{m_2}, l_{m_2}, g'_{m_2} and g_{m_2} refer to the isotope, order of Legendre expansion, and energy groups associated with the parameter s_{m_2}, respectively. Noting that

$$
\begin{aligned}
\frac{\partial \Sigma_s^{g\to g'}(s;\mathbf{\Omega}\to\mathbf{\Omega}')}{\partial s_{m_2}} &= \frac{\partial \Sigma_s^{g\to g'}(s;\mathbf{\Omega}\to\mathbf{\Omega}')}{\partial \sigma_{s,l_{m_2},i_{m_2}}^{g'_{m_2}\to g_{m_2}}} = \frac{\partial \left[\sum\limits_{m=1}^{M}\sum\limits_{i=1}^{I} N_{i,m}\sigma_{s,i}^{g\to g'}(s;\mathbf{\Omega}\to\mathbf{\Omega}')\right]}{\partial \sigma_{s,l_{m_2},i_{m_2}}^{g'_{m_2}\to g_{m_2}}} \\
&= \frac{\partial \left[\sum\limits_{m=1}^{M}\sum\limits_{i=1}^{I}\sum\limits_{l=0}^{ISCT} N_{i,m}(2l+1)\sigma_{s,l,i}^{g\to g'}P_l(\mathbf{\Omega}'\cdot\mathbf{\sigma})\right]}{\partial \sigma_{s,l_{m_2},i_{m_2}}^{g'_{m_2}\to g_{m_2}}} = \delta_{g'_{m_2}g}\delta_{g_{m_2}g'}N_{i_{m_2},m_{m_2}}(2l_{m_2}+1)P_{l_{m_2}}(\mathbf{\Omega}'\cdot\mathbf{\Omega}),
\end{aligned}
\tag{68}
$$

$$
\frac{\partial \Sigma_s^{g'\to g}(s;\mathbf{\Omega}'\to\mathbf{\Omega})}{\partial s_{m_2}} = \frac{\partial \Sigma_s^{g'\to g}(s;\mathbf{\Omega}'\to\mathbf{\Omega})}{\partial \sigma_{s,l_{m_2},i_{m_2}}^{g'_{m_2}\to g_{m_2}}} = \delta_{g_{m_2}g}\delta_{g'_{m_2}g'}N_{i_{m_2},m_{m_2}}(2l_{m_2}+1)P_{l_{m_2}}(\mathbf{\Omega}'\cdot\mathbf{\Omega}),
\tag{69}
$$

inserting the results obtained in Equations (68) and (69) into Equation (67), using the addition theorem for spherical harmonics in one-dimensional geometry, performing the respective angular integrations, and finally setting $l_{m_2}=0$ in the resulting expression yields the following simplified expression for Equation (67):

$$
\left(\frac{\partial^2 L}{\partial f_j \partial s_{m_2}}\right)^{(1)}_{(f=\sigma_f, s=\sigma_{s,l=0})} = N_{i_{m_2},m_{m_2}} \int_V dV \left[\xi_0^{(1),g_{m_2}}(r)U_{1,j;0}^{(2),g'_{m_2}}(r) + \varphi_0^{g'_{m_2}}(r)U_{2,j;0}^{(2),g_{m_2}}(r)\right],
\tag{70}
$$

where the 0th-order moments $\varphi_0^{g'_{m_2}}(r)$, $\xi_0^{(1),g_{m_2}}(r)$, $U_{1,j;0}^{(2),g'_{m_2}}(r)$ and $U_{2,j;0}^{(2),g_{m_2}}(r)$ have been defined previously in Equations (15), (16), (27) and (28), respectively.

Using Equation (158) in [5] in conjunction with the relations $\frac{\partial^2 L}{\partial t_j \partial t_{m_2}}\frac{\partial t_j}{\partial f_j}\frac{\partial t_{m_2}}{\partial s_{m_2}} = \frac{\partial^2 L}{\partial f_j \partial s_{m_2}}$, $\frac{\partial \Sigma_t^g}{\partial t_{m_2}}\frac{\partial t_{m_2}}{\partial s_{m_2}} = \frac{\partial \Sigma_t^g}{\partial s_{m_2}}$ and $\frac{\partial^2 \Sigma_t^g}{\partial t_j \partial t_{m_2}}\frac{\partial t_j}{\partial f_j}\frac{\partial t_{m_2}}{\partial s_{m_2}} = \frac{\partial^2 \Sigma_t^g}{\partial f_j \partial s_{m_2}}$ yields the following contributions:

$$
\begin{aligned}
\left(\frac{\partial^2 L}{\partial f_j \partial s_{m_2}}\right)^{(2)}_{(f=\sigma_f, s=\sigma_{s,l=0})} &= -\sum_{g=1}^{G} \int_V dV \int_{4\pi} d\mathbf{\Omega}\, \psi^{(1),g}(r,\mathbf{\Omega})\varphi^g(r,\mathbf{\Omega}) \frac{\partial^2 \Sigma_t^g}{\partial f_j \partial s_{m_2}} \\
&- \sum_{g=1}^{G} \int_V dV \int_{4\pi} d\mathbf{\Omega} \left[\psi_{1,j}^{(2),g}(r,\mathbf{\Omega})\psi^{(1),g}(r,\mathbf{\Omega}) + \psi_{2,j}^{(2),g}(r,\mathbf{\Omega})\varphi^g(r,\mathbf{\Omega})\right]\frac{\partial \Sigma_t^g}{\partial s_{m_2}},
\end{aligned}
\tag{71}
$$

$$
\text{for } j=1,\dots,J_{\sigma f}, \ m_2=1,\dots,J_{\sigma s,l=0},
$$

where the adjoint functions $\psi_{1,j}^{(2),g}(r,\mathbf{\Omega})$ and $\psi_{2,j}^{(2),g}(r,\mathbf{\Omega})$, $j=1,\dots,J_{\sigma f}$; $g=1,\dots,G$ are the solutions of the 2nd-Level Adjoint Sensitivity System (2nd-LASS) presented in Equations (33), (35), (39) and (40).

Noting that,

$$
\frac{\partial^2 \Sigma_t^g}{\partial f_j \partial s_{m_2}} = \frac{\partial^2 \Sigma_t^g}{\partial \sigma_{f,i_j}^{g_j}\partial \sigma_{s,l_{m_2},i_{m_2}}^{g'_{m_2}\to g_{m_2}}} = 0,
\tag{72}
$$

$$
\begin{aligned}
\frac{\partial \Sigma_t^g}{\partial s_{m_2}} &= \frac{\partial \left[\sum\limits_{m=1}^{M} \sum\limits_{i=1}^{I} N_{i,m} \sigma_{t,i}^g \right]}{\partial \sigma_{s,l m_2 = 0, i m_2}^{g' m_2 \to g m_2}} = \frac{\partial \left\{ \sum\limits_{m=1}^{M} \sum\limits_{i=1}^{I} N_{i,m} \left[\sigma_{f,i}^g + \sigma_{c,i}^g + \sum\limits_{g'=1}^{G} \sigma_{s,l=0,i}^{g \to g'} \right] \right\}}{\partial \sigma_{s,l m_2 = 0, i m_2}^{g' m_2 \to g m_2}} \\
&= \frac{\partial \left[\sum\limits_{m=1}^{M} \sum\limits_{i=1}^{I} \sum\limits_{g'=1}^{G} N_{i,m} \sigma_{s,l=0,i}^{g \to g'} \right]}{\partial \sigma_{s,l m_2 = 0, i m_2}^{g' m_2 \to g m_2}} = \delta_{g'_{m_2} g} N_{i_{m_2}, m_{m_2}},
\end{aligned}
\tag{73}
$$

and inserting the results obtained in Equations (72) and (73) into Equation (71), yields the following simplified expression for Equation (71):

$$
\begin{aligned}
&\left(\frac{\partial^2 L}{\partial f_j \partial s_{m_2}} \right)^{(2)}_{(f = \sigma_f, s = \sigma_{s,l=0})} \\
&= -N_{i_{m_2}, m_{m_2}} \int_V dV \int_{4\pi} d\Omega \left[\psi_{1,j}^{(2), g'_{m_2}}(r, \Omega) \psi^{(1), g'_{m_2}}(r, \Omega) + \psi_{2,j}^{(2), g'_{m_2}}(r, \Omega) \varphi^{g'_{m_2}}(r, \Omega) \right].
\end{aligned}
\tag{74}
$$

Additional contributions stem from Equation (159) in [5], which takes on the following particular form:

$$
\begin{aligned}
&\left(\frac{\partial^2 L}{\partial f_j \partial s_{m_2}} \right)^{(3)}_{(f = \sigma_f, s = \sigma_{s,l=0})} \\
&= \sum_{g=1}^{G} \int_V dV \int_{4\pi} d\Omega \, \psi_{1,j}^{(2), g}(r, \Omega) \sum_{g'=1}^{G} \int_{4\pi} d\Omega' \psi^{(1), g'}(r, \Omega') \frac{\partial \Sigma_s^{g \to g'}(s; \Omega \to \Omega')}{\partial s_{m_2}} \\
&+ \sum_{g=1}^{G} \int_V dV \int_{4\pi} d\Omega \, \psi_{2,j}^{(2), g}(r, \Omega) \sum_{g'=1}^{G} \int_{4\pi} d\Omega' \varphi^{g'}(r, \Omega') \frac{\partial \Sigma_s^{g' \to g}(s; \Omega' \to \Omega)}{\partial s_{m_2}}, \\
&\quad for \ j = 1, \dots, J_{\sigma f}; \ m_2 = 1, \dots, J_{\sigma s, l=0}.
\end{aligned}
\tag{75}
$$

Inserting the results obtained in Equations (68) and (69) into Equation (75), using the addition theorem for spherical harmonics in one-dimensional geometry and performing the respective angular integrations, and setting $l_{m_2} = 0$, yields the following simplified expression for Equation (75):

$$
\left(\frac{\partial^2 L}{\partial f_j \partial s_{m_2}} \right)^{(3)}_{(f = \sigma_f, s = \sigma_{s,l=0})} = N_{i_{m_2}, m_{m_2}} \int_V dV \left[\xi_0^{(1), g_{m_2}}(r) \xi_{1,j;0}^{(2), g'_{m_2}}(r) + \varphi_0^{g'_{m_2}}(r) \xi_{2,j;0}^{(2), g_{m_2}}(r) \right],
\tag{76}
$$

where the 0th-order moments $\xi_{1,j;0}^{(2), g'_{m_2}}(r)$ and $\xi_{2,j;0}^{(2), g_{m_2}}(r)$ have been defined previously in Equations (43) and (44), respectively.

Using Equation (177) in [5] in conjunction with the relation $\frac{\partial \Sigma_t^g}{\partial t_{m_2}} = \frac{\partial \Sigma_t^g}{\partial t_{m_2}} \frac{\partial t_{m_2}}{\partial s_{m_2}} = \frac{\partial \Sigma_t^g}{\partial s_{m_2}}$ yields the final set of contributions, namely:

$$
\begin{aligned}
&\left(\frac{\partial^2 L}{\partial f_j \partial s_{m_2}} \right)^{(4)}_{(f = \sigma_f, s = \sigma_{s,l=0})} \\
&= -\sum_{g=1}^{G} \int_V dV \int_{4\pi} d\Omega \left[u_{1,j}^{(2), g}(r, \Omega) \psi^{(1), g}(r, \Omega) + u_{2,j}^{(2), g}(r, \Omega) \varphi^g(r, \Omega) \right] \frac{\partial \Sigma_t^g}{\partial s_{m_2}}, \\
&\quad for \ j = 1, \dots, J_{\sigma f}; \ m_2 = 1, \dots, J_{\sigma s, l=0}.
\end{aligned}
\tag{77}
$$

Replacing the result obtained in Equation (73) into Equation (77) yields the following simplified expression:

$$
\begin{aligned}
&\left(\frac{\partial^2 L}{\partial f_j \partial s_{m_2}} \right)^{(4)}_{(f = \sigma_f, s = \sigma_{s,l=0})} \\
&= -N_{i_{m_2}, m_{m_2}} \int_V dV \int_{4\pi} d\Omega \left[u_{1,j}^{(2), g'_{m_2}}(r, \Omega) \psi^{(1), g'_{m_2}}(r, \Omega) + u_{2,j}^{(2), g'_{m_2}}(r, \Omega) \varphi^{g'_{m_2}}(r, \Omega) \right].
\end{aligned}
\tag{78}
$$

Collecting the partial contributions obtained in Equations (70), (74), (76) and (78), yields the following result:

$$
\begin{aligned}
\left(\frac{\partial^2 L}{\partial f_j \partial s_{m_2}}\right)_{(f=\sigma_f, s=\sigma_{s,l=0})} &= \sum_{i=1}^{4}\left(\frac{\partial^2 L}{\partial f_j \partial s_{m_2}}\right)^{(i)}_{(f=\sigma_f, s=\sigma_{s,l=0})} \\
&= N_{i_{m_2}, m_{m_2}}\Bigg\{\int_V dV \xi_0^{(1),g m_2}(r)\left[\xi_{1,j;0}^{(2),g' m_2}(r) + U_{1,j;0}^{(2),g' m_2}(r)\right] + \int_V dV \varphi_0^{g' m_2}(r)\left[\xi_{2,j;0}^{(2),g m_2}(r) + U_{2,j;0}^{(2),g m_2}(r)\right] \\
&\quad - \int_V dV \int_{4\pi} d\Omega\left[\psi_{1,j}^{(2),g' m_2}(r,\Omega)\psi^{(1),g' m_2}(r,\Omega) + \psi_{2,j}^{(2),g' m_2}(r,\Omega)\varphi^{g' m_2}(r,\Omega)\right] \\
&\quad - \int_V dV \int_{4\pi} d\Omega\left[u_{1,j}^{(2),g' m_2}(r,\Omega)\psi^{(1),g' m_2}(r,\Omega) + u_{2,j}^{(2),g' m_2}(r,\Omega)\varphi^{g' m_2}(r,\Omega)\right]\Bigg\}, \\
&\quad for\ j = 1,\ldots,J_{\sigma f}; m_2 = 1,\ldots,J_{\sigma s, l=0}.
\end{aligned}
\tag{79}
$$

4.1.2. Second-Order Sensitivities $\left(\frac{\partial^2 L}{\partial f_j \partial s_{m_2}}\right)_{(f=\sigma_f, s=\sigma_{s,l\geq 1})}$

For computing the 2nd-order sensitivities $\left(\frac{\partial^2 L}{\partial f_j \partial s_{m_2}}\right)_{(f=\sigma_f, s=\sigma_{s,l\geq 1})}$, the parameters $f_j \equiv \sigma_{f,i_j}^{g_j}$ correspond to the fission cross sections, and the parameters $s_{m_2} \equiv \sigma_{s,l_{m_2},i_{m_2}}^{g' m_2 \to g m_2}$ correspond to the lth-order ($l \geq 1$) scattering cross sections. In this case, only the fission cross sections contribute to the total cross sections, since the lth-order ($l \geq 1$) scattering cross sections are not comprised in the total cross sections. The expression of $\left(\frac{\partial^2 L}{\partial f_j \partial s_{m_2}}\right)_{(f=\sigma_f, s=\sigma_{s,l\geq 1})}$ is obtained by particularizing Equations (159) and (178) in [5] to the PERP benchmark, which yields,

$$
\begin{aligned}
&\left(\frac{\partial^2 L}{\partial f_j \partial s_{m_2}}\right)_{(f=\sigma_f, s=\sigma_{s,l\geq 1})} \\
&= \sum_{g=1}^{G} \int_V dV \int_{4\pi} d\Omega\, u_{1,j}^{(2),g}(r,\Omega) \times \sum_{g'=1}^{G} \int_{4\pi} d\Omega' \psi^{(1),g'}(r,\Omega') \frac{\partial \Sigma_s^{g \to g'}(s;\Omega \to \Omega')}{\partial s_{m_2}} \\
&+ \sum_{g=1}^{G} \int_V dV \int_{4\pi} d\Omega\, u_{2,j}^{(2),g}(r,\Omega) \sum_{g'=1}^{G} \int_{4\pi} d\Omega' \varphi^{g'}(r,\Omega') \frac{\partial \Sigma_s^{g' \to g}(s;\Omega' \to \Omega)}{\partial s_{m_2}} \\
&+ \sum_{g=1}^{G} \int_V dV \int_{4\pi} d\Omega\, \psi_{1,j}^{(2),g}(r,\Omega) \sum_{g'=1}^{G} \int_{4\pi} d\Omega' \psi^{(1),g'}(r,\Omega') \frac{\partial \Sigma_s^{g \to g'}(s;\Omega \to \Omega')}{\partial s_{m_2}} \\
&+ \sum_{g=1}^{G} \int_V dV \int_{4\pi} d\Omega\, \psi_{2,j}^{(2),g}(r,\Omega) \sum_{g'=1}^{G} \int_{4\pi} d\Omega' \varphi^{g'}(r,\Omega') \frac{\partial \Sigma_s^{g' \to g}(s;\Omega' \to \Omega)}{\partial s_{m_2}}, \\
&\quad for\ j = 1,\ldots,J_{\sigma f}; m_2 = 1,\ldots,J_{\sigma s, l\geq 1},
\end{aligned}
\tag{80}
$$

where the first two terms arise from Equation (178) while the last two terms arise from Equations (159). Inserting the results obtained in Equations (68) and (69) into Equation (80), using the addition theorem for spherical harmonics in one-dimensional geometry and performing the respective angular integrations, yields the following expression:

$$
\begin{aligned}
&\left(\frac{\partial^2 L}{\partial f_j \partial s_{m_2}}\right)_{(f=\sigma_f, s=\sigma_{s,l\geq 1})} = N_{i_{m_2}, m_{m_2}}(2l_{m_2} + 1)\Bigg\{\int_V dV \xi_{l_{m_2}}^{(1),g m_2}(r)\left[\xi_{1,j;l_{m_2}}^{(2),g' m_2}(r) + U_{1,j;l_{m_2}}^{(2),g' m_2}(r)\right] \\
&+ \int_V dV \varphi_{l_{m2}}^{g' m_2}(r)\left[\xi_{2,j;l_{m2}}^{(2),g m_2}(r) + U_{2,j;l_{m2}}^{(2),g m_2}(r)\right]\Bigg\},\ j = 1,\ldots,J_{\sigma f}; m_2 = 1,\ldots,J_{\sigma s, l\geq 1}; l_{m_2} = 1,\ldots,ISCT,
\end{aligned}
\tag{81}
$$

where the moments $\varphi_{l_{m2}}^{g' m_2}(r)$, $\xi_{l_{m2}}^{(1),g m_2}(r)$, $\xi_{1,j;l_{m2}}^{(2),g' m_2}(r)$, $\xi_{2,j;l_{m2}}^{(2),g m_2}(r)$, $U_{1,j;l_{m2}}^{(2),g' m_2}(r)$ and $U_{2,j;l_{m2}}^{(2),g m_2}(r)$ are defined as follows:

$$
\varphi_l^g(r) \triangleq \int_{4\pi} d\Omega\, P_l(\Omega)\varphi^g(r,\Omega'),
\tag{82}
$$

$$
\xi_l^{(1),g}(r) \triangleq \int_{4\pi} d\Omega\, P_l(\Omega)\psi^{(1),g}(r,\Omega'),
\tag{83}
$$

$$\xi_{1,j;l}^{(2),g}(r) \triangleq \int_{4\pi} d\mathbf{\Omega}\, P_l(\mathbf{\Omega})\psi_{1,j}^{(2),g}(r,\mathbf{\Omega}'), \tag{84}$$

$$\xi_{2,j;l}^{(2),g}(r) \triangleq \int_{4\pi} d\mathbf{\Omega}\, P_l(\mathbf{\Omega})\psi_{2,j}^{(2),g}(r,\mathbf{\Omega}'), \tag{85}$$

$$U_{1,j;l}^{(2),g}(r) \triangleq \int_{4\pi} d\mathbf{\Omega}\, P_l(\mathbf{\Omega})u_{1,j}^{(2),g}(r,\mathbf{\Omega}'), \tag{86}$$

$$U_{2,j;l}^{(2),g}(r) \triangleq \int_{4\pi} d\mathbf{\Omega}\, P_l(\mathbf{\Omega})u_{2,j}^{(2),g}(r,\mathbf{\Omega}'). \tag{87}$$

4.2. Alternative Path: Computing the Second-Order Sensitivities $\partial^2 L(\boldsymbol{\alpha})/\partial\boldsymbol{\sigma}_s\partial\boldsymbol{\sigma}_f$

The results to be computed using the expressions for $\partial^2 L(\boldsymbol{\alpha})/\partial\boldsymbol{\sigma}_f\partial\boldsymbol{\sigma}_s$ obtained in Equations (79) and (81) can be verified, because of the symmetry of the mixed 2nd-order sensitivities, by obtaining the expressions for $\partial^2 L(\boldsymbol{\alpha})/\partial\boldsymbol{\sigma}_s\partial\boldsymbol{\sigma}_f$, which also requires separate consideration of the zeroth-order scattering cross sections. The two cases involved are as follows:

(1) $\left(\frac{\partial^2 L}{\partial s_j \partial f_{m_2}}\right)_{(s=\sigma_{s,l=0},f=\sigma_f)}$, $j = 1,\ldots,J_{\sigma s,l=0}; m_2 = 1,\ldots,J_{\sigma f}$, where the quantities s_j refer to the parameters underlying the 0th-order scattering cross sections, while the quantities f_{m_2} refer to the parameters underlying the fission cross sections;

(2) $\left(\frac{\partial^2 L}{\partial s_j \partial f_{m_2}}\right)_{(s=\sigma_{s,l\geq1},f=\sigma_f)}$, $j = 1,\ldots,\sigma_{s,l\geq1}; m_2 = 1,\ldots,J_{\sigma f}$, where the quantities s_j refer to the parameters underlying the lth-order ($l \geq 1$) scattering cross sections, and the quantities f_{m_2} refer to the parameters underlying the fission cross sections.

4.2.1. Second-Order Sensitivities $\left(\frac{\partial^2 L}{\partial s_j \partial f_{m_2}}\right)_{(s=\sigma_{s,l=0},f=\sigma_f)}$

The equations needed for deriving the expression of the 2nd-order mixed sensitivities $\left(\frac{\partial^2 L}{\partial s_j \partial f_{m_2}}\right)_{(s=\sigma_{s,l=0},f=\sigma_f)}$ are obtained by particularizing Equations (158), (160), (167) and (169) in [5] to the PERP benchmark. The expression obtained by particularizing Equation (169) in [5] to the PERP benchmark is as follows:

$$\left(\frac{\partial^2 L}{\partial s_j \partial f_{m_2}}\right)_{(s=\sigma_{s,l=0},f=\sigma_f)}^{(1)} = \sum_{g=1}^{G} \int_V dV \int_{4\pi} d\mathbf{\Omega}\, \theta_{1,j}^{(2),g}(r,\mathbf{\Omega}')\frac{\partial\left[(v\Sigma_f)^g\right]}{\partial f_{m_2}} \sum_{g'=1}^{G} \int_{4\pi} d\mathbf{\Omega}'\chi^{g'}\psi^{(1),g'}(r,\mathbf{\Omega}')$$
$$+ \sum_{g=1}^{G} \int_V dV \int_{4\pi} d\mathbf{\Omega}\, \theta_{2,j}^{(2),g}(r,\mathbf{\Omega}') \sum_{g'=1}^{G} \int_{4\pi} d\mathbf{\Omega}'\varphi^{g'}(r,\mathbf{\Omega}')\chi^g\frac{\partial\left[(v\Sigma_f)^{g'}\right]}{\partial f_{m_2}}, \tag{88}$$
$$for \quad j = 1,\ldots,J_{\sigma s,l=0}; m_2 = 1,\ldots,J_{\sigma f}$$

where the 2nd-level adjoint functions, $\theta_{1,j}^{(2),g}(r,\mathbf{\Omega}')$ and $\theta_{2,j}^{(2),g}(r,\mathbf{\Omega}'), j = 1,\ldots,J_{\sigma s}; g = 1,\ldots,G$, are the solutions of the 2nd-Level Adjoint Sensitivity System (2nd-LASS) presented in Equations (46), (48), (51) and (52) of Part II [2], which are reproduced below for convenient reference:

$$B^g(\boldsymbol{\alpha}^0)\theta_{1,j}^{(2),g}(r,\mathbf{\Omega}) = \delta_{gjg}N_{i_j,m_j}(2l_j+1)P_{l_j}(\mathbf{\Omega})\phi_l^{g'_j}(r), \quad j = 1,\ldots,J_{\sigma s}; g = 1,\ldots,G; l = 0,\ldots,ISCT, \tag{89}$$

$$\theta_{1,j}^{(2),g}(r_d,\mathbf{\Omega}) = 0, \mathbf{\Omega}\cdot\mathbf{n} < 0; j = 1,\ldots,J_{\sigma s}; g = 1,\ldots,G. \tag{90}$$

$$A^{(1)g}(\boldsymbol{\alpha}^0)\theta_{2,j}^{(2),g}(r,\mathbf{\Omega}) = \delta_{g'jg}N_{i_j,m_j}(2l_j+1)P_{l_j}(\mathbf{\Omega})\xi_{l_j}^{(1),g_j}(r), j = 1,\ldots,J_{\sigma s}; g = 1,\ldots,G; l = 0,\ldots,ISCT, \tag{91}$$

$$\theta_{2,j}^{(2),g}(r_d,\mathbf{\Omega}) = 0, \mathbf{\Omega}\cdot\mathbf{n} > 0; j = 1,\ldots,J_{\sigma s}; g = 1,\ldots,G. \tag{92}$$

In Equation (88), the parameters indexed by s_j correspond to the 0th-order scattering cross sections, so that $s_j \equiv \sigma_{s,l_j=0,i_j}^{g'_j \rightarrow g_j}$, while the parameters indexed by f_{m_2} correspond to the fission cross sections, so that $f_{m_2} \equiv \sigma_{f,i_{m_2}}^{g_{m_2}}$. Inserting the results obtained in Equations (23) and (24) into Equation (88), yields the following simplified expression for Equation (88):

$$\left(\frac{\partial^2 L}{\partial s_j \partial f_{m_2}}\right)^{(1)}_{(s=\sigma_{s,l=0}, f=\sigma_f)} = N_{i_{m_2}, m_{m_2}} \nu_{i_{m_2}}^{g_{m_2}} \int_V dV \left[\Theta_{1,j;0}^{(2),g_{m_2}}(r) \sum_{g'=1}^{G} \chi^{g'} \xi_0^{(1),g'}(r) + \varphi_0^{g_{m_2}}(r) \sum_{g=1}^{G} \chi^g \Theta_{2,j;0}^{(2),g}(r)\right], \tag{93}$$

where the 0th-order moments $\Theta_{1,j;0}^{(2),g_{m_2}}(r)$ and $\Theta_{2,j;0}^{(2),g}(r)$ are defined as follows:

$$\Theta_{1,j;0}^{(2),g}(r) \triangleq \int_{4\pi} d\mathbf{\Omega}\, \theta_{1,j}^{(2),g}(r, \mathbf{\Omega}'), \tag{94}$$

$$\Theta_{2,j;0}^{(2),g}(r) \triangleq \int_{4\pi} d\mathbf{\Omega}\, \theta_{2,j}^{(2),g}(r, \mathbf{\Omega}'). \tag{95}$$

Using Equation (158) in [5] in conjunction with the relations $\frac{\partial^2 L}{\partial t_j \partial t_{m_2}} \frac{\partial t_j}{\partial s_j} \frac{\partial t_{m_2}}{\partial f_{m_2}} = \frac{\partial^2 L}{\partial s_j \partial f_{m_2}}$, $\frac{\partial \Sigma_t^g}{\partial t_{m_2}} \frac{\partial t_{m_2}}{\partial f_{m_2}} = \frac{\partial \Sigma_t^g}{\partial f_{m_2}}$ and $\frac{\partial^2 \Sigma_t^g}{\partial t_j \partial t_{m_2}} \frac{\partial t_j}{\partial s_j} \frac{\partial t_{m_2}}{\partial f_{m_2}} = \frac{\partial^2 \Sigma_t^g}{\partial s_j \partial f_{m_2}}$ yields the following contributions:

$$\left(\frac{\partial^2 L}{\partial s_j \partial f_{m_2}}\right)^{(2)}_{(s=\sigma_{s,l=0}, f=\sigma_f)} = -\sum_{g=1}^{G} \int_V dV \int_{4\pi} d\mathbf{\Omega}\, \psi^{(1),g}(r, \mathbf{\Omega}) \varphi^g(r, \mathbf{\Omega}) \frac{\partial^2 \Sigma_t^g}{\partial s_j \partial f_{m_2}}$$
$$- \sum_{g=1}^{G} \int_V dV \int_{4\pi} d\mathbf{\Omega} \left[\psi_{1,j}^{(2),g}(r, \mathbf{\Omega}) \psi^{(1),g}(r, \mathbf{\Omega}) + \psi_{2,j}^{(2),g}(r, \mathbf{\Omega}) \varphi^g(r, \mathbf{\Omega})\right] \frac{\partial \Sigma_t^g}{\partial f_{m_2}}, \tag{96}$$
$$for\ j = 1, \ldots, J_{\sigma s, l=0},\ m_2 = 1, \ldots, J_{\sigma f},$$

where the 2nd-level adjoint functions, $\psi_{1,j}^{(2),g}(r, \mathbf{\Omega})$ and $\psi_{2,j}^{(2),g}(r, \mathbf{\Omega})$, $j = 1, \ldots, J_{\sigma s, l=0}$; $g = 1, \ldots, G$, are the solutions of the 2nd-Level Adjoint Sensitivity System (2nd-LASS) presented in Equations (30), (32), (36) and (37) of Part II [2], which are reproduced below for convenient reference:

$$B^g(\boldsymbol{\alpha}^0) \psi_{1,j}^{(2),g}(r, \mathbf{\Omega}) = -\delta_{g'_j g} N_{i_j, m_j} \varphi^g(r, \mathbf{\Omega}), \quad j = 1, \ldots, J_{\sigma s, l=0}; \ g = 1, \ldots, G, \tag{97}$$

$$\psi_{1,j}^{(2),g}(r_d, \mathbf{\Omega}) = 0, \ \mathbf{\Omega} \cdot \mathbf{n} < 0; \ j = 1, \ldots, J_{\sigma s, l=0}; \ g = 1, \ldots, G, \tag{98}$$

$$A^{(1),g}(\boldsymbol{\alpha}^0) \psi_{2,j}^{(2),g}(r, \mathbf{\Omega}) = -\delta_{g'_j g} N_{i_j, m_j} \psi^{(1),g}(r, \mathbf{\Omega}), \quad j = 1, \ldots, J_{\sigma s, l=0}; \ g = 1, \ldots, G, \tag{99}$$

$$\psi_{2,j}^{(2),g}(r_d, \mathbf{\Omega}) = 0, \ \mathbf{\Omega} \cdot \mathbf{n} > 0; \ j = 1, \ldots, J_{\sigma s, l=0}; \ g = 1, \ldots, G. \tag{100}$$

Noting that

$$\frac{\partial^2 \Sigma_t^g}{\partial s_j \partial f_{m_2}} = \frac{\partial^2 \Sigma_t^g}{\partial \sigma_{s,l_j,i_j}^{g'_j \rightarrow g_j} \partial \sigma_{f,i_{m_2}}^{g_{m_2}}} = 0, \tag{101}$$

and inserting the results obtained in Equations (101) and (37) into Equation (96), yields the following simplified expression for Equation (96):

$$\left(\frac{\partial^2 L}{\partial s_j \partial f_{m_2}}\right)^{(2)}_{(s=\sigma_{s,l=0}, f=\sigma_f)}$$
$$= -N_{i_{m_2}, m_{m_2}} \int_V dV \int_{4\pi} d\mathbf{\Omega} \left[\psi_{1,j}^{(2),g_{m_2}}(r, \mathbf{\Omega}) \psi^{(1),g_{m_2}}(r, \mathbf{\Omega}) + \psi_{2,j}^{(2),g_{m_2}}(r, \mathbf{\Omega}) \varphi^{g_{m_2}}(r, \mathbf{\Omega})\right]. \tag{102}$$

Additional contributions stem from Equation (160) in [5], which takes on the following particular form:

$$
\left(\frac{\partial^2 L}{\partial s_j \partial f_{m_2}}\right)^{(3)}_{(s=\sigma_{s,l=0}, f=\sigma_f)} = \sum_{g=1}^{G} \int_V dV \int_{4\pi} d\Omega\, \psi^{(2),g}_{2,j}(r,\Omega') \sum_{g'=1}^{G} \int_{4\pi} d\Omega'\, \varphi^{g'}(r,\Omega')\chi^g \frac{\partial\left[(\nu\Sigma_f)^{g'}\right]}{\partial f_{m_2}}
$$
$$
+ \sum_{g=1}^{G} \int_V dV \int_{4\pi} d\Omega\, \psi^{(2),g}_{1,j}(r,\Omega') \frac{\partial\left[(\nu\Sigma_f)^g\right]}{\partial f_{m_2}} \sum_{g'=1}^{G} \int_{4\pi} d\Omega'\, \chi^{g'} \psi^{(1),g'}(r,\Omega'),
$$
$$
for\ \ j=1,\ldots,J_{\sigma s,l=0};\ \ m_2=1,\ldots,J_{\sigma f}. \tag{103}
$$

Inserting the results obtained in Equations (23) and (24) into Equation (103), yields the following simplified expression for Equation (103):

$$
\left(\frac{\partial^2 L}{\partial s_j \partial f_{m_2}}\right)^{(3)}_{(s=\sigma_{s,l=0}, f=\sigma_f)} = N_{i_{m_2},m_{m_2}} \nu^{g_{m_2}}_{i_{m_2}} \int_V dV \left[\xi^{(2),g_{m_2}}_{1,j;0}(r) \sum_{g'=1}^{G} \chi^{g'} \xi^{(1),g'}_0(r) + \varphi^{g_{m_2}}_0(r) \sum_{g=1}^{G} \chi^g \xi^{(2),g}_{2,j;0}(r) \right],
$$
$$
for\ \ j=1,\ldots,J_{\sigma s,l=0};\ \ m_2=1,\ldots,J_{\sigma f}. \tag{104}
$$

Using Equation (167) in [5] in conjunction with the relation $\frac{\partial\Sigma_t^g}{\partial t_{m_2}}\frac{\partial t_{m_2}}{\partial f_{m_2}} = \frac{\partial\Sigma_t^g}{\partial f_{m_2}}$ yields the following contributions:

$$
\left(\frac{\partial^2 L}{\partial s_j \partial f_{m_2}}\right)^{(4)}_{(s=\sigma_{s,l=0}, f=\sigma_f)}
$$
$$
= -\sum_{g=1}^{G} \int_V dV \int_{4\pi} d\Omega \left[\theta^{(2),g}_{1,j}(r,\Omega)\psi^{(1),g}(r,\Omega) + \theta^{(2),g}_{2,j}(r,\Omega)\varphi^g(r,\Omega) \right]\frac{\partial\Sigma_t^g}{\partial f_{m_2}},
$$
$$
for\ \ j=1,\ldots,J_{\sigma s,l=0};\ \ m_2=1,\ldots,J_{\sigma f}. \tag{105}
$$

Inserting the results obtained in Equation (37) into Equation (105), yields the following simplified expression:

$$
\left(\frac{\partial^2 L}{\partial s_j \partial f_{m_2}}\right)^{(4)}_{(s=\sigma_{s,l=0}, f=\sigma_f)}
$$
$$
= -N_{i_{m_2},m_{m_2}} \int_V dV \int_{4\pi} d\Omega \left[\theta^{(2),g_{m_2}}_{1,j}(r,\Omega)\psi^{(1),g_{m_2}}(r,\Omega) + \theta^{(2),g_{m_2}}_{2,j}(r,\Omega)\varphi^{g_{m_2}}(r,\Omega) \right]. \tag{106}
$$

Collecting the partial contributions obtained in Equations (93), (102), (104) and (106), yields the following result:

$$
\left(\frac{\partial^2 L}{\partial s_j \partial f_{m_2}}\right)_{(s=\sigma_{s,l=0}, f=\sigma_f)} = \sum_{i=1}^{4}\left(\frac{\partial^2 L}{\partial s_j \partial f_{m_2}}\right)^{(i)}_{(s=\sigma_{s,l=0}, f=\sigma_f)}
$$
$$
= N_{i_{m_2},m_{m_2}} \nu^{g_{m_2}}_{i_{m_2}} \int_V dV \left[\Theta^{(2),g_{m_2}}_{1,j;0}(r) \sum_{g'=1}^{G} \chi^{g'} \xi^{(1),g'}_0(r) + \varphi^{g_{m_2}}_0(r) \sum_{g=1}^{G} \chi^g \Theta^{(2),g}_{2,j;0}(r) \right]
$$
$$
- N_{i_{m_2},m_{m_2}} \int_V dV \int_{4\pi} d\Omega \left[\psi^{(2),g_{m_2}}_{1,j}(r,\Omega)\psi^{(1),g_{m_2}}(r,\Omega) + \psi^{(2),g_{m_2}}_{2,j}(r,\Omega)\varphi^{g_{m_2}}(r,\Omega) \right]
$$
$$
+ N_{i_{m_2},m_{m_2}} \nu^{g_{m_2}}_{i_{m_2}} \int_V dV \left[\xi^{(2),g_{m_2}}_{1,j;0}(r) \sum_{g'=1}^{G} \chi^{g'} \xi^{(1),g'}_0(r) + \varphi^{g_{m_2}}_0(r) \sum_{g=1}^{G} \chi^g \xi^{(2),g}_{2,j;0}(r) \right]
$$
$$
- N_{i_{m_2},m_{m_2}} \int_V dV \int_{4\pi} d\Omega \left[\theta^{(2),g_{m_2}}_{1,j}(r,\Omega)\psi^{(1),g_{m_2}}(r,\Omega) + \theta^{(2),g_{m_2}}_{2,j}(r,\Omega)\varphi^{g_{m_2}}(r,\Omega) \right],
$$
$$
for\ \ j=1,\ldots,J_{\sigma s,l=0};\ m_2=1,\ldots,J_{\sigma f}. \tag{107}
$$

4.2.2. Second-Order Sensitivities $\left(\frac{\partial^2 L}{\partial s_j \partial f_{m_2}}\right)_{(s=\sigma_{s,l\geq1}, f=\sigma_f)}$

For this case, only the fission cross sections contribute to the total cross sections, so the parameters s_j correspond to the lth-order ($l \geq 1$) scattering cross sections, denoted as $s_j \equiv \sigma^{g_j' \to g_j}_{s,l_j,i_j}$, and the

parameters f_{m_2} correspond to the fission cross sections, denoted as $f_{m_2} \equiv \sigma^{g_{m_2}}_{f,i_{m_2}}$. The expression of $\left(\frac{\partial^2 L}{\partial s_j \partial f_{m_2}}\right)_{(s=\sigma_{s,l\geq 1}, f=\sigma_f)}$ is obtained by particularizing Equations (167) and (169) in [5] to the PERP benchmark, which yields,

$$
\begin{aligned}
\left(\frac{\partial^2 L}{\partial s_j \partial f_{m_2}}\right)_{(s=\sigma_{s,l\geq 1}, f=\sigma_f)} &= -\sum_{g=1}^{G} \int_V dV \int_{4\pi} d\Omega \left[\theta^{(2),g}_{1,j}(r,\Omega)\psi^{(1),g}(r,\Omega) + \theta^{(2),g}_{2,j}(r,\Omega)\varphi^{g}(r,\Omega)\right]\frac{\partial \Sigma_t^{g}}{\partial f_{m_2}} \\
&+ \sum_{g=1}^{G} \int_V dV \int_{4\pi} d\Omega\, \theta^{(2),g}_{1,j}(r,\Omega)\frac{\partial\left[(\nu\Sigma_f)^g\right]}{\partial f_{m_2}} \sum_{g'=1}^{G} \int_{4\pi} d\Omega' \chi^{g'}\psi^{(1),g'}(r,\Omega') \\
&+ \sum_{g=1}^{G} \int_V dV \int_{4\pi} d\Omega\, \theta^{(2),g}_{2,j}(r,\Omega) \sum_{g'=1}^{G} \int_{4\pi} d\Omega' \varphi^{g'}(r,\Omega')\chi^{g}\frac{\partial\left[(\nu\Sigma_f)^{g'}\right]}{\partial f_{m_2}}, \\
&\text{for } j = 1,\ldots,J_{\sigma s,l\geq 1}; m_2 = 1,\ldots,J_{\sigma f}.
\end{aligned}
\tag{108}
$$

Inserting the results obtained in Equations (23), (24) and (37) into Equation (108), yields the final expression as follows:

$$
\begin{aligned}
&\left(\frac{\partial^2 L}{\partial s_j \partial f_{m_2}}\right)_{(s=\sigma_{s,l\geq 1}, f=\sigma_f)} \\
&= -N_{i_{m_2},m_{m_2}} \int_V dV \int_{4\pi} d\Omega \left[\theta^{(2),g_{m_2}}_{1,j}(r,\Omega)\psi^{(1),g_{m_2}}(r,\Omega) + \theta^{(2),g_{m_2}}_{2,j}(r,\Omega)\varphi^{g_{m_2}}(r,\Omega)\right] \\
&+ N_{i_{m_2},m_{m_2}} \nu^{g_{m_2}}_{i_{m_2}} \int_V dV \left[\Theta^{(2),g_{m_2}}_{1,j;0}(r) \sum_{g'=1}^{G} \chi^{g'}\xi^{(1),g'}_0(r) + \phi^{g_{m_2}}_0(r) \sum_{g=1}^{G} \chi^{g}\Theta^{(2),g}_{2,j;0}(r)\right], \\
&\text{for } j = 1,\ldots,J_{\sigma s,l\geq 1}; m_2 = 1,\ldots,J_{\sigma f}.
\end{aligned}
\tag{109}
$$

4.3. Numerical Results for $\partial^2 L(\boldsymbol{\alpha})/\partial\boldsymbol{\sigma}_f\partial\boldsymbol{\sigma}_s$

Computing the second-order absolute sensitivities, $\partial^2 L(\boldsymbol{\alpha})/\partial\boldsymbol{\sigma}_f\partial\boldsymbol{\sigma}_s$, using Equations (79) and (81) requires $J_{\sigma f} = G \times N_f = 30 \times 2 = 60$ forward and adjoint PARTISN computations to obtain the adjoint functions $u^{(2),g}_{1,j}(r,\Omega)$ and $u^{(2),g}_{2,j}(r,\Omega)$, $j = 1,\ldots,J_{\sigma f}$; $g = 1,\ldots,G$, as well as $J_{\sigma f} = 60$ forward and adjoint PARTISN computations to obtain the adjoint functions $\psi^{(2),g}_{1,j}(r,\Omega)$ and $\psi^{(2),g}_{2,j}(r,\Omega)$, $j = 1,\ldots,J_{\sigma f}$; $g = 1,\ldots,G$. Thus, a total of 120 forward and adjoint PARTISN computations are required to obtain all of the 2nd-order sensitivities $\partial^2 L(\boldsymbol{\alpha})/\partial\boldsymbol{\sigma}_f\partial\boldsymbol{\sigma}_s$ using Equations (79) and (81).

On the other hand, computing the alternative expression $\partial^2 L(\boldsymbol{\alpha})/\partial\boldsymbol{\sigma}_s\partial\boldsymbol{\sigma}_f$ using Equations (107) and (109), requires 7101 forward and adjoint PARTISN computations to obtain the adjoint functions $\theta^{(2),g}_{1,j}(r,\Omega)$ and $\theta^{(2),g}_{2,j}(r,\Omega)$, $j = 1,\ldots,J_{\sigma s}$; $g = 1,\ldots,G$. The reason for needing "only" 7101, rather than 21,600, PARTISN computations is that all of the up-scattering and some of the down-scattering cross sections are zero for the PERP benchmark. Thus, computing $\partial^2 L(\boldsymbol{\alpha})/\partial\boldsymbol{\sigma}_f\partial\boldsymbol{\sigma}_s$ using Equations (79) and (81) is about $60 (\approx 7101/120)$ times more efficient than computing $\partial^2 L(\boldsymbol{\alpha})/\partial\boldsymbol{\sigma}_s\partial\boldsymbol{\sigma}_f$ by using Equations (107) and (109).

The dimensions of the matrix $\partial^2 L/\partial f_j \partial s_{m_2}$, $j = 1,\ldots,J_{\sigma f}$; $m_2 = 1,\ldots,J_{\sigma f}$ is $J_{\sigma f} \times J_{\sigma s} (= 60 \times 21,600)$, where $J_{\sigma f} = G \times N_f = 30 \times 2 = 60$ and $J_{\sigma s} = G \times G \times (ISCT + 1) \times I = 30 \times 30 \times 4 \times 6 = 21,600$. The matrix of 2nd-order relative sensitivities corresponding to $\partial^2 L/\partial f_j \partial s_{m_2}$, $j = 1,\ldots,J_{\sigma f}$; $m_2 = 1,\ldots,J_{\sigma f}$, denoted as $\mathbf{S}^{(2)}\left(\sigma^g_{f,i}, \sigma^{g'\to h}_{s,l,k}\right)$, is defined as follows:

$$
\mathbf{S}^{(2)}\left(\sigma^g_{f,i}, \sigma^{g'\to h}_{s,l,k}\right) \triangleq \frac{\partial^2 L}{\partial \sigma^g_{f,i} \partial \sigma^{g'\to h}_{s,l,k}}\left(\frac{\sigma^g_{f,i}\sigma^{g'\to h}_{s,l,k}}{L}\right), \quad l = 0,\ldots,3; \ i = 1,2; k = 1,\ldots,6; \ g,g',h = 1,\ldots,30.
\tag{110}
$$

To facilitate the presentation and interpretation of the numerical results, the $J_{\sigma f} \times J_{\sigma s} (= 60 \times 21,600)$ matrix $\mathbf{S}^{(2)}\left(\sigma^g_{f,i}, \sigma^{g'\to h}_{s,l,k}\right)$ has been partitioned into $N_f \times I \times (ISCT + 1) = 2 \times 6 \times 4$ submatrices, each of dimensions $G \times (G \cdot G) = 30 \times 900$. The results for scattering orders $l = 0$, $l = 1$, $l = 2$, and $l = 3$, respectively, are summarized below, in Sections 4.3.1–4.3.4.

4.3.1. Results for the Relative Sensitivities $\mathbf{S}^{(2)}\left(\sigma_{f,i}^g, \sigma_{s,l=0,k}^{g'\to h}\right)$

Table 8 presents the results for 2nd-order relative sensitivities of the leakage response with respect to the fission cross sections and the 0th-order scattering cross sections for all isotopes, $\mathbf{S}^{(2)}\left(\sigma_{f,i}^g, \sigma_{s,l=0,k}^{g'\to h}\right) \triangleq \left(\partial^2 L/\partial\sigma_{f,i}^g \partial\sigma_{s,l=0,k}^{g'\to h}\right)\left(\sigma_{f,i}^g \sigma_{s,l=0,k}^{g'\to h}/L\right)$, $l = 0$; $i = 1,2$; $k = 1,\ldots,6$; $g,g',h = 1,\ldots,30$. All of these 2nd-order relative sensitivities are smaller than 1.0. The value of the largest element of each of the respective sub-matrices is presented in Table 8, together with the phase-space coordinates of the respective element. For the 2nd-order mixed sensitivities with respect to the 0th-order scattering cross sections, the values can be positive or negative, but there are more positive values than negative ones. For example, the submatrix $\mathbf{S}^{(2)}\left(\sigma_{f,1}^g, \sigma_{s,l=0,1}^{g'\to h}\right)$, having dimensions $G \times (G \cdot G) = 30 \times 900$, comprises 7577 positive elements, 2563 negative elements, while the remaining elements are zero. The largest absolute values of the mixed 2nd-order sensitivities all involve the fission cross sections for the 12th energy group of isotopes ^{239}Pu or ^{240}Pu, and (mostly) the 0th-order self-scattering cross sections in the 12th energy group for isotopes ^{239}Pu, ^{240}Pu, ^{69}Ga, ^{71}Ga andC, or (occasionally) the 0th-order out-scattering cross section $\sigma_{s,l=0,k=6}^{16\to 17}$ for isotope ^{1}H. All of the largest elements in the respective sub-matrix are positive, and the vast majority of them are very small. The overall largest element in the matrix $\mathbf{S}^{(2)}\left(\sigma_{f,i}^g, \sigma_{s,l=0,k}^{g'\to h}\right)$ is $S^{(2)}\left(\sigma_{f,1}^{g=12}, \sigma_{s,l=0,1}^{12\to 12}\right) = 3.03 \times 10^{-1}$.

Table 8. Summary presentation of the matrix $\mathbf{S}^{(2)}\left(\sigma_{f,i}^g, \sigma_{s,l=0,k}^{g'\to h}\right)$.

Isotopes	k=1 (^{239}Pu)	k=2 (^{240}Pu)	k=3 (^{69}Ga)	k=4 (^{71}Ga)	k=5 (C)	k=6 (^{1}H)
$i = 1$ (^{239}Pu)	$\mathbf{S}^{(2)}\left(\begin{smallmatrix}\sigma_{f,1'}^g\\\sigma_{s,l=0,1}^{g'\to h}\end{smallmatrix}\right)$ Max. value = 3.03×10^{-1} at $g = 12$, $g' = 12$ $\to$ h = 12	$\mathbf{S}^{(2)}\left(\begin{smallmatrix}\sigma_{f,1'}^g\\\sigma_{s,l=0,2}^{g'\to h}\end{smallmatrix}\right)$ Max. value = 2.01×10^{-2} at $g = 12$, $g' = 12$ $\to$ h = 12	$\mathbf{S}^{(2)}\left(\begin{smallmatrix}\sigma_{f,1'}^g\\\sigma_{s,l=0,3}^{g'\to h}\end{smallmatrix}\right)$ Max. value = 1.16×10^{-3} at $g = 12$, $g' = 12$ $\to$ h = 12	$\mathbf{S}^{(2)}\left(\begin{smallmatrix}\sigma_{f,1'}^g\\\sigma_{s,l=0,4}^{g'\to h}\end{smallmatrix}\right)$ Max. value = 7.44×10^{-4} at $g = 12$, $g' = 12$ $\to$ h = 12	$\mathbf{S}^{(2)}\left(\begin{smallmatrix}\sigma_{f,1'}^g\\\sigma_{s,l=0,5}^{g'\to h}\end{smallmatrix}\right)$ Max. value = 1.37×10^{-1} at $g = 12$, $g' = 12$ $\to$ h = 12	$\mathbf{S}^{(2)}\left(\begin{smallmatrix}\sigma_{f,1'}^g\\\sigma_{s,l=0,6}^{g'\to h}\end{smallmatrix}\right)$ Max. value = 2.30×10^{-1} at $g = 12$, $g' = 16$ $\to$ h = 17
$i = 2$ (^{240}Pu)	$\mathbf{S}^{(2)}\left(\begin{smallmatrix}\sigma_{f,2'}^g\\\sigma_{s,l=0,1}^{g'\to h}\end{smallmatrix}\right)$ Max. value = 1.56×10^{-2} at $g = 12$, $g' = 12$ $\to$ h = 12	$\mathbf{S}^{(2)}\left(\begin{smallmatrix}\sigma_{f,2'}^g\\\sigma_{s,l=0,2}^{g'\to h}\end{smallmatrix}\right)$ Max. value = 1.04×10^{-3} at $g = 12$, $g' = 12$ $\to$ h = 12	$\mathbf{S}^{(2)}\left(\begin{smallmatrix}\sigma_{f,2'}^g\\\sigma_{s,l=0,3}^{g'\to h}\end{smallmatrix}\right)$ Max. value = 5.99×10^{-5} at $g = 12$, $g' = 12$ $\to$ h = 12	$\mathbf{S}^{(2)}\left(\begin{smallmatrix}\sigma_{f,2'}^g\\\sigma_{s,l=0,4}^{g'\to h}\end{smallmatrix}\right)$ Max. value = 3.84×10^{-5} at $g = 12$, $g' = 12$ $\to$ h = 12	$\mathbf{S}^{(2)}\left(\begin{smallmatrix}\sigma_{f,2'}^g\\\sigma_{s,l=0,5}^{g'\to h}\end{smallmatrix}\right)$ Max. value = 7.10×10^{-3} at $g = 12$, $g' = 12$ $\to$ h = 12	$\mathbf{S}^{(2)}\left(\begin{smallmatrix}\sigma_{f,2'}^g\\\sigma_{s,l=0,6}^{g'\to h}\end{smallmatrix}\right)$ Max. value = 1.19×10^{-2} at $g = 12$, $g' = 16$ $\to$ h = 17

4.3.2. Results for the Relative Sensitivities $\mathbf{S}^{(2)}\left(\sigma_{f,i}^g, \sigma_{s,l=1,k}^{g'\to h}\right)$

Table 9 summarizes the results for the 2nd-order mixed relative sensitivities of the leakage response with respect to the fission cross sections and the 1st-order scattering cross sections for all isotopes, $\mathbf{S}^{(2)}\left(\sigma_{f,i}^g, \sigma_{s,l=1,k}^{g'\to h}\right) \triangleq \left(\partial^2 L/\partial\sigma_{f,i}^g \partial\sigma_{s,l=1,k}^{g'\to h}\right)\left(\sigma_{f,i}^g \sigma_{s,l=1,k}^{g'\to h}/L\right)$, $l = 1$; $i = 1,2$; $k = 1,\ldots,6$; $g,g',h = 1,\ldots,30$. Most of these 2nd-order mixed sensitivities are zero; the non-zero ones are mostly negative. For example, the submatrix $\mathbf{S}^{(2)}\left(\sigma_{f,1}^g, \sigma_{s,l=1,1}^{g'\to h}\right)$, having dimensions $G \times (G \cdot G) = 30 \times 900$, comprises 7798 elements with negative values, 2342 elements with positive values, while the remaining elements are zero. As shown in Table 9, the largest absolute values of the mixed 2nd-order sensitivities all involve the fission cross sections $\sigma_{f,i}^{g=12}$, $i = 1,2$ for the 12th energy group of isotopes ^{239}Pu or ^{240}Pu, and either the 1st-order self-scattering cross sections $\sigma_{s,l=1,k}^{7\to 7}$, $k = 1,\ldots,4$ in the 7th energy group for isotopes ^{239}Pu, ^{240}Pu, ^{69}Ga and ^{71}Ga, or the 1st-order self-scattering cross sections $\sigma_{s,l=1,k}^{12\to 12}$, $k = 5,6$ in the 12th energy group for isotopes C and ^{1}H. All of the largest (in absolute value) elements are negative, and the vast majority of them are very small. The overall most negative element in the matrix $\mathbf{S}^{(2)}\left(\sigma_{f,i}^g, \sigma_{s,l=1,k}^{g'\to h}\right)$ is $S^{(2)}\left(\sigma_{f,1}^{g=12}, \sigma_{s,l=1,1}^{7\to 7}\right) = -1.70 \times 10^{-1}$.

Table 9. Summary presentation of the matrix $\mathbf{S}^{(2)}\left(\sigma_{f,i}^{g},\sigma_{s,l=1,k}^{g'\to h}\right)$.

Isotopes	$k=1$ (^{239}Pu)	$k=2$ (^{240}Pu)	$k=3$ (^{69}Ga)	$k=4$ (^{71}Ga)	$k=5$ (C)	$k=6$ (^{1}H)
$i=1$ (^{239}Pu)	$\mathbf{S}^{(2)}\left(\begin{smallmatrix}\sigma_{f,1'}^{g}\\ \sigma_{s,l=1,1}^{g'\to h}\end{smallmatrix}\right)$ Min. value = -1.70×10^{-1} at $g=12,\,g'=7$ $\to h=7$	$\mathbf{S}^{(2)}\left(\begin{smallmatrix}\sigma_{f,1'}^{g}\\ \sigma_{s,l=1,2}^{g'\to h}\end{smallmatrix}\right)$ Min. value = -1.02×10^{-2} at $g=12,\,g'=7$ $\to h=7$	$\mathbf{S}^{(2)}\left(\begin{smallmatrix}\sigma_{f,1'}^{g}\\ \sigma_{s,l=1,3}^{g'\to h}\end{smallmatrix}\right)$ Min. value = -3.43×10^{-4} at $g=12,\,g'=7$ $\to h=7$	$\mathbf{S}^{(2)}\left(\begin{smallmatrix}\sigma_{f,1'}^{g}\\ \sigma_{s,l=1,4}^{g'\to h}\end{smallmatrix}\right)$ Min. value = -2.08×10^{-4} at $g=12,\,g'=7$ $\to h=7$	$\mathbf{S}^{(2)}\left(\begin{smallmatrix}\sigma_{f,1'}^{g}\\ \sigma_{s,l=1,5}^{g'\to h}\end{smallmatrix}\right)$ Min. value = 1.37×10^{-1} at $g=12,\,g'=12$ $\to h=12$	$\mathbf{S}^{(2)}\left(\begin{smallmatrix}\sigma_{f,1'}^{g}\\ \sigma_{s,l=1,6}^{g'\to h}\end{smallmatrix}\right)$ Min. value = -5.63×10^{-2} at $g=12,\,g'=12$ $\to h=12$
$i=2$ (^{240}Pu)	$\mathbf{S}^{(2)}\left(\begin{smallmatrix}\sigma_{f,2'}^{g}\\ \sigma_{s,l=1,1}^{g'\to h}\end{smallmatrix}\right)$ Min. value = -8.78×10^{-3} at $g=12,\,g'=7$ $\to h=7$	$\mathbf{S}^{(2)}\left(\begin{smallmatrix}\sigma_{f,2'}^{g}\\ \sigma_{s,l=1,2}^{g'\to h}\end{smallmatrix}\right)$ Min. value = -5.28×10^{-4} at $g=12,\,g'=7$ $\to h=7$	$\mathbf{S}^{(2)}\left(\begin{smallmatrix}\sigma_{f,2'}^{g}\\ \sigma_{s,l=1,3}^{g'\to h}\end{smallmatrix}\right)$ Min. value = -1.78×10^{-5} at $g=12,\,g'=7$ $\to h=7$	$\mathbf{S}^{(2)}\left(\begin{smallmatrix}\sigma_{f,2'}^{g}\\ \sigma_{s,l=1,4}^{g'\to h}\end{smallmatrix}\right)$ Min. value = -1.08×10^{-5} at $g=12,\,g'=7$ $\to h=7$	$\mathbf{S}^{(2)}\left(\begin{smallmatrix}\sigma_{f,2'}^{g}\\ \sigma_{s,l=1,5}^{g'\to h}\end{smallmatrix}\right)$ Min. value = -2.91×10^{-3} at $g=12,\,g'=12$ $\to h=12$	$\mathbf{S}^{(2)}\left(\begin{smallmatrix}\sigma_{f,2'}^{g}\\ \sigma_{s,l=1,6}^{g'\to h}\end{smallmatrix}\right)$ Min. value = -9.15×10^{-3} at $g=12,\,g'=12$ $\to h=12$

4.3.3. Results for the Relative Sensitivities $\mathbf{S}^{(2)}\left(\sigma_{f,i}^{g},\sigma_{s,l=2,k}^{g'\to h}\right)$

Table 10 presents the results for the 2nd-order mixed relative sensitivities $\mathbf{S}^{(2)}\left(\sigma_{f,i}^{g},\sigma_{s,l=2,k}^{g'\to h}\right) \triangleq \left(\partial^2 L/\partial\sigma_{f,i}^{g}\partial\sigma_{s,l=2,k}^{g'\to h}\right)\left(\sigma_{f,i}^{g}\sigma_{s,l=2,k}^{g'\to h}/L\right)$, $l=2$; $i=1,2$; $k=1,\ldots,6$; $g,g',h=1,\ldots,30$, of the leakage response with respect to the fission cross sections and the 2nd-order scattering cross sections for all isotopes. Most of the non-zero elements of $\mathbf{S}^{(2)}\left(\sigma_{f,i}^{g},\sigma_{s,l=2,k}^{g'\to h}\right)$ are positive. For example, the submatrix $\mathbf{S}^{(2)}\left(\sigma_{f,1}^{g},\sigma_{s,l=2,1}^{g'\to h}\right)$, having dimensions $G\times(G\cdot G)=30\times900$, comprises 6308 positive elements and 3832 negative elements, while the remaining elements are zero. As shown in Table 10, all of the largest absolute values of the mixed 2nd-order sensitivities involve the fission cross sections $\sigma_{f,i}^{g=12}$, $i=1,2$ for the 12th energy group of isotopes ^{239}Pu or ^{240}Pu, and involve either the 2nd-order self-scattering cross sections $\sigma_{s,l=2,i=6}^{12\to12}$ in the 12th energy group for isotope ^{1}H, or the 2nd-order self-scattering cross sections $\sigma_{s,l=2,k}^{7\to7}$, $k=1,\ldots,5$ in the 7th energy group for isotopes ^{239}Pu, ^{240}Pu, ^{69}Ga, ^{71}Ga and C. As shown in Table 10, all of the largest elements in the respective sub-matrix are positive, and the vast majority of them are very small. The overall largest element in the matrix $\mathbf{S}^{(2)}\left(\sigma_{f,i}^{g},\sigma_{s,l=2,k}^{g'\to h}\right)$ is $S^{(2)}\left(\sigma_{f,1}^{g=12},\sigma_{s,l=2,1}^{7\to7}\right)=1.02\times10^{-2}$.

Table 10. Summary presentation of the matrix $\mathbf{S}^{(2)}\left(\sigma_{f,i}^{g},\sigma_{s,l=2,k}^{g'\to h}\right)$.

Isotopes	$k=1$ (^{239}Pu)	$k=2$ (^{240}Pu)	$k=3$ (^{69}Ga)	$k=4$ (^{71}Ga)	$k=5$ (C)	$k=6$ (^{1}H)
$i=1$ (^{239}Pu)	$\mathbf{S}^{(2)}\left(\begin{smallmatrix}\sigma_{f,1'}^{g}\\ \sigma_{s,l=2,1}^{g'\to h}\end{smallmatrix}\right)$ Max. value = 1.02×10^{-2} at $g=12,\,g'=7$ $\to h=7$	$\mathbf{S}^{(2)}\left(\begin{smallmatrix}\sigma_{f,1'}^{g}\\ \sigma_{s,l=2,2}^{g'\to h}\end{smallmatrix}\right)$ Max. value = 6.25×10^{-4} at $g=12,\,g'=7$ $\to h=7$	$\mathbf{S}^{(2)}\left(\begin{smallmatrix}\sigma_{f,1'}^{g}\\ \sigma_{s,l=2,3}^{g'\to h}\end{smallmatrix}\right)$ Max. value = 1.87×10^{-5} at $g=12,\,g'=7$ $\to h=7$	$\mathbf{S}^{(2)}\left(\begin{smallmatrix}\sigma_{f,1'}^{g}\\ \sigma_{s,l=2,4}^{g'\to h}\end{smallmatrix}\right)$ Max. value = 1.16×10^{-5} at $g=12,\,g'=7$ $\to h=7$	$\mathbf{S}^{(2)}\left(\begin{smallmatrix}\sigma_{f,1'}^{g}\\ \sigma_{s,l=2,5}^{g'\to h}\end{smallmatrix}\right)$ Max. value = 1.39×10^{-2} at $g=12,\,g'=7$ $\to h=7$	$\mathbf{S}^{(2)}\left(\begin{smallmatrix}\sigma_{f,1'}^{g}\\ \sigma_{s,l=2,6}^{g'\to h}\end{smallmatrix}\right)$ Max. value = 5.94×10^{-2} at $g=12,\,g'=12$ $\to h=12$
$i=2$ (^{240}Pu)	$\mathbf{S}^{(2)}\left(\begin{smallmatrix}\sigma_{f,2'}^{g}\\ \sigma_{s,l=2,1}^{g'\to h}\end{smallmatrix}\right)$ Max. value = 5.29×10^{-4} at $g=12,\,g'=7$ $\to h=7$	$\mathbf{S}^{(2)}\left(\begin{smallmatrix}\sigma_{f,2'}^{g}\\ \sigma_{s,l=2,2}^{g'\to h}\end{smallmatrix}\right)$ Max. value = 3.24×10^{-5} at $g=12,\,g'=7$ $\to h=7$	$\mathbf{S}^{(2)}\left(\begin{smallmatrix}\sigma_{f,2'}^{g}\\ \sigma_{s,l=2,3}^{g'\to h}\end{smallmatrix}\right)$ Max. value = 9.71×10^{-7} at $g=12,\,g'=7$ $\to h=7$	$\mathbf{S}^{(2)}\left(\begin{smallmatrix}\sigma_{f,2'}^{g}\\ \sigma_{s,l=2,4}^{g'\to h}\end{smallmatrix}\right)$ Max. value = 6.03×10^{-7} at $g=12,\,g'=7$ $\to h=7$	$\mathbf{S}^{(2)}\left(\begin{smallmatrix}\sigma_{f,2'}^{g}\\ \sigma_{s,l=2,5}^{g'\to h}\end{smallmatrix}\right)$ Max. value = 7.18×10^{-4} at $g=12,\,g'=7$ $\to h=7$	$\mathbf{S}^{(2)}\left(\begin{smallmatrix}\sigma_{f,2'}^{g}\\ \sigma_{s,l=2,6}^{g'\to h}\end{smallmatrix}\right)$ Max. value = 3.07×10^{-3} at $g=12,\,g'=12$ $\to h=12$

4.3.4. Results for the Relative Sensitivities $\mathbf{S}^{(2)}\left(\sigma_{f,i}^{g},\sigma_{s,l=3,k}^{g'\to h}\right)$

Table 11 presents the results for the 2nd-order mixed relative sensitivities $\mathbf{S}^{(2)}\left(\sigma_{f,i}^{g},\sigma_{s,l=3,k}^{g'\to h}\right) \triangleq \left(\partial^2 L/\partial\sigma_{f,i}^{g}\partial\sigma_{s,l=3,k}^{g'\to h}\right)\left(\sigma_{f,i}^{g}\sigma_{s,l=3,k}^{g'\to h}/L\right)$, $l=3$; $i=1,2$; $k=1,\ldots,6$; $g,g',h=1,\ldots,30$, of the leakage

response with respect to the fission cross sections and the 3rd-order scattering cross sections for all isotopes. Most of the elements of $\mathbf{S}^{(2)}\left(\sigma_{f,i}^{g}, \sigma_{s,l=3,k}^{g' \to h}\right)$ are zero; the non-zero elements are very small, and the negative ones slightly outnumber the positive ones. For example, the $G \times (G \cdot G) = 30 \times 900$ -dimensional submatrix $\mathbf{S}^{(2)}\left(\sigma_{f,1}^{g}, \sigma_{s,l=3,1}^{g' \to h}\right)$ comprises 5288 negative elements and 4822 positive elements, while the remaining ones are zero. As shown in Table 11, the mixed 2nd-order sensitivities having the largest absolute values involve the fission cross sections $\sigma_{f,i}^{g=12}$, $i = 1, 2$ for the 12th energy group of isotopes ^{239}Pu or^{240}Pu, and either the 3rd-order self-scattering cross sections $\sigma_{s,l=3,i=6}^{12 \to 12}$ for the 12th energy group for isotope ^{1}H or the 3rd-order self-scattering cross sections $\sigma_{s,l=3,k}^{7 \to 7}$, $k = 1, \dots, 5$ for the 7th energy group for isotopes^{239}Pu, ^{240}Pu, ^{69}Ga, ^{71}Ga and C. The overall largest (in absolute value) element of the matrix $\mathbf{S}^{(2)}\left(\sigma_{f,i}^{g}, \sigma_{s,l=3,k}^{g' \to h}\right)$ is $S^{(2)}\left(\sigma_{f,i=1}^{g=12}, \sigma_{s,l=3,k=6}^{12 \to 12}\right) = -1.25 \times 10^{-2}$.

Table 11. Summary presentation of the matrix $\mathbf{S}^{(2)}\left(\sigma_{f,i}^{g}, \sigma_{s,l=3,k}^{g' \to h}\right)$.

Isotopes	k=1 (^{239}Pu)	k=2 (^{240}Pu)	k=3 (^{69}Ga)	k=4 (^{71}Ga)	k=5 (C)	k=6 (^{1}H)
$i = 1$ (^{239}Pu)	$\mathbf{S}^{(2)}\left(\sigma_{f,1'}^{g}, \sigma_{s,l=3,1}^{g' \to h}\right)$ Min. value = -1.79×10^{-5} at $g = 12$, $g' = 7$ $\to$ h = 7	$\mathbf{S}^{(2)}\left(\sigma_{f,1'}^{g}, \sigma_{s,l=3,2}^{g' \to h}\right)$ Min. value = -1.10×10^{-6} at $g = 12$, $g' = 7$ $\to$ h = 7	$\mathbf{S}^{(2)}\left(\sigma_{f,1'}^{g}, \sigma_{s,l=3,3}^{g' \to h}\right)$ Min. value = -3.12×10^{-8} at $g = 12$, $g' = 7$ $\to$ h = 7	$\mathbf{S}^{(2)}\left(\sigma_{f,1'}^{g}, \sigma_{s,l=3,4}^{g' \to h}\right)$ Min. value = -1.96×10^{-8} at $g = 12$, $g' = 7$ $\to$ h = 7	$\mathbf{S}^{(2)}\left(\sigma_{f,1'}^{g}, \sigma_{s,l=3,5}^{g' \to h}\right)$ Min. value = -3.48×10^{-3} at $g = 12$, $g' = 7$ $\to$ h = 7	$\mathbf{S}^{(2)}\left(\sigma_{f,1'}^{g}, \sigma_{s,l=3,6}^{g' \to h}\right)$ Min. value = -1.25×10^{-2} at $g = 12$, $g' = 12$ $\to$ h = 12
$i = 2$ (^{240}Pu)	$\mathbf{S}^{(2)}\left(\sigma_{f,2'}^{g}, \sigma_{s,l=3,1}^{g' \to h}\right)$ Min. value = -9.26×10^{-7} at $g = 12$, $g' = 7$ $\to$ h = 7	$\mathbf{S}^{(2)}\left(\sigma_{f,2'}^{g}, \sigma_{s,l=3,2}^{g' \to h}\right)$ Min. value = -5.70×10^{-8} at $g = 12$, $g' = 7$ $\to$ h = 7	$\mathbf{S}^{(2)}\left(\sigma_{f,2'}^{g}, \sigma_{s,l=3,3}^{g' \to h}\right)$ Min. value = -1.62×10^{-9} at $g = 12$, $g' = 7$ $\to$ h = 7	$\mathbf{S}^{(2)}\left(\sigma_{f,2'}^{g}, \sigma_{s,l=3,4}^{g' \to h}\right)$ Min. value = -1.02×10^{-9} at $g = 12$, $g' = 7$ $\to$ h = 7	$\mathbf{S}^{(2)}\left(\sigma_{f,2'}^{g}, \sigma_{s,l=3,5}^{g' \to h}\right)$ Min. value = -1.80×10^{-4} at $g = 12$, $g' = 7$ $\to$ h = 7	$\mathbf{S}^{(2)}\left(\sigma_{f,2'}^{g}, \sigma_{s,l=3,6}^{g' \to h}\right)$ Min. value = -6.44×10^{-4} at $g = 12$, $g' = 12$ $\to$ h = 12

The results in Tables 9–11 indicate that the largest mixed second-order relative sensitivities in matrices $\mathbf{S}^{(2)}\left(\sigma_{f,i}^{g}, \sigma_{s,l=1,k}^{g' \to h}\right)$, $\mathbf{S}^{(2)}\left(\sigma_{f,i}^{g}, \sigma_{s,l=2,k}^{g' \to h}\right)$ and $\mathbf{S}^{(2)}\left(\sigma_{f,i}^{g}, \sigma_{s,l=3,k}^{g' \to h}\right)$ frequently involve the self-scattering cross sections in the 7th-energy group namely, $\sigma_{s,l,k}^{7 \to 7}$, $l = 1, 2, 3$; $k = 1, \dots, 4$, which is likely due to the fact that, for isotope ^{239}Pu, the scattering cross section $\sigma_{s,l,k=1}^{7 \to 7}$, $l = 1, 2, 3$ has the largest value among all scattering cross sections $\sigma_{s,l,k=1}^{g' \to h}$, $g', h = 1, \dots, 30$, for $l = 1, 2, 3$.

Figure 4 shows the energy-group structure of the fission spectrum for isotope ^{239}Pu, highlighting that most of the spectrum is concentrated in the energy region $g = 7, \dots, 14$, with the largest portion contained in group 12. It is therefore not surprising that most of the large mixed 2nd-order relative sensitivities of $\partial^2 L(\boldsymbol{\alpha})/\partial\boldsymbol{\sigma}_f\partial\boldsymbol{\sigma}_f$, $\partial^2 L(\boldsymbol{\alpha})/\partial\boldsymbol{\sigma}_f\partial\boldsymbol{\sigma}_t$, $\partial^2 L(\boldsymbol{\alpha})/\partial\boldsymbol{\sigma}_f\partial\boldsymbol{\sigma}_s$ and $\partial^2 L(\boldsymbol{\alpha})/\partial\boldsymbol{\nu}\partial\boldsymbol{\sigma}_f$ are concentrated in the energy region $g = 7, \dots, 14$ of the fission cross sections of ^{239}Pu. In particular, the 1st- and 2nd-order sensitivities of leakage response to the fission cross sections of ^{239}Pu are both related to the 12th energy group, which is expected since energy-group 12 contains the largest portion of the fission spectrum of ^{239}Pu.
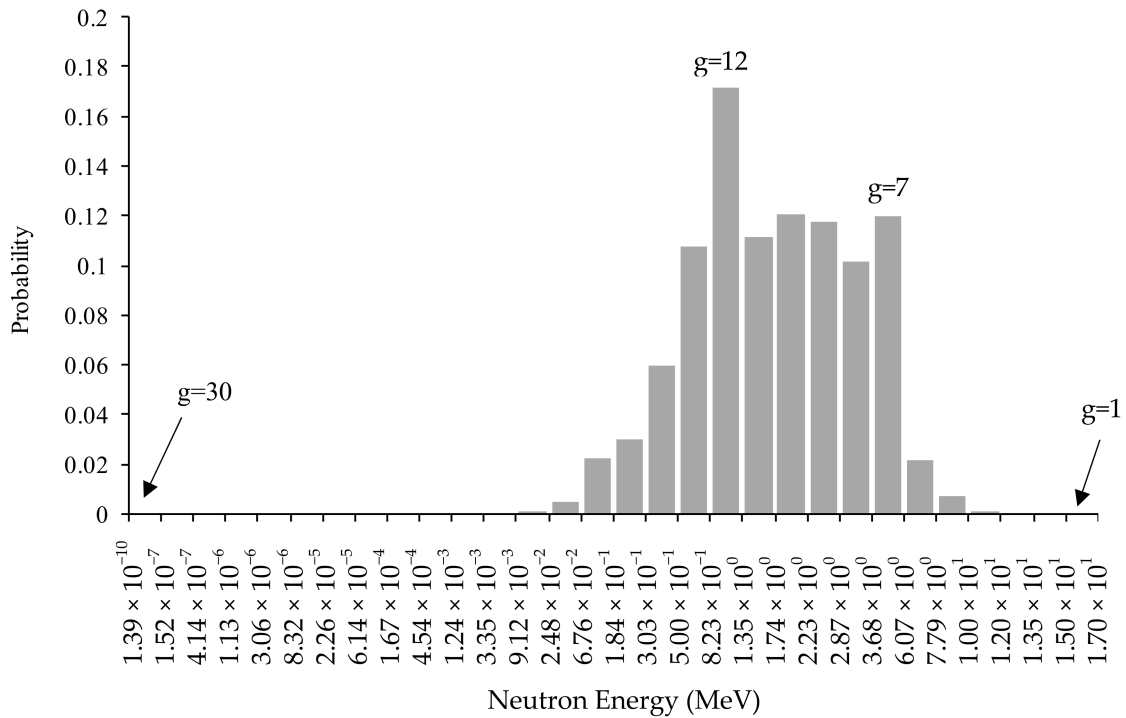
Figure 4. Histogram plot of fission spectrum $\chi_{i=1}^g$, $g = 1, \ldots, 30$ for isotope ^{239}Pu.

5. Computation of the 1st- and 2nd-Order Sensitivities of the PERP Leakage Response to the Average Number of Neutrons Per Fission

This Section reports the computational results for the 1st-order sensitivities $\partial L(\boldsymbol{\alpha})/\partial \boldsymbol{\nu}$ and for the 2nd-order sensitivities $\partial^2 L(\boldsymbol{\alpha})/\partial \boldsymbol{\nu} \partial \boldsymbol{\nu}$. Sections 6–8 report the equations and results for $\partial^2 L(\boldsymbol{\alpha})/\partial \boldsymbol{\nu} \partial \boldsymbol{\sigma}_t$, $\partial^2 L(\boldsymbol{\alpha})/\partial \boldsymbol{\nu} \partial \boldsymbol{\sigma}_s$, $\partial^2 L(\boldsymbol{\alpha})/\partial \boldsymbol{\nu} \partial \boldsymbol{\sigma}_f$, respectively.

5.1. First-Order Sensitivities $\partial L(\boldsymbol{\alpha})/\partial \boldsymbol{\nu}$

The expressions for computing the 1st-order sensitivities of the leakage response with respect to the parameters underlying the average number of neutrons per fission are derived using Equations (152), (156) and (157) in [5], as follows:

$$\left[\frac{\partial L(\boldsymbol{\alpha})}{\partial f_j}\right]_{f=\nu} = \sum_{g=1}^{G} \int_V dV \int_{4\pi} d\boldsymbol{\Omega}\, \psi^{(1),g}(r, \boldsymbol{\Omega}) \sum_{g'=1}^{G} \int_{4\pi} d\boldsymbol{\Omega}' \frac{\partial \left[\left(\nu\Sigma_f\right)^{g'}\right]}{\partial f_j} \chi^g \varphi^{g'}(r, \boldsymbol{\Omega}')\,, \tag{111}$$

$$\text{for } j = J_{\sigma f} + 1, \ldots, J_{\sigma f} + J_\nu,$$

where the parameters f_j, $j = J_{\sigma f} + 1, \ldots, J_{\sigma f} + J_\nu$ correspond to the components of the vector

$\boldsymbol{\nu} \triangleq \left[f_{J_{\sigma f}+1}, \ldots, f_{J_{\sigma f}+J_\nu}\right]^\dagger \triangleq \left[\nu_{i=1}^1, \nu_{i=1}^2, \ldots, \nu_{i=1}^G, \ldots, \nu_i^g, \ldots, \nu_{i=N_f}^1, \ldots, \nu_{i=N_f}^G\right]^\dagger$, $i = 1, \ldots, N_f$; $g = 1, \ldots, G$; $J_\nu = G \times N_f$, as defined in Equation (A13) in Appendix A.

The multigroup adjoint fluxes $\psi^{(1),g}(r, \boldsymbol{\Omega})$, $g = 1, \ldots, G$ in Equation (111) are the solutions of the 1st-Level Adjoint Sensitivity System (1st-LASS) as previously defined in Equations (7) and (8).

When the parameters f_j correspond to the average number of neutrons per fission, i.e., $f_j \equiv \nu_{i_j}^{g_j}$, the following relation holds:

$$\frac{\partial \left[\left(\nu\Sigma_f\right)^{g'}\right]}{\partial f_j} = \frac{\partial \sum_{m=1}^{M} \sum_{i=1}^{I} N_{i,m} \left(\nu\sigma_f\right)_i^{g'}}{\partial \nu_{i_j}^{g_j}} = \frac{\partial \sum_{m=1}^{M} \sum_{i=1}^{I} N_{i,m} \nu_i^{g'} \sigma_{f,i}^{g'}}{\partial \nu_{i_j}^{g_j}} = \delta_{g_j g'} N_{i_j,m_j} \sigma_{f,i_j}^{g'}. \tag{112}$$

Inserting Equation (112) into Equation (111) yields the following simplified expression for computational purposes:

$$\frac{\partial L(\boldsymbol{\alpha})}{\partial v_i^g} = N_{i,m} \int_V dV \sigma_{f,i}^g \varphi_0^g(r) \sum_{g'=1}^{G} \chi^{g'} \xi_0^{(1),g'}(r) \ , \quad i = 1,\ldots,I; \ g = 1,\ldots,G; \ m = 1,\ldots,M. \tag{113}$$

The numerical values of the 1st-order relative sensitivities, $S^{(1)}\left(v_i^g\right) \triangleq \left(\partial L/\partial v_i^g\right)\left(v_i^g/L\right)$, $i = 1, 2$; $g = 1,\ldots,30$, of the leakage response with respect to the average number of neutrons per fission for the two fissionable isotopes contained in the PERP benchmark will be presented in Section 5.3, below, in tables that will also include comparisons with the numerical values of the corresponding 2nd-order unmixed relative sensitivities $S^{(2)}\left(v_i^g, v_i^g\right) \triangleq \left(\partial^2 L/\partial v_i^g \partial v_i^g\right)\left(v_i^g v_i^g/L\right)$, $i = 1, 2$; $g = 1,\ldots,30$.

5.2. Second-Order Sensitivities $\partial^2 L(\boldsymbol{\alpha})/\partial \mathbf{v} \partial \mathbf{v}$

The equations needed for deriving the expression of the 2nd-order sensitivities $\partial^2 L(\boldsymbol{\alpha})/\partial \mathbf{v} \partial \mathbf{v}$ are obtained by particularizing Equation (179) in [5] to the PERP benchmark, which takes the following particular form:

$$
\begin{aligned}
\left(\frac{\partial^2 L}{\partial f_j \partial f_{m_2}}\right)_{(f=v, f=v)} &= \sum_{g=1}^{G} \int_V dV \int_{4\pi} d\boldsymbol{\Omega} \, \psi^{(1),g}(r,\boldsymbol{\Omega}) \sum_{g'=1}^{G} \int_{4\pi} d\boldsymbol{\Omega}' \varphi^{g'}(r,\boldsymbol{\Omega}') \chi^g \frac{\partial^2 \left[(v\Sigma_f)^{g'}\right]}{\partial f_j \partial f_{m_2}} \\
&+ \sum_{g=1}^{G} \int_V dV \int_{4\pi} d\boldsymbol{\Omega} \, u_{1,j}^{(2),g}(r,\boldsymbol{\Omega}) \frac{\partial \left[(v\Sigma_f)^g\right]}{\partial f_{m_2}} \sum_{g'=1}^{G} \int_{4\pi} d\boldsymbol{\Omega}' \chi^{g'} \psi^{(1),g'}(r,\boldsymbol{\Omega}') \\
&+ \sum_{g=1}^{G} \int_V dV \int_{4\pi} d\boldsymbol{\Omega} \, u_{2,j}^{(2),g}(r,\boldsymbol{\Omega}) \sum_{g'=1}^{G} \int_{4\pi} d\boldsymbol{\Omega}' \varphi^{g'}(r,\boldsymbol{\Omega}') \chi^g \frac{\partial \left[(v\Sigma_f)^{g'}\right]}{\partial f_{m_2}}, \\
&\text{for} \quad j = J_{\sigma f} + 1, \ldots, J_{\sigma f} + J_v; m_2 = J_{\sigma f} + 1, \ldots, J_{\sigma f} + J_v,
\end{aligned}
\tag{114}
$$

where the 2nd-level adjoint functions, $u_{1,j}^{(2),g}(r,\boldsymbol{\Omega})$ and $u_{2,j}^{(2),g}(r,\boldsymbol{\Omega})$, $j = J_{\sigma f} + 1,\ldots,J_{\sigma f} + J_v$; $g = 1,\ldots,G$, are the solutions of the following 2nd-Level Adjoint Sensitivity System (2nd-LASS) presented in Equations (183)–(185) in [5]:

$$B^g\left(\boldsymbol{\alpha}^0\right) u_{1,j}^{(2),g}(r,\boldsymbol{\Omega}) = \sum_{g'=1}^{G} \int_{4\pi} d\boldsymbol{\Omega}' \varphi^{g'}(r,\boldsymbol{\Omega}') \chi^g \frac{\partial \left[(v\Sigma_f)^{g'}\right]}{\partial f_j}, j = J_{\sigma f} + 1,\ldots,J_{\sigma f} + J_v; \ g = 1,\ldots,G, \tag{115}$$

$$u_{1,j}^{(2),g}(r_d,\boldsymbol{\Omega}) = 0, \ \boldsymbol{\Omega} \cdot \mathbf{n} < 0; \ j = J_{\sigma f} + 1,\ldots,J_{\sigma f} + J_v; \ g = 1,\ldots,G, \tag{116}$$

$$A^{(1),g}\left(\boldsymbol{\alpha}^0\right) u_{2,j}^{(2),g}(r,\boldsymbol{\Omega}) = \frac{\partial \left[(v\Sigma_f)^g\right]}{\partial f_j} \sum_{g'=1}^{G} \int_{4\pi} d\boldsymbol{\Omega}' \psi^{(1),g'}(r,\boldsymbol{\Omega}') \chi^{g'}, j = J_{\sigma f} + 1,\ldots,J_{\sigma f} + J_v; \ g = 1,\ldots,G, \tag{117}$$

$$u_{2,j}^{(2),g}(r_d,\boldsymbol{\Omega}) = 0, \ \boldsymbol{\Omega} \cdot \mathbf{n} > 0; \ j = J_{\sigma f} + 1,\ldots,J_{\sigma f} + J_v; \ g = 1,\ldots,G. \tag{118}$$

The parameters f_j and f_{m_2} in Equations (114), (115) and (117) correspond to the average number of neutrons per fission, and are therefore denoted as $f_j \equiv v_{i_j}^{g_j}$ and $f_{m_2} \equiv v_{i_{m_2}}^{g_{m_2}}$, respectively. Noting that,

$$\frac{\partial^2 \Sigma_t^g}{\partial f_j \partial f_{m_2}} = \frac{\partial^2 \Sigma_t^g}{\partial v_{i_j}^{g_j} \partial v_{i_{m_2}}^{g_{m_2}}} = \frac{\partial \left[\frac{\partial \Sigma_t^g}{\partial v_{i_j}^{g_j}}\right]}{\partial v_{i_{m_2}}^{g_{m_2}}} = 0, \tag{119}$$

$$
\frac{\partial\left[(\nu\Sigma_f)^g\right]}{\partial f_{m_2}} = \frac{\partial \sum\limits_{m=1}^{M} \sum\limits_{i=1}^{I} N_{i,m}(\nu\sigma_f)_i^g}{\partial \nu_{i_{m_2}}^{g_{m_2}}} = \frac{\partial \sum\limits_{m=1}^{M} \sum\limits_{i=1}^{I} N_{i,m}\nu_i^g \sigma_{f,i}^g}{\partial \nu_{i_{m_2}}^{g_{m_2}}} = \delta_{g_{m_2}g} N_{i_{m_2},m_{m_2}} \sigma_{f,i_{m_2}}^g, \tag{120}
$$

$$
\frac{\partial\left[(\nu\Sigma_f)^{g'}\right]}{\partial f_{m_2}} = \frac{\partial \sum\limits_{m=1}^{M} \sum\limits_{i=1}^{I} N_{i,m}(\nu\sigma_f)_i^{g'}}{\partial \nu_{i_{m_2}}^{g_{m_2}}} = \frac{\partial \sum\limits_{m=1}^{M} \sum\limits_{i=1}^{I} N_{i,m}\nu_i^{g'} \sigma_{f,i}^{g'}}{\partial \nu_{i_{m_2}}^{g_{m_2}}} = \delta_{g_{m_2}g'} N_{i_{m_2},m_{m_2}} \sigma_{f,i_{m_2}}^{g'}, \tag{121}
$$

$$
\frac{\partial\left[(\nu\Sigma_f)^g\right]}{\partial f_j} = \frac{\partial \sum\limits_{m=1}^{M} \sum\limits_{i=1}^{I} N_{i,m}(\nu\sigma_f)_i^g}{\partial \nu_{i_j}^{g_j}} = \frac{\partial \sum\limits_{m=1}^{M} \sum\limits_{i=1}^{I} N_{i,m}\nu_i^g \sigma_{f,i}^g}{\partial \nu_{i_j}^{g_j}} = \delta_{g_j g} N_{i_j,m_j} \sigma_{f,i_j}^g, \tag{122}
$$

and inserting the results obtained in Equation (112) and Equations (119)–(122) into Equations (115), (117) and (114) reduces the latter equation to the following simplified expression:

$$
\left(\frac{\partial^2 L}{\partial f_j \partial f_{m_2}}\right)_{(f=\nu, f=\nu)} = N_{i_{m_2},m_{m_2}} \sigma_{f,i_{m_2}}^{g_{m_2}} \int_V dV \left[U_{1,j;0}^{(2),g_{m_2}}(r) \sum\limits_{g'=1}^{G} \chi^{g'} \xi_0^{(1),g'}(r) + \varphi_0^{g_{m_2}}(r) \sum\limits_{g=1}^{G} \chi^g U_{2,j;0}^{(2),g}(r) \right], \tag{123}
$$

$$
for \quad j = J_{\sigma f}+1,\dots,J_{\sigma f}+J_\nu; m_2 = J_{\sigma f}+1,\dots,J_{\sigma f}+J_\nu,
$$

where the 2nd-level adjoint functions, $u_{1,j}^{(2),g}(r,\mathbf{\Omega})$ and $u_{2,j}^{(2),g}(r,\mathbf{\Omega})$, $j = J_{\sigma f}+1,\dots,J_{\sigma f}+J_\nu$; $g = 1,\dots,G$ are the solutions of the following simplified form of the 2nd-Level Adjoint Sensitivity System (2nd-LASS) obtained from Equations (115) and (117):

$$
B^g(\boldsymbol{\alpha}^0) u_{1,j}^{(2),g}(r,\mathbf{\Omega}) = N_{i_j,m_j} \sigma_{f,i_j}^{g_j} \chi^g \varphi_0^{g_j}(r), \quad j = J_{\sigma f}+1,\dots,J_{\sigma f}+J_\nu; g = 1,\dots,G, \tag{124}
$$

$$
A^{(1),g}(\boldsymbol{\alpha}^0) u_{2,j}^{(2),g}(r,\mathbf{\Omega}) = \delta_{g_j g} N_{i_j,m_j} \sigma_{f,i_j}^{g_j} \sum\limits_{g'=1}^{G} \chi^{g'} \xi_0^{(1),g'}(r), \quad j = J_{\sigma f}+1,\dots,J_{\sigma f}+J_\nu; g = 1,\dots,G, \tag{125}
$$

and subject to the boundary conditions shown in Equations (116) and (118), respectively.

5.3. Numerical Results for $\partial^2 L(\boldsymbol{\alpha})/\partial\mathbf{v}\partial\mathbf{v}$

The 2nd-order absolute sensitivities of the leakage response with respect to the parameters underlying the average number of neutrons per fission, i.e., $\partial^2 L/\partial\nu_i^g \partial\nu_k^{g'}$, $i,k = 1,\dots,N_f$; $g,g' = 1,\dots,G$, for the $N_f = 2$ fissionable isotopes and $G = 30$ energy groups of the PERP benchmark are computed using Equation (123). The (Hessian) matrix $(\partial^2 L/\partial f_j \partial f_{m_2})_{(f=\nu, f=\nu)}$, $j, m_2 = J_{\sigma f}+1,\dots,J_{\sigma f}+J_\nu$ of the 2nd-order absolute sensitivities has dimensions $J_\nu \times J_\nu (= 60 \times 60)$, since $J_\nu = G \times N_f = 30 \times 2$. The relative sensitivities corresponding to $(\partial^2 L/\partial f_j \partial f_{m_2})_{(f=\nu, f=\nu)}$, $j, m_2 = J_{\sigma f}+1,\dots,J_{\sigma f}+J_\nu$, which are denoted as $\mathbf{S}^{(2)}(\nu_i^g, \nu_k^{g'})$ and are defined as follows:

$$
\mathbf{S}^{(2)}(\nu_i^g, \nu_k^{g'}) \triangleq \frac{\partial^2 L}{\partial\nu_i^g \partial\nu_k^{g'}}\left(\frac{\nu_i^g \nu_k^{g'}}{L}\right), \quad i,k = 1,2; \ g,g' = 1,\dots,30. \tag{126}
$$

The numerical results obtained for the matrix $\mathbf{S}^{(2)}(\nu_i^g, \nu_k^{g'})$, $i,k = 1,2$; $g,g' = 1,\dots,30$ have been partitioned into $N_f \times N_f = 4$ submatrices, each of dimensions $G \times G (= 30 \times 30)$, and the summary of the main features of each submatrix is presented in Table 12.

Table 12. Summary presentation of the matrix $\mathbf{S}^{(2)}\left(v_i^g, v_k^{g'}\right)$, $i, k = 1, 2$; $g, g' = 1, \ldots, 30$.

Isotopes	k=1 (^{239}Pu)	k=2 (^{240}Pu)
$i = 1$ (^{239}Pu)	$\mathbf{S}^{(2)}\left(v_1^g, v_1^{g'}\right)$ 52 elements with absolute values > 1.0	$\mathbf{S}^{(2)}\left(v_1^g, v_2^{g'}\right)$ Max. value = 1.54×10^{-1} at $g = 12$, $g' = 12$
$i = 2$ (^{240}Pu)	$\mathbf{S}^{(2)}\left(v_2^g, v_1^{g'}\right)$ Max. value = 1.54×10^{-1} at $g = 12$, $g' = 12$	$\mathbf{S}^{(2)}\left(v_2^g, v_2^{g'}\right)$ Max. value = 8.01×10^{-3} at $g = 12$, $g' = 12$

The 2nd-order mixed sensitivities $\mathbf{S}^{(2)}\left(v_i^g, v_k^{g'}\right)$, $i, k = 1, 2$; $g, g' = 1, \ldots, 30$ are all positive. Most of the $J_v \times J_v$ (= 60×60) elements are very small, but 52 elements have very large relative sensitivities, with values greater than 1.0, as summarized in Table 12. All of these 52 large sensitivities belong to the sub-matrix $\mathbf{S}^{(2)}\left(v_1^g, v_1^{g'}\right)$, and relate to the parameters corresponding to the average number of neutrons per fission in isotope ^{239}Pu. The overall maximum relative sensitivity is $S^{(2)}\left(v_1^{12}, v_1^{12}\right) = 2.963$. Additional details about the sub-matrix $\mathbf{S}^{(2)}\left(v_1^g, v_1^{g'}\right)$, $g, g' = 1, \ldots, 30$ is provided in the following Section. Also noted in Table 12 is that all of the mixed 2nd-order relative sensitivities involving v_2^g, $g = 1, \ldots, G$ have absolute values smaller than 1.0. The elements with the maximum absolute value in each of the respective submatrices relate to the 12th energy group of v_i^g for isotopes ^{239}Pu and ^{240}Pu.

5.3.1. Second-Order Unmixed Relative Sensitivities $S^{(2)}\left(v_i^g, v_i^g\right)$, $i = 1, 2$; $g = 1, \ldots, 30$

The 2nd-order unmixed sensitivities $S^{(2)}\left(v_i^g, v_i^g\right) \triangleq \left(\partial^2 L / \partial v_i^g \partial v_i^g\right)\left(v_i^g v_i^g / L\right)$, $i = 1, 2$; $g = 1, \ldots, 30$, which are the elements on the diagonal of the matrix $S^{(2)}\left(v_i^g, v_k^{g'}\right)$, $i, k = 1, 2$; $g, g' = 1, \ldots, 30$, can be directly compared to the values of the 1st-order relative sensitivities $S^{(1)}\left(v_i^g\right) \triangleq \left(\partial L / \partial v_i^g\right)\left(v_i^g / L\right)$, $i = 1, 2$; $g = 1, \ldots, 30$, for the leakage response with respect to the average number of neutrons per fission.

Table 13 presents the results obtained for the 1st- and 2nd-order unmixed relative sensitivities with respect to the average number of neutrons per fission $\mathbf{v}$ for isotope 1 (^{239}Pu). These results indicate that for energy groups $g = 7, \ldots, 14$, the values of the 2nd-order sensitivities are significantly larger than the corresponding values of the 1st-order sensitivities for the same energy group; for other energy groups, the 2nd-order relative sensitivities are smaller than the corresponding values of the 1st-order sensitivities. All of the 1st- and 2nd-order relative sensitivities are positive, and the largest values for the 1st-order and 2nd-order relative sensitivities are both related to the 12th energy group.

Table 14 presents the 1st-order and 2nd-order unmixed relative sensitivities for isotope 2 (^{240}Pu). The results in this table indicate that the values for both the 1st- and 2nd-order relative sensitivities are all very small, and the values of the 2nd-order unmixed relative sensitivities are at least one order of magnitude smaller than the corresponding values of the 1st-order ones for all energy groups. The largest 1st-order relative sensitivity is $S^{(1)}\left(v_{i=2}^{12}\right) = 6.316 \times 10^{-2}$, and the largest 2nd-order unmixed relative sensitivity is $S^{(2)}\left(v_{i=2}^{12}, v_{k=2}^{12}\right) = 8.011 \times 10^{-3}$, both occur for the 12th energy group of the average number of neutrons per fission for isotope ^{240}Pu.

Table 13. 1st-order relative sensitivities $\left(\partial L/\partial v_{i=1}^g\right)\left(v_{i=1}^g/L\right), g = 1,\ldots,30$ and 2nd-order relative sensitivities $\left(\partial^2 L/\partial v_1^g \partial v_1^g\right)\left(v_1^g v_1^g/L\right)$, $g = 1,\ldots,30$, for isotope 1 (^{239}Pu).

g	1st-Order	2nd-Order	g	1st-Order	2nd-Order
1	0.0005266	0.0000006	16	0.297	0.177
2	0.0010690	0.0000025	17	0.117	0.027
3	0.0030646	0.0000206	18	0.068	0.009
4	0.0140	0.0004	19	0.060	0.007
5	0.0672	0.0097	20	0.065	0.009
6	0.169	0.060	21	0.071	0.010
7	0.762	**1.192**	22	0.064	0.008
8	0.659	0.880	23	0.064	0.008
9	0.802	**1.299**	24	0.042	0.004
10	0.843	**1.430**	25	0.055	0.006
11	0.786	**1.243**	26	0.051	0.005
12	**1.215**	**2.963**	27	0.026	0.001
13	0.847	**1.444**	28	0.012	0.0003
14	0.555	0.620	29	0.034	0.002
15	0.321	0.208	30	0.461	0.429

Table 14. Comparison of 1st-order relative sensitivities $\left(\partial L/\partial v_{i=2}^g\right)\left(v_{i=2}^g/L\right), g = 1,\ldots,30$ and 2nd-order relative sensitivities $\left(\partial^2 L/\partial v_2^g \partial v_2^g\right)\left(v_2^g v_2^g/L\right)$, $g = 1,\ldots,30$, for isotope 2 (^{240}Pu).

g	1st-Order	2nd-Order	g	1st-Order	2nd-Order
1	3.278×10^{-5}	2.395×10^{-9}	16	9.569×10^{-4}	1.834×10^{-6}
2	6.388×10^{-5}	9.027×10^{-9}	17	4.337×10^{-4}	3.745×10^{-7}
3	1.790×10^{-4}	7.043×10^{-8}	18	2.251×10^{-4}	1.009×10^{-7}
4	8.648×10^{-4}	1.627×10^{-6}	19	1.278×10^{-4}	3.261×10^{-8}
5	4.197×10^{-3}	3.767×10^{-5}	20	2.292×10^{-4}	1.050×10^{-7}
6	1.003×10^{-2}	2.115×10^{-4}	21	1.298×10^{-4}	3.374×10^{-8}
7	4.313×10^{-2}	3.819×10^{-3}	22	1.227×10^{-5}	3.019×10^{-10}
8	3.774×10^{-2}	2.890×10^{-3}	23	8.578×10^{-6}	1.480×10^{-10}
9	4.397×10^{-2}	3.904×10^{-3}	24	1.631×10^{-6}	5.347×10^{-12}
10	4.475×10^{-2}	4.034×10^{-3}	25	7.522×10^{-6}	1.140×10^{-10}
11	3.985×10^{-2}	3.192×10^{-3}	26	1.225×10^{-7}	3.010×10^{-14}
12	6.316×10^{-2}	8.011×10^{-3}	27	8.661×10^{-6}	1.505×10^{-10}
13	2.649×10^{-2}	1.411×10^{-3}	28	9.563×10^{-6}	1.845×10^{-10}
14	4.768×10^{-3}	4.572×10^{-5}	29	4.853×10^{-8}	4.752×10^{-15}
15	1.289×10^{-3}	3.338×10^{-6}	30	2.463×10^{-6}	1.222×10^{-11}

5.3.2. Second-Order Relative Sensitivities $\mathbf{S}^{(2)}\left(v_{i=1}^g, v_{k=1}^{g'}\right), g, g' = 1,\ldots,30$

Table 15 presents the 2nd-order mixed relative sensitivity results obtained for $\mathbf{S}^{(2)}\left(v_1^g, v_1^{g'}\right) \triangleq \left(\partial^2 L/\partial v_{i=1}^g \partial v_{k=1}^{g'}\right)\left(v_{i=1}^g v_{k=1}^{g'}/L\right)$, $g, g' = 1,\ldots,30$, for the leakage response with respect to the parameters underlying the average number of neutrons per fission of isotope ^{239}Pu. The majority of the larger 2nd-order relative sensitivities are concentrated in the energy region confined by the energy groups $g = 7,\ldots,14$ and $g' = 7,\ldots,14$. Shown in bold in Table 15 are the numerical values of 52 elements that have values greater than 1.0. The largest value among these sensitivities is attained by the relative 2nd-order unmixed sensitivity $S^{(2)}\left(v_1^{g=12}, v_1^{g'=12}\right) = 2.963$.

Table 15. Components of $\mathbf{S}^{(2)}\left(v_1^g, v_1^{g'}\right)$, $g, g' = 1, \ldots, 30$ having values greater than 1.0.

Groups	$g' = 6$	7	8	9	10	11	12	13	14	15
$g = 6$	0.060	0.267	0.230	0.279	0.293	0.273	0.422	0.294	0.193	0.112
7	0.267	**1.192**	**1.024**	**1.244**	**1.306**	**1.217**	**1.879**	**1.312**	0.860	0.497
8	0.230	**1.024**	**0.880**	**1.069**	**1.122**	**1.046**	**1.615**	**1.127**	0.739	0.427
9	0.279	**1.244**	**1.069**	**1.299**	**1.363**	**1.271**	**1.962**	**1.370**	0.897	0.519
10	0.293	**1.306**	**1.122**	**1.363**	**1.430**	**1.333**	**2.059**	**1.437**	0.942	0.545
11	0.273	**1.217**	**1.046**	**1.271**	**1.333**	**1.243**	**1.919**	**1.340**	0.878	0.508
12	0.422	**1.879**	**1.615**	**1.962**	**2.059**	**1.919**	**2.963**	**2.068**	**1.356**	0.784
13	0.294	**1.312**	**1.127**	**1.370**	**1.437**	**1.340**	**2.068**	**1.444**	0.946	0.547
14	0.193	0.860	0.739	0.897	0.942	0.878	1.356	0.946	0.620	0.359
15	0.112	0.497	0.427	0.519	0.545	0.508	0.784	0.547	0.359	0.208

In addition to the sensitivities presented in Table 15, the following 2nd-order relative sensitivities in the matrix $\mathbf{S}^{(2)}\left(v_1^g, v_1^{g'}\right)$, $g, g' = 1, \ldots, 30$ have values greater than 1.0: $S^{(2)}\left(v_{i=1}^{30}, v_{k=1}^{12}\right) = S^{(2)}\left(v_{i=1}^{12}, v_{k=1}^{30}\right) = 1.062$. Also, as shown in Table 15, the values of the mixed sensitivities in row $g = 12$ are the largest among all $g = 1, \ldots, 30$ rows. Likewise, the values of the mixed sensitivities in column $g' = 12$ are the largest among all groups $g' = 1, \ldots, 30$.

6. Mixed Second-Order Sensitivities of the PERP Total Leakage Response with Respect to the Parameters Underlying the Average Number of Neutrons Per Fission and Total Cross Sections

This section presents the computation and analysis of the numerical results for the 2nd-order mixed sensitivities $\partial^2 L(\boldsymbol{\alpha}) / \partial \mathbf{v} \partial \boldsymbol{\sigma}_t$ of the leakage response with respect to the average number of neutrons per fission and total microscopic cross sections of all isotopes of the PERP benchmark. Similarly, these mixed sensitivities can be computed using either the computation of $\partial^2 L(\boldsymbol{\alpha}) / \partial \mathbf{v} \partial \boldsymbol{\sigma}_t$ or the computation of $\partial^2 L(\boldsymbol{\alpha}) / \partial \boldsymbol{\sigma}_t \partial \mathbf{v}$. These two distinct paths will be presented in Sections 6.1 and 6.2, respectively.

6.1. Second-Order Sensitivities $\partial^2 L(\boldsymbol{\alpha}) / \partial \mathbf{v} \partial \boldsymbol{\sigma}_t$

The equations needed for deriving the expression of the 2nd-order sensitivities $\partial^2 L(\boldsymbol{\alpha}) / \partial \mathbf{v} \partial \boldsymbol{\sigma}_t$ are obtained by particularizing Equation (177) in [5] to the PERP benchmark, which takes the following form:

$$\left(\frac{\partial^2 L}{\partial f_j \partial t_{m_2}}\right)_{(f=v, t=\sigma_t)} = -\sum_{g=1}^{G} \int_V dV \int_{4\pi} d\mathbf{\Omega} \left[u_{1,j}^{(2),g}(r, \mathbf{\Omega}) \psi^{(1),g}(r, \mathbf{\Omega}) + u_{2,j}^{(2),g}(r, \mathbf{\Omega}) \varphi^g(r, \mathbf{\Omega})\right] \frac{\partial \Sigma_t^g}{\partial t_{m_2}},$$

$$for \quad j = J_{\sigma f} + 1, \ldots, J_{\sigma f} + J_v; \quad m_2 = 1, \ldots, J_{\sigma t}. \tag{127}$$

The parameters f_j and t_{m_2} in Equation (127) correspond to the average number of neutrons per fission and total cross sections, and are therefore denoted as $f_j \equiv v_{i_j}^{g_j}$ and $t_{m_2} \equiv \sigma_{t,i_{m_2}}^{g_{m_2}}$, respectively.

Inserting the results obtained in Equation (50) into Equation (127), yields:

$$\left(\frac{\partial^2 L}{\partial f_j \partial t_{m_2}}\right)_{(f=v, t=\sigma_t)} = -N_{i_{m_2}, m_{m_2}} \int_V dV \int_{4\pi} d\mathbf{\Omega} \left[u_{1,j}^{(2),g_{m_2}}(r, \mathbf{\Omega}) \psi^{(1),g_{m_2}}(r, \mathbf{\Omega}) + u_{2,j}^{(2),g_{m_2}}(r, \mathbf{\Omega}) \varphi^{g_{m_2}}(r, \mathbf{\Omega})\right],$$

$$for \quad j = J_{\sigma f} + 1, \ldots, J_{\sigma f} + J_v; \quad m_2 = 1, \ldots, J_{\sigma t}. \tag{128}$$

6.2. Alternative Path: Computing the Second-Order Sensitivities $\partial^2 L(\boldsymbol{\alpha})/\partial\boldsymbol{\sigma}_t\partial\boldsymbol{\nu}$

The equations needed for deriving the expression for $\partial^2 L(\boldsymbol{\alpha})/\partial\boldsymbol{\sigma}_t\partial\boldsymbol{\nu}$ are obtained by particularizing Equation (160) in [5] to the PERP benchmark, which takes the following form:

$$
\begin{aligned}
\left(\frac{\partial^2 L}{\partial t_j\partial f_{m_2}}\right)_{(t=\sigma_t,f=\nu)} &= \sum_{g=1}^{G}\int_V dV\int_{4\pi}d\boldsymbol{\Omega}\,\psi_{1,j}^{(2),g}(r,\boldsymbol{\Omega})\frac{\partial\left[(\nu\Sigma_f)^g\right]}{\partial f_{m_2}}\sum_{g'=1}^{G}\int_{4\pi}d\boldsymbol{\Omega}'\chi^{g'}\psi^{(1),g'}(r,\boldsymbol{\Omega}') \\
&+ \sum_{g=1}^{G}\int_V dV\int_{4\pi}d\boldsymbol{\Omega}\,\psi_{2,j}^{(2),g}(r,\boldsymbol{\Omega})\sum_{g'=1}^{G}\int_{4\pi}d\boldsymbol{\Omega}'\varphi^{g'}(r,\boldsymbol{\Omega}')\chi^g\frac{\partial\left[(\nu\Sigma_f)^{g'}\right]}{\partial f_{m_2}}, \\
&\quad for\ \ j=1,\ldots,J_{\sigma t};\ \ m_2=J_{\sigma f}+1,\ldots,J_{\sigma f}+J_\nu\,,
\end{aligned}
\tag{129}
$$

where the adjoint functions $\psi_{1,j}^{(2),g}(r,\boldsymbol{\Omega})$ and $\psi_{2,j}^{(2),g}(r,\boldsymbol{\Omega})$, $j=1,\ldots,J_{\sigma t}$; $g=1,\ldots,G$ are the solutions of the 2nd-Level Adjoint Sensitivity System (2nd-LASS) presented in Equations (32), (34), (39) and (40) of Part I [1], which have been reproduced as Equations (57)–(60) in Section 3.2.

The parameters t_j and f_{m_2} in Equation (129) correspond to the total cross sections and the average number of neutrons per fission, respectively, and are therefore denoted as $t_j\equiv\sigma_{t,i_j}^{g_j}$ and $f_{m_2}\equiv\nu_{i_{m_2}}^{g_{m_2}}$. Inserting the results obtained in Equations (121) and (122) into Equation (129) yields:

$$
\begin{aligned}
\left(\frac{\partial^2 L}{\partial t_j\partial f_{m_2}}\right)_{(t=\sigma_t,f=\nu)} &= N_{i_{m_2},m_{m_2}}\sigma_{f,i_{m_2}}^{g_{m_2}}\int_V dV\left[\xi_{1,j;0}^{(2),g_{m_2}}(r)\sum_{g'=1}^{G}\chi^{g'}\xi_0^{(1),g'}(r)+\varphi_0^{g_{m_2}}(r)\sum_{g=1}^{G}\chi^g\xi_{2,j;0}^{(2),g}(r)\right], \\
&\quad for\ \ j=1,\ldots,J_{\sigma t};\ \ m_2=J_{\sigma f}+1,\ldots,J_{\sigma f}+J_\nu\,,
\end{aligned}
\tag{130}
$$

where the flux moments $\xi_{1,j;0}^{(2),g_{m_2}}(r)$ and $\xi_{2,j;0}^{(2),g}(r)$ have been defined in Equations (43) and (44).

6.3. Numerical Results for $\partial^2 L(\boldsymbol{\alpha})/\partial\boldsymbol{\nu}\partial\boldsymbol{\sigma}_t$

The second-order absolute sensitivities, $\partial^2 L(\boldsymbol{\alpha})/\partial\boldsymbol{\nu}\partial\boldsymbol{\sigma}_t$, of the leakage response with respect to the average number of neutrons per fission and the total cross sections for all isotopes of the PERP benchmark have been computed using Equation (128), and have been independently verified by computing $\partial^2 L(\boldsymbol{\alpha})/\partial\boldsymbol{\sigma}_t\partial\boldsymbol{\nu}$ using Equation (130). Similarly, computing $\partial^2 L(\boldsymbol{\alpha})/\partial\boldsymbol{\nu}\partial\boldsymbol{\sigma}_t$ by using Equation (128) requires 120 PARTISN computations while computing $\partial^2 L(\boldsymbol{\alpha})/\partial\boldsymbol{\sigma}_t\partial\boldsymbol{\nu}$ using Equation (130) requires $J_{\sigma t}=G\times I=30\times 6=360$ PARTISN computations. Thus, computing $\partial^2 L(\boldsymbol{\alpha})/\partial\boldsymbol{\nu}\partial\boldsymbol{\sigma}_t$ using Equation (128) is 3 times more efficient than computing $\partial^2 L(\boldsymbol{\alpha})/\partial\boldsymbol{\sigma}_t\partial\boldsymbol{\nu}$ using Equation (130).

The matrix $\left(\partial^2 L/\partial f_j\partial t_{m_2}\right)_{(f=\nu,t=\sigma_t)}$, $j=J_{\sigma f}+1,\ldots,J_{\sigma f}+J_\nu$; $m_2=1,\ldots,J_{\sigma f}$; has dimensions $J_\nu\times J_{\sigma t}\,(=\ 60\times 180)$. The matrix of 2nd-order relative sensitivities corresponding to $\left(\partial^2 L/\partial f_j\partial t_{m_2}\right)_{(f=\nu,t=\sigma_t)}$, $j=J_{\sigma f}+1,\ldots,J_{\sigma f}+J_\nu$; $m_2=1,\ldots,J_{\sigma f}$; denoted as $\mathbf{S}^{(2)}\left(\nu_i^g,\sigma_{t,k}^{g'}\right)$, is defined as follows:

$$
\mathbf{S}^{(2)}\left(\nu_i^g,\sigma_{t,k}^{g'}\right)\triangleq\frac{\partial^2 L}{\partial\nu_i^g\partial\sigma_{t,k}^{g'}}\left(\frac{\partial\nu_i^g\partial\sigma_{t,k}^{g'}}{L}\right),\ \ i=1,2;\ k=1,\ldots,6;\ g,g'=1,\ldots,30.
\tag{131}
$$

To facilitate the presentation and interpretation of the numerical results, the $J_\nu\times J_{\sigma t}\,(=60\times 180)$ matrix $\mathbf{S}^{(2)}\left(\nu_i^g,\sigma_{t,k}^{g'}\right)$ has been partitioned into $N_f\times I=2\times 6$ submatrices, each of dimensions $G\times G=30\times 30$. The main features of each of these submatrices is presented in Table 16.

Table 16. Summary presentation of the matrix $\mathbf{S}^{(2)}\left(v_i^g, \sigma_{t,k}^{g'}\right)$.

Isotopes	k=1 (^{239}Pu)	k=2 (^{240}Pu)	k=3 (^{69}Ga)	k=4 (^{71}Ga)	k=5 (C)	k=6 (^{1}H)
$i = 1$ (^{239}Pu)	$\mathbf{S}^{(2)}\left(v_1^g, \sigma_{t,1}^{g'}\right)$ 72 elements with absolute values > 1.0	$\mathbf{S}^{(2)}\left(v_1^g, \sigma_{t,2}^{g'}\right)$ Min. value = -2.39×10^{-1} at $g = 12$, $g' = 12$	$\mathbf{S}^{(2)}\left(v_1^g, \sigma_{t,3}^{g'}\right)$ Min. value = -1.08×10^{-2} at $g = 12$, $g' = 12$	$\mathbf{S}^{(2)}\left(v_1^g, \sigma_{t,4}^{g'}\right)$ Min. value = -7.31×10^{-3} at $g = 12$, $g' = 12$	$\mathbf{S}^{(2)}\left(v_1^g, \sigma_{t,5}^{g'}\right)$ 7 elements with absolute values > 1.0	$\mathbf{S}^{(2)}\left(v_1^g, \sigma_{t,6}^{g'}\right)$ 99 elements with absolute values > 1.0
$i = 2$ (^{240}Pu)	$\mathbf{S}^{(2)}\left(v_2^g, \sigma_{t,1}^{g'}\right)$ Min. value = -1.97×10^{-1} at $g = 12$, $g' = 12$	$\mathbf{S}^{(2)}\left(v_2^g, \sigma_{t,2}^{g'}\right)$ Min. value = -1.25×10^{-2} at $g = 12$, $g' = 12$	$\mathbf{S}^{(2)}\left(v_2^g, \sigma_{t,3}^{g'}\right)$ Min. value = -5.60×10^{-4} at $g = 12$, $g' = 12$	$\mathbf{S}^{(2)}\left(v_2^g, \sigma_{t,4}^{g'}\right)$ Min. value = -3.80×10^{-4} at $g = 12$, $g' = 12$	$\mathbf{S}^{(2)}\left(v_2^g, \sigma_{t,5}^{g'}\right)$ Min. value = -8.41×10^{-2} at $g = 12$, $g' = 30$	$\mathbf{S}^{(2)}\left(v_2^g, \sigma_{t,6}^{g'}\right)$ 1 element with absolute value > 1.0

Most of the values of the $J_v \times J_{\sigma t}$ ($= 10{,}800$) elements in the matrix $\mathbf{S}^{(2)}\left(v_i^g, \sigma_{t,k}^{g'}\right)$, $i = 1, 2$; $k = 1, \ldots, 6$; $g, g' = 1, \ldots, 30$ are very small, and the majority (10,780 out of 10,800) of these elements have negative values. The results in Table 16 indicate that, when the 2nd-order mixed relative sensitivities involve v_2^g, $g = 1, \ldots, 30$ or the total cross sections of isotopes ^{240}Pu, ^{69}Ga and ^{71}Ga, their absolute values are all smaller than 1.0, except for one element in the submatrix $\mathbf{S}^{(2)}\left(v_2^g, \sigma_{t,6}^{g'}\right)$. The element with the most negative value in each of the submatrices is always related to v_i^g, $i = 1, 2$ for the 12th energy group and $\sigma_{t,k}^{g'}$, $k = 1, \ldots, 6$ for either the 12th or the 30th energy group. There are 179 elements with large relative sensitivities, having absolute values greater than 1.0, as indicated in Table 16. Those large sensitivities reside in the submatrices $\mathbf{S}^{(2)}\left(v_1^g, \sigma_{t,1}^{g'}\right)$, $\mathbf{S}^{(2)}\left(v_1^g, \sigma_{t,5}^{g'}\right)$, $\mathbf{S}^{(2)}\left(v_1^g, \sigma_{t,6}^{g'}\right)$ and $\mathbf{S}^{(2)}\left(v_2^g, \sigma_{t,6}^{g'}\right)$, respectively, and 178 out of the 179 large sensitivities involve the average number of neutrons per fission of isotope ^{239}Pu, namely, v_1^g, and the total cross sections of isotopes ^{239}Pu, C and ^{1}H. Of the sensitivities summarized in Table 16, the single largest relative value is $S^{(2)}\left(v_1^{12}, \sigma_{t,6}^{30}\right) = -19.29$.

6.3.1. Second-Order Relative Sensitivities $\mathbf{S}^{(2)}\left(v_1^g, \sigma_{t,1}^{g'}\right)$, $g, g' = 1, \ldots, 30$

The submatrix $\mathbf{S}^{(2)}\left(v_{i=1}^g, \sigma_{t,k=1}^{g'}\right) \triangleq \left(\partial^2 L / \partial v_{i=1}^g \partial \sigma_{t,k=1}^{g'}\right)\left(v_{i=1}^g \sigma_{t,k=1}^{g'} / L\right)$ comprises the 2nd-order mixed relative sensitivity results obtained for, $g, g' = 1, \ldots, 30$, for the leakage response with respect to the average number of neutrons per fission of ^{239}Pu and to the total microscopic cross sections of ^{239}Pu. All elements in this submatrix have negative 2nd-order relative sensitivities. The largest 2nd-order mixed relative sensitivities are concentrated in the energy region confined by the energy groups $g = 7, \ldots, 14$ and $g' = 7, \ldots, 16$. The numerical values of these large elements are presented in Table 17, which indicates (in bold) the 72 elements that have values greater than 1.0. The largest absolute value in this submatrix is attained by the relative 2nd-order mixed sensitivity $S^{(2)}\left(v_{i=1}^{g=12}, \sigma_{t,k=1}^{g'=12}\right) = -3.785$, involving the parameters representing the average number of neutrons per fission and total cross section of isotope ^{239}Pu in the 12th energy group.

Table 17. Components of $\mathbf{S}^{(2)}\left(v_{i=1}^g, \sigma_{t,k=1}^{g'}\right)$, $g, g' = 1, \ldots, 30$ having values greater than 1.0.

Groups	$g' = 6$	7	8	9	10	11	12	13	14	15	16
$g = 6$	−0.139	−0.256	−0.236	−0.274	−0.274	−0.251	−0.426	−0.373	−0.310	−0.226	−0.257
7	−0.202	**−1.635**	**−1.051**	**−1.220**	**−1.222**	**−1.119**	**−1.901**	**−1.666**	**−1.382**	**−1.008**	**−1.146**
8	−0.172	−0.997	**−1.334**	**−1.049**	**−1.051**	−0.962	**−1.634**	**−1.432**	**−1.188**	−0.866	−0.985
9	−0.209	**−1.207**	**−1.124**	**−1.787**	**−1.277**	**−1.169**	**−1.986**	**−1.740**	**−1.444**	**−1.053**	**−1.197**
10	−0.220	**−1.262**	**−1.165**	**−1.363**	**−1.856**	**−1.226**	**−2.084**	**−1.826**	**−1.515**	**−1.105**	**−1.257**
11	−0.205	**−1.178**	**−1.083**	**−1.259**	**−1.275**	**−1.612**	**−1.942**	**−1.702**	**−1.413**	**−1.030**	**−1.171**
12	−0.316	**−1.825**	**−1.677**	**−1.948**	**−1.953**	**−1.802**	**−3.785**	**−2.629**	**−2.181**	**−1.590**	**−1.809**
13	−0.221	**−1.279**	**−1.176**	**−1.366**	**−1.369**	**−1.252**	**−2.148**	**−2.513**	**−1.523**	**−1.110**	**−1.263**
14	−0.145	−0.840	−0.773	−0.898	−0.900	−0.825	**−1.406**	**−1.247**	**−1.565**	−0.728	−0.828
15	−0.084	−0.486	−0.448	−0.521	−0.522	−0.478	−0.815	−0.719	−0.613	−0.821	−0.479

In addition to the sensitivities presented in Table 17, the following 2nd-order relative sensitivities in the matrix $\mathbf{S}^{(2)}\left(\nu_{i=1}^{g}, \sigma_{t,k=1}^{g'}\right)$, $g, g' = 1, \ldots, 30$ have absolute values greater than 1.0: $S^{(2)}\left(\nu_{i=1}^{30}, \sigma_{t,k=1}^{12}\right) = -1.175$, $S^{(2)}\left(\nu_{i=1}^{30}, \sigma_{t,k=1}^{13}\right) = -1.053$ and $S^{(2)}\left(\nu_{i=1}^{12}, \sigma_{t,k=1}^{30}\right) = -1.064$. The absolute values of the mixed sensitivities in row $g = 12$ are the largest among all $g = 1, \ldots, 30$ rows, including rows not presented in Table 17. Similarly, the values of the mixed sensitivities in group $g' = 12$ are the most negative among all groups $g' = 1, \ldots, 30$, except for the sensitivity value located in groups $g = 13$ and $g' = 12$, which is less negative than the value located in groups $g = 13$ and $g' = 13$.

6.3.2. Second-Order Relative Sensitivities $\mathbf{S}^{(2)}\left(\nu_{1}^{g}, \sigma_{t,5}^{g'}\right)$, $g, g' = 1, \ldots, 30$

As presented in Table 18, the submatrix $\mathbf{S}^{(2)}\left(\nu_{1}^{g}, \sigma_{t,5}^{g'}\right)$, $g, g' = 1, \ldots, 30$, comprising the 2nd-order relative sensitivities of the leakage response with respect to the average number of neutrons per fission of isotope 1 (^{239}Pu) and the total cross sections of isotope 5 (C), includes 7 elements that have values greater than 1.0. All of these 7 large elements involve the total cross section $\sigma_{t,5}^{g'=30}$ for group $g' = 30$ of isotope 5 (C).

Table 18. Components of $\mathbf{S}^{(2)}\left(\nu_{1}^{g}, \sigma_{t,5}^{g'}\right)$, $g, g' = 1, \ldots, 30$ having values greater than 1.0.

Energy Groups	$g = 7$ $g' = 30$	$g = 9$ $g' = 30$	$g = 10$ $g' = 30$	$g = 11$ $g' = 30$	$g = 12$ $g' = 30$	$g = 13$ $g' = 30$	$g = 30$ $g' = 30$
Values	-1.022	-1.070	-1.122	-1.046	-1.617	-1.129	-1.258

6.3.3. Second-Order Relative Sensitivities $\mathbf{S}^{(2)}\left(\nu_{1}^{g}, \sigma_{t,6}^{g'}\right)$, $g, g' = 1, \ldots, 30$

The submatrix $\mathbf{S}^{(2)}\left(\nu_{1}^{g}, \sigma_{t,6}^{g'}\right)$, $g, g' = 1, \ldots, 30$, comprises the 2nd-order relative sensitivities of the leakage response with respect to the average number of neutrons per fission of isotope 1 (^{239}Pu) and the total microscopic cross sections of isotope 6 (^{1}H). The submatrix $\mathbf{S}^{(2)}\left(\nu_{1}^{g}, \sigma_{t,6}^{g'}\right)$, $g, g' = 1, \ldots, 30$ includes 99 elements that have absolute values greater than 1.0, as specified (in bold) in Tables 19 and 20. Of these 99 elements, 71 elements are located in the energy phase-space confined by the energy groups $g = 7, \ldots, 14$ and $g' = 14, \ldots, 29$, while the other 28 elements are located in energy groups $g = 30$ or $g' = 30$; some of these sensitivities have very large negative values. The largest negative value is displayed by the 2nd-order relative sensitivity of the leakage response with respect to the 12th energy group of the parameter underlying the average number of neutrons per fission for ^{239}Pu and the 30th energy group of the total cross section for ^{1}H, namely, $S^{(2)}\left(\nu_{1}^{12}, \sigma_{t,6}^{30}\right) = -19.29$.

Table 19. Elements of $\mathbf{S}^{(2)}\left(v_{i=1}^{g}, \sigma_{t,k=6}^{g'}\right)$, $g, g' = 1, \ldots, 30$, having absolute values greater than 1.0.

Groups	$g' = 13$	14	15	16	17	18	19	20	21
$g = 5$	−0.054	−0.061	−0.063	−0.130	−0.134	−0.131	−0.126	−0.120	−0.112
6	−0.134	−0.153	−0.158	−0.325	−0.333	−0.327	−0.315	−0.298	−0.280
7	−0.600	−0.682	−0.707	**−1.451**	**−1.488**	**−1.460**	**−1.406**	**−1.331**	**−1.251**
8	−0.517	−0.587	−0.608	**−1.248**	**−1.280**	**−1.256**	**−1.209**	**−1.145**	**−1.076**
9	−0.628	−0.714	−0.740	**−1.518**	**−1.557**	**−1.528**	**−1.471**	**−1.393**	**−1.308**
10	−0.660	−0.750	−0.777	**−1.593**	**−1.634**	**−1.603**	**−1.543**	**−1.461**	**−1.373**
11	−0.615	−0.699	−0.724	**−1.486**	**−1.523**	**−1.495**	**−1.439**	**−1.362**	**−1.280**
12	−0.950	**−1.080**	**−1.118**	**−2.295**	**−2.352**	**−2.308**	**−2.223**	**−2.104**	**−1.977**
13	−0.691	−0.754	−0.781	**−1.602**	**−1.643**	**−1.612**	**−1.552**	**−1.470**	**−1.381**
14	−0.448	−0.524	−0.512	**−1.050**	**−1.077**	**−1.057**	**−1.018**	−0.964	−0.906
15	−0.260	−0.299	−0.323	−0.609	−0.624	−0.613	−0.590	−0.559	−0.525
16	−0.246	−0.282	−0.295	−0.629	−0.580	−0.569	−0.548	−0.519	−0.488
17	−0.103	−0.119	−0.125	−0.261	−0.293	−0.227	−0.219	−0.208	−0.195
18	−0.064	−0.074	−0.078	−0.165	−0.174	−0.195	−0.130	−0.123	−0.116
19	−0.057	−0.067	−0.071	−0.150	−0.158	−0.159	−0.180	−0.108	−0.102
20	−0.063	−0.074	−0.078	−0.165	−0.174	−0.175	−0.172	−0.197	−0.111
21	−0.069	−0.081	−0.086	−0.181	−0.191	−0.191	−0.188	−0.182	−0.211
22	−0.062	−0.073	−0.078	−0.163	−0.172	−0.172	−0.169	−0.163	−0.157
23	−0.063	−0.074	−0.079	−0.166	−0.174	−0.174	−0.171	−0.165	−0.158
24	−0.042	−0.049	−0.052	−0.110	−0.115	−0.115	−0.113	−0.109	−0.104
25	−0.054	−0.064	−0.068	−0.142	−0.149	−0.149	−0.146	−0.140	−0.135
26	−0.051	−0.059	−0.063	−0.132	−0.139	−0.139	−0.136	−0.131	−0.125
27	−0.026	−0.031	−0.033	−0.069	−0.073	−0.072	−0.071	−0.068	−0.065
28	−0.012	−0.014	−0.015	−0.031	−0.033	−0.033	−0.032	−0.031	−0.030
29	−0.035	−0.041	−0.043	−0.091	−0.095	−0.095	−0.093	−0.089	−0.085
30	−0.470	−0.550	−0.584	**−1.224**	**−1.281**	**−1.278**	**−1.250**	**−1.201**	**−1.151**

Table 20. Continuation of Table 19.

Groups	$g' = 22$	23	24	25	26	27	28	29	30
$g = 5$	−0.103	−0.095	−0.086	−0.082	−0.076	−0.067	−0.063	−0.063	**−1.096**
6	−0.257	−0.238	−0.215	−0.204	−0.188	−0.168	−0.157	−0.158	**−2.732**
7	**−1.148**	**−1.063**	−0.962	−0.913	−0.841	−0.750	−0.703	−0.706	**−12.20**
8	−0.988	−0.915	−0.828	−0.785	−0.724	−0.645	−0.605	−0.607	**−10.49**
9	**−1.202**	**−1.113**	**−1.007**	−0.955	−0.880	−0.785	−0.736	−0.739	**−12.77**
10	**−1.261**	**−1.167**	**−1.056**	**−1.002**	−0.924	−0.823	−0.772	−0.775	**−13.39**
11	**−1.176**	**−1.088**	−0.985	−0.934	−0.861	−0.767	−0.720	−0.723	**−12.49**
12	**−1.816**	**−1.681**	**−1.521**	**−1.443**	**−1.330**	**−1.186**	**−1.112**	**−1.116**	**−19.29**
13	**−1.268**	**−1.174**	**−1.063**	**−1.008**	−0.929	−0.828	−0.777	−0.780	**−13.48**
14	−0.832	−0.770	−0.697	−0.661	−0.609	−0.543	−0.509	−0.512	**−8.843**
15	−0.482	−0.447	−0.404	−0.383	−0.353	−0.315	−0.295	−0.297	**−5.129**
16	−0.448	−0.415	−0.376	−0.357	−0.329	−0.293	−0.275	−0.276	**−4.777**
17	−0.180	−0.167	−0.151	−0.143	−0.132	−0.118	−0.111	−0.111	**−1.921**
18	−0.107	−0.099	−0.090	−0.085	−0.078	−0.070	−0.066	−0.066	**−1.142**
19	−0.094	−0.087	−0.079	−0.075	−0.069	−0.062	−0.058	−0.058	**−1.004**
20	−0.102	−0.095	−0.086	−0.082	−0.075	−0.067	−0.063	−0.063	**−1.096**
21	−0.111	−0.103	−0.093	−0.089	−0.082	−0.073	−0.069	−0.069	**−1.190**
22	−0.183	−0.093	−0.084	−0.080	−0.073	−0.065	−0.062	−0.062	**−1.068**
23	−0.151	−0.179	−0.085	−0.080	−0.074	−0.066	−0.062	−0.062	**−1.077**
24	−0.099	−0.095	−0.113	−0.053	−0.049	−0.043	−0.041	−0.041	−0.708
25	−0.127	−0.122	−0.116	−0.144	−0.063	−0.056	−0.053	−0.053	−0.915
26	−0.118	−0.113	−0.107	−0.104	−0.129	−0.052	−0.049	−0.049	−0.849
27	−0.062	−0.059	−0.055	−0.054	−0.052	−0.064	−0.025	−0.026	−0.443
28	−0.028	−0.027	−0.025	−0.024	−0.023	−0.022	−0.028	−0.012	−0.200
29	−0.081	−0.077	−0.072	−0.070	−0.067	−0.063	−0.062	−0.083	−0.578
30	**−1.085**	**−1.031**	−0.967	−0.936	−0.893	−0.836	−0.811	−0.817	**−15.02**

6.3.4. Second-Order Relative Sensitivities $\mathbf{S}^{(2)}\left(\nu_2^g, \sigma_{t,6}^{g'}\right)$, $g, g' = 1, \ldots, 30$

The submatrix $\mathbf{S}^{(2)}\left(\nu_2^g, \sigma_{t,6}^{g'}\right)$, $g, g' = 1, \ldots, 30$, comprising the 2nd-order sensitivities of the leakage response with respect to the average number of neutrons per fission of isotope 2 (^{240}Pu) and the total cross sections of isotope 6 (^{1}H), contains a single large element that has an absolute value greater than 1.0, namely, $S^{(2)}\left(\nu_2^{12}, \sigma_{t,6}^{30}\right) = -1.003$.

7. Mixed Second-Order Sensitivities of the PERP Total Leakage Response with Respect to the Parameters Underlying the Average Number of Neutrons Per Fission and Scattering Cross Sections

This Section presents the computation and analysis of the numerical results for the 2nd-order mixed sensitivities, $\partial^2 L(\boldsymbol{\alpha}) / \partial \boldsymbol{\nu} \partial \boldsymbol{\sigma}_s$, of the leakage response with respect to the average number of neutrons per fission and scattering microscopic cross sections of all isotopes of the PERP benchmark. The numerical values of the 2nd-order mixed sensitivities $\partial^2 L(\boldsymbol{\alpha}) / \partial \boldsymbol{\nu} \partial \boldsymbol{\sigma}_s$ can alternatively be computed by using the symmetric expression $\partial^2 L(\boldsymbol{\alpha}) / \partial \boldsymbol{\sigma}_s \partial \boldsymbol{\nu}$. The path for computing the 2nd-order mixed sensitivities $\partial^2 L(\boldsymbol{\alpha}) / \partial \boldsymbol{\nu} \partial \boldsymbol{\sigma}_s$ will be presented in Section 7.1. The path for computing the alternative expressions for $\partial^2 L(\boldsymbol{\alpha}) / \partial \boldsymbol{\sigma}_s \partial \boldsymbol{\nu}$ will be presented in Section 7.2.

7.1. Computation of the Second-Order Sensitivities $\partial^2 L(\boldsymbol{\alpha}) / \partial \boldsymbol{\nu} \partial \boldsymbol{\sigma}_s$

Similar to the computation of $\partial^2 L(\boldsymbol{\alpha}) / \partial \boldsymbol{\sigma}_f \partial \boldsymbol{\sigma}_s$ as presented in Section 4.1, the equations needed for deriving the expressions of the 2nd-order sensitivities $\partial^2 L / \partial f_j \partial s_{m_2}$, $j = J_{\sigma f} + 1, \ldots, J_{\sigma f} + J_\nu$; $m_2 = 1, \ldots, J_{\sigma s}$ will differ from each other depending on whether the parameter s_{m_2} corresponds to the 0th-order ($l = 0$) scattering cross sections or to the higher-order ($l \geq 1$) scattering cross sections. The two distinct cases are as follows:

(1) $\left(\frac{\partial^2 L}{\partial f_j \partial s_{m_2}}\right)_{(f=\nu, s=\sigma_{s,l=0})}$, $j = J_{\sigma f} + 1, \ldots, J_{\sigma f} + J_\nu$; $m_2 = 1, \ldots, J_{\sigma s, l=0}$, where the quantities f_j enumerate the parameters underlying the average number of neutrons per fission, and the quantities s_{m_2} enumerate parameters underlying the 0th-order scattering microscopic cross sections;

(2) $\left(\frac{\partial^2 L}{\partial f_j \partial s_{m_2}}\right)_{(f=\nu, s=\sigma_{s,l\geq 1})}$, $j = J_{\sigma f} + 1, \ldots, J_{\sigma f} + J_\nu$; $m_2 = 1, \ldots, \sigma_{s,l\geq 1}$, where the quantities f_j enumerate the parameters underlying the average number of neutrons per fission, and the quantities s_{m_2} enumerate parameters underlying the lth-order ($l \geq 1$) scattering microscopic cross sections.

7.1.1. Computation of the Second-Order Sensitivities $\left(\frac{\partial^2 L}{\partial f_j \partial s_{m_2}}\right)_{(f=\nu, s=\sigma_{s,l=0})}$

The equations needed for deriving the expression of the 2nd-order mixed sensitivities $\left(\partial^2 L / \partial f_j \partial s_{m_2}\right)_{(f=\nu, s=\sigma_{s,l=0})}$ are obtained by particularizing Equations (177) and (178) presented in [5] to the PERP benchmark, where Equation (178) provides the contributions arising directly from the parameters underlying the average number of neutrons per fission and scattering cross sections, while Equation (177) provides contributions arising indirectly through the total cross sections, since the 0th-order scattering cross sections are part of the total cross sections. The expression obtained by particularizing Equation (178) in [5] to the PERP benchmark yields:

$$
\begin{aligned}
\left(\frac{\partial^2 L}{\partial f_j \partial s_{m_2}}\right)_{(f=\nu, s=\sigma_{s,l=0})}^{(1)} &= \sum_{g=1}^{G} \int_V dV \int_{4\pi} d\mathbf{\Omega}\, u_{1,j}^{(2),g}(r, \mathbf{\Omega}) \sum_{g'=1}^{G} \int_{4\pi} d\mathbf{\Omega}'\, \psi^{(1),g'}(r, \mathbf{\Omega}') \frac{\partial \Sigma_s^{g \to g'}(\mathbf{s}; \mathbf{\Omega} \to \mathbf{\Omega}')}{\partial s_{m_2}} \\
&+ \sum_{g=1}^{G} \int_V dV \int_{4\pi} d\mathbf{\Omega}\, u_{2,j}^{(2),g}(r, \mathbf{\Omega}) \sum_{g'=1}^{G} \int_{4\pi} d\mathbf{\Omega}'\, \varphi^{g'}(\mathbf{r}, \mathbf{\Omega}') \frac{\partial \Sigma_s^{g' \to g}(\mathbf{s}; \mathbf{\Omega}' \to \mathbf{\Omega})}{\partial s_{m_2}}, \\
&\quad for \ j = J_{\sigma f} + 1, \ldots, J_{\sigma f} + J_\nu; m_2 = 1, \ldots, J_{\sigma s, l=0}.
\end{aligned}
\tag{132}
$$

In Equation (132), the parameters indexed by f_j correspond to the average number of neutrons per fission, so that $f_j \equiv v_{i_j}^{g_j}$, while the parameters indexed by s_{m_2} correspond to the 0th-order scattering cross sections, so that $s_{m_2} \equiv \sigma_{s,l_{m_2}=0,i_{m_2}}^{g'_{m_2} \to g_{m_2}}$, respectively.

Inserting the results obtained in Equations (68) and (69) into Equation (132), using the addition theorem for spherical harmonics in one-dimensional geometry, performing the respective angular integrations, and setting $l_{m_2} = 0$ in the resulting expression yields the following simplified form for Equation (132):

$$\left(\frac{\partial^2 L}{\partial f_j \partial s_{m_2}}\right)^{(1)}_{(f=v,s=\sigma_s,l=0)} = N_{i_{m_2},m_{m_2}} \int_V dV \left[\xi_0^{(1),g_{m_2}}(r) U_{1,j;0}^{(2),g'_{m_2}}(r) + \varphi_0^{g'_{m_2}}(r) U_{2,j;0}^{(2),g_{m_2}}(r) \right], \tag{133}$$

where the 0th-order moments $\varphi_0^{g'_{m_2}}(r)$, $\xi_0^{(1),g_{m_2}}(r)$, $U_{1,j;0}^{(2),g'_{m_2}}(r)$ and $U_{2,j;0}^{(2),g_{m_2}}(r)$ have been defined previously in Equations (15), (16), (27) and (28), respectively.

The contributions stemming from the specialized form of Equation (177) of [5], in conjunction with the relation $\frac{\partial \Sigma_t^g}{\partial t_{m_2}} = \frac{\partial \Sigma_t^g}{\partial t_{m_2}} \frac{\partial t_{m_2}}{\partial s_{m_2}} = \frac{\partial \Sigma_t^g}{\partial s_{m_2}}$, are as follows:

$$\left(\frac{\partial^2 L}{\partial f_j \partial s_{m_2}}\right)^{(2)}_{(f=v,s=\sigma_s,l=0)} = -\sum_{g=1}^{G} \int_V dV \int_{4\pi} d\Omega \left[u_{1,j}^{(2),g}(r,\Omega)\psi^{(1),g}(r,\Omega) + u_{2,j}^{(2),g}(r,\Omega)\varphi^g(r,\Omega) \right]\frac{\partial \Sigma_t^g}{\partial s_{m_2}},$$
$$\text{for } j = J_{\sigma f}+1,\ldots,J_{\sigma f}+J_v; \ m_2 = 1,\ldots,J_{\sigma s,l=0}. \tag{134}$$

Inserting the result obtained in Equation (73) into Equation (134) yields the following simplified expression:

$$\left(\frac{\partial^2 L}{\partial f_j \partial s_{m_2}}\right)^{(2)}_{(f=v,s=\sigma_s,l=0)}$$
$$= -N_{i_{m_2},m_{m_2}} \int_V dV \int_{4\pi} d\Omega \left[u_{1,j}^{(2),g'_{m_2}}(r,\Omega)\psi^{(1),g'_{m_2}}(r,\Omega) + u_{2,j}^{(2),g'_{m_2}}(r,\Omega)\varphi^{g'_{m_2}}(r,\Omega) \right]. \tag{135}$$

Collecting the partial contributions obtained in Equations (133) and (135), yields the following result:

$$\left(\frac{\partial^2 L}{\partial f_j \partial s_{m_2}}\right)_{(f=v,s=\sigma_s,l=0)} = \sum_{i=1}^{2} \left(\frac{\partial^2 L}{\partial f_j \partial s_{m_2}}\right)^{(i)}_{(f=v,s=\sigma_s,l=0)}$$
$$= N_{i_{m_2},m_{m_2}} \int_V dV \left[\xi_0^{(1),g_{m_2}}(r) U_{1,j;0}^{(2),g'_{m_2}}(r) + \varphi_0^{g'_{m_2}}(r) U_{2,j;0}^{(2),g_{m_2}}(r) \right]$$
$$-N_{i_{m_2},m_{m_2}} \int_V dV \int_{4\pi} d\Omega \left[u_{1,j}^{(2),g'_{m_2}}(r,\Omega)\psi^{(1),g'_{m_2}}(r,\Omega) + u_{2,j}^{(2),g'_{m_2}}(r,\Omega)\varphi^{g'_{m_2}}(r,\Omega) \right], \tag{136}$$
$$\text{for } j = J_{\sigma f}+1,\ldots,J_{\sigma f}+J_v; m_2 = 1,\ldots,J_{\sigma s,l=0}.$$

7.1.2. Second-Order Sensitivities $\left(\frac{\partial^2 L}{\partial f_j \partial s_{m_2}}\right)_{(f=v,s=\sigma_{s,l\geq 1})}$

When computing the 2nd-order sensitivities $\left(\partial^2 L/\partial f_j \partial s_{m_2}\right)_{(f=v,s=\sigma_{s,l\geq 1})}$, the parameters $f_j \equiv v_j^{g_j}$ correspond to the average number of neutrons per fission, while the parameters $s_{m_2} \equiv \sigma_{s,l_{m_2},i_{m_2}}^{g'_{m_2} \to g_{m_2}}$ correspond to the lth-order ($l \geq 1$) scattering cross sections, neither of which contribute to the total cross

sections. Thus, the expression of $\left(\partial^2 L / \partial f_j \partial s_{m_2}\right)_{(f=v, s=\sigma_{s,l\geq1})}$ is obtained by particularizing Equation (178) in [5] to the PERP benchmark, which yields,

$$
\begin{aligned}
\left(\frac{\partial^2 L}{\partial f_j \partial s_{m_2}}\right)_{(f=v, s=\sigma_{s,l\geq1})} &= \sum_{g=1}^{G} \int_V dV \int_{4\pi} d\Omega\, u_{1,j}^{(2),g}(r,\Omega) \sum_{g'=1}^{G} \int_{4\pi} d\Omega'\, \psi^{(1),g'}(r,\Omega') \frac{\partial \Sigma_s^{g\to g'}(s;\Omega\to\Omega')}{\partial s_{m_2}} \\
&+ \sum_{g=1}^{G} \int_V dV \int_{4\pi} d\Omega\, u_{2,j}^{(2),g}(r,\Omega) \sum_{g'=1}^{G} \int_{4\pi} d\Omega'\, \varphi^{g'}(r,\Omega') \frac{\partial \Sigma_s^{g'\to g}(s;\Omega'\to\Omega)}{\partial s_{m_2}}, \\
&\quad for\ j = J_{\sigma f}+1,\dots,J_{\sigma f}+J_v;\, m_2 = 1,\dots,J_{\sigma s,l\geq1}.
\end{aligned}
\tag{137}
$$

Inserting the results obtained in Equations (68) and (69) into Equation (137), using the addition theorem for spherical harmonics in one-dimensional geometry and performing the respective angular integrations yields the following simplified form for Equation (137):

$$
\begin{aligned}
\left(\frac{\partial^2 L}{\partial f_j \partial s_{m_2}}\right)_{(f=v, s=\sigma_{s,l\geq1})} \\
= N_{i_{m_2}, m_{m_2}} (2l_{m_2}+1)\left[\int_V dV \xi_{l_{m_2}}^{(1),g_{m_2}}(r) U_{1,j;l_{m_2}}^{(2),g'\,m_2}(r) + \int_V dV \varphi_{l_{m_2}}^{g'\,m_2}(r) U_{2,j;l_{m_2}}^{(2),g_{m_2}}(r) \right] \\
for\ j = J_{\sigma f}+1,\dots,J_{\sigma f}+J_v;\, m_2 = 1,\dots,J_{\sigma s,l\geq1};\, l_{m_2} = 1,\dots,ISCT,
\end{aligned}
\tag{138}
$$

where the moments $\varphi_{l_{m_2}}^{g'\,m_2}(r)$, $\xi_{l_{m_2}}^{(1),g_{m_2}}(r)$, $U_{1,j;l_{m_2}}^{(2),g'\,m_2}(r)$ and $U_{2,j;l_{m_2}}^{(2),g_{m_2}}(r)$ have been defined in Equations (82), (83), (86) and (87), respectively.

7.2. Alternative Path: Computing the Second-Order Sensitivities $\partial^2 L(\boldsymbol{\alpha})/\partial\boldsymbol{\sigma}_s\partial\mathbf{v}$

Due to the symmetry of the mixed 2nd-order sensitivities, the results computed using Equations (136) and (138) for $\partial^2 L(\boldsymbol{\alpha})/\partial\mathbf{v}\partial\boldsymbol{\sigma}_s$ can be verified by computing the expressions of the sensitivities $\partial^2 L(\boldsymbol{\alpha})/\partial\boldsymbol{\sigma}_s\partial\mathbf{v}$, which also requires separate consideration of the zeroth-order scattering cross sections. The two cases involved are as follows:

(1) $\left(\frac{\partial^2 L}{\partial s_j \partial f_{m_2}}\right)_{(s=\sigma_{s,l=0}, f=v)}$, $j = 1,\dots,J_{\sigma s,l=0};\, m_2 = J_{\sigma f}+1,\dots,J_{\sigma f}+J_v$, where the quantities s_j refer to the parameters underlying the 0th-order scattering cross sections, while the quantities f_{m_2} refer to the parameters underlying the average number of neutrons per fission;

(2) $\left(\frac{\partial^2 L}{\partial s_j \partial f_{m_2}}\right)_{(s=\sigma_{s,l\geq1}, f=v)}$, $j = 1,\dots,J_{s,l\geq1};\, m_2 = J_{\sigma f}+1,\dots,J_{\sigma f}+J_v$, where the quantities s_j refer to the parameters underlying the lth-order ($l \geq 1$) scattering cross sections, and the quantities f_{m_2} refer to the parameters underlying the average number of neutrons per fission.

7.2.1. Second-Order Sensitivities $\left(\frac{\partial^2 L}{\partial s_j \partial f_{m_2}}\right)_{(s=\sigma_{s,l=0}, f=v)}$

The equations needed for deriving the expression of the 2nd-order mixed sensitivities $\left(\partial^2 L / \partial s_j \partial f_{m_2}\right)_{(s=\sigma_{s,l=0}, f=v)}$ are obtained by particularizing Equations (160) and (169) in [5] to the PERP benchmark. Particularizing Equation (169) in [5] to the PERP benchmark yields the following expression:

$$
\begin{aligned}
\left(\frac{\partial^2 L}{\partial s_j \partial f_{m_2}}\right)_{(s=\sigma_{s,l=0}, f=v)}^{(1)} &= \sum_{g=1}^{G} \int_V dV \int_{4\pi} d\Omega\, \theta_{1,j}^{(2),g}(r,\Omega') \frac{\partial\left[(v\Sigma_f)^g\right]}{\partial f_{m_2}} \sum_{g'=1}^{G} \int_{4\pi} d\Omega'\, \chi^{g'} \psi^{(1),g'}(r,\Omega') \\
&+ \sum_{g=1}^{G} \int_V dV \int_{4\pi} d\Omega\, \theta_{2,j}^{(2),g}(r,\Omega') \sum_{g'=1}^{G} \int_{4\pi} d\Omega'\, \varphi^{g'}(r,\Omega') \chi^g \frac{\partial\left[(v\Sigma_f)^{g'}\right]}{\partial f_{m_2}}, \\
&\quad for\ j = 1,\dots,J_{\sigma s,l=0};\, m_2 = J_{\sigma f}+1,\dots,J_{\sigma f}+J_v,
\end{aligned}
\tag{139}
$$

where the 2nd-level adjoint functions, $\theta_{1,j}^{(2),g}(r,\Omega')$ and $\theta_{2,j}^{(2),g}(r,\Omega')$, $j = 1,\dots,J_{\sigma s};\, g = 1,\dots,G$, are the solutions of the 2nd-Level Adjoint Sensitivity System (2nd-LASS) presented in Equations (46), (48), (51) and (52) of Part II [2], which have been reproduced previously in Equations (89)–(92).

In Equation (139), the parameters indexed by s_j correspond to the 0th-order scattering cross sections, so that $s_j \equiv \sigma_{s,l_j=0,i_j}^{g'_j \to g_j}$, while the parameters indexed by f_{m_2} correspond to the average number of neutrons per fission, so that $f_{m_2} \equiv \nu_{i_{m_2}}^{g_{m_2}}$. Inserting the results obtained in Equations (121) and (122) into Equation (139), yields the following simplified expression for Equation (139):

$$\left(\frac{\partial^2 L}{\partial s_j \partial f_{m_2}}\right)^{(1)}_{(s=\sigma_s,l=0,f=\nu)} = N_{i_{m_2},m_{m_2}} \sigma_{f,i_{m_2}}^{g_{m_2}} \int_V dV \left[\Theta_{1,j;0}^{(2),g_{m_2}}(r) \sum_{g'=1}^{G} \chi^{g'} \xi_0^{(1),g'}(r) + \varphi_0^{g_{m_2}}(r) \sum_{g=1}^{G} \chi^g \Theta_{2,j;0}^{(2),g}(r)\right], \tag{140}$$

where the 0th-order moments $\Theta_{1,j;0}^{(2),g_{m_2}}(r)$ and $\Theta_{2,j;0}^{(2),g}(r)$ have been previously defined in Equations (94) and (95), respectively.

The contributions stemming from Equation (160) in [5] takes on the following particular form:

$$\left(\frac{\partial^2 L}{\partial s_j \partial f_{m_2}}\right)^{(2)}_{(s=\sigma_s,l=0,f=\nu)} = \sum_{g=1}^{G} \int_V dV \int_{4\pi} d\mathbf{\Omega}\, \psi_{2,j}^{(2),g}(r,\mathbf{\Omega}') \sum_{g'=1}^{G} \int_{4\pi} d\mathbf{\Omega}' \varphi^{g'}(r,\mathbf{\Omega}') \chi^g \frac{\partial\left[(\nu\Sigma_f)^{g'}\right]}{\partial f_{m_2}}$$
$$+ \sum_{g=1}^{G} \int_V dV \int_{4\pi} d\mathbf{\Omega}\, \psi_{1,j}^{(2),g}(r,\mathbf{\Omega}') \frac{\partial\left[(\nu\Sigma_f)^g\right]}{\partial f_{m_2}} \sum_{g'=1}^{G} \int_{4\pi} d\mathbf{\Omega}' \chi^{g'} \psi^{(1),g'}(r,\mathbf{\Omega}'), \tag{141}$$
$$for \ j = 1,\ldots,J_{\sigma s,l=0}; \ m_2 = J_{\sigma f}+1,\ldots,J_{\sigma f}+J_\nu,$$

where the 2nd-level adjoint functions $\psi_{1,j}^{(2),g}(r,\mathbf{\Omega}')$ and $\psi_{2,j}^{(2),g}(r,\mathbf{\Omega}')$, $j = 1,\ldots,J_{\sigma s,l=0}$; $g = 1,\ldots,G$ are the solutions of the 2nd-Level Adjoint Sensitivity System (2nd-LASS) presented in Equations (30), (32), (36) and (37) of Part II [2], which were reproduced previously in Equations (97)–(100), respectively.

Inserting the results obtained in Equations (121) and (122) into Equation (141), yields the following simplified expression for Equation (141):

$$\left(\frac{\partial^2 L}{\partial s_j \partial f_{m_2}}\right)^{(2)}_{(s=\sigma_s,l=0,f=\nu)} = N_{i_{m_2},m_{m_2}} \sigma_{f,i_{m_2}}^{g_{m_2}} \int_V dV \left[\xi_{1,j;0}^{(2),g_{m_2}}(r) \sum_{g'=1}^{G} \chi^{g'} \xi_0^{(1),g'}(r) + \varphi_0^{g_{m_2}}(r) \sum_{g=1}^{G} \chi^g \xi_{2,j;0}^{(2),g}(r)\right], \tag{142}$$
$$for \ j = 1,\ldots,J_{\sigma s,l=0}; \ m_2 = J_{\sigma f}+1,\ldots,J_{\sigma f}+J_\nu,$$

Collecting the partial contributions obtained in Equations (140) and (142), yields the following result:

$$\left(\frac{\partial^2 L}{\partial s_j \partial f_{m_2}}\right)_{(s=\sigma_s,l=0,f=\nu)} = \sum_{i=1}^{2} \left(\frac{\partial^2 L}{\partial s_j \partial f_{m_2}}\right)^{(i)}_{(s=\sigma_s,l=0,f=\nu)}$$
$$= N_{i_{m_2},m_{m_2}} \sigma_{f,i_{m_2}}^{g_{m_2}} \int_V dV \left\{\left[\Theta_{1,j;0}^{(2),g_{m_2}}(r) + \xi_{1,j;0}^{(2),g_{m_2}}(r)\right] \sum_{g'=1}^{G} \chi^{g'} \xi_0^{(1),g'}(r) + \varphi_0^{g_{m_2}}(r) \sum_{g=1}^{G} \chi^g \left[\Theta_{2,j;0}^{(2),g}(r) + \xi_{2,j;0}^{(2),g}(r)\right]\right\}, \tag{143}$$
$$for\ j = 1,\ldots,J_{\sigma s,l=0}; m_2 = J_{\sigma f}+1,\ldots,J_{\sigma f}+J_\nu.$$

7.2.2. Second-Order Sensitivities $\left(\frac{\partial^2 L}{\partial s_j \partial f_{m_2}}\right)_{(s=\sigma_s,l\geq 1,f=\nu)}$

For this case, the parameters s_j correspond to the lth-order ($l \geq 1$) scattering cross sections, denoted as $s_j \equiv \sigma_{s,l_j,i_j}^{g'_j \to g_j}$, while the parameters f_{m_2} correspond to the average number of neutrons per fission, denoted as $f_{m_2} \equiv \nu_{i_{m_2}}^{g_{m_2}}$, neither of them contribute to the total cross sections. Therefore, the expression of $\left(\partial^2 L/\partial s_j \partial f_{m_2}\right)_{(s=\sigma_s,l\geq 1,f=\nu)}$ is obtained by particularizing Equation (169) in [5] to the PERP benchmark, which yields,

$$\left(\frac{\partial^2 L}{\partial s_j \partial f_{m_2}}\right)_{(s=\sigma_s,l\geq 1,f=\nu)} = \sum_{g=1}^{G} \int_V dV \int_{4\pi} d\mathbf{\Omega}\, \theta_{1,j}^{(2),g}(r,\mathbf{\Omega}) \frac{\partial\left[(\nu\Sigma_f)^g\right]}{\partial f_{m_2}} \sum_{g'=1}^{G} \int_{4\pi} d\mathbf{\Omega}' \chi^{g'} \psi^{(1),g'}(r,\mathbf{\Omega}')$$
$$+ \sum_{g=1}^{G} \int_V dV \int_{4\pi} d\mathbf{\Omega}\, \theta_{2,j}^{(2),g}(r,\mathbf{\Omega}) \sum_{g'=1}^{G} \int_{4\pi} d\mathbf{\Omega}' \varphi^{g'}(r,\mathbf{\Omega}') \chi^g \frac{\partial\left[(\nu\Sigma_f)^{g'}\right]}{\partial f_{m_2}}, \tag{144}$$
$$for\ j = 1,\ldots,J_{\sigma s,l\geq 1}; m_2 = J_{\sigma f}+1,\ldots,J_{\sigma f}+J_\nu.$$

Inserting the results obtained in Equations (121) and (122) into Equation (144) yields the following expression:

$$\left(\frac{\partial^2 L}{\partial s_j \partial f_{m_2}}\right)_{(s=\sigma_s, l\geq 1, f=\nu)} = N_{i_{m_2}, m_{m_2}} \sigma_{f, i_{m_2}}^{g_{m_2}} \int_V dV \left[\Theta_{1, j; 0}^{(2), g_{m_2}}(r) \sum_{g'=1}^{G} \chi^{g'} \xi_0^{(1), g'}(r) + \phi_0^{g_{m_2}}(r) \sum_{g=1}^{G} \chi^g \Theta_{2, j; 0}^{(2), g}(r)\right],$$

$$for \; j = 1, \ldots, J_{\sigma s, l\geq 1}; m_2 = J_{\sigma f} + 1, \ldots, J_{\sigma f} + J_\nu.$$

(145)

7.3. Numerical Results for $\partial^2 L(\boldsymbol{\alpha})/\partial \boldsymbol{\nu} \partial \boldsymbol{\sigma}_s$

The second-order absolute sensitivities, $\partial^2 L(\boldsymbol{\alpha})/\partial \boldsymbol{\nu} \partial \boldsymbol{\sigma}_s$ for the PERP benchmark, have been computed using Equations (136) and (138), and have been verified by computing $\partial^2 L(\boldsymbol{\alpha})/\partial \boldsymbol{\sigma}_s \partial \boldsymbol{\nu}$ using Equations (143) and (145). Similar to the computation of $\partial^2 L(\boldsymbol{\alpha})/\partial \boldsymbol{\sigma}_f \partial \boldsymbol{\sigma}_s$ as shown in Section 4.3, computing the second-order sensitivities $\partial^2 L(\boldsymbol{\alpha})/\partial \boldsymbol{\nu} \partial \boldsymbol{\sigma}_s$ using Equations (136) and (138) requires a total of 120 forward and adjoint PARTISN computations to obtain all the adjoint functions to compute the 2nd-order sensitivities $\partial^2 L(\boldsymbol{\alpha})/\partial \boldsymbol{\nu} \partial \boldsymbol{\sigma}_s$.

On the other hand, computing the alternative expression $\partial^2 L(\boldsymbol{\alpha})/\partial \boldsymbol{\sigma}_s \partial \boldsymbol{\nu}$ using Equations (143) and (145) would require 7101 forward and adjoint PARTISN computations to obtain the adjoint functions $\theta_{1,j}^{(2), g}(r, \boldsymbol{\Omega})$ and $\theta_{2,j}^{(2), g}(r, \boldsymbol{\Omega}), j = 1, \ldots, J_{\sigma s}; g = 1, \ldots, G$. As has been explained in Section 4.3, the reason for needing "only" 7101, instead of $J_{\sigma s} = 21600$, PARTISN computations is that all of the up-scattering and some of the down-scattering cross sections are zero for the PERP benchmark. Thus, computing $\partial^2 L(\boldsymbol{\alpha})/\partial \boldsymbol{\nu} \partial \boldsymbol{\sigma}_s$ using Equations (136) and (138) is about $60(\approx 7101/120)$ times more efficient than computing $\partial^2 L(\boldsymbol{\alpha})/\partial \boldsymbol{\sigma}_s \partial \boldsymbol{\nu}$ by using Equations (143) and (145).

The matrix $\partial^2 L/\partial f_j \partial s_{m_2}, j = J_{\sigma f} + 1, \ldots, J_{\sigma f} + J_\nu; m_2 = 1, \ldots, J_{\sigma f};$ has dimensions $J_\nu \times J_{\sigma s} (= 60 \times 21,600)$. The matrix of 2nd-order relative sensitivities corresponding to $\partial^2 L/\partial f_j \partial s_{m_2}, j = J_{\sigma f} + 1, \ldots, J_{\sigma f} + J_\nu; m_2 = 1, \ldots, J_{\sigma f};$, denoted as $\mathbf{S}^{(2)}\left(v_i^g, \sigma_{s,l,k}^{g' \to h}\right)$, is defined as follows:

$$\mathbf{S}^{(2)}\left(v_i^g, \sigma_{s,l,k}^{g' \to h}\right) \triangleq \frac{\partial^2 L}{\partial v_i^g \partial \sigma_{s,l,k}^{g' \to h}}\left(\frac{v_i^g \sigma_{s,l,k}^{g' \to h}}{L}\right), \; l = 0, \ldots, 3; \; i = 1, 2; k = 1, \ldots, 6; \; g, g', h = 1, \ldots, 30. \quad (146)$$

To facilitate the presentation and interpretation of the numerical results, the $J_\nu \times J_{\sigma s} (= 60 \times 21600)$ matrix $\mathbf{S}^{(2)}\left(v_i^g, \sigma_{s,l,k}^{g' \to h}\right)$ has been partitioned into $N_f \times I \times (ISCT + 1) = 2 \times 6 \times 4$ submatrices, each of dimensions $G \times (G \cdot G) = 30 \times 900$. The results for scattering orders $l = 0, l = 1, l = 2,$ and $l = 3$, respectively, are summarized below, in Sections 7.3.1–7.3.4.

7.3.1. Results for the Relative Sensitivities $\mathbf{S}^{(2)}\left(v_i^g, \sigma_{s,l=0,k}^{g' \to h}\right)$

Table 21 presents the results for 2nd-order relative sensitivities $\mathbf{S}^{(2)}\left(v_i^g, \sigma_{s,l=0,k}^{g' \to h}\right) \triangleq \left(\partial^2 L/\partial v_i^g \partial \sigma_{s,l=0,k}^{g' \to h}\right)\left(v_i^g \sigma_{s,l=0,k}^{g' \to h}/L\right), i = 1, 2; k = 1, \ldots, 6; g, g', h = 1, \ldots, 30$ of the leakage response with respect to the average number of neutrons per fission and the 0th-order scattering cross sections for all isotopes. All of these 2nd-order relative sensitivities are smaller than 1.0. For the 2nd-order mixed sensitivities $\mathbf{S}^{(2)}\left(v_i^g, \sigma_{s,l=0,k}^{g' \to h}\right)$, the values can be positive or negative, but there are more positive values than negative ones. For example, the submatrix $\mathbf{S}^{(2)}\left(v_1^g, \sigma_{s,l=0,1}^{g' \to h}\right)$, having dimensions $G \times (G \cdot G) = 30 \times 900$, comprises 7601 positive elements, 2539 negative elements, while the remaining elements are zero. The largest absolute values of the mixed 2nd-order sensitivities in the submatrices all involve the 12th energy group of v_i^g for isotopes ^{239}Pu or ^{240}Pu, and (mostly) the 0th-order self-scattering cross sections in the 12th energy group of isotopes ^{239}Pu, ^{240}Pu, ^{69}Ga, ^{71}Ga andC, or (occasionally) the 0th-order out-scattering cross section $\sigma_{s,l=0,k=6}^{16 \to 17}$ of isotope ^{1}H. All of the

largest elements in the respective sub-matrix are positive, and the vast majority of them are very small. The overall largest element in the matrix $\mathbf{S}^{(2)}\left(v_i^g, \sigma_{s,l=0,k}^{g'\to h}\right)$ is $S^{(2)}\left(v_1^{g=12}, \sigma_{s,l=0,k=1}^{12\to 12}\right) = 4.65\times 10^{-1}$.

Table 21. Summary presentation of the matrix $\mathbf{S}^{(2)}\left(v_i^g, \sigma_{s,l=0,k}^{g'\to h}\right)$.

Isotopes	$k=1$ (^{239}Pu)	$k=2$ (^{240}Pu)	$k=3$ (^{69}Ga)	$k=4$ (^{71}Ga)	$k=5$ (C)	$k=6$ (^{1}H)
$i=1$ (^{239}Pu)	$\mathbf{S}^{(2)}\left(\begin{smallmatrix}v_{1'}^g\\ \sigma_{s,l=0,1}^{g'\to h}\end{smallmatrix}\right)$ Max. value = 4.65×10^{-1} at $g=12, g'=12$ $\to h=12$	$\mathbf{S}^{(2)}\left(\begin{smallmatrix}v_{1'}^g\\ \sigma_{s,l=0,2}^{g'\to h}\end{smallmatrix}\right)$ Max. value = 3.08×10^{-2} at $g=12, g'=12$ $\to h=12$	$\mathbf{S}^{(2)}\left(\begin{smallmatrix}v_{1'}^g\\ \sigma_{s,l=0,3}^{g'\to h}\end{smallmatrix}\right)$ Max. value = 1.78×10^{-3} at $g=12, g'=12$ $\to h=12$	$\mathbf{S}^{(2)}\left(\begin{smallmatrix}v_{1'}^g\\ \sigma_{s,l=0,4}^{g'\to h}\end{smallmatrix}\right)$ Max. value = 1.14×10^{-3} at $g=12, g'=12$ $\to h=12$	$\mathbf{S}^{(2)}\left(\begin{smallmatrix}v_{1'}^g\\ \sigma_{s,l=0,5}^{g'\to h}\end{smallmatrix}\right)$ Max. value = 1.98×10^{-1} at $g=12, g'=12$ $\to h=12$	$\mathbf{S}^{(2)}\left(\begin{smallmatrix}v_{1'}^g\\ \sigma_{s,l=0,6}^{g'\to h}\end{smallmatrix}\right)$ Max. value = 3.18×10^{-1} at $g=12, g'=16$ $\to h=17$
$i=2$ (^{240}Pu)	$\mathbf{S}^{(2)}\left(\begin{smallmatrix}v_{2'}^g\\ \sigma_{s,l=0,1}^{g'\to h}\end{smallmatrix}\right)$ Max. value = 2.42×10^{-2} at $g=12, g'=12$ $\to h=12$	$\mathbf{S}^{(2)}\left(\begin{smallmatrix}v_{2'}^g\\ \sigma_{s,l=0,2}^{g'\to h}\end{smallmatrix}\right)$ Max. value = 1.60×10^{-3} at $g=12, g'=12$ $\to h=12$	$\mathbf{S}^{(2)}\left(\begin{smallmatrix}v_{2'}^g\\ \sigma_{s,l=0,3}^{g'\to h}\end{smallmatrix}\right)$ Max. value = 9.25×10^{-5} at $g=12, g'=12$ $\to h=12$	$\mathbf{S}^{(2)}\left(\begin{smallmatrix}v_{2'}^g\\ \sigma_{s,l=0,4}^{g'\to h}\end{smallmatrix}\right)$ Max. value = 5.94×10^{-5} at $g=12, g'=12$ $\to h=12$	$\mathbf{S}^{(2)}\left(\begin{smallmatrix}v_{2'}^g\\ \sigma_{s,l=0,5}^{g'\to h}\end{smallmatrix}\right)$ Max. value = 1.03×10^{-2} at $g=12, g'=12$ $\to h=12$	$\mathbf{S}^{(2)}\left(\begin{smallmatrix}v_{2'}^g\\ \sigma_{s,l=0,6}^{g'\to h}\end{smallmatrix}\right)$ Max. value = 1.65×10^{-2} at $g=12, g'=16$ $\to h=17$

7.3.2. Results for the Relative Sensitivities $\mathbf{S}^{(2)}\left(v_i^g, \sigma_{s,l=1,k}^{g'\to h}\right)$

Table 22 summarizes the results for 2nd-order mixed relative sensitivities $\mathbf{S}^{(2)}\left(v_i^g, \sigma_{s,l=1,k}^{g'\to h}\right) \triangleq \left(\partial^2 L/\partial v_i^g \partial\sigma_{s,l=1,k}^{g'\to h}\right)\left(v_i^g \sigma_{s,l=1,k}^{g'\to h}/L\right)$, $l=1$; $i=1,2; k=1,\ldots,6$; $g,g',h=1,\ldots,30$ of the leakage response with respect to the average number of neutrons per fission and the 1st-order scattering cross sections for all isotopes. Most of these 2nd-order mixed sensitivities are zero; the non-zero ones are mostly negative. For example, the submatrix $\mathbf{S}^{(2)}\left(v_1^g, \sigma_{s,l=1,k=1}^{g'\to h}\right)$, having dimensions $G\times(G\cdot G)=30\times 900$, comprises 7918 elements with negative values, 2222 elements with positive values, while the remaining elements are zero. As shown in Table 22, the largest absolute values of the mixed 2nd-order sensitivities in the submatrices involve the 12th energy group of v_i^g for isotopes ^{239}Pu or ^{240}Pu, and (mostly) the 1st-order self-scattering cross sections for the 12th energy group of isotopes ^{239}Pu, ^{240}Pu, ^{69}Ga, C and ^{1}H, or (occasionally) the 1st-order self-scattering cross sections for the 7th energy group of isotope ^{71}Ga. All of the largest (in absolute value) elements are negative, and the vast majority of them are very small. The overall most negative value in the matrix $\mathbf{S}^{(2)}\left(v_1^g, \sigma_{s,l=1,k}^{g'\to h}\right)$ is $S^{(2)}\left(v_1^{g=12}, \sigma_{s,l=1,k=6}^{12\to 12}\right) = -2.64\times 10^{-1}$.

Table 22. Summary presentation of the matrix $\mathbf{S}^{(2)}\left(v_i^g, \sigma_{s,l=1,k}^{g'\to h}\right)$.

Isotopes	$k=1$ (^{239}Pu)	$k=2$ (^{240}Pu)	$k=3$ (^{69}Ga)	$k=4$ (^{71}Ga)	$k=5$ (C)	$k=6$ (^{1}H)
$i=1$ (^{239}Pu)	$\mathbf{S}^{(2)}\left(\begin{smallmatrix}v_{1'}^g\\ \sigma_{s,l=1,1}^{g'\to h}\end{smallmatrix}\right)$ Min. value = -2.37×10^{-1} at $g=12, g'=12$ $\to h=12$	$\mathbf{S}^{(2)}\left(\begin{smallmatrix}v_{1'}^g\\ \sigma_{s,l=1,2}^{g'\to h}\end{smallmatrix}\right)$ Min. value = -1.48×10^{-2} at $g=12, g'=12$ $\to h=12$	$\mathbf{S}^{(2)}\left(\begin{smallmatrix}v_{1'}^g\\ \sigma_{s,l=1,3}^{g'\to h}\end{smallmatrix}\right)$ Min. value = -4.88×10^{-4} at $g=12, g'=12$ $\to h=12$	$\mathbf{S}^{(2)}\left(\begin{smallmatrix}v_{1'}^g\\ \sigma_{s,l=1,4}^{g'\to h}\end{smallmatrix}\right)$ Min. value = -2.78×10^{-4} at $g=12, g'=7$ $\to h=7$	$\mathbf{S}^{(2)}\left(\begin{smallmatrix}v_{1'}^g\\ \sigma_{s,l=1,5}^{g'\to h}\end{smallmatrix}\right)$ Min. value = -8.40×10^{-2} at $g=12, g'=12$ $\to h=12$	$\mathbf{S}^{(2)}\left(\begin{smallmatrix}v_{1'}^g\\ \sigma_{s,l=1,6}^{g'\to h}\end{smallmatrix}\right)$ Min. value = -2.64×10^{-1} at $g=12, g'=12$ $\to h=12$
$i=2$ (^{240}Pu)	$\mathbf{S}^{(2)}\left(\begin{smallmatrix}v_{2'}^g\\ \sigma_{s,l=1,1}^{g'\to h}\end{smallmatrix}\right)$ Min. value = -1.23×10^{-2} at $g=12, g'=12$ $\to h=12$	$\mathbf{S}^{(2)}\left(\begin{smallmatrix}v_{2'}^g\\ \sigma_{s,l=1,2}^{g'\to h}\end{smallmatrix}\right)$ Min. value = -7.70×10^{-4} at $g=12, g'=12$ $\to h=12$	$\mathbf{S}^{(2)}\left(\begin{smallmatrix}v_{2'}^g\\ \sigma_{s,l=1,3}^{g'\to h}\end{smallmatrix}\right)$ Min. value = -2.54×10^{-5} at $g=12, g'=12$ $\to h=12$	$\mathbf{S}^{(2)}\left(\begin{smallmatrix}v_{2'}^g\\ \sigma_{s,l=1,4}^{g'\to h}\end{smallmatrix}\right)$ Min. value = -1.50×10^{-5} at $g=12, g'=7$ $\to h=7$	$\mathbf{S}^{(2)}\left(\begin{smallmatrix}v_{2'}^g\\ \sigma_{s,l=1,5}^{g'\to h}\end{smallmatrix}\right)$ Min. value = -4.37×10^{-3} at $g=12, g'=12$ $\to h=12$	$\mathbf{S}^{(2)}\left(\begin{smallmatrix}v_{2'}^g\\ \sigma_{s,l=1,6}^{g'\to h}\end{smallmatrix}\right)$ Min. value = -1.37×10^{-2} at $g=12, g'=12$ $\to h=12$

7.3.3. Results for the Relative Sensitivities $\mathbf{S}^{(2)}\left(v_i^g, \sigma_{s,l=2,k}^{g'\to h}\right)$

Table 23 presents the results for 2nd-order mixed relative sensitivities $\mathbf{S}^{(2)}\left(v_i^g, \sigma_{s,l=2,k}^{g'\to h}\right) \triangleq \left(\partial^2 L/\partial v_i^g \partial\sigma_{s,l=2,k}^{g'\to h}\right)\left(v_i^g \sigma_{s,l=2,k}^{g'\to h}/L\right)$, $l=2$; $i=1,2$; $k=1,\ldots,6$; $g,g',h=1,\ldots,30$, of the leakage response

with respect to the average number of neutrons per fission and the 2nd-order scattering cross sections for all isotopes. Most of the non-zero elements of $\mathbf{S}^{(2)}\left(v_i^g, \sigma_{s,l=2,k}^{g' \to h}\right)$ are positive. For example, the submatrix $\mathbf{S}^{(2)}\left(v_{i=1}^g, \sigma_{s,l=2,k=1}^{g' \to h}\right)$, having dimensions $G \times (G \cdot G) = 30 \times 900$, comprises 6439 positive elements, 3701 negative elements, while the remaining elements are zero. As shown in Table 23, all of the largest absolute values of the mixed 2nd-order sensitivities involve $v_i^{g=12}$, $i = 1,2$ for the 12th energy group or the 7th energy group of isotopes ^{239}Pu or^{240}Pu, and (most of the time) involve either the 2nd-order self-scattering cross sections $\sigma_{s,l=2,k}^{7 \to 7}$, $k = 1, \ldots, 5$ for the 7th energy group of isotopes ^{239}Pu, ^{240}Pu, ^{69}Ga, ^{71}Ga and C or (occasionally) the 2nd-order self-scattering cross sections $\sigma_{s,l=2,i=6}^{12 \to 12}$ for the 12th energy group of isotope^{1}H. As shown in Table 23, all of the largest elements in the respective sub-matrix are positive, and the vast majority of them are very small. The overall largest element in the matrix $\mathbf{S}^{(2)}\left(v_i^g, \sigma_{s,l=2,k}^{g' \to h}\right)$ is $S^{(2)}\left(v_1^{g=12}, \sigma_{s,l=2,k=6}^{12 \to 12}\right) = 9.03 \times 10^{-2}$.

Table 23. Summary presentation of the matrix $\mathbf{S}^{(2)}\left(v_i^g, \sigma_{s,l=2,k}^{g' \to h}\right)$.

Isotopes	k=1 (^{239}Pu)	k=2 (^{240}Pu)	k=3 (^{69}Ga)	k=4 (^{71}Ga)	k=5 (C)	k=6 (^{1}H)
$i = 1$ (^{239}Pu)	$\mathbf{S}^{(2)}\left(\begin{matrix} v_{1'}^g, \\ \sigma_{s,l=2,1}^{g' \to h} \end{matrix}\right)$ Max. value = 1.35×10^{-2} at $g = 12, g' = 7$ $\to$ h = 7	$\mathbf{S}^{(2)}\left(\begin{matrix} v_{1'}^g, \\ \sigma_{s,l=2,2}^{g' \to h} \end{matrix}\right)$ Max. value = 8.24×10^{-4} at $g = 12, g' = 7$ $\to$ h = 7	$\mathbf{S}^{(2)}\left(\begin{matrix} v_{1'}^g, \\ \sigma_{s,l=2,3}^{g' \to h} \end{matrix}\right)$ Max. value = 2.47×10^{-5} at $g = 12, g' = 7$ $\to$ h = 7	$\mathbf{S}^{(2)}\left(\begin{matrix} v_{1'}^g, \\ \sigma_{s,l=2,4}^{g' \to h} \end{matrix}\right)$ Max. value = 1.53×10^{-5} at $g = 12, g' = 7$ $\to$ h = 7	$\mathbf{S}^{(2)}\left(\begin{matrix} v_{1'}^g, \\ \sigma_{s,l=2,5}^{g' \to h} \end{matrix}\right)$ Max. value = 1.86×10^{-2} at $g = 12, g' = 7$ $\to$ h = 7	$\mathbf{S}^{(2)}\left(\begin{matrix} v_{1'}^g, \\ \sigma_{s,l=2,6}^{g' \to h} \end{matrix}\right)$ Max. value = 9.03×10^{-2} at $g = 12, g' = 12$ $\to$ h = 12
$i = 2$ (^{240}Pu)	$\mathbf{S}^{(2)}\left(\begin{matrix} v_{2'}^g, \\ \sigma_{s,l=2,1}^{g' \to h} \end{matrix}\right)$ Max. value = 7.16×10^{-4} at $g = 7, g' = 7 \to$ h = 7	$\mathbf{S}^{(2)}\left(\begin{matrix} v_{2'}^g, \\ \sigma_{s,l=2,2}^{g' \to h} \end{matrix}\right)$ Max. value = 4.38×10^{-5} at $g = 7, g' = 7 \to$ h = 7	$\mathbf{S}^{(2)}\left(\begin{matrix} v_{2'}^g, \\ \sigma_{s,l=2,3}^{g' \to h} \end{matrix}\right)$ Max. value = 1.31×10^{-6} at $g = 7, g' = 7 \to$ h = 7	$\mathbf{S}^{(2)}\left(\begin{matrix} v_{2'}^g, \\ \sigma_{s,l=2,4}^{g' \to h} \end{matrix}\right)$ Max. value = 8.16×10^{-7} at $g = 7, g' = 7 \to$ h = 7	$\mathbf{S}^{(2)}\left(\begin{matrix} v_{2'}^g, \\ \sigma_{s,l=2,5}^{g' \to h} \end{matrix}\right)$ Max. value = 9.85×10^{-4} at $g = 7, g' = 7 \to$ h = 7	$\mathbf{S}^{(2)}\left(\begin{matrix} v_{2'}^g, \\ \sigma_{s,l=2,6}^{g' \to h} \end{matrix}\right)$ Max. value = 4.70×10^{-3} at $g = 12, g' = 12$ $\to$ h = 12

7.3.4. Results for the Relative Sensitivities $\mathbf{S}^{(2)}\left(v_i^g, \sigma_{s,l=3,k}^{g' \to h}\right)$

Table 24 presents the results for 2nd-order mixed relative sensitivities $\mathbf{S}^{(2)}\left(v_i^g, \sigma_{s,l=3,k}^{g' \to h}\right) \triangleq \left(\partial^2 L / \partial v_i^g \partial \sigma_{s,l=3,k}^{g' \to h}\right)\left(v_i^g \sigma_{s,l=3,k}^{g' \to h} / L\right)$, $l = 3$; $i = 1,2; k = 1, \ldots, 6$; $g, g', h = 1, \ldots, 30$, of the leakage response with respect to the average number of neutrons per fission and the 3rd-order scattering cross sections for all isotopes. Most of the elements of $\mathbf{S}^{(2)}\left(v_i^g, \sigma_{s,l=3,k}^{g' \to h}\right)$ are zero; the non-zero elements are very small, and the negative ones slightly outnumber the positive ones. For example, the $G \times (G \cdot G) = 30 \times 900$ -dimensional submatrix $\mathbf{S}^{(2)}\left(v_{i=1}^g, \sigma_{s,l=3,k=1}^{g' \to h}\right)$ comprises 5375 negative elements, 4735 positive elements, while the remaining ones are zero. As shown in Table 24, the mixed 2nd-order sensitivities having the largest absolute values involve $v_i^{g=12}$, $i = 1,2$ for the 12th energy group or (occasionally) the 7th energy group of isotopes ^{239}Pu or^{240}Pu, and the 3rd-order self-scattering cross sections $\sigma_{s,l=3,k}^{7 \to 7}$, $k = 1, \ldots, 5$ for the 7th energy group of isotopes^{239}Pu, ^{240}Pu, ^{69}Ga, ^{71}Ga and C, or (occasionally) the 3rd-order self-scattering cross sections $\sigma_{s,l=3,i=6}^{12 \to 12}$ for the 12th energy group of isotope ^{1}H. The overall largest (in absolute value) element of the matrix $\mathbf{S}^{(2)}\left(v_i^g, \sigma_{s,l=3,k}^{g' \to h}\right)$ is $S^{(2)}\left(v_1^{g=12}, \sigma_{s,l=3,k=6}^{12 \to 12}\right) = -1.94 \times 10^{-2}$.

Table 24. Summary presentation of the matrix $\mathbf{S}^{(2)}\left(v_i^g, \sigma_{s,l=3,k}^{g'\to h}\right)$.

Isotopes	$k=1$ (^{239}Pu)	$k=2$ (^{240}Pu)	$k=3$ (^{69}Ga)	$k=4$ (^{71}Ga)	$k=5$ (C)	$k=6$ (^{1}H)
$i=1$ (^{239}Pu)	$\mathbf{S}^{(2)}\left(\begin{smallmatrix}v_{1'}^g\\ \sigma_{s,l=3,1}^{g'\to h}\end{smallmatrix}\right)$ Min. value = -2.08×10^{-5} at $g=12, g'=7$ $\to h=7$	$\mathbf{S}^{(2)}\left(\begin{smallmatrix}v_{1'}^g\\ \sigma_{s,l=3,2}^{g'\to h}\end{smallmatrix}\right)$ Min. value = -1.28×10^{-6} at $g=12, g'=7$ $\to h=7$	$\mathbf{S}^{(2)}\left(\begin{smallmatrix}v_{1'}^g\\ \sigma_{s,l=3,3}^{g'\to h}\end{smallmatrix}\right)$ Min. value = -3.64×10^{-8} at $g=12, g'=7$ $\to h=7$	$\mathbf{S}^{(2)}\left(\begin{smallmatrix}v_{1'}^g\\ \sigma_{s,l=3,4}^{g'\to h}\end{smallmatrix}\right)$ Min. value = -2.28×10^{-8} at $g=12, g'=7$ $\to h=7$	$\mathbf{S}^{(2)}\left(\begin{smallmatrix}v_{1'}^g\\ \sigma_{s,l=3,5}^{g'\to h}\end{smallmatrix}\right)$ Min. value = -4.66×10^{-3} at $g=12, g'=7$ $\to h=7$	$\mathbf{S}^{(2)}\left(\begin{smallmatrix}v_{1'}^g\\ \sigma_{s,l=3,6}^{g'\to h}\end{smallmatrix}\right)$ Min. value = -1.94×10^{-2} at $g=12, g'=12$ $\to h=12$
$i=2$ (^{240}Pu)	$\mathbf{S}^{(2)}\left(\begin{smallmatrix}v_{2'}^g\\ \sigma_{s,l=3,1}^{g'\to h}\end{smallmatrix}\right)$ Min. value = -1.08×10^{-6} at $g=12, g'=7$ $\to h=7$	$\mathbf{S}^{(2)}\left(\begin{smallmatrix}v_{2'}^g\\ \sigma_{s,l=3,2}^{g'\to h}\end{smallmatrix}\right)$ Min. value = -6.67×10^{-8} at $g=12, g'=7$ $\to h=7$	$\mathbf{S}^{(2)}\left(\begin{smallmatrix}v_{2'}^g\\ \sigma_{s,l=3,3}^{g'\to h}\end{smallmatrix}\right)$ Min. value = -1.89×10^{-9} at $g=12, g'=7$ $\to h=7$	$\mathbf{S}^{(2)}\left(\begin{smallmatrix}v_{2'}^g\\ \sigma_{s,l=3,4}^{g'\to h}\end{smallmatrix}\right)$ Min. value = -1.19×10^{-9} at $g=12, g'=7$ $\to h=7$	$\mathbf{S}^{(2)}\left(\begin{smallmatrix}v_{2'}^g\\ \sigma_{s,l=3,5}^{g'\to h}\end{smallmatrix}\right)$ Min. value = -2.59×10^{-4} at $g=7, g'=7 \to$ h $=7$	$\mathbf{S}^{(2)}\left(\begin{smallmatrix}v_{2'}^g\\ \sigma_{s,l=3,6}^{g'\to h}\end{smallmatrix}\right)$ Min. value = -1.01×10^{-3} at $g=12, g'=12$ $\to h=12$

8. Mixed Second-Order Sensitivities of the PERP Total Leakage Response with Respect to the Parameters Underlying the Average Number of Neutrons per Fission and Fission Cross Sections

This Section presents the computation and analysis of the numerical results for the 2nd-order mixed sensitivities $\partial^2 L(\boldsymbol{\alpha})/\partial v \partial \boldsymbol{\sigma}_f$ of the leakage response with respect to the average number of neutrons per fission and fission microscopic cross sections of all isotopes of the PERP benchmark. Likewise, the numerical values of the 2nd-order mixed sensitivities $\partial^2 L(\boldsymbol{\alpha})/\partial v \partial \boldsymbol{\sigma}_f$ can also be computed by using the alternative expression for $\partial^2 L(\boldsymbol{\alpha})/\partial \boldsymbol{\sigma}_f \partial v$. The formulas for computing the 2nd-order mixed sensitivities $\partial^2 L(\boldsymbol{\alpha})/\partial v \partial \boldsymbol{\sigma}_f$ are presented in Section 8.1, while the formulas for computing, alternatively, the expressions for $\partial^2 L(\boldsymbol{\alpha})/\partial \boldsymbol{\sigma}_f \partial v$ are presented in Section 8.2.

8.1. Computing the Second-Order Sensitivities $\partial^2 L(\boldsymbol{\alpha})/\partial v \partial \boldsymbol{\sigma}_f$

The equations needed for deriving the expression of the 2nd-order sensitivities $\partial^2 L(\boldsymbol{\alpha})/\partial v \partial \boldsymbol{\sigma}_f$ are obtained by particularizing Equations (177) and (179) in [5] to the PERP benchmark and adding their respective contributions. The expression obtained by particularizing Equation (179) in [5] takes on the following form:

$$
\begin{aligned}
\left(\frac{\partial^2 L}{\partial f_j \partial f_{m_2}}\right)^{(1)}_{(f=v, f=\sigma_f)} &= \sum_{g=1}^{G} \int_V dV \int_{4\pi} d\mathbf{\Omega}\, \psi^{(1),g}(r,\mathbf{\Omega}) \sum_{g'=1}^{G} \int_{4\pi} d\mathbf{\Omega}'\varphi^{g'}(r,\mathbf{\Omega}')\chi^g \frac{\partial^2\left[(v\Sigma_f)^{g'}\right]}{\partial f_j \partial f_{m_2}} \\
&+ \sum_{g=1}^{G} \int_V dV \int_{4\pi} d\mathbf{\Omega}\, u_{1,j}^{(2),g}(r,\mathbf{\Omega}) \frac{\partial\left[(v\Sigma_f)^g\right]}{\partial f_{m_2}} \sum_{g'=1}^{G} \int_{4\pi} d\mathbf{\Omega}'\chi^{g'} \psi^{(1),g'}(r,\mathbf{\Omega}') \\
&+ \sum_{g=1}^{G} \int_V dV \int_{4\pi} d\mathbf{\Omega}\, u_{2,j}^{(2),g}(r,\mathbf{\Omega}) \sum_{g'=1}^{G} \int_{4\pi} d\mathbf{\Omega}'\varphi^{g'}(r,\mathbf{\Omega}')\chi^g \frac{\partial\left[(v\Sigma_f)^{g'}\right]}{\partial f_{m_2}},
\end{aligned}
$$

$$for \quad j = J_{\sigma f}+1,\ldots,J_{\sigma f}+J_v; m_2 = 1,\ldots,J_{\sigma f}. \tag{147}$$

The parameters f_j and t_{m_2} in Equation (147) correspond to the average number of neutrons per fission and fission cross sections, and are therefore denoted as $f_j \equiv v_{i_j}^{g_j}$ and $f_{m_2} \equiv \sigma_{f,i_{m_2}}^{g_{m_2}}$, respectively. Noting that

$$
\frac{\partial^2\left[(v\Sigma_f)^{g'}\right]}{\partial f_j \partial f_{m_2}} = \frac{\partial\left[\dfrac{\partial \sum_{m=1}^{M}\sum_{i=1}^{I} N_{i,m}(v\sigma_f)_i^{g'}}{\partial v_{i_j}^{g_j}}\right]}{\partial \sigma_{f,i_{m_2}}^{g_{m_2}}} = \frac{\partial\left[\delta_{g_j g'} N_{i_j,m_j}\sigma_{f,i_j}^{g'}\right]}{\partial \sigma_{f,i_{m_2}}^{g_{m_2}}} = \delta_{i_j i_{m_2}}\delta_{g_j g'}\delta_{g_{m_2} g'} N_{i_{m_2},m_{m_2}}, \tag{148}
$$

and inserting the results obtained in Equations (148), (23) and (24) into Equation (147), yields the following simplified expression for Equation (147):

$$
\begin{aligned}
\left(\frac{\partial^2 L}{\partial f_j \partial f_{m_2}}\right)^{(1)}_{(f=v, f=\sigma_f)} &= \delta_{i_j i_{m_2}} \delta_{g_j g_{m_2}} N_{i_{m_2}, m_{m_2}} \int_V dV \varphi_0^{g_{m_2}}(r) \sum_{g=1}^{G} \chi^g \xi_0^{(1),g}(r) \\
&+ N_{i_{m_2}, m_{m_2}} v_{i_{m_2}}^{g_{m_2}} \int_V dV \left[U_{1,j;0}^{(2),g_{m_2}}(r) \sum_{g'=1}^{G} \chi^{g'} \xi_0^{(1),g'}(r) + \varphi_0^{g_{m_2}}(r) \sum_{g=1}^{G} \chi^g U_{2,j;0}^{(2),g}(r) \right], \\
&\quad for \quad j = J_{\sigma f} + 1, \ldots, J_{\sigma f} + J_v; m_2 = 1, \ldots, J_{\sigma f}.
\end{aligned}
\tag{149}
$$

The contributions stemming from Equation (177) in [5], in conjunction with the relations $\frac{\partial \Sigma_t^g}{\partial t_{m_2}} = \frac{\partial \Sigma_t^g}{\partial t_{m_2}} \frac{\partial t_{m_2}}{\partial f_{m_2}} = \frac{\partial \Sigma_t^g}{\partial f_{m_2}}$, take on the following particular form:

$$
\begin{aligned}
\left(\frac{\partial^2 L}{\partial f_j \partial f_{m_2}}\right)^{(2)}_{(f=v, f=\sigma_f)} &= -\sum_{g=1}^{G} \int_V dV \int_{4\pi} d\Omega \left[u_{1,j}^{(2),g}(r,\Omega) \psi^{(1),g}(r,\Omega) + u_{2,j}^{(2),g}(r,\Omega) \varphi^g(r,\Omega) \right] \frac{\partial \Sigma_t^g}{\partial f_{m_2}}, \\
&\quad for \quad j = J_{\sigma f} + 1, \ldots, J_{\sigma f} + J_v; m_2 = 1, \ldots, J_{\sigma f}.
\end{aligned}
\tag{150}
$$

Inserting the results obtained in Equation (37) into Equation (150), yields the following simplified expression for Equation (150):

$$
\left(\frac{\partial^2 L}{\partial f_j \partial f_{m_2}}\right)^{(2)}_{(f=v, f=\sigma_f)} = -N_{i_{m_2}, m_{m_2}} \int_V dV \int_{4\pi} d\Omega \left[u_{1,j}^{(2),g_{m_2}}(r,\Omega) \psi^{(1),g_{m_2}}(r,\Omega) + u_{2,j}^{(2),g_{m_2}}(r,\Omega) \varphi^{g_{m_2}}(r,\Omega) \right],
\tag{151}
$$

Collecting the partial contributions obtained in Equations (149) and (151), yields the following final expression:

$$
\begin{aligned}
\left(\frac{\partial^2 L}{\partial f_j \partial f_{m_2}}\right)_{(f=v, f=\sigma_f)} &= \sum_{i=1}^{2} \left(\frac{\partial^2 L}{\partial f_j \partial f_{m_2}}\right)^{(1)}_{(f=v, f=\sigma_f)} \\
&= \delta_{i_j i_{m_2}} \delta_{g_j g_{m_2}} N_{i_{m_2}, m_{m_2}} \int_V dV \varphi_0^{g_{m_2}}(r) \sum_{g=1}^{G} \chi^g \xi_0^{(1),g}(r) \\
&+ N_{i_{m_2}, m_{m_2}} v_{i_{m_2}}^{g_{m_2}} \int_V dV \left[U_{1,j;0}^{(2),g_{m_2}}(r) \sum_{g'=1}^{G} \chi^{g'} \xi_0^{(1),g'}(r) + \varphi_0^{g_{m_2}}(r) \sum_{g=1}^{G} \chi^g U_{2,j;0}^{(2),g}(r) \right] \\
&- N_{i_{m_2}, m_{m_2}} \int_V dV \int_{4\pi} d\Omega \left[u_{1,j}^{(2),g_{m_2}}(r,\Omega) \psi^{(1),g_{m_2}}(r,\Omega) + u_{2,j}^{(2),g_{m_2}}(r,\Omega) \varphi^{g_{m_2}}(r,\Omega) \right], \\
&\quad for \quad j = J_{\sigma f} + 1, \ldots, J_{\sigma f} + J_v; m_2 = 1, \ldots, J_{\sigma f}.
\end{aligned}
\tag{152}
$$

8.2. Alternative Path: Computing the Second-Order Sensitivities $\partial^2 L(\boldsymbol{\alpha})/\partial \boldsymbol{\sigma}_f \partial \boldsymbol{v}$

The equations needed for deriving the expression of the 2nd-order sensitivities $\partial^2 L(\boldsymbol{\alpha})/\partial \boldsymbol{\sigma}_f \partial \boldsymbol{v}$ are obtained by particularizing Equations (160) and (179) in [5] to the PERP benchmark. The expression obtained by particularizing Equation (179) in [5] to the PERP benchmark, takes on the following form:

$$
\begin{aligned}
\left(\frac{\partial^2 L}{\partial f_j \partial f_{m_2}}\right)^{(1)}_{(f=\sigma_f, f=v)} &= \sum_{g=1}^{G} \int_V dV \int_{4\pi} d\Omega \, \psi^{(1),g}(r,\Omega) \sum_{g'=1}^{G} \int_{4\pi} d\Omega' \varphi^{g'}(r,\Omega') \chi^g \frac{\partial^2 \left[(v\Sigma_f)^{g'} \right]}{\partial f_j \partial f_{m_2}} \\
&+ \sum_{g=1}^{G} \int_V dV \int_{4\pi} d\Omega \, u_{1,j}^{(2),g}(r,\Omega) \frac{\partial \left[(v\Sigma_f)^g \right]}{\partial f_{m_2}} \sum_{g'=1}^{G} \int_{4\pi} d\Omega' \chi^{g'} \psi^{(1),g'}(r,\Omega') \\
&+ \sum_{g=1}^{G} \int_V dV \int_{4\pi} d\Omega \, u_{2,j}^{(2),g}(r,\Omega) \sum_{g'=1}^{G} \int_{4\pi} d\Omega' \varphi^{g'}(r,\Omega') \chi^g \frac{\partial \left[(v\Sigma_f)^{g'} \right]}{\partial f_{m_2}}, \\
&\quad for \quad j = 1, \ldots, J_{\sigma f}; m_2 = J_{\sigma f} + 1, \ldots, J_{\sigma f} + J_v.
\end{aligned}
\tag{153}
$$

In Equation (153), the 2nd-level adjoint functions $u_{1,j}^{(2),g}(r,\mathbf{\Omega})$, and $u_{2,j}^{(2),g}(r,\mathbf{\Omega})$, $j=1,\ldots,J_{\sigma f}$; $g=1,\ldots,G$, are the solutions of the 2nd-Level Adjoint Sensitivity System (2nd-LASS) presented in Equations (18)–(21) in Section 2.2.

The parameters f_j and t_{m_2} in Equation (153) correspond to the fission cross sections and the average number of neutrons per fission, and are therefore denoted as $f_j \equiv \sigma_{f,i_j}^{g_j}$ and $f_{m_2} \equiv \nu_{i_{m_2}}^{g_{m_2}}$, respectively. Noting that,

$$\frac{\partial^2 \left[(\nu\Sigma_f)^{g'}\right]}{\partial f_j \partial f_{m_2}} = \frac{\partial \left[\frac{\partial \sum\limits_{m=1}^{M}\sum\limits_{i=1}^{I} N_{i,m}(\nu\sigma_f)_i^{g'}}{\partial \sigma_{f,i_j}^{g_j}}\right]}{\partial \nu_{i_{m_2}}^{g_{m_2}}} = \frac{\partial \left[\delta_{g_j g'} N_{i_j,m_j} \nu_{i_j}^{g'}\right]}{\partial \nu_{i_{m_2}}^{g_{m_2}}} = \delta_{i_j i_{m_2}} \delta_{g_j g'} \delta_{g_{m_2} g'} N_{i_{m_2},m_{m_2}}, \qquad (154)$$

and inserting the results obtained in Equations (120), (121) and (154) into Equation (153), yields the following simplified expression for Equation (153):

$$\left(\frac{\partial^2 L}{\partial f_j \partial f_{m_2}}\right)^{(1)}_{(f=\sigma_f,f=\nu)} = \delta_{i_j i_{m_2}} \delta_{g_j g_{m_2}} N_{i_{m_2},m_{m_2}} \int_V dV \varphi_0^{g_{m_2}}(r) \sum_{g=1}^{G} \chi^g \xi_0^{(1),g}(r)$$

$$+ N_{i_{m_2},m_{m_2}} \sigma_{f,i_{m_2}}^{g_{m_2}} \int_V dV \left[U_{1,j;0}^{(2),g_{m_2}}(r) \sum_{g'=1}^{G} \chi^{g'} \xi_0^{(1),g'}(r) + \varphi_0^{g_{m_2}}(r) \sum_{g=1}^{G} \chi^g U_{2,j;0}^{(2),g}(r)\right], \qquad (155)$$

$$for \quad j=1,\ldots,J_{\sigma f}; m_2 = J_{\sigma f}+1,\ldots,J_{\sigma f}+J_\nu.$$

The contributions stemming from Equation (160) in [5], in conjunction with the relations $\frac{\partial^2 L}{\partial t_j \partial f_{m_2}} \frac{\partial t_j}{\partial f_j} = \frac{\partial^2 L}{\partial f_j \partial f_{m_2}}$, yield the following particular form for these contributions:

$$\left(\frac{\partial^2 L}{\partial f_j \partial f_{m_2}}\right)^{(2)}_{(f=\sigma_f,f=\nu)} = \sum_{g=1}^{G} \int_V dV \int_{4\pi} d\mathbf{\Omega}\, \psi_{1,j}^{(2),g}(r,\mathbf{\Omega}) \frac{\partial \left[(\nu\Sigma_f)^g\right]}{\partial f_{m_2}} \sum_{g'=1}^{G} \int_{4\pi} d\mathbf{\Omega}' \chi^{g'} \psi^{(1),g'}(r,\mathbf{\Omega}')$$

$$+ \sum_{g=1}^{G} \int_V dV \int_{4\pi} d\mathbf{\Omega}\, \psi_{2,j}^{(2),g}(r,\mathbf{\Omega}) \sum_{g'=1}^{G} \int_{4\pi} d\mathbf{\Omega}' \varphi^{g'}(r,\mathbf{\Omega}') \chi^g \frac{\partial \left[(\nu\Sigma_f)^g\right]}{\partial f_{m_2}}, \qquad (156)$$

$$for \quad j=1,\ldots,J_{\sigma f}; m_2 = J_{\sigma f}+1,\ldots,J_{\sigma f}+J_\nu,$$

where the 2nd-level adjoint functions $\psi_{1,j}^{(2),g}(r,\mathbf{\Omega})$, and $\psi_{2,j}^{(2),g}(r,\mathbf{\Omega})$, $j=1,\ldots,J_{\sigma f}$; $g=1,\ldots,G$, are the solutions of the 2nd-Level Adjoint Sensitivity System (2nd-LASS) presented in Equations (33), (35), (39) and (40) in Section 2.2.

Inserting the results obtained in Equations (120) and (121) into Equation (156) and performing the respective angular integrations yields the following simplified expression for Equation (156):

$$\left(\frac{\partial^2 L}{\partial f_j \partial f_{m_2}}\right)^{(2)}_{(f=\sigma_f,f=\nu)} = N_{i_{m_2},m_{m_2}} \sigma_{f,i_{m_2}}^{g_{m_2}} \int_V dV \left[\xi_{1,j;0}^{(2),g_{m_2}}(r) \sum_{g'=1}^{G} \chi^{g'} \xi_0^{(1),g'}(r) + \varphi_0^{g_{m_2}}(r) \sum_{g=1}^{G} \chi^g \xi_{2,j;0}^{(2),g}(r)\right], \qquad (157)$$

Collecting the partial contributions obtained in Equations (155) and (157), yields the following final expression:

$$
\begin{aligned}
\left(\frac{\partial^2 L}{\partial f_j \partial f_{m_2}}\right)_{(f=\sigma_f, f=v)} &= \sum_{i=1}^{2}\left(\frac{\partial^2 L}{\partial f_j \partial f_{m_2}}\right)_{(f=\sigma_f, f=v)}^{(i)} \\
&= \delta_{i_j i_{m_2}} \delta_{g_j g_{m_2}} N_{i_{m_2}, m_{m_2}} \int_V dV \varphi_0^{g_{m_2}}(r) \sum_{g=1}^{G} \chi^g \xi_0^{(1),g}(r) \\
&+ N_{i_{m_2}, m_{m_2}} \sigma_{f, i_{m_2}}^{g_{m_2}} \int_V dV \left[U_{1,j;0}^{(2),g_{m_2}}(r) \sum_{g'=1}^{G} \chi^{g'} \xi_0^{(1),g'}(r) + \varphi_0^{g_{m_2}}(r) \sum_{g=1}^{G} \chi^g U_{2,j;0}^{(2),g}(r) \right. \\
&+ \left. \xi_{1,j;0}^{(2),g_{m_2}}(r) \sum_{g'=1}^{G} \chi^{g'} \xi_0^{(1),g'}(r) + \varphi_0^{g_{m_2}}(r) \sum_{g=1}^{G} \chi^g \xi_{2,j;0}^{(2),g}(r) \right], \\
&\quad for \quad j = 1, \ldots, J_{\sigma f}; m_2 = J_{\sigma f} + 1, \ldots, J_{\sigma f} + J_v.
\end{aligned}
\tag{158}
$$

8.3. Numerical Results for $\partial^2 L(\boldsymbol{\alpha})/\partial \mathbf{v} \partial \boldsymbol{\sigma}_f$

The second-order absolute sensitivities, $\partial^2 L(\boldsymbol{\alpha})/\partial \mathbf{v} \partial \boldsymbol{\sigma}_f$, of the leakage response with respect to the average number of neutrons per fission and fission cross sections for all isotopes of the PERP benchmark have been computed using Equation (152), and have been independently verified by computing $\partial^2 L(\boldsymbol{\alpha})/\partial \boldsymbol{\sigma}_f \partial \mathbf{v}$ using Equation (158). For this case, computing $\partial^2 L(\boldsymbol{\alpha})/\partial \mathbf{v} \partial \boldsymbol{\sigma}_f$ using Equation (152) is as efficient as computing $\partial^2 L(\boldsymbol{\alpha})/\partial \boldsymbol{\sigma}_f \partial \mathbf{v}$ using Equation (158) since either path requires 120 forward and adjoint PARTISN computations to obtain all the needed 2nd-level adjoint functions.

The matrix $\left(\partial^2 L/\partial f_j \partial f_{m_2}\right)_{(f=v, f=\sigma_f)}$, $j = J_{\sigma f} + 1, \ldots, J_{\sigma f} + J_v; m_2 = 1, \ldots, J_{\sigma f}$ of 2nd-order absolute sensitivities has dimensions $J_v \times J_{\sigma f} (= 60 \times 60)$, since $J_{\sigma f} = J_v = G \times N_f = 60$. For convenient comparisons, the numerical results presented in this section are presented in unit-less values of the relative sensitivities that correspond to $\left(\partial^2 L/\partial f_j \partial f_{m_2}\right)_{(f=v, f=\sigma_f)}$, $j = J_{\sigma f} + 1, \ldots, J_{\sigma f} + J_v; m_2 = 1, \ldots, J_{\sigma f}$, which are denoted as $\mathbf{S}^{(2)}\left(v_i^g, \sigma_{f,k}^{g'}\right)$ and are defined as follows:

$$
\mathbf{S}^{(2)}\left(v_i^g, \sigma_{f,k}^{g'}\right) \triangleq \frac{\partial^2 L}{\partial v_i^g \partial \sigma_{f,k}^{g'}}\left(\frac{v_i^g \sigma_{f,k}^{g'}}{L}\right), \quad i,k = 1,2; \ g,g' = 1, \ldots, 30.
\tag{159}
$$

The numerical results obtained for the matrix $\mathbf{S}^{(2)}\left(v_i^g, \sigma_{f,k}^{g'}\right)$, $i,k = 1,2; \ g,g' = 1, \ldots, 30$ have been partitioned into $N_f \times N_f = 4$ submatrices, each of dimensions $G \times G (= 30 \times 30)$. The summary of the main features of each submatrix is presented in Table 25.

Table 25. Summary presentation of the matrix $\mathbf{S}^{(2)}\left(v_i^g, \sigma_{f,k}^{g'}\right)$, $i,k = 1,2; \ g,g' = 1, \ldots, 30$.

Isotopes	k=1 (^{239}Pu)	k=2 (^{240}Pu)
$i = 1$ (^{239}Pu)	$\mathbf{S}^{(2)}\left(v_{i=1}^g, \sigma_{f,k=1}^{g'}\right)$ 28 elements with absolute values > 1.0	$\mathbf{S}^{(2)}\left(v_{i=1}^g, \sigma_{f,k=2}^{g'}\right)$ Max. value = 1.04×10^{-1} at $g = 12, g' = 12$
$i = 2$ (^{240}Pu)	$\mathbf{S}^{(2)}\left(v_{i=2}^g, \sigma_{f,k=1}^{g'}\right)$ Max. value = 1.05×10^{-1} at $g = 12, g' = 12$	$\mathbf{S}^{(2)}\left(v_{i=2}^g, \sigma_{f,k=2}^{g'}\right)$ Max. value = 6.86×10^{-2} at $g = 12, g' = 12$

The 2nd-order mixed sensitivities $\partial^2 L(\boldsymbol{\alpha})/\partial \mathbf{v} \partial \boldsymbol{\sigma}_f$ are mostly positive. Among the $J_v \times J_{\sigma f} (= 60 \times 60)$ elements in the matrix $\mathbf{S}^{(2)}\left(v_i^g, \sigma_{f,k}^{g'}\right)$, $i,k = 1,2; \ g,g' = 1, \ldots, 30$, 3557 out of 3600 elements have positive values, and most of them are very small; however, 28 out of these 3600 elements

have large relative sensitivities, with values greater than 1.0, as noted in Table 25. All of these larger sensitivities reside in the sub-matrix $\mathbf{S}^{(2)}\left(v_{i=1}^{g}, \sigma_{f,k=1}^{g'}\right)$, and relate to the fission parameters for isotope ^{239}Pu. The overall maximum relative sensitivity is $S^{(2)}\left(v_1^{12}, \sigma_{f,1}^{12}\right) = 3.225$. Additional details about the sub-matrix $\mathbf{S}^{(2)}\left(v_{i=1}^{g}, \sigma_{f,k=1}^{g'}\right)$ are provided in the following section. The results in Table 25 also indicate that all of the mixed 2nd-order relative sensitivities involving the fission parameters (either $v_{i=2}^{g}$ or $\sigma_{f,k=2}^{g'}$) of isotope ^{240}Pu have absolute values smaller than 1.0. Moreover, as shown in this table, the elements with the maximum absolute value in each of the respective submatrices all involve the fission parameters for the 12th energy group (i.e., $v_i^{g=12}, i = 1, 2$ or $\sigma_{f,k}^{g'=12}, k = 1, 2$) of isotopes ^{239}Pu and ^{240}Pu.

The numerical results for the elements of the submatrix $\mathbf{S}^{(2)}\left(v_{i=1}^{g}, \sigma_{f,k=1}^{g'}\right) \triangleq \left(\partial^2 L/\partial v_{i=1}^{g}\partial\sigma_{f,k=1}^{g'}\right)\left(v_{i=1}^{g}\sigma_{f,k=1}^{g'}/L\right)$, $g, g' = 1, \ldots, 30$, of 2nd-order mixed relative sensitivities of the leakage response with respect to the average number of neutrons per fission and fission cross sections of isotope ^{239}Pu, indicate that the majority (899 out of 900) of the elements of this submatrix have positive 2nd-order relative sensitivities; only 1 element is negative. Table 26 presents the 28 elements (in bold) of $\mathbf{S}^{(2)}\left(v_{i=1}^{g}, \sigma_{f,k=1}^{g'}\right)$, $g, g' = 1, \ldots, 30$ which have values greater than 1.0. The largest value among these sensitivities is attained by the relative 2nd-order mixed sensitivity $S^{(2)}\left(v_1^{12}, \sigma_{f,1}^{12}\right) = 3.225$.

Table 26. Components of $\mathbf{S}^{(2)}\left(v_{i=1}^{g}, \sigma_{f,k=1}^{g'}\right)$, $g, g' = 1, \ldots, 30$ having values greater than 1.0.

Groups	$g' = 6$	7	8	9	10	11	12	13	14
$g = 6$	0.188	0.210	0.175	0.210	0.218	0.203	0.314	0.218	0.140
7	0.207	**1.587**	0.779	0.936	0.973	0.904	**1.401**	0.971	0.625
8	0.179	0.801	**1.227**	0.804	0.836	0.776	**1.203**	0.834	0.537
9	0.217	0.974	0.807	**1.649**	**1.015**	0.943	**1.462**	**1.013**	0.652
10	0.228	**1.023**	0.850	**1.018**	**1.767**	0.990	**1.534**	**1.063**	0.684
11	0.212	0.953	0.793	0.952	0.986	**1.577**	**1.430**	0.991	0.638
12	0.328	**1.470**	**1.223**	**1.469**	**1.527**	**1.414**	**3.225**	**1.530**	0.985
13	0.229	**1.025**	0.853	**1.024**	**1.064**	0.989	**1.528**	**1.777**	0.688
14	0.150	0.671	0.558	0.670	0.697	0.647	**1.002**	0.691	0.910
15	0.087	0.388	0.323	0.388	0.403	0.374	0.579	0.400	0.255

9. Quantification of Uncertainties in the PERP Leakage Response Due to Uncertainties in Fission Cross Sections

Correlations between the group-averaged microscopic fission cross sections or correlations between these cross sections and other cross sections are not available for the PERP benchmark. When such correlations are unavailable, the maximum entropy principle (see, e.g., [9]) indicates that neglecting them minimizes the inadvertent introduction of spurious information into the computations of the various moments of the response's distribution in parameter space. The formulas for computing the expected value, variance and skewness of the response distribution by taking into account the 2nd-order response sensitivities together with the standard deviations of the group-averaged fission microscopic cross sections parameter correlations are as follows:

1. The expected value, $[E(L)]_f$, of the leakage response $L(\boldsymbol{\alpha})$ has the following expression:

$$[E(L)]_f = L\left(\boldsymbol{\alpha}^0\right) + [E(L)]_f^{(2,U)}, \tag{160}$$

where the subscript "f" indicates contributions *solely* from the *group-averaged uncorrelated fission microscopic cross sections,* and where the term $[E(L)]_f^{(2,U)}$, which provides the 2nd-order contributions, is given by the following expression:

$$[E(L)]_f^{(2,U)} = \frac{1}{2} \sum_{g=1}^{G} \sum_{i=1}^{I} \frac{\partial^2 L(\boldsymbol{\alpha})}{\partial \sigma_{f,i}^g \partial \sigma_{f,i}^g} \left(s_{f,i}^g \right)^2, \quad G = 30, \ I = 6 \tag{161}$$

In Equation (161), the quantity $s_{f,i}^g$ denotes the standard deviation associated with the imprecisely known model parameter $\sigma_{f,i}^g$:

2. Taking into account contributions solely from the *group-averaged <u>u</u>ncorrelated and <u>n</u>ormally-distributed microscopic fission cross sections* (which will be indicated by using the superscript "(U,N)" in the following equations), the expression for computing the variance, denoted as $[\mathrm{var}(L)]_f^{(U,N)}$, of the PERP leakage response has the following form:

$$[\mathrm{var}(L)]_f^{(U,N)} = [\mathrm{var}\,(L)]_f^{(1,U,N)} + [\mathrm{var}\,(L)]_f^{(2,U,N)}, \tag{162}$$

where the first-order contribution term, $[\mathrm{var}\,(L)]_f^{(1,U,N)}$, to the variance $[\mathrm{var}(L)]_f^{(U,N)}$ is defined as

$$[\mathrm{var}\,(L)]_f^{(1,U,N)} \triangleq \sum_{g=1}^{G} \sum_{i=1}^{I} \left[\frac{\partial L(\boldsymbol{\alpha})}{\partial \sigma_{f,i}^g} \right]^2 \left(s_{f,i}^g \right)^2, \quad G = 30, \ I = 6, \tag{163}$$

while the second-order contribution term, $[\mathrm{var}\,(L)]_f^{(2,U,N)}$, to the variance $[\mathrm{var}(L)]_f^{(U,N)}$ is defined as

$$[\mathrm{var}\,(L)]_f^{(2,U,N)} \triangleq \frac{1}{2} \sum_{g=1}^{G} \sum_{i=1}^{I} \left[\frac{\partial^2 L(\boldsymbol{\alpha})}{\partial \sigma_{f,i}^g \partial \sigma_{f,i}^g} \left(s_{f,i}^g \right)^2 \right]^2, \quad G = 30, \ I = 6. \tag{164}$$

3. Taking into account contributions solely from the group-averaged uncorrelated normally-distributed fission microscopic cross sections, the third-order moment, $[\mu_3(L)]_f^{(U,N)}$, of the leakage response for the PERP benchmark takes on the following form:

$$[\mu_3(L)]_f^{(U,N)} = 3 \sum_{g=1}^{G} \sum_{i=1}^{I} \left[\frac{\partial L(\boldsymbol{\alpha})}{\partial \sigma_{f,i}^g} \right]^2 \frac{\partial^2 L(\boldsymbol{\alpha})}{\partial \sigma_{f,i}^g \partial \sigma_{f,i}^g} \left(s_{f,i}^g \right)^4, \quad G = 30, \ I = 6. \tag{165}$$

As Equation (165) indicates, if the 2nd-order sensitivities were unavailable, the third moment $[\mu_3(L)]_f^{(U,N)}$ would vanish and the response distribution would by default be assumed to be Gaussian.

4. The skewness, $[\gamma_1(L)]_f^{(U,N)}$, due to the variances of microscopic fission cross sections in the leakage response, *L*, is defined as follows:

$$[\gamma_1(L)]_f^{(U,N)} = [\mu_3(L)]_f^{(U,N)} / \left\{ [\mathrm{var}(L)]_f^{(U,N)} \right\}^{3/2} \tag{166}$$

The effects of the first- and, respectively, second-order sensitivities on the response's expected value, variance and skewness can be quantified by considering typical values for the standard deviations for the uncorrelated group-averaged isotopic fission cross sections, using these values together with the respective sensitivities computed in Section 2 in Equations (161)–(166). The results thus obtained are presented in Table 27, considering uniform parameter standard deviations of 1%, 5%, and 10%, respectively. These results indicate that the effects of both the 1st- and 2nd-order sensitivities on the

expected response value, standard deviation and skewness are small, which is not surprising in view of the small values for the 1st- and 2nd-order sensitivities already presented in Tables 2 and 3.

Table 27. Comparison of Response Moments Induced by Various Relative Standard Deviations Assumed for the Parameters $\sigma_{f,i}^g$, $i = 1, 2$; $g = 1, \ldots, 30$.

Relative Standard Deviation	10%	5%	1%
$[E(L)]_f^{(2,U)}$	3.7191×10^4	9.2976×10^3	3.7191×10^2
$L(\boldsymbol{\alpha}^0)$	1.7648×10^6	1.7648×10^6	1.7648×10^6
$[E(L)]_f = L(\boldsymbol{\alpha}^0) + [E(L)]_f^{(2,U)}$	1.8020×10^6	1.7741×10^6	1.7652×10^6
$[\text{var}(L)]_f^{(1,U,N)}$	9.5932×10^{10}	2.3983×10^{10}	9.5932×10^8
$[\text{var}(L)]_f^{(2,U,N)}$	5.4830×10^8	3.4269×10^7	5.4830×10^4
$[\text{var}(L)]_f^{(U,N)} = [\text{var}(L)]_f^{(1,U,N)} + [\text{var}(L)]_f^{(2,U,N)}$	9.6480×10^{10}	2.4017×10^{10}	9.5938×10^8
$[\mu_3(L)]_f^{(U,N)}$	3.5136×10^{15}	2.1960×10^{14}	3.5136×10^{11}
$[\gamma_1(L)]_f^{(U,N)} = [\mu_3(L)]_f^{(U,N)} / \left\{ [\text{var}(L)]_f^{(U,N)} \right\}^{3/2}$	0.1172	5.8999×10^{-2}	1.1824×10^{-2}

The relative effects of uncertainties in the fission cross sections can be compared to the corresponding effects stemming from the total and, respectively, scattering cross sections, by considering standard deviations of 10% for all of these cross sections and by comparing the corresponding results shown in Table 27 with the corresponding results presented in Table 25 of Part I [1] and Table 19 of Part II [2]. This comparison reveals that the following relations hold:

$$[E(L)]_s^{(2,U)} = -1.3473 \times 10^4 < [E(L)]_f^{(2,U)} = 3.7191 \times 10^4 \ll [E(L)]_t^{(2,U)} = 4.5980 \times 10^6,$$

$$[\text{var}(L)]_s^{(1,U,N)} = 1.2379 \times 10^{10} < [\text{var}(L)]_f^{(1,U,N)} = 9.5932 \times 10^{10} \ll [\text{var}(L)]_t^{(1,U,N)} = 3.4196 \times 10^{12},$$

$$[\text{var}(L)]_s^{(2)} = 4.3207 \times 10^7 \ll [\text{var}(L)]_f^{(2)} = 5.4830 \times 10^8 \ll [\text{var}(L)]_t^{(2)} = 2.8789 \times 10^{13},$$

$$\left| [\gamma_1(L)]_s^{(U,N)} \right| = 3.5595 \times 10^{-3} \ll [\gamma_1(L)]_f^{(U,N)} = 0.1172 < [\gamma_1(L)]_t^{(U,N)} = 0.3407.$$

The above relations indicate that the contributions to the leakage response moments stemming from the group-averaged uncorrelated microscopic fission cross sections are much smaller than the corresponding contributions stemming from the group-averaged uncorrelated microscopic total cross sections but are much greater than the corresponding contributions stemming from the group-averaged uncorrelated microscopic scattering cross sections.

It is important to note that the results presented in Table 27 consider only the standard deviations of the group-averaged microscopic fission cross sections, since correlations between these parameters are unavailable. On the other hand, the results presented in Section 3 indicated that the largest values are displayed by several mixed 2nd-order sensitivities of the leakage response with respect to the total and fission cross sections, which are by several times larger than the values of the unmixed sensitivities. Recall that the following sensitivities have absolute values larger than 1.0: (a) 11 elements of the matrix $\mathbf{S}^{(2)}\left(\sigma_{f,1}^g, \sigma_{f,1}^{g'} \right)$, $g, g', h = 1, \ldots, 30$, presented in Table 4, in which only one of them is included in the above computations; (b) 35 elements of the matrix $\mathbf{S}^{(2)}\left(\sigma_{f,1}^g, \sigma_{t,1}^{g'} \right)$, $g, g', h = 1, \ldots, 30$, presented in Table 5; (c) 1 elements of the matrix $\mathbf{S}^{(2)}\left(\sigma_{f,1}^g, \sigma_{t,5}^{g'} \right)$, $g, g', h = 1, \ldots, 30$, as listed in Table 5; (d) 48

elements of the matrix $\mathbf{S}^{(2)}\left(\sigma_{f,1}^g, \sigma_{t,6}^{g'}\right)$, $g, g' = 1, \ldots, 30$, presented in Table 5. However, the effects of these sensitivities on the uncertainties in the response distribution can be taken into account only if the corresponding correlations among the various model parameters were available.

10. Uncertainties in the PERP Leakage Response Stemming from Uncertainties in the Average Number of Neutrons per Fission

The correlations between the average number of neutrons per fission are unknown, so these parameters will be assumed to be uncorrelated, since this assumption is the least biased, according to the maximum entropy principle [9] in avoiding the introduction of spurious information in the uncertainty quantification computations. Similar to those formulas presented in Section 9, upto 2nd-order response sensitivities, the expected value, $[E(L)]_\nu$, of the leakage response $L(\boldsymbol{\alpha})$ has the following expression:

$$[E(L)]_\nu = L\left(\boldsymbol{\alpha}^0\right) + [E(L)]_\nu^{(2,U)}, \tag{167}$$

where the subscript "ν" and superscript "U" indicate contributions *solely* from the *group-averaged uncorrelated parameters underlying the average number of neutrons per fission,* and where the term $[E(L)]_\nu^{(2,U)}$, which provides the 2nd-order contributions, is given by the following expression:

$$[E(L)]_\nu^{(2,U)} = \frac{1}{2}\sum_{g=1}^{G}\sum_{i=1}^{I} \frac{\partial^2 L(\boldsymbol{\alpha})}{\partial \nu_i^g \partial \nu_i^g}\left(s_{\nu,i}^g\right)^2, \quad G = 30, \ I = 6. \tag{168}$$

In Equation (168), the quantity $s_{\nu,i}^g$ denotes the standard deviation associated with the imprecisely known model parameter ν_i^g.

Considering contributions solely from the group-averaged uncorrelated parameters underlying the average number of neutrons per fission, the expression for computing the variance, denoted as $[\mathrm{var}(L)]_\nu^{(U,N)}$, of the PERP leakage response has the following form:

$$[\mathrm{var}(L)]_\nu^{(U,N)} = [\mathrm{var}\,(L)]_\nu^{(1,U,N)} + [\mathrm{var}\,(L)]_\nu^{(2,U,N)}. \tag{169}$$

In Equation (169), the term $[\mathrm{var}\,(L)]_\nu^{(1,U,N)}$ denotes the first-order contributions to the variance $[\mathrm{var}(L)]_\nu^{(U,N)}$ and is defined as follows:

$$[\mathrm{var}\,(L)]_\nu^{(1,U,N)} \triangleq \sum_{g=1}^{G}\sum_{i=1}^{I}\left[\frac{\partial L(\boldsymbol{\alpha})}{\partial \nu_i^g}\right]^2 \left(s_{\nu,i}^g\right)^2, \quad G = 30, \ I = 6, \tag{170}$$

while the second-order contribution term, $[\mathrm{var}\,(L)]_\nu^{(2,U,N)}$ to the variance $[\mathrm{var}(L)]_\nu^{(U,N)}$ is defined as follows:

$$[\mathrm{var}\,(L)]_\nu^{(2,U,N)} \triangleq \frac{1}{2}\sum_{g=1}^{G}\sum_{i=1}^{I}\left[\frac{\partial^2 L(\boldsymbol{\alpha})}{\partial \nu_i^g \partial \nu_i^g}\left(s_{\nu,i}^g\right)^2\right]^2, \quad G = 30, \ I = 6. \tag{171}$$

Again, taking into account contributions solely from the group-averaged uncorrelated parameters underlying the average number of neutrons per fission, the third-order moment, $[\mu_3(L)]_\nu^{(U,N)}$, of the leakage response for the PERP benchmark takes on the following form:

$$[\mu_3(L)]_\nu^{(U,N)} = 3\sum_{g=1}^{G}\sum_{i=1}^{I}\left[\frac{\partial L(\boldsymbol{\alpha})}{\partial \nu_i^g}\right]^2 \frac{\partial^2 L(\boldsymbol{\alpha})}{\partial \nu_i^g \partial \nu_i^g}\left(s_{\nu,i}^g\right)^4, \quad G = 30, \ I = 6. \tag{172}$$

As Equation (172) indicates, if the 2nd-order sensitivities were unavailable, the third moment $[\mu_3(L)]_\nu^{(U,N)}$ would vanish and the response distribution would need, by default, to be assumed to

be Gaussian. The skewness, $[\gamma_1(L)]_\nu^{(U,N)}$, of the leakage response, L, which indicates the degree of the distribution's asymmetry with respect to its mean, due to the variances of the average number of neutrons per fission, is defined as follows:

$$[\gamma_1(L)]_\nu^{(U,N)} = [\mu_3(L)]_\nu^{(U,N)} / \left\{ [\text{var}(L)]_\nu^{(U,N)} \right\}^{3/2} \tag{173}$$

Table 28 shows the results computed using Equations (167)–(173) together with the 1st- and 2nd-order respective sensitivity values presented in Section 5.3, for uniform parameter standard deviations of 1%, 5%, and 10% of ν_i^g, $i = 1, 2$; $g = 1, \ldots, 30$, respectively.

Table 28. Comparison of Response Moments Induced by Various Relative Standard Deviations Assumed for the Parameters ν_i^g, $i = 1, 2$; $g = 1, \ldots, 30$.

Relative Standard Deviation	10%	5%	1%
$[E(L)]_\nu^{(2,U)}$	1.0659×10^5	2.6647×10^4	1.0659×10^2
$L(\alpha^0)$	1.7648×10^6	1.7648×10^6	1.7648×10^6
$[E(L)]_\nu = L(\alpha^0) + [E(L)]_\nu^{(2,U)}$	1.8714×10^6	1.7915×10^6	1.7659×10^6
$[\text{var}(L)]_\nu^{(1,U,N)}$	1.8649×10^{11}	4.6623×10^{10}	1.8649×10^9
$[\text{var}(L)]_\nu^{(2,U,N)}$	2.9566×10^9	1.8479×10^8	2.9566×10^5
$[\text{var}(L)]_\nu^{(U,N)} = [\text{var}(L)]_\nu^{(1,U,N)} + [\text{var}(L)]_\nu^{(2,U,N)}$	1.8945×10^{11}	4.6807×10^{10}	1.8652×10^9
$[\mu_3(L)]_\nu^{(U,N)}$	1.5540×10^{16}	9.7125×10^{14}	1.5540×10^{12}
$[\gamma_1(L)]_\nu^{(U,N)} = [\mu_3(L)]_\nu^{(U,N)} / \left\{ [\text{var}(L)]_\nu^{(U,N)} \right\}^{3/2}$	0.1885	9.5909×10^{-2}	1.9291×10^{-2}

The relative effects on the leakage response of uncertainties in the average number of neutrons per fission can be compared to the corresponding effects stemming from the fission and total cross sections. A final comparison, with corresponding conclusions, will be made after all of the 2nd-order sensitivities of the PERP leakage response to the PERP benchmark's underlying nuclear data are obtained. Thus, comparing the results shown in Table 28 for standard deviations of 10% with the corresponding results presented in Table 27 for the fission cross sections and Table 25 of Part I [1] for the total cross sections reveals that:

$$[E(L)]_f^{(2,U)} = 3.7191 \times 10^4 < [E(L)]_\nu^{(2,U)} = 1.0659 \times 10^5 \ll [E(L)]_t^{(2,U)} = 4.5980 \times 10^6,$$

$$[\text{var}(L)]_f^{(1,U,N)} = 9.5932 \times 10^{10} < [\text{var}(L)]_\nu^{(1,U,N)} = 1.8649 \times 10^{11} \ll [\text{var}(L)]_t^{(1,U,N)} = 3.4196 \times 10^{12},$$

$$[\text{var}(L)]_f^{(2)} = 5.4830 \times 10^8 < [\text{var}(L)]_\nu^{(2,U,N)} = 2.9566 \times 10^9 \ll [\text{var}(L)]_t^{(2,U,N)} = 2.8789 \times 10^{13},$$

$$[\gamma_1(L)]_f^{(U,N)} = 0.1172 < [\gamma_1(L)]_\nu^{(U,N)} = 0.1885 < [\gamma_1(L)]_t^{(U,N)} = 0.3407.$$

The above comparisons indicate that the contributions to the leakage response moments stemming from the group-averaged uncorrelated parameters underlying the average number of neutrons per fission are much smaller than the corresponding contributions stemming from the group-averaged uncorrelated microscopic total cross sections but are bigger than the corresponding contributions stemming from the group-averaged uncorrelated microscopic fission cross sections. Again, it is important to note that the results presented in Table 28 consider only the standard deviations of the uncorrelated parameters underlying the average number of neutrons per fission, since correlations between these parameters are unavailable. On the other hand, the results presented in Sections 5–7 indicated that the largest values are displayed by several mixed 2nd-order sensitivities of the leakage

response with respect to ν and $\boldsymbol{\sigma}_t$, and with respect to ν and $\boldsymbol{\sigma}_f$, which are much larger than the values of the unmixed sensitivities. Recall that the following sensitivities have absolute values larger than 1.0: (a) 52 elements of the matrix $\mathbf{S}^{(2)}\left(\nu_1^g, \nu_1^{g'}\right)$, $g, g', h = 1, \ldots, 30$, as summarized in Table 15; only 6 of these are included in the computations leading to the results shown in Table 28; (b) 72 elements of the matrix $\mathbf{S}^{(2)}\left(\nu_1^g, \sigma_{t,1}^{g'}\right)$, $g, g', h = 1, \ldots, 30$, presented in Table 17; (c) 7 elements of the matrix $\mathbf{S}^{(2)}\left(\nu_1^g, \sigma_{t,5}^{g'}\right)$, $g, g' = 1, \ldots, 30$ as listed in Table 18; (d) 99 elements of the matrix $\mathbf{S}^{(2)}\left(\nu_1^g, \sigma_{t,6}^{g'}\right)$, $g, g' = 1, \ldots, 30$ presented in Tables 19 and 20; (e) 1 element of the matrix $\mathbf{S}^{(2)}\left(\nu_2^g, \sigma_{t,6}^{g'}\right)$, $g, g' = 1, \ldots, 30$ presented in Section 6.3.4; and (f) 28 elements of the matrix $\mathbf{S}^{(2)}\left(\nu_{i=1}^g, \sigma_{f,k=1}^{g'}\right)$, $g, g' = 1, \ldots, 30$ presented in Table 26. However, the effect of these large sensitivities on the uncertainties in the response distribution cannot be considered presently because the corresponding correlations among the various model parameters are not available.

11. Conclusions

This work has presented results for the first-order sensitivities, $\partial L(\boldsymbol{\alpha})/\partial \boldsymbol{\sigma}_f$, and the second-order sensitivities $\partial^2 L(\boldsymbol{\alpha})/\partial \boldsymbol{\sigma}_f \partial \boldsymbol{\sigma}_f$ of the PERP total leakage response with respect to the group-averaged microscopic fission cross sections, and the mixed second-order sensitivities $\partial^2 L(\boldsymbol{\alpha})/\partial \boldsymbol{\sigma}_f \partial \boldsymbol{\sigma}_t$ and $\partial^2 L(\boldsymbol{\alpha})/\partial \boldsymbol{\sigma}_f \partial \boldsymbol{\sigma}_s$ of the leakage response with respect to the group-averaged microscopic fission/total cross sections and corresponding fission and scattering cross sections. In addition, this work has also presented results for $\partial L(\boldsymbol{\alpha})/\partial \nu$ and $\partial^2 L(\boldsymbol{\alpha})/\partial \nu \partial \nu$, i.e., the first- and, respectively, second-order sensitivities of the PERP total leakage response with respect to the parameters underlying the benchmark's average number of neutrons per fission, as well as results for the mixed second-order sensitivities for $\partial^2 L(\boldsymbol{\alpha})/\partial \nu \partial \boldsymbol{\sigma}_t$, $\partial^2 L(\boldsymbol{\alpha})/\partial \nu \partial \boldsymbol{\sigma}_s$, and $\partial^2 L(\boldsymbol{\alpha})/\partial \nu \partial \boldsymbol{\sigma}_f$.

For the sensitivities with respect to the fission cross sections, the following conclusions can be drawn from the results reported in this work:

1. The 1st-order relative sensitivities of the PERP leakage response with respect to the group-averaged microscopic fission cross sections for the two fissionable PERP isotopes are positive, as shown in Tables 2 and 3, signifying that an increase in $\sigma_{f,i}^g$, $i = 1, 2$; $g = 1, \ldots, 30$ will cause an increase in the PERP leakage response L (i.e., more neutrons will leak out of the sphere). The 2nd-order unmixed relative sensitivities of the PERP leakage response with respect to the group-averaged microscopic fission cross sections are positive for the energy groups $g = 7, \ldots, 15$, but are negative for the other energy groups;

2. Comparing the results for the 1st-order relative sensitivities to those obtained for the 2nd-order unmixed relative sensitivities for isotope 1 (^{239}Pu) indicates that the values of the 2nd-order sensitivities are close to, and generally smaller than, the corresponding values of the 1st-order sensitivities for the same energy group, except for the 12th energy group, where the 2nd-order relative sensitivity is larger. For isotope 2 (^{240}Pu), the values for both the 1st- and 2nd-order relative sensitivities are very small, and the values of the 2nd-order unmixed relative sensitivities are at least an order of magnitude smaller than the corresponding values of the 1st-order ones. The largest values of the 1st-order and 2nd-order relative sensitivities are always related to the 12th energy group for both isotopes ^{239}Pu and ^{240}Pu;

3. The 1st-order relative sensitivities with respect to the fission cross sections are up to 50% smaller than the corresponding values with respect to the total cross sections, and are approximately one order of magnitude larger than the corresponding 1st-order relative sensitivities with respect to the 0th-order scattering cross sections for isotope ^{239}Pu. Likewise, the absolute values of the 2nd-order unmixed relative sensitivities with respect to the fission cross sections are 50–90% smaller than the corresponding values with respect to total cross sections but are approximately

one to two orders of magnitudes larger than the 2nd-order sensitivities corresponding to the 0th-order scattering cross sections for ^{239}Pu;

4. The 2nd-order mixed sensitivities $\partial^2 L(\boldsymbol{\alpha})/\partial\boldsymbol{\sigma}_f\partial\boldsymbol{\sigma}_f$ are mostly positive. Among the $J_{\sigma f} \times J_{\sigma f}$ ($= 60 \times 60$) elements in the matrix $\mathbf{S}^{(2)}\left(\sigma_{f,i}^g, \sigma_{f,k}^{g'}\right)$, $i, k = 1, 2$; $g, g' = 1, \ldots, 30$, 11 elements have relative sensitivities greater than 1.0. All of these 11 large sensitivities belong to the submatrix $\mathbf{S}^{(2)}\left(\sigma_{f,1}^g, \sigma_{f,1}^{g'}\right)$, and involve the 12th energy group of the fission cross sections of isotope ^{239}Pu; the largest of these sensitivities is $S^{(2)}\left(\sigma_{f,1}^{12}, \sigma_{f,1}^{12}\right) = 1.348$. The values of the mixed 2nd-order relative sensitivities involving the fission cross sections of isotope ^{240}Pu are all smaller than 1.0;

5. The 2nd-order mixed sensitivities $\partial^2 L(\boldsymbol{\alpha})/\partial\boldsymbol{\sigma}_f\partial\boldsymbol{\sigma}_t$ are mostly negative. Among the $J_{\sigma f} \times J_{\sigma t}$ ($= 60 \times 180$) elements of the matrix $\mathbf{S}^{(2)}\left(\sigma_{f,i}^g, \sigma_{t,k}^{g'}\right)$, $i = 1, 2$; $k = 1, \ldots, 6$; $g, g' = 1, \ldots, 30$, 84 elements belonging to the submatrices $\mathbf{S}^{(2)}\left(\sigma_{f,1}^g, \sigma_{t,1}^{g'}\right)$, $\mathbf{S}^{(2)}\left(\sigma_{f,1}^g, \sigma_{t,5}^{g'}\right)$ and $\mathbf{S}^{(2)}\left(\sigma_{f,1}^g, \sigma_{t,6}^{g'}\right)$ have absolute values greater than 1.0. These 84 large sensitivities involve the fission cross sections of isotope ^{239}Pu, and the total cross sections of isotopes ^{239}Pu, C and 1H. The largest (negative) relative sensitivity is $S^{(2)}\left(\sigma_{f,1}^{12}, \sigma_{t,6}^{30}\right) = -13.92$. The mixed 2nd-order relative sensitivities involving the fission cross sections of the isotope ^{240}Pu or the total cross sections of isotopes ^{240}Pu, 69Ga and 71Ga have absolute values smaller than 1.0;

6. The $J_{\sigma f} \times J_{\sigma s}$ ($= 60 \times 21,600$) dimensional matrix $\mathbf{S}^{(2)}\left(\sigma_{f,i}^g, \sigma_{s,l,k}^{g'\rightarrow h}\right)$ comprises more elements having positive (rather than negative) values when involving even-orders ($l = 0, 2$) scattering cross sections, and vice-versa when involving odd-orders ($l = 1, 3$) scattering cross sections. Overall, however, the total number of positive elements in this matrix is comparable to that of negative elements in the sensitivity matrix. As shown in Tables 8–11, in each submatrix of $\mathbf{S}^{(2)}\left(\sigma_{f,i}^g, \sigma_{s,l,k}^{g'\rightarrow h}\right)$, $l = 0, \ldots, 3$; $i = 1, 2$; $k = 1, \ldots, 6$; $g, g', h = 1, \ldots, 30$, the largest absolute values of the 2nd-order relative sensitivities corresponding to even-order scattering parameters are all positive, while those corresponding to odd-orders scattering parameters are all negative;

7. The absolute values of all the $J_{\sigma f} \times J_{\sigma s}$ ($= 60 \times 21,600$) elements of the matrix $\mathbf{S}^{(2)}\left(\sigma_{f,i}^g, \sigma_{s,l,k}^{g'\rightarrow h}\right)$ are less than 1.0, and the vast majority of them are very small; also, the higher the order of scattering cross sections, the smaller the absolute values of these sensitivities. Also, it is observed that the largest absolute value of the 2nd-order relative sensitivities in each submatrix of $\mathbf{S}^{(2)}\left(\sigma_{f,i}^g, \sigma_{s,l,k}^{g'\rightarrow h}\right)$, $l = 0, \ldots, 3$; $i = 1, 2$; $k = 1, \ldots, 6$; $g, g', h = 1, \ldots, 30$, generally involve the fission cross sections for the 12th energy group of isotopes ^{239}Pu or^{240}Pu, and the self-scattering cross sections in the 12th or 7th energy group for all isotopes. The largest sensitivity comprised in $\mathbf{S}^{(2)}\left(\sigma_{f,i}^g, \sigma_{s,l,k}^{g'\rightarrow h}\right)$ is $S^{(2)}\left(\sigma_{f,1}^{g=12}, \sigma_{s,l=0,1}^{12\rightarrow 12}\right) = 3.03 \times 10^{-1}$, i.e., the 2nd-order mixed sensitivity of the PERP leakage response with respect to the 12th energy group of the fission and 0th-order self-scattering cross sections of isotope ^{239}Pu;

8. The alternative paths for computing the mixed 2nd-order sensitivities, which are due to the symmetry of these sensitivities, provide multiple reciprocal "solution verifications" possibilities, ensuring that the respective computations were performed correctly. However, one of the alternative paths is much more efficient computationally than the other. For example, computing $\partial^2 L(\boldsymbol{\alpha})/\partial\boldsymbol{\sigma}_f\partial\boldsymbol{\sigma}_t$ is around 3 times more efficient than computing alternatively the symmetric sensitivities $\partial^2 L(\boldsymbol{\alpha})/\partial\boldsymbol{\sigma}_t\partial\boldsymbol{\sigma}_f$. Also, computing $\partial^2 L(\boldsymbol{\alpha})/\partial\boldsymbol{\sigma}_f\partial\boldsymbol{\sigma}_s$ is about 60 times more efficient than computing alternatively the sensitivities $\partial^2 L(\boldsymbol{\alpha})/\partial\boldsymbol{\sigma}_s\partial\boldsymbol{\sigma}_f$;

9. Many mixed 2nd-order sensitivities of the leakage response to the group-averaged fission and total microscopic cross sections are significantly larger than the unmixed 2nd-order sensitivities of the leakage response with respect to the group-averaged fission microscopic cross sections. Therefore,

it would be very important to obtain correlations among the various model parameter, since the correlations among the respective fission and total cross sections could provide significantly larger contributions to the response moments than the standard deviations of the fission cross sections.

For the sensitivities with respect to the parameters underlying the average number of neutrons per fission, the following conclusions can be drawn from the results reported in this work:

10. The 1st-order relative sensitivities of $\partial L(\boldsymbol{\alpha})/\partial \boldsymbol{\nu}$ for the two fissionable PERP isotopes are positive, as shown in Tables 13 and 14, signifying that an increase in ν_i^g, $i = 1, 2$; $g = 1, \ldots, 30$ will cause an increase in the PERP leakage response L. The 2nd-order unmixed relative sensitivities of the leakage response with respect to the average number of neutrons per fission are also positive;

11. Comparing the results for the 1st-order relative sensitivities of $\partial L(\boldsymbol{\alpha})/\partial \boldsymbol{\nu}$ to those 2nd-order unmixed relative sensitivities for isotope 1 (^{239}Pu) indicate that, for energy groups $g = 7, \ldots, 14$, the values of the 2nd-order unmixed sensitivities are significantly larger than the corresponding values of the 1st-order sensitivities for the same energy group, and they are smaller for other energy groups. For isotope 2 (^{240}Pu), the values for both the 1st- and 2nd-order relative sensitivities are all very small, and the values of the 2nd-order unmixed relative sensitivities are at least an order of magnitude smaller than the corresponding values of the 1st-order ones. The largest values of the 1st-order and 2nd-order unmixed relative sensitivities are always related to the 12th energy group of the parameters underlying the average number of neutrons per fission for both isotopes ^{239}Pu and ^{240}Pu;

12. The 1st-order relative sensitivities of $\partial L(\boldsymbol{\alpha})/\partial \boldsymbol{\nu}$ are comparable to the corresponding values with respect to the total cross sections for energy groups $g = 7, \ldots, 12$, but for energy groups $g = 13, \ldots, 22$, they are considerably smaller. On the other hand, the 1st-order relative sensitivities of $\partial L(\boldsymbol{\alpha})/\partial \boldsymbol{\nu}$ are 30% to 50% larger than the corresponding values to $\partial L(\boldsymbol{\alpha})/\partial \boldsymbol{\sigma}_f$ for ^{239}Pu. Likewise, the values of the 2nd-order unmixed relative sensitivities with respect to the average number of neutrons per fission are significantly smaller than the corresponding values with respect to total cross sections, but larger than the corresponding values with respect to fission cross sections;

13. The 2nd-order mixed sensitivities $\partial^2 L(\boldsymbol{\alpha})/\partial \boldsymbol{\nu} \partial \boldsymbol{\nu}$ are all positive. Among the $J_\nu \times J_\nu = (60 \times 60)$ elements in the matrix $\mathbf{S}^{(2)}\left(\nu_i^g, \nu_k^{g'}\right)$, $i, k = 1, 2$; $g, g' = 1, \ldots, 30$, 52 elements have relative sensitivities greater than 1.0. All of these 52 large sensitivities belong to the submatrix $\mathbf{S}^{(2)}\left(\nu_1^g, \nu_1^{g'}\right)$, and involve the parameters underlying the average number of neutrons per fission of isotope ^{239}Pu. The largest of these sensitivities is $S^{(2)}\left(\nu_1^{12}, \nu_1^{12}\right) = 2.963$. The values of the mixed 2nd-order relative sensitivities involving the parameters underlying the average number of neutrons per fission of isotope ^{240}Pu are all smaller than 1.0;

14. The 2nd-order mixed sensitivities $\partial^2 L(\boldsymbol{\alpha})/\partial \boldsymbol{\nu} \partial \boldsymbol{\sigma}_t$ are mostly negative. Among the $J_\nu \times J_{\sigma t}$ ($= 10{,}800$) elements of the matrix $\mathbf{S}^{(2)}\left(\nu_i^g, \sigma_{t,k}^{g'}\right)$, $i = 1, 2$; $k = 1, \ldots, 6$; $g, g' = 1, \ldots, 30$, there are 179 elements belonging to the submatrices $\mathbf{S}^{(2)}\left(\nu_1^g, \sigma_{t,1}^{g'}\right)$, $\mathbf{S}^{(2)}\left(\nu_1^g, \sigma_{t,5}^{g'}\right)$ and $\mathbf{S}^{(2)}\left(\nu_1^g, \sigma_{t,6}^{g'}\right)$ which have absolute values greater than 1.0; 178 of these large sensitivities involve the parameters underlying the average number of neutrons per fission of isotope ^{239}Pu, and the total cross sections of isotopes ^{239}Pu, C and 1H. The largest (negative) relative sensitivity is $S^{(2)}\left(\nu_1^{12}, \sigma_{t,6}^{30}\right) = -19.29$. In addition, the mixed 2nd-order relative sensitivities involving isotopes ^{240}Pu, 69Ga and 71Ga generally have absolute values smaller than 1.0;

15. The $J_\nu \times J_{\sigma s}$ ($= 60 \times 21{,}600$) dimensional matrix $\mathbf{S}^{(2)}\left(\nu_i^g, \sigma_{s,l,k}^{g' \to h}\right)$ comprises more elements having positive (rather than negative) values for even-orders ($l = 0, 2$) scattering cross sections and vice-versa when involving odd-orders ($l = 1, 3$) scattering cross sections. Overall, however, this matrix contains about as many positive elements as negative ones. As shown in Tables 21–24,

in each submatrix of $\mathbf{S}^{(2)}\left(v_i^g, \sigma_{s,l,k}^{g' \rightarrow h}\right)$, $l = 0, \ldots, 3$; $i = 1, 2$; $k = 1, \ldots, 6$; $g, g', h = 1, \ldots, 30$, the largest absolute values of the 2nd-order relative sensitivities corresponding to even-order scattering parameters are all positive, while those corresponding to odd-orders scattering parameters are all negative;

16. The absolute values of all the $J_v \times J_{\sigma s} (= 60 \times 21,600)$ elements of the matrix $\mathbf{S}^{(2)}\left(v_i^g, \sigma_{s,l,k}^{g' \rightarrow h}\right)$ are less than 1.0, and the vast majority of them are very small; also, the higher the order of scattering cross sections, the smaller the absolute values of these sensitivities. Furthermore, it is observed that in each submatrix of $\mathbf{S}^{(2)}\left(v_i^g, \sigma_{s,l,k}^{g' \rightarrow h}\right)$, $l = 0, \ldots, 3$; $i = 1, 2$; $k = 1, \ldots, 6$; $g, g', h = 1, \ldots, 30$ the largest 2nd-order relative sensitivities generally involve v_i^g for the 12th energy group of isotopes ^{239}Pu or^{240}Pu, and the self-scattering cross sections in the 12th or 7th energy group for all isotopes. The largest 2nd-order sensitivity comprised in $\mathbf{S}^{(2)}\left(v_i^g, \sigma_{s,l,k}^{g' \rightarrow h}\right)$ is $S^{(2)}\left(v_1^{g=12}, \sigma_{s,l=0,k=1}^{12 \rightarrow 12}\right) = 4.65 \times 10^{-1}$;

17. The 2nd-order mixed sensitivities $\partial^2 L(\boldsymbol{\alpha}) / \partial \boldsymbol{v} \partial \boldsymbol{\sigma}_f$ are mostly positive. Among the $J_v \times J_{\sigma f} (= 60 \times 60)$ elements in the matrix $\mathbf{S}^{(2)}\left(v_i^g, \sigma_{f,k}^{g'}\right)$, $i, k = 1, 2$; $g, g' = 1, \ldots, 30$, 28 elements have relative sensitivities greater than 1.0. All of these 28 large sensitivities belong to the submatrix $\mathbf{S}^{(2)}\left(v_{i=1}^g, \sigma_{f,k=1}^{g'}\right)$, and relate to the average number of neutrons per fission of isotope ^{239}Pu. The largest of these sensitivities is $S^{(2)}\left(v_1^{12}, \sigma_{f,1}^{12}\right) = 3.225$. The values of the mixed 2nd-order relative sensitivities involving isotope ^{240}Pu are all smaller than 1.0;

18. Many mixed 2nd-order relative sensitivities in the matrices $\mathbf{S}^{(2)}\left(v_i^g, v_k^{g'}\right)$, $\mathbf{S}^{(2)}\left(v_i^g, \sigma_{t,k}^{g'}\right)$ and $\mathbf{S}^{(2)}\left(v_i^g, \sigma_{f,k}^{g'}\right)$ are significantly larger than the unmixed 2nd-order sensitivities of the leakage response with respect to the parameters underlying the average number of neutrons per fission. Therefore, it would be very important to obtain correlations among the average number of neutrons per fission, total and fission cross sections, so that significantly larger contributions from those mixed sensitivities to the response moments can be accounted for.

Subsequent works [10,11] will report the values and effects of the 1st-order and 2nd-order sensitivities of the PERP's leakage response with respect to the group-averaged source parameters, fission spectrum, and isotopic number densities, along with the overall conclusions and implications of this pioneering and uniquely comprehensive 2nd-order sensitivity analysis and uncertainty quantification of the PERP reactor physics benchmark.

Appendix A. Definitions of PERP Model Parameters

As presented in Part I [1], the components of the vector of 1st-order sensitivities of the leakage response with respect to the model parameters, denoted as $\mathbf{S}^{(1)}(\boldsymbol{\alpha})$, was defined as follows:

$$\mathbf{S}^{(1)}(\boldsymbol{\alpha}) \triangleq \left[\frac{\partial L(\boldsymbol{\alpha})}{\partial \boldsymbol{\sigma}_t}; \frac{\partial L(\boldsymbol{\alpha})}{\partial \boldsymbol{\sigma}_s}; \frac{\partial L(\boldsymbol{\alpha})}{\partial \boldsymbol{\sigma}_f}; \frac{\partial L(\boldsymbol{\alpha})}{\partial \boldsymbol{\nu}}; \frac{\partial L(\boldsymbol{\alpha})}{\partial \mathbf{p}}; \frac{\partial L(\boldsymbol{\alpha})}{\partial \mathbf{q}}; \frac{\partial L(\boldsymbol{\alpha})}{\partial \mathbf{N}} \right]^{\dagger}. \tag{A1}$$

The symmetric matrix of 2nd-order sensitivities of the leakage response with respect to the model parameters, denoted as $\mathbf{S}^{(2)}(\boldsymbol{\alpha})$, was defined as follows:

$$\mathbf{S}^{(2)}(\boldsymbol{\alpha}) \triangleq \begin{bmatrix} \frac{\partial^2 L(\boldsymbol{\alpha})}{\partial \boldsymbol{\sigma}_t \partial \boldsymbol{\sigma}_t} & * & * & * & * & * & * \\ \frac{\partial^2 L(\boldsymbol{\alpha})}{\partial \boldsymbol{\sigma}_s \partial \boldsymbol{\sigma}_t} & \frac{\partial^2 L(\boldsymbol{\alpha})}{\partial \boldsymbol{\sigma}_s \partial \boldsymbol{\sigma}_s} & * & * & * & * & * \\ \frac{\partial^2 L(\boldsymbol{\alpha})}{\partial \boldsymbol{\sigma}_f \partial \boldsymbol{\sigma}_t} & \frac{\partial^2 L(\boldsymbol{\alpha})}{\partial \boldsymbol{\sigma}_f \partial \boldsymbol{\sigma}_s} & \frac{\partial^2 L(\boldsymbol{\alpha})}{\partial \boldsymbol{\sigma}_f \partial \boldsymbol{\sigma}_f} & * & * & * & * \\ \frac{\partial^2 L(\boldsymbol{\alpha})}{\partial \boldsymbol{\nu} \partial \boldsymbol{\sigma}_t} & \frac{\partial^2 L(\boldsymbol{\alpha})}{\partial \boldsymbol{\nu} \partial \boldsymbol{\sigma}_s} & \frac{\partial^2 L(\boldsymbol{\alpha})}{\partial \boldsymbol{\nu} \partial \boldsymbol{\sigma}_f} & \frac{\partial^2 L(\boldsymbol{\alpha})}{\partial \boldsymbol{\nu} \partial \boldsymbol{\nu}} & * & * & * \\ \frac{\partial^2 L(\boldsymbol{\alpha})}{\partial \mathbf{p} \partial \boldsymbol{\sigma}_t} & \frac{\partial^2 L(\boldsymbol{\alpha})}{\partial \mathbf{p} \partial \boldsymbol{\sigma}_s} & \frac{\partial^2 L(\boldsymbol{\alpha})}{\partial \mathbf{p} \partial \boldsymbol{\sigma}_f} & \frac{\partial^2 L(\boldsymbol{\alpha})}{\partial \mathbf{p} \partial \boldsymbol{\nu}} & \frac{\partial^2 L(\boldsymbol{\alpha})}{\partial \mathbf{p} \partial \mathbf{p}} & * & * \\ \frac{\partial^2 L(\boldsymbol{\alpha})}{\partial \mathbf{q} \partial \boldsymbol{\sigma}_t} & \frac{\partial^2 L(\boldsymbol{\alpha})}{\partial \mathbf{q} \partial \boldsymbol{\sigma}_s} & \frac{\partial^2 L(\boldsymbol{\alpha})}{\partial \mathbf{q} \partial \boldsymbol{\sigma}_f} & \frac{\partial^2 L(\boldsymbol{\alpha})}{\partial \mathbf{q} \partial \boldsymbol{\nu}} & \frac{\partial^2 L(\boldsymbol{\alpha})}{\partial \mathbf{q} \partial \mathbf{p}} & \frac{\partial^2 L(\boldsymbol{\alpha})}{\partial \mathbf{q} \partial \mathbf{q}} & * \\ \frac{\partial^2 L(\boldsymbol{\alpha})}{\partial \mathbf{N} \partial \boldsymbol{\sigma}_t} & \frac{\partial^2 L(\boldsymbol{\alpha})}{\partial \mathbf{N} \partial \boldsymbol{\sigma}_s} & \frac{\partial^2 L(\boldsymbol{\alpha})}{\partial \mathbf{N} \partial \boldsymbol{\sigma}_f} & \frac{\partial^2 L(\boldsymbol{\alpha})}{\partial \mathbf{N} \partial \boldsymbol{\nu}} & \frac{\partial^2 L(\boldsymbol{\alpha})}{\partial \mathbf{N} \partial \mathbf{p}} & \frac{\partial^2 L(\boldsymbol{\alpha})}{\partial \mathbf{N} \partial \mathbf{q}} & \frac{\partial^2 L(\boldsymbol{\alpha})}{\partial \mathbf{N} \partial \mathbf{N}} \end{bmatrix}. \tag{A2}$$

As defined in Equation (1), the vector $\boldsymbol{\alpha} \triangleq \left[\boldsymbol{\sigma}_t; \boldsymbol{\sigma}_s; \boldsymbol{\sigma}_f; \boldsymbol{\nu}; \mathbf{p}; \mathbf{q}; \mathbf{N} \right]^{\dagger}$ denotes the "vector of imprecisely known model parameters", with vector-components $\boldsymbol{\sigma}_t$, $\boldsymbol{\sigma}_s$, $\boldsymbol{\sigma}_f$, $\boldsymbol{\nu}$, $\mathbf{p}$, $\mathbf{q}$ and $\mathbf{N}$, comprising the various model parameters for the microscopic total cross sections, scattering cross sections, fission cross sections, average number of neutrons per fission, fission spectra, sources, and isotopic number densities, which have been described in Part I [1]. For easy referencing, the definitions of these model parameters will be recalled in the remainder of this Appendix.

The total cross section Σ_t^g for energy group g, $g = 1, \dots, G$, is computed for the PERP benchmark using the following expression:

$$\Sigma_t^g = \sum_{m=1}^{M=2} \Sigma_{t,m}^g; \quad \Sigma_{t,m}^g = \sum_i^I N_{i,m} \sigma_{t,i}^g = \sum_i^I N_{i,m} \left[\sigma_{f,i}^g + \sigma_{c,i}^g + \sum_{g'=1}^G \sigma_{s,l=0,i}^{g \to g'} \right], \quad m = 1, 2, \tag{A3}$$

where m denotes the materials in the PERP benchmark; $\sigma_{f,i}^g$ and $\sigma_{c,i}^g$ denote, respectively, the tabulated group microscopic fission and neutron capture cross sections for group g, $g = 1, \dots, G$. Other nuclear reactions are negligible in the PERP benchmark. As discussed in Part I [1], the total cross section $\Sigma_t^g \to \Sigma_t^g(\mathbf{t})$ will depend on the vector of parameters $\mathbf{t}$, which is defined as follows:

$$\mathbf{t} \triangleq \left[t_1, \dots, t_{J_t} \right]^{\dagger} \triangleq \left[t_1, \dots, t_{J_{\sigma t}}; n_1, \dots, n_{J_n} \right]^{\dagger} \triangleq \left[\boldsymbol{\sigma}_t; \mathbf{N} \right]^{\dagger}, \quad J_t = J_{\sigma t} + J_n, \tag{A4}$$

where

$$\mathbf{N} \triangleq \left[n_1, \dots, n_{J_n} \right]^{\dagger} \triangleq [N_{1,1}, N_{2,1}, N_{3,1}, N_{4,1}, N_{5,2}, N_{6,2}]^{\dagger}, \quad J_n = 6, \tag{A5}$$

$$\boldsymbol{\sigma}_t \triangleq \left[t_1, \dots, t_{J_{\sigma t}} \right]^{\dagger} \triangleq \left[\sigma_{t,i=1}^1, \sigma_{t,i=1}^2, \dots, \sigma_{t,i=1}^G, \dots, \sigma_{t,i}^g, \dots, \sigma_{t,i=I}^1, \dots, \sigma_{t,i=I}^G \right]^{\dagger},$$
$$i = 1, \dots, I = 6; \ g = 1, \dots, G = 30; \ J_{\sigma t} = I \times G. \tag{A6}$$

In Equations (A4)–(A6), the dagger denotes "transposition," $\sigma_{t,i}^g$ denotes the microscopic total cross section for isotope i and energy group g, $N_{i,m}$ denotes the respective isotopic number density, and J_n denotes the total number of isotopic number densities in the model. Thus, the vector $\mathbf{t}$ comprises a total of $J_t = J_{\sigma t} + J_n = 30 \times 6 + 6 = 186$ imprecisely known "model parameters" as its components.

The scattering transfer cross section $\Sigma_s^{g'\to g}(\Omega' \to \Omega)$ from energy group g', $g' = 1,\ldots,G$ into energy group g, $g = 1,\ldots,G$, is computed using the finite Legendre polynomial expansion of order $ISCT = 3$:

$$\Sigma_s^{g'\to g}(\Omega' \to \Omega) = \sum_{m=1}^{M=2} \Sigma_{s,m}^{g'\to g}(\Omega' \to \Omega),$$

$$\Sigma_{s,m}^{g'\to g}(\Omega' \to \Omega) \cong \sum_{i=1}^{I=6} N_{i,m} \sum_{l=0}^{ISCT=3} (2l+1)\ \sigma_{s,l,i}^{g'\to g} P_l(\Omega'\cdot\Omega), \quad m = 1,2, \tag{A7}$$

where $\sigma_{s,l,i}^{g'\to g}$ denotes the *l*-th order Legendre-expanded microscopic scattering cross section from energy group g' into energy group g for isotope i. In view of Equation (A7), the scattering cross section $\Sigma_s^{g'\to g}(\Omega' \to \Omega) \to \Sigma_s^{g'\to g}(\mathbf{s};\Omega' \to \Omega)$ depends on the vector of parameters $\mathbf{s}$, which is defined as follows:

$$\mathbf{s} \triangleq \left[s_1,\ldots,s_{J_s}\right]^\dagger \triangleq \left[s_1,\ldots,s_{J_{\sigma s}};n_1,\ldots,n_{J_n}\right]^\dagger \triangleq \left[\boldsymbol{\sigma}_s;\mathbf{N}\right]^\dagger, \ J_s = J_{\sigma s} + J_n, \tag{A8}$$

$$\boldsymbol{\sigma}_s \triangleq \left[s_1,\ldots,s_{J_{\sigma s}}\right]^\dagger \triangleq \left[\sigma_{s,l=0,i=1}^{g'=1\to g=1},\sigma_{s,l=0,i=1}^{g'=2\to g=1},\ldots,\sigma_{s,l=0,i=1}^{g'=G\to g=1},\sigma_{s,l=0,i=1}^{g'=1\to g=2},\sigma_{s,l=0,i=1}^{g'=2\to g=2},\ldots,\sigma_{s,l,i}^{g'\to g},\ldots,\sigma_{s,ISCT,i=I}^{G\to G}\right]^\dagger,$$
$$l = 0,\ldots,ISCT;\ i = 1,\ldots,I;\ g,g' = 1,\ldots,G;\ J_{\sigma s} = (G\times G)\times I\times(ISCT+1). \tag{A9}$$

The expressions in Equations (A7) and (A3) indicate that the zeroth order (i.e., $l = 0$) scattering cross sections must be considered separately from the higher order (i.e., $l \geq 1$) scattering cross sections, since the former contribute to the total cross sections, while the latter do not. Therefore, the total number of zeroth-order scattering cross section comprise in $\boldsymbol{\sigma}_s$ is denoted as $J_{\sigma s,l=0}$, where $J_{\sigma s,l=0} = G\times G\times I$; and the total number of higher order (i.e., $l \geq 1$) scattering cross sections comprised in $\boldsymbol{\sigma}_s$ is denoted as $J_{\sigma s,l\geq 1}$, where $J_{\sigma s,l\geq 1} = G\times G\times I\times ISCT$, with $J_{\sigma s,l=0} + J_{\sigma s,l\geq 1} = J_{\sigma s}$. Thus, the vector $\mathbf{s}$ comprises a total of $J_{\sigma s} + J_n = 30\times 30\times 6\times(3+1) + 6 = 21606$ imprecisely known components ("model parameters").

The transport code PARTISN [4] computes the quantity $\left(\nu\Sigma_f\right)^g$ using directly the quantities $(\nu\sigma)_{f,i}^g$, which are provided in data files for each isotope i, and energy group g, as follows

$$\left(\nu\Sigma_f\right)^g = \sum_{m=1}^{M=2}\left(\nu\Sigma_f\right)_m^g;\quad \left(\nu\Sigma_f\right)_m^g = \sum_{i=1}^{I=6} N_{i,m}\left(\nu\sigma_f\right)_i^g,\quad m = 1,2. \tag{A10}$$

In view of Equation (A10), the quantity $\left(\nu\Sigma_f\right)^g \to \left(\nu\Sigma_f\right)^g(\mathbf{f};r)$ depends on the vector of parameters $\mathbf{f}$, which is defined as follows:

$$\mathbf{f} \triangleq \left[f_1,\ldots,f_{J_{\sigma f}};f_{J_{\sigma f}+1},\ldots,f_{J_{\sigma f}+J_\nu};f_{J_{\sigma f}+J_\nu+1},\ldots,f_{J_f}\right]^\dagger \triangleq \left[\boldsymbol{\sigma}_f;\boldsymbol{\nu};\mathbf{N}\right]^\dagger, \ J_f = J_{\sigma f} + J_\nu + J_n, \tag{A11}$$

where

$$\boldsymbol{\sigma}_f \triangleq \left[\sigma_{f,i=1}^1,\sigma_{f,i=1}^2,\ldots,\sigma_{f,i=1}^G,\ldots,\sigma_{f,i}^g,\ldots,\sigma_{f,i=N_f}^1,\ldots,\sigma_{f,i=N_f}^G\right]^\dagger \triangleq \left[f_1,\ldots,f_{J_{\sigma f}}\right]^\dagger,$$
$$i = 1,\ldots,N_f;\ g = 1,\ldots,G;\ J_{\sigma f} = G\times N_f, \tag{A12}$$

$$\boldsymbol{\nu} \triangleq \left[\nu_{i=1}^1,\nu_{i=1}^2,\ldots,\nu_{i=1}^G,\ldots,\nu_i^g,\ldots,\nu_{i=N_f}^1,\ldots,\nu_{i=N_f}^G\right]^\dagger \triangleq \left[f_{J_{\sigma f}+1},\ldots,f_{J_{\sigma f}+J_\nu}\right]^\dagger,$$
$$i = 1,\ldots,N_f;\ g = 1,\ldots,G;\ J_\nu = G\times N_f, \tag{A13}$$

and where $\sigma_{f,i}^g$ denotes the microscopic fission cross section for isotope i and energy group g, ν_i^g denotes the average number of neutrons per fission for isotope i and energy group g, and N_f denotes the total number of fissionable isotopes. For the purposes of sensitivity analysis, the quantity ν_i^g, can be obtained by using the relation $\nu_{f,i}^g = (\nu\sigma)_{f,i}^g/\sigma_{f,i}^g$, where the isotopic fission cross sections $\sigma_{f,i}^g$ are available in data files for computing reaction rates.

The quantity χ^g in Equation (3) quantifies the material fission spectrum in energy group g, and is defined in PARTISN [4] as follows:

$$\chi^g \triangleq \frac{\sum\limits_{i=1}^{N_f} \chi_i^g N_{i,m} \sum\limits_{g'=1}^{G} \left(\nu\sigma_f\right)_i^{g'} f_i^{g'}}{\sum\limits_{i=1}^{N_f} N_{i,m} \sum\limits_{g'=1}^{G} \left(\nu\sigma_f\right)_i^{g'} f_i^{g'}}, \quad \text{with } \sum\limits_{g=1}^{G} \chi_i^g = 1, \tag{A14}$$

where the quantity χ_i^g denotes the isotopic fission spectrum in energy group g, while the quantity f_i^g denotes the corresponding spectrum weighting function.

Appendix B.

The sensitivities presented in this work have been computed by specializing the general expressions derived by Cacuci [5] to the PERP benchmark. For easy reference, the equations from Ref. [5] used in this work are reproduced in the following:

Equation (149) in [5]:

$$A^{(1),g}(\boldsymbol{\alpha})\psi^{(1),g}(\mathbf{r},\boldsymbol{\Omega}) \triangleq -\boldsymbol{\Omega}\cdot\nabla\psi^{(1),g}(\mathbf{r},\boldsymbol{\Omega}) + \Sigma_t^g(t^g;\mathbf{r})\,\psi^{(1),g}(\mathbf{r},\boldsymbol{\Omega})$$
$$-\sum_{g'=1}^{G}\int_{4\pi} d\boldsymbol{\Omega}'\Sigma_s^{g\to g'}\left(s^{gg'};\mathbf{r},\boldsymbol{\Omega}\to\boldsymbol{\Omega}'\right)\psi^{(1),g'}(\mathbf{r},\boldsymbol{\Omega}') \;-\nu\Sigma_f^g(f^g;\mathbf{r})\sum_{g'=1}^{G}\int_{4\pi} d\boldsymbol{\Omega}'\chi^{g\to g'}\left(p^{gg'};\mathbf{r}\right)\psi^{(1),g'}(\mathbf{r},\boldsymbol{\Omega}'). \tag{A15}$$

Equation (150) in [5]:

$$\frac{\partial R\left(\boldsymbol{\alpha},\varphi;\boldsymbol{\psi}^{(1)}\right)}{\partial t_j} = -\sum_{g=1}^{G}\int dV\int_{4\pi} d\boldsymbol{\Omega}\,\psi^{(1),g}(\mathbf{r},\boldsymbol{\Omega})\varphi^g(\mathbf{r},\boldsymbol{\Omega})\frac{\partial\Sigma_t^g(t;\mathbf{r})}{\partial t_j}, \quad j=1,\ldots,J_t. \tag{A16}$$

Equation (152) in [5]:

$$\frac{\partial R\left(\boldsymbol{\alpha},\varphi;\boldsymbol{\psi}^{(1)}\right)}{\partial f_j} = \sum_{g=1}^{G}\int dV\int_{4\pi} d\boldsymbol{\Omega}\,\psi^{(1),g}(\mathbf{r},\boldsymbol{\Omega}')\sum_{g'=1}^{G}\int_{4\pi} d\boldsymbol{\Omega}'\frac{\partial\left[\left(\nu\Sigma_f\right)^{g'}(f;\mathbf{r})\right]}{\partial f_j}\chi^{g'\to g}(p;\mathbf{r})\varphi^{g'}(\mathbf{r},\boldsymbol{\Omega}'), \quad j=1,\ldots,J_f. \tag{A17}$$

Equations (156) and (157) in [5]:

$$A^{(1),g}(\boldsymbol{\alpha})\psi^{(1),g}(\mathbf{r},\boldsymbol{\Omega}) = \sum_{d}^{g}\left(d^0;\mathbf{r},\boldsymbol{\Omega}\right), \quad g=1,\ldots,G, \tag{A18}$$

$$\psi^{(1),g}(\mathbf{r}_s,\boldsymbol{\Omega}) = 0, \mathbf{r}_s \in \partial V, \boldsymbol{\Omega}\cdot\mathbf{n} > 0. \tag{A19}$$

Equation (158) in [5]:

$$\frac{\partial^2 R}{\partial t_j \partial t_{m_2}} = -\sum_{g=1}^{G}\int dV\int_{4\pi} d\boldsymbol{\Omega}\,\psi^{(1),g}(\mathbf{r},\boldsymbol{\Omega})\varphi^g(\mathbf{r},\boldsymbol{\Omega})\frac{\partial^2\Sigma_t^g(t;\mathbf{r},\boldsymbol{\Omega})}{\partial t_j \partial t_{m_2}}$$
$$-\sum_{g=1}^{G}\int dV\int_{4\pi} d\boldsymbol{\Omega}\left[\psi_{1,j}^{(2),g}(\mathbf{r},\boldsymbol{\Omega})\psi^{(1),g}(\mathbf{r},\boldsymbol{\Omega}) + \psi_{2,j}^{(2),g}(\mathbf{r},\boldsymbol{\Omega})\varphi^g(\mathbf{r},\boldsymbol{\Omega})\right]\frac{\partial\Sigma_t^g(t;\mathbf{r},\boldsymbol{\Omega})}{\partial t_{m_2}}, \tag{A20}$$
$$\text{for } j=1,\ldots,J_t; m_2=1,\ldots,J_t.$$

Equation (159) in [5]:

$$\frac{\partial^2 R}{\partial t_j \partial s_{m_2}} = \sum_{g=1}^{G} \int dV \int_{4\pi} d\mathbf{\Omega}\, \psi_{1,j}^{(2),g}(\mathbf{r},\mathbf{\Omega}) \sum_{g'=1}^{G} \int_{4\pi} d\mathbf{\Omega'}\, \psi^{(1),g'}(\mathbf{r},\mathbf{\Omega'}) \frac{\partial \Sigma_s^{g\to g'}(\mathbf{s};\mathbf{r},\mathbf{\Omega}\to\mathbf{\Omega'})}{\partial s_{m_2}}$$
$$+ \sum_{g=1}^{G} \int dV \int_{4\pi} d\mathbf{\Omega}\, \psi_{2,j}^{(2),g}(\mathbf{r},\mathbf{\Omega}) \sum_{g'=1}^{G} \int_{4\pi} d\mathbf{\Omega'}\, \varphi^{g'}(\mathbf{r},\mathbf{\Omega'}) \frac{\partial \Sigma_s^{g'\to g}(\mathbf{s};\mathbf{r},\mathbf{\Omega'}\to\mathbf{\Omega})}{\partial s_{m_2}},$$
$$for \ \ j=1,\dots,J_t; m_2=1,\dots,J_s. \tag{A21}$$

Equation (160) in [5]:

$$\frac{\partial^2 R}{\partial t_j \partial f_{m_2}} = \sum_{g=1}^{G} \int dV \int_{4\pi} d\mathbf{\Omega}\, \psi_{2,j}^{(2),g}(\mathbf{r},\mathbf{\Omega}) \sum_{g'=1}^{G} \int_{4\pi} d\mathbf{\Omega'}\, \varphi^{g'}(\mathbf{r},\mathbf{\Omega'})\chi^{g'\to g}(\mathbf{p};\mathbf{r}) \frac{\partial\left[(v\Sigma_f)^{g'}(\mathbf{f};\mathbf{r})\right]}{\partial f_{m_2}}$$
$$+ \sum_{g=1}^{G} \int dV \int_{4\pi} d\mathbf{\Omega}\, \psi_{1,j}^{(2),g}(\mathbf{r},\mathbf{\Omega}) \frac{\partial\left[(v\Sigma_f)^{g}(\mathbf{f};\mathbf{r})\right]}{\partial f_{m_2}} \sum_{g'=1}^{G} \int_{4\pi} d\mathbf{\Omega'}\, \chi^{g\to g'}(\mathbf{p};\mathbf{r})\psi^{(1),g'}(\mathbf{r},\mathbf{\Omega'}),$$
$$for \ \ j=1,\dots,J_t; \ \ m_2=1,\dots,J_f. \tag{A22}$$

Equations (164)–(166) in [5]:

$$L^g(\boldsymbol{\alpha}^0)\psi_{1,j}^{(2),g}(\mathbf{r},\mathbf{\Omega}) = -\varphi^g(\mathbf{r},\mathbf{\Omega})\frac{\partial\Sigma_t^g(\mathbf{t};\mathbf{r})}{\partial t_j}, \ j=1,\dots,J_t; \ g=1,\dots,G, \tag{A23}$$

$$A^{(1),g}(\boldsymbol{\alpha}^0)\psi_{2,j}^{(2),g}(\mathbf{r},\mathbf{\Omega}) = -\psi^{(1),g}(\mathbf{r},\mathbf{\Omega})\frac{\partial\Sigma_t^g(\mathbf{t};\mathbf{r})}{\partial t_j}, \ j=1,\dots,J_t; \ g=1,\dots,G, \tag{A24}$$

$$\psi_{1,j}^{(2),g}(\mathbf{r}_s,\mathbf{\Omega})=0, \ \mathbf{\Omega}\cdot\mathbf{n}<0; \psi_{2,j}^{(2),g}(\mathbf{r}_s,\mathbf{\Omega})=0, \ \mathbf{\Omega}\cdot\mathbf{n}>0; \ \mathbf{r}_s\in\partial V; \ j=1,\dots,J_t; \ g=1,\dots,G. \tag{A25}$$

Equation (167) in [5]:

$$\frac{\partial^2 R}{\partial s_j \partial t_{m_2}} = -\sum_{g=1}^{G} \int dV \int_{4\pi} d\mathbf{\Omega}\left[\theta_{1,j}^{(2),g}(\mathbf{r},\mathbf{\Omega})\psi^{(1),g}(\mathbf{r},\mathbf{\Omega}) + \theta_{2,j}^{(2),g}(\mathbf{r},\mathbf{\Omega})\varphi^g(\mathbf{r},\mathbf{\Omega})\right]\frac{\partial\Sigma_t^g(\mathbf{t};\mathbf{r},\mathbf{\Omega})}{\partial t_{m_2}},$$
$$for \ \ j=1,\dots,J_s; \ m_2=1,\dots,J_t. \tag{A26}$$

Equation (169) in [5]:

$$\frac{\partial^2 R}{\partial s_j \partial f_{m_2}} = \sum_{g=1}^{G} \int dV \int_{4\pi} d\mathbf{\Omega}\, \theta_{1,j}^{(2),g}(\mathbf{r},\mathbf{\Omega}) \frac{\partial\left[(v\Sigma_f)^{g}(\mathbf{f};\mathbf{r})\right]}{\partial f_{m_2}} \sum_{g'=1}^{G} \int_{4\pi} d\mathbf{\Omega'}\, \chi^{g\to g'}(\mathbf{p};\mathbf{r})\psi^{(1),g'}(\mathbf{r},\mathbf{\Omega'})$$
$$+ \sum_{g=1}^{G} \int dV \int_{4\pi} d\mathbf{\Omega}\, \theta_{2,j}^{(2),g}(\mathbf{r},\mathbf{\Omega}) \sum_{g'=1}^{G} \int_{4\pi} d\mathbf{\Omega'}\, \varphi^{g'}(\mathbf{r},\mathbf{\Omega'})\chi^{g'\to g}(\mathbf{p};\mathbf{r}) \frac{\partial\left[(v\Sigma_f)^{g'}(\mathbf{f};\mathbf{r})\right]}{\partial f_{m_2}},$$
$$for \ \ j=1,\dots,J_s; \ m_2=1,\dots,J_f. \tag{A27}$$

Equations (173) through (175) in [5]:

$$L^g(\boldsymbol{\alpha}^0)\theta_{1,j}^{(2),g}(\mathbf{r},\mathbf{\Omega}) = \sum_{g'=1}^{G} \int_{4\pi} d\mathbf{\Omega'}\, \frac{\partial\Sigma_s^{g'\to g}(\mathbf{s};\mathbf{r},\mathbf{\Omega'}\to\mathbf{\Omega})}{\partial s_j}\varphi^{g'}(\mathbf{r},\mathbf{\Omega'}), \ j=1,\dots,J_s; \ g=1,\dots,G, \tag{A28}$$

$$A^{(1),g}(\boldsymbol{\alpha}^0)\theta_{2,j}^{(2),g}(\mathbf{r},\mathbf{\Omega}) = \sum_{g'=1}^{G} \int_{4\pi} d\mathbf{\Omega'}\, \psi^{(1),g'}(\mathbf{r},\mathbf{\Omega'})\frac{\partial\Sigma_s^{g\to g'}(\mathbf{s};\mathbf{r},\mathbf{\Omega}\to\mathbf{\Omega'})}{\partial s_j}, \ j=1,\dots,J_s; \ g=1,\dots,G, \tag{A29}$$

$$\theta_{1,j}^{(2),g}(\mathbf{r}_s,\mathbf{\Omega})=0, \ \mathbf{\Omega}\cdot\mathbf{n}<0; \theta_{2,j}^{(2),g}(\mathbf{r}_s,\mathbf{\Omega})=0, \ \mathbf{\Omega}\cdot\mathbf{n}>0; \ \mathbf{r}_s\in\partial V; \ j=1,\dots,J_s; \ g=1,\dots,G. \tag{A30}$$

Equation (177) in [5]:

$$\frac{\partial^2 R}{\partial f_j \partial t_{m_2}} = -\sum_{g=1}^{G} \int dV \int_{4\pi} d\mathbf{\Omega} \left[u_{1,j}^{(2),g}(\mathbf{r},\mathbf{\Omega}) \psi^{(1),g}(\mathbf{r},\mathbf{\Omega}) + u_{2,j}^{(2),g}(\mathbf{r},\mathbf{\Omega}) \varphi^g(\mathbf{r},\mathbf{\Omega}) \right] \frac{\partial \Sigma_t^g(\mathbf{t};\mathbf{r},\mathbf{\Omega})}{\partial t_{m_2}},$$

$$for \quad j = 1, \ldots, J_f; \ m_2 = 1, \ldots, J_t.$$

(A31)

Equation (178) in [5]:

$$\frac{\partial^2 R}{\partial f_j \partial s_{m_2}} = \sum_{g=1}^{G} \int dV \int_{4\pi} d\mathbf{\Omega} \, u_{1,j}^{(2),g}(\mathbf{r},\mathbf{\Omega}) \sum_{g'=1}^{G} \int_{4\pi} d\mathbf{\Omega}' \psi^{(1),g'}(\mathbf{r},\mathbf{\Omega}') \frac{\partial \Sigma_s^{g \to g'}(\mathbf{s};\mathbf{r},\mathbf{\Omega} \to \mathbf{\Omega}')}{\partial s_{m_2}}$$

$$+ \sum_{g=1}^{G} \int dV \int_{4\pi} d\mathbf{\Omega} \, u_{2,j}^{(2),g}(\mathbf{r},\mathbf{\Omega}) \sum_{g'=1}^{G} \int_{4\pi} d\mathbf{\Omega}' \varphi^{g'}(\mathbf{r},\mathbf{\Omega}') \frac{\partial \Sigma_s^{g' \to g}(\mathbf{s};\mathbf{r},\mathbf{\Omega}' \to \mathbf{\Omega})}{\partial s_{m_2}},$$

$$for \quad j = 1, \ldots, J_f; m_2 = 1, \ldots, J_s.$$

(A32)

Equation (179) in [5]:

$$\frac{\partial^2 R}{\partial f_j \partial f_{m_2}} = \sum_{g=1}^{G} \int dV \int_{4\pi} d\mathbf{\Omega} \, \psi^{(1),g}(\mathbf{r},\mathbf{\Omega}) \sum_{g'=1}^{G} \int_{4\pi} d\mathbf{\Omega}' \varphi^{g'}(\mathbf{r},\mathbf{\Omega}') \chi^{g' \to g}(\mathbf{p};\mathbf{r}) \frac{\partial^2 \left[(\nu \Sigma_f)^{g'}(\mathbf{f};\mathbf{r}) \right]}{\partial f_j \partial f_{m_2}}$$

$$+ \sum_{g=1}^{G} \int dV \int_{4\pi} d\mathbf{\Omega} \, u_{1,j}^{(2),g}(\mathbf{r},\mathbf{\Omega}) \frac{\partial \left[(\nu \Sigma_f)^g(\mathbf{f};\mathbf{r}) \right]}{\partial f_{m_2}} \sum_{g'=1}^{G} \int_{4\pi} d\mathbf{\Omega}' \chi^{g \to g'}(\mathbf{p};\mathbf{r}) \psi^{(1),g'}(\mathbf{r},\mathbf{\Omega}')$$

$$+ \sum_{g=1}^{G} \int dV \int_{4\pi} d\mathbf{\Omega} \, u_{2,j}^{(2),g}(\mathbf{r},\mathbf{\Omega}) \sum_{g'=1}^{G} \int_{4\pi} d\mathbf{\Omega}' \varphi^{g'}(\mathbf{r},\mathbf{\Omega}') \chi^{g' \to g}(\mathbf{p};\mathbf{r}) \frac{\partial \left[(\nu \Sigma_f)^{g'}(\mathbf{f};\mathbf{r}) \right]}{\partial f_{m_2}},$$

$$for \quad j = 1, \ldots, J_f; m_2 = 1, \ldots, J_f.$$

(A33)

Equations (183)–(185) in [5]:

$$L^g(\boldsymbol{\alpha}^0) u_{1,j}^{(2),g}(\mathbf{r},\mathbf{\Omega}) = \sum_{g'=1}^{G} \int_{4\pi} d\mathbf{\Omega}' \varphi^{g'}(\mathbf{r},\mathbf{\Omega}') \chi^{g' \to g}(\mathbf{p}^0;\mathbf{r}) \frac{\partial \left[(\nu \Sigma_f)^{g'}(\mathbf{f};\mathbf{r}) \right]}{\partial f_j}, j = 1, \ldots, J_f; \ g = 1, \ldots, G,$$

(A34)

$$A^{(1),g}(\boldsymbol{\alpha}^0) u_{2,j}^{(2),g}(\mathbf{r},\mathbf{\Omega}) = \frac{\partial \left[(\nu \Sigma_f)^g(\mathbf{f};\mathbf{r}) \right]}{\partial f_j} \sum_{g'=1}^{G} \int_{4\pi} d\mathbf{\Omega}' \psi^{(1),g'}(\mathbf{r},\mathbf{\Omega}') \chi^{g \to g'}(\mathbf{p}^0;\mathbf{r}), j = 1, \ldots, J_f; \ g = 1, \ldots, G,$$

(A35)

$$u_{2,j}^{(2),g}(\mathbf{r}_s,\mathbf{\Omega}) = 0, \ \mathbf{\Omega} \cdot \mathbf{n} > 0; u_{1,j}^{(2),g}(\mathbf{r}_s,\mathbf{\Omega}) = 0, \ \mathbf{\Omega} \cdot \mathbf{n} < 0; \ \mathbf{r}_s \in \partial V; \ j = 1, \ldots, J_f; \ g = 1, \ldots, G.$$

(A36)

Nomenclature

Symbols

$A^{(1)}$	adjoint operator
a_k, b_k	parameters used in Watt's fission spectra approximation for isotope k
B	forward operator
E^g	boundary of energy group g
$[E(L)]_\alpha$	expected value of the leakage response taking into account contributions from the uncorrelated parameters α, where α can be t, s, f, ν, respectively
$[E(L)]_\alpha^{(2,U)}$	2nd-order contributions to the expected value $[E(L)]_\alpha$ due to uncorrelated parameters of α, where α can be t, s, f, ν, respectively
F_k^{SF}	fraction of isotope k decays that are spontaneous fission events
f_j, f_{m_2}	parameters in vector $\boldsymbol{\sigma}_f$ indexed by j and m_2
G	total number of energy groups
I	total number of isotopes
J_n	total number of parameters in vector $\mathbf{N}$
J_p	total number of parameters in vector $\mathbf{p}$
J_q	total number of parameters in vector $\mathbf{q}$
$J_{\sigma f}$	total number of parameters in vector $\boldsymbol{\sigma}_f$
$J_{\sigma s}$	total number of parameters in vector $\boldsymbol{\sigma}_s$

$J_{\sigma t}$	total number of parameters in vector $\boldsymbol{\sigma}_t$
J_t	total number of parameters in vector $\mathbf{t}$
J_v	total number of parameters in vector $\boldsymbol{\nu}$
l	variable for the order of Legendre-expansion of the microscopic scattering cross sections, $l = 1, \ldots, ISCT$
$L(\boldsymbol{\alpha})$	total neutron leakage from the PERP sphere
M	total number of materials
N_f	total number of fissionable isotopes
$N_{i,m}$	atom number density for isotope i and material m
$P_l(\boldsymbol{\Omega}' \cdot \boldsymbol{\Omega})$	Legendre and associated Legendre polynomials appropriate for the geometry under consideration
$Q^g(r)$	source term in group g
r	spatial variable
r_d	external radius of the PERP benchmark
S_b	outer surface of the PERP sphere
$s_{f,i}^g$	standard deviation associated with the model parameter $\sigma_{f,i}^g$
$s_{v,i}^g$	standard deviation associated with the model parameter ν_i^g
s_j, s_{m_2}	parameters in vector $\boldsymbol{\sigma}_s$ indexed by j and m_2
t_j, t_{m_2}	parameters in vector $\boldsymbol{\sigma}_t$ indexed by j and m_2
$u_{1,j}^{(2),g}(r,\boldsymbol{\Omega}), u_{2,j}^{(2),g}(r,\boldsymbol{\Omega})$	2nd-level adjoint functions in group g at point r in direction $\boldsymbol{\Omega}$ associated with the fission parameter indexed by j (e.g., f_j)
$U_{1,j;0}^{(2),g}(r), U_{2,j;0}^{(2),g}(r)$	zeroth order 2nd-level adjoint flux moments in group g at point r, $U_{1,j;l}^{(2),g}(r) \triangleq \int_{4\pi} d\boldsymbol{\Omega}\, P_l(\boldsymbol{\Omega}) u_{1,j}^{(2),g}(r,\boldsymbol{\Omega}),\ \ U_{2,j;l}^{(2),g}(r) \triangleq \int_{4\pi} d\boldsymbol{\Omega}\, P_l(\boldsymbol{\Omega}) u_{2,j}^{(2),g}(r,\boldsymbol{\Omega})$
$U_{1,j;l}^{(2),g}(r), U_{2,j;l}^{(2),g}(r)$	l^{th} $(l=1,\ldots,ISCT)$ order 2nd-level adjoint flux moments in group g at point r, $U_{1,j;l}^{(2),g}(r) \triangleq \int_{4\pi} d\boldsymbol{\Omega}\, P_l(\mu) u_{1,j}^{(2),g}(r,\boldsymbol{\Omega}),\ \ U_{2,j;l}^{(2),g}(r) \triangleq \int_{4\pi} d\boldsymbol{\Omega}\, P_l(\mu) u_{2,j}^{(2),g}(r,\boldsymbol{\Omega})$
$[\mathrm{var}(L)]_\alpha^{(U,N)}$	variance of the leakage response taking into account contributions solely from the uncorrelated and normally-distributed parameters α, where α can be t, s, f, v, respectively
$[\mathrm{var}(L)]_\alpha^{(1,U,N)}$	first-order contributions to the variance $[\mathrm{var}(L)]_\alpha^{(U,N)}$
$[\mathrm{var}(L)]_\alpha^{(2,U,N)}$	second-order contributions to the variance $[\mathrm{var}(L)]_\alpha^{(U,N)}$

Vectors and Matrices

$\boldsymbol{\alpha}$	vector of imprecisely known model parameters, $\boldsymbol{\alpha} \triangleq \left[\boldsymbol{\sigma}_t; \boldsymbol{\sigma}_s; \boldsymbol{\sigma}_f; \boldsymbol{\nu}; \mathbf{p}; \mathbf{q}; \mathbf{N}\right]^\dagger$
$\boldsymbol{\alpha}^0$	nominal values of the parameters in the vector $\boldsymbol{\alpha}$
$\mathbf{t}$	vector of imprecisely known total parameters, $\mathbf{t} \triangleq [\boldsymbol{\sigma}_t; \mathbf{N}]^\dagger$
$\mathbf{s}$	vector of imprecisely known scatter parameters, $\mathbf{s} \triangleq [\boldsymbol{\sigma}_s; \mathbf{N}]^\dagger$
$\mathbf{f}$	vector of imprecisely known fission parameters, $\mathbf{f} \triangleq \left[\boldsymbol{\sigma}_f; \boldsymbol{\nu}; \mathbf{N}\right]^\dagger$
$\boldsymbol{\sigma}_t$	vector of imprecisely known total cross sections
$\boldsymbol{\sigma}_s$	vector of imprecisely known scattering cross sections
$\boldsymbol{\sigma}_f$	vector of imprecisely known fission cross sections
$\boldsymbol{\nu}$	vector of imprecisely known parameters underlying the average number of neutrons per fission
$\mathbf{N}$	vector of imprecisely known atom number densities
$\mathbf{p}$	vector of imprecisely known fission spectrum parameters
$\mathbf{q}$	vector of imprecisely known source parameters
$\mathbf{S}^{(1)}$	vector of first-order relative sensitivities of the leakage response
$\mathbf{S}^{(2)}$	matrix of first-order relative sensitivities of the leakage response

Greek Symbols

$[\gamma_1(L)]_\alpha^{(U,N)}$	the skewness due to the variances of parameters α in the leakage response, where α can be t, s, f, v, respectively
δ	Kronecker-delta functionals
$\theta_{1,j}^{(2),g}(r,\boldsymbol{\Omega}), \theta_{2,j}^{(2),g}(r,\boldsymbol{\Omega})$	2nd-level adjoint functions in group g at point r in direction $\boldsymbol{\Omega}$ associated with the scattering cross section parameter indexed by j (e.g., s_j)
$\Theta_{1,j;0}^{(2),g}(r), \Theta_{2,j;0}^{(2),g}(r)$	zeroth order 2nd-level adjoint flux moments in group g at point r, $\Theta_{1,j;0}^{(2),g}(r) \triangleq \int_{4\pi} d\boldsymbol{\Omega}\, \theta_{1,j}^{(2),g}(r,\boldsymbol{\Omega})$ and $\Theta_{2,j;0}^{(2),g}(r) \triangleq \int_{4\pi} d\boldsymbol{\Omega}\, \theta_{2,j}^{(2),g}(r,\boldsymbol{\Omega})$
λ_k	decay constant for isotope k
$[\mu_3(L)]_\alpha^{(U,N)}$	third-order moment of the leakage response with contributions solely from the uncorrelated and normally-distributed parameters α, where α can be t, s, f, v, respectively

ν_i^g	number of neutrons produced per fission by isotope i and energy group g
ν_k^{SF}	the spontaneous emission of an average neutrons of an isotope k
$\xi_0^{(1),g}(r)$	zeroth order of adjoint flux moment in group g at point r
$\xi_l^{(1),g}(r)$	l^{th} $(l = 1,\dots,ISCT)$ order adjoint flux moment in group g at point r, $\xi_l^{(1),g}(r) \triangleq \int_{4\pi} d\Omega\, P_l(\Omega)\psi^{(1),g}(r,\Omega),\ \ l = 1,\dots,ISCT$
$\xi_{1,j;0}^{(2),g}(r), \xi_{2,j;0}^{(2),g}(r)$	zeroth order moments for $\xi_{1,j;0}^{(2),g}(r) \triangleq \int_{4\pi} d\Omega\, \psi_{1,j}^{(2),g}(r,\Omega)$ and $\xi_{2,j;0}^{(2),g}(r) \triangleq \int_{4\pi} d\Omega\, \psi_{2,j}^{(2),g}(r,\Omega)$
$\xi_{1,j;l}^{(2),g}(r), \xi_{2,j;l}^{(2),g}(r)$	l^{th} $(l = 1,\dots,ISCT)$ order 2nd-level adjoint flux moments in group g at point r, $\xi_{1,j;l}^{(2),g}(r) \triangleq \int_{4\pi} d\Omega\, P_l(\Omega)\psi_{1,j}^{(2),g}(r,\Omega),\ \ \xi_{2,j;l}^{(2),g}(r) \triangleq \int_{4\pi} d\Omega\, P_l(\Omega)\psi_{2,j}^{(2),g}(r,\Omega)$
σ	cross sections
$\sigma_{f,i}^g$	microscopic fission cross section in group g of isotope i
$\sigma_{s,l,i}^{g'\to g}$	the lth order Legendre-expanded microscopic scattering cross section from energy group g' into energy group g for isotope i
$\sigma_{t,i}^g$	microscopic total cross section in group g of isotope i
$\Sigma_t^g(\mathbf{t};r)$	macroscopic total cross section for energy group g
$\Sigma_f^g(\mathbf{f};r)$	macroscopic fission cross section for energy group g
$\Sigma_s^{g'\to g}(\mathbf{s};r,\Omega'\to\Omega)$	macroscopic scattering transfer cross section from energy group g' into energy group g
$\varphi^g(r,\Omega)$	forward angular flux in group g at point r in direction Ω
$\varphi_0^g(r)$	zeroth order of forward flux moment in group g at point r
$\varphi_l^g(r)$	l^{th} $(l = 1,\dots,ISCT)$ order forward flux moment in group g at point r, $\varphi_l^g(r) \triangleq \int_{4\pi} d\Omega\, P_l(\mu)\varphi^g(r,\Omega),\ \ l = 1,\dots,ISCT$
$\chi^g(r)$	material fission spectrum in energy group g
$\psi^{(1),g}(r,\Omega)$	adjoint angular flux in group g at point r in direction Ω
$\psi_{1,j}^{(2),g}(r,\Omega), \psi_{2,j}^{(2),g}(r,\Omega)$	2nd-level adjoint functions in group g at point r in direction Ω associated with the total cross section parameter indexed by j (e.g., t_j)
Ω, Ω'	directional variable
Subscripts, Superscripts	
f	fission
g, g'	energy group variable $g, g' = 1,\dots,G$
g_j, g_{m_2}	energy group associated with parameter indexed by j (e.g., f_j, t_j and s_j) or m_2 (e.g., f_{m_2}, t_{m_2} and s_{m_2})
i	index variable for isotopes, $i = 1,\dots,I$
i_j, i_{m_2}	isotope associated with the parameter indexed by j (e.g., f_j, t_j and s_j) or m_2 (e.g., f_{m_2}, t_{m_2} and s_{m_2})
j	index variable for parameters
k	index variable for isotopes, $k = 1,\dots,I$
l	order of Legendre expansion
l_j, l_{m_2}	order of Legendre expansion associated with the microscopic scattering cross section parameters indexed by j (e.g., s_j) or m_2 (e.g., s_{m_2})
ν	number of neutrons produced per fission
m	index variable for materials, $m = 1,\dots,M$
m_2	index variable for parameters
m_j, m_{m_2}	material associated with parameter indexed by j (e.g., f_j, t_j and s_j) s_j) or m_2 (e.g., f_{m_2}, t_{m_2} and s_{m_2})
t	total
s	scatter
$(1, U, N)$	first-order contributions from uncorrelated and normally-distributed parameters
$(2, U)$	2nd-order contributions from uncorrelated parameters
$(2, U, N)$	2nd-order contributions from uncorrelated and normally-distributed parameters
(U, N)	uncorrelated and normally-distributed parameters
Abbreviations	
$1^{st} - LASS$	1st-Level adjoint sensitivity system
$2^{nd} - ASAM$	second-order adjoint sensitivity analysis methodology
$2^{nd} - LASS$	2nd-Level adjoint sensitivity system
$ISCT$	order of the finite expansion in Legendre polynomial
$PERP$	polyethylene-reflected plutonium

References

1. Cacuci, D.G.; Fang, R.; Favorite, J.A. Comprehensive Second-Order Adjoint Sensitivity Analysis Methodology (2nd-ASAM) Applied to a Subcritical Experimental Reactor Physics Benchmark: I. Effects of Imprecisely Known Microscopic Total and Capture Cross Sections. *Energies*, accepted for publication.

2. Fang, R.; Cacuci, D.G. Comprehensive Second-Order Adjoint Sensitivity Analysis Methodology (2nd-ASAM) Applied to a Subcritical Experimental Reactor Physics Benchmark: II. Effects of Imprecisely Known Microscopic Scattering Cross Sections. *Energies*, accepted for publication.

3. Mattingly, J. *Polyethylene-Reflected Plutonium Metal Sphere: Subcritical Neutron and Gamma Measurements*; SAND2009-5804 Rev. 3; Sandia National Laboratories: Albuquerque, NM, USA, July 2012.

4. Alcouffe, R.E.; Baker, R.S.; Dahl, J.A.; Turner, S.A.; Ward, R. *PARTISN: A Time-Dependent, Parallel Neutral Particle Transport Code System*; LA-UR-08-07258 (Revised Nov. 2008); Los Alamos National Laboratories: Los Alamos, NM, USA.

5. Cacuci, D.G. Application of the Second-Order Comprehensive Adjoint Sensitivity Analysis Methodology to Compute 1st- and 2nd-Order Sensitivities of Flux Functionals in a Multiplying System with Source. *Nucl. Sci. Eng.* **2019**, *193*, 555–600. [CrossRef]

6. Wilson, W.B.; Perry, R.T.; Shores, E.F.; Charlton, W.S.; Parish, T.A.; Estes, G.P.; Brown, T.H.; Arthur, E.D.; Bozoian, M.; England, T.R.; et al. SOURCES4C: A Code for Calculating (α,n), Spontaneous Fission, and Delayed Neutron Sources and Spectra. In Proceedings of the American Nuclear Society/Radiation Protection and Shielding Division 12th Biennial Topical Meeting, Santa Fe, NM, USA, 14–18 April 2002; LA-UR-02-1839.

7. Conlin, J.L.; Parsons, D.K.; Gardiner, S.J.; Gray, M.G.; Lee, M.B.; White, M.C. *MENDF71X: Multigroup Neutron Cross-Section Data Tables Based upon ENDF/B-VII.1X*; LA-UR-15-29571 (7 October 2013); Los Alamos National Laboratories: Los Alamos, NM, USA. [CrossRef]

8. Chadwick, M.B.; Herman, M.; Obložinský, P.; Dunn, M.E.; Danon, Y.; Kahler, A.C.; Smith, D.L.; Pritychenko, B.; Arbanas, G.; Arcilla, R.; et al. ENDF/B-VII.1: Nuclear Data for Science and Technology: Cross Sections, Covariances, Fission Product Yields and Decay Data. *Nucl. Data Sheets* **2011**, *112*, 2887–2996. [CrossRef]

9. Cacuci, D.G. *BERRU Predictive Modeling: Best Estimate Results with Reduced Uncertainties*; Springer: Heidelberg, Germany; New York, NY, USA, 2018.

10. Fang, R.; Cacuci, D.G. Comprehensive Second-Order Adjoint Sensitivity Analysis Methodology (2nd-ASAM) Applied to a Subcritical Experimental Reactor Physics Benchmark: IV. Effects of Imprecisely Known Source Parameters. *Energies*, under review.

11. Cacuci, D.G.; Fang, R.; Favorite, J.A. Comprehensive Second-Order Adjoint Sensitivity Analysis Methodology (2nd-ASAM) Applied to a Subcritical Experimental Reactor Physics Benchmark: V. Effects of Imprecisely Known Isotopic Number Densities, Fission Spectrum and Overall Conclusions. *Energies*, (under review).